Thesis for the
Doctor of Philosophy Award of a Research Degree
From the University of London

Véronique Maxence BLANC

Expression, regulation and roles of semaphorins and their receptors in prostate and prostate cancer

Supervisors
Professor John Masters, University College London
Doctor Magali Williamson[1], University College London

Examiners
Professor Paul Abel, Imperial College London
Professor Fouad Habib, University of Edinburgh

Prostate Cancer Research Centre (PCRC)
Institute of Urology and Nephrology
University College London (UCL)
63-67 Riding House Street
London W1W7EJ
+44(0) 207 679 9597[1]

ProQuest LLC
789 East Eisenhower Parkway
P.O. Box 1346
Ann Arbor, MI 48106-1346

To Nicole and Yves,
To Helene, Lucie and Marcel,
To Erwann,

ACKNOWLEDGEMENTS

I thank the Pilkington Trust for funding the following research project. I thank Professor John Masters and Doctor Magali Williamson for allowing and supervising my research work at the Prostate Cancer Research Centre (Institute of Urology and Nephrology, University College London), as well as for their support and supervision during completion.

I thank all my colleagues for their encouragements and support, particularly Dr. Simon Bott, Dr. Charlotte Foley, Dr. Manit Araya, Dr. Aamir Ahmed, Dr. Andy Symes, Dr. Tharani Nitkunan, Dr. Joseph Nariculam, Dr. Jason Constantinou...

I deeply thank all my friends for their support in this hard and long labour, to which they have largely contributed in one way or another, particularly Dr. Isabelle Bisson, Dr. Roger Tatoud, Dr. Rena Meimaridou, Dr. Tahirah Alam, Marthin Louis Vorster, Patrice Renault, Jennifer McNair Wilson...

I dedicate this work to my parents, my grand parents, and especially to Erwann Thomassain, who has seen the worst of me during completion, and without whom, I would not have succeeded.

Thank you for your continuous support and your confidence in my success.

Declaration that the work presented in the following thesis is my own

I, Véronique Maxence BLANC, confirm that the work presented in this thesis is my own. Where information has been derived from other sources, I confirm that this has been indicated in the thesis (e.g. site-directed mutagenesis and subsequent stable transfection, SSCP, some figures in the introduction annotated with a reference).

ABSTRACT

Prostate cancer (PCa) has become a major public health issue; it is the second most common cause of cancer-related death in the UK. PCa preferentially metastasises to the bone. Semaphorins are an important family of membrane bound or secreted signalling proteins, which control cell movement (or chemotaxis). They have a role in the nervous, immune and vascular systems, but have not previously been studied in prostate. To determine if semaphorins and their receptors are expressed in normal and pathological prostate, profiling experiments were performed by (q)RT-PCR in prostate cell lines and tissues. Results show that semaphorins and receptors are ubiquitously expressed, suggesting autocrine and paracrine regulation of semaphorin signalling in prostate; particularly an autocrine signalling of Semaphorin3A in bone metastasis derived cells. Results also show that expression of secreted semaphorins is regulated by hypoxia; which strongly downregulates semaphorin 3e in primary tumour derived cells, whereas semaphorin 3c is strongly upregulated. Particular focus was brought on semaphorin 3e, whose expression is strongly increased in epithelial cells derived from benign prostate hyperplasia, non-neoplastic tissue, and bone metastasis derived cells. A Semaphorin3E expression construct was made and the protein produced in mammalian cells to study its effects on cell morphology and adhesion by immunocytochemistry and adhesion assays. Results show that Semaphorin3E inhibits integrin-mediated cell adhesion while it initiates vinculin-mediated focal adhesion formation, which suggest that Semaphorin3E may play important regulatory roles in prostate cancer metastasis. The effects on cell movement of frequent missense mutations of PlexinB1 receptor, associated with prostate primary tumours and metastases, was studied by migration assays. Results show that the three mutations of PlexinB1 increase cell migration in absence of ligand Semaphorin4D, and further increase migration in its presence. Together these results suggest that semaphorin signalling has a key role in prostate cancer progression.

INTRODUCTION

The following thesis is divided into four chapters: **(1)** literature review, **(2)** materials and methods, **(3)** results and discussions, **(4)** conclusion and future work.

(1) The 'literature review' chapter comprises three sections. **(a)** The prostate and its pathologies, with emphasis on prostate adenocarcinoma, the second most common cause of death due to cancer in the UK. **(b)** The theories of cancer progression, summarising the molecular-based theory of cancer, which describes nine cancer gene pathways, eventually all leading to activation of the hypoxia/HIF1 pathway, which promotes angiogenesis and survival of the cancer cells. **(c)** The sema domain containing superfamily describes three family members with common and specific features, details the HGF and MET, and Semaphorin4D and PlexinB1 signalling pathways, and summarise their roles in cell guidance and migration, invasive growth, and tumour angiogenesis.

(2) The 'materials and methods' chapter is divided into two sections, **(a)** materials and **(b)** methods.

(3) The 'results and discussions' chapter contains three sections. **(a)** The first section resumes the results of expression profiling experiments under normoxic and hypoxic conditions in 10 prostate cell lines. Results show that semaphorins and their receptors are largely expressed in prostate cell lines, and that the expression of secreted semaphorins is strongly regulated by hypoxia. **(b)** The second section summarises the study of three mutations of PlexinB1 receptor, associated with prostate tumours and metastases. The mutations modulate cell migration in presence or absence of Semaphorin4D ligand. **(c)** The last section describes the production of Semaphorin3E protein and its effects on cell phenotype and behaviour. Semaphorin3E inhibits β1-integrin-mediated cell adhesion and initiates vinculin-mediated cell motility, spreading.

(4) Finally, the 'conclusions and future work' chapter summarises all findings and suggests further studies.

TABLE OF CONTENTS

LIST OF FIGURES

LIST OF TABLES

LIST OF ABBREVIATIONS

(b)FGF: (basic) fibroblast growth factor
β-IFN: interferon beta
(q)RT-PCR: (quantitative) reverse transcription-polymerase chain reaction
(r)EGF: (recombinant) epidermal growth factor
42C: 1542CPTX prostate cell line, primary tumour
42F: 1542FTX prostate cell line, fibroblastic
42N: 1542NPTX prostate cell line, non-neoplastic "normal"
A: alanine
aa: amino acids
ALT: alternative lengthening of telomeres
AP: alkaline phosphatase
APC: adenomatous polyposis coil
AR: androgen receptor
BAD: Bcl2-antagonist of cell death
BAX: Bcl2-associated X protein
BER: base excision repair
bp: base pair
BPE: bovine pituitary extract
BPH: benign prostate hyperplasia
CAM: cell adhesion molecule
CD100: Semaphorin4D protein
Cdc42: cell division cycle 42
cDNA: complementary DNA
CIAP: calf intestinal alkaline phosphatase
COLL-5: Semaphorin3E
CRD: cystin-rich domain
CRIB: cdc42/rac-interactive binding
CUB: complement binding domain
Cyt-c: cytochrome c
DAPI: 4',6-diamidino-2-phenylindole
DHR: Dlg homologous region
DHR: Dlg homologous region
DNA: deoxyribonucleic acid
dNTP: deoxy-nucleoside triphosphate
DOC: sodium deoxycholate
DRG: dorsal root ganglion
DTT; dithiothreitol
E: glutamate
ECM: extracellular matrix
ErbB2: v-erb-b2 erythroblastic leukemia viral oncogene homolog 2
ERG: v-ets erythroblastosis virus E26 oncogene homolog
Erk1/2: mitogene-activated protein kinase 1
ETS: ets transcription factors
ETV1: ets *variant gene 1*
FASR: Fas receptor
FCS: foetal calf serum
FITC: fluorescein isothyiocyanate
Gab1: Grb2-associated binding protein 1
GAG: glycosaminoglycan
GAP: GTPases activating protein
GAPDH: glycerol 3 phosphate dehydrogenase
GEF: guanosine exchange factor
GF: growth factor
GLI: glioma-associated oncogene
GPI: glycosylphosphatidylinositol
Grb2: growth factor receptor-bound protein 2
GSC: Gleason score
GSP: Gleason grades
GST: glutathione transferase
GTPAse: guanosine triphosphatase
HA:
HGF: hepatocyte growth factor
HIF1(α): hypoxia-inducible factor 1 (alpha)
His: histidine
HRP: Horseradish peroxidase
HT29: colon cancer cell line
Ig: immunoglobulin
IGF1,2: Insulin growth factor 1 and 2
IGFR-1: Insulin growth factor receptor 1
IL3: interleukin 3
IL3R: interleulin 3 receptor
IPT/TIG: repeats found in immunoglobulins, plexins and transcription factors
kb: kilobase
kDa: kilodalton
KIAA0331: Semaphorin3E
KLF6: kruppel-like factor 6
L1-CAM: L1 cell adhesion molecule
LARG: leukemia-associated Rho guanine nucleotide exchange factor GEF
LB: luria bertani broth
LOH: loss of heterozygocy
M: distant metastases
MAM: meprin/A5/Mu-phosphatase domain
MAPK: mitogene-activated protein kinase
Max: Myc-associated factor X
MBD: MET binding domain
MMP: matrix metalloproteinase
MRS: MET-related sequence
MSP: macrophage stimulating protein
N: regional lymph node metastasis
NaAc: sodium acetate
NER: nucleotide excision repair
NFKB/REL/Dorsal: NF kappa B/v-rel reticuloendotheliosis viral oncogene homolog
NGF: nerve growth factor
NIP: neuropilin-interacting protein
NKX3.1: NK3 homeobox 1
NMR: mismatch repair
Np: Neuropilin
OTK: off track receptor
P14ARF: p16INK4
p16INK4A: cyclin-dependent kinase inhibitor 2A
p27KIP1: cyclin-dependent kinase inhibitor 1B
p53: tumour protein 53
PAGE: polyacrylamide gel
PAK: p21-activated kinase
PBS: phosphate buffer
PCa: prostate cancer
PI3K: phosphoinositide 3 kinase
PIN: prostate intraepithelial neoplasia
PLC-γ: phospholipase C-gamma

Plx: Plexin
PNS: peripheral nervous system
POT1: protection of telomere 1 homolog
pRB: retinoblastoma protein
PRGF: plasminogen-related growth factor
PSI: domain found in plexins, semaphorin and integrins
pT: tumour stage
PTB: phosphotyrosine binding
PTEN: phosphate and tensin homolog
PYK2: proline-rich tyrosine kinase 2
R: recurrence
RNA: ribonucleic acid
Rnd1: Rho family GTPase 1
RON: macrophage stimulating 1 receptor
rpm: rotation per minute
RTK: receptor tyrosine kinase
S: serine
SDS: sodium dodecyl sulfate
SEM: standard error of the mean
Sema: semaphorin domain
Sema3: semaphorin class 3
Semaphorin 3e: gene
Semaphorin3E: protein
SemaH: Semaphorin3E
SF: scatter factor
SH2/SH3: Src-homolgy 2 and 3 domains
Shc: (Src homology 2 domain containing) transforming protein
SHP2: Src homology 2-containing tyrosine phosphatase
SMT: somatic mutation theory
SP: sex and plexin domain
Src: v-src sarcoma viral oncogene homolog
STAT: signal transducer and activator of transcription
TCF4: Transcription factor 4
TEMED: N,N,N',N'-tetramethylenediamine
TGFβ: transforming growth facto beta
TIN2: TRF1-interacting nuclear factor 2
TNFα: tumour necrosis factor alpha
TNFR-1: tumour necrosis factor receptor 1
TOFT: tissue organization theory
tPA: plasminogen activator, tissue
TPP1: tripeptidyl peptidase telomere
TRF1/2: telomeric repeat binding factor ½
TRITC: tetramethyl rhodamine iso-thyociante
TSP-1: thrombospondin 1
UK: united kingdom
uPA: plasminogen activator, urokinase
UTR: untranslated region
VEGF: vascular endothelial growth factor
VEGFR: vascular endothelial growth factor receptor
VSV: vesicular somatitis virus
WT: wild type
Y: tyrosine

REMARKS:

Names of genes are written in lower case: plexin b1, semaphorin 3e

Names of proteins are written in caps: PlexinB1, Semaphorin3E

Expression, regulation and roles of semaphorins and their receptors in prostate and prostate cancer

CHAPTER 1: LITERATURE REVIEW

Section 1: The Prostate and its pathologies

1. Role and structure of the prostate

Prostate is a gland of the male reproductive system that makes and stores seminal fluid, which nourishes sperm. The gland has the size of a walnut, and is located below the bladder and in front of the rectum (Figure 1). It surrounds the upper part of the urethra that empties urine from the bladder. The prostate gland is made of acini and ducts and comprises three anatomical zones: the peripheral zone, the transition zone, and the central zone (McNeal, 1981a). The peripheral zone, approximately 65% of the prostate volume, is characterised by small, simple, acinar spaces lined by tall columnar secretory epithelial cells. The central zone, approximately 25% of normal prostatic volume, is made of large acini with irregular contours that are lined by low columnar cuboidal epithelium. This central zone surrounds the ejaculatory ducts. The transition zone, 5 to 10% of the prostate volume, is separated from the other two zones by a narrow band of fibromuscular stroma. The ducts of this transition zone empty bilaterally into the urethra.

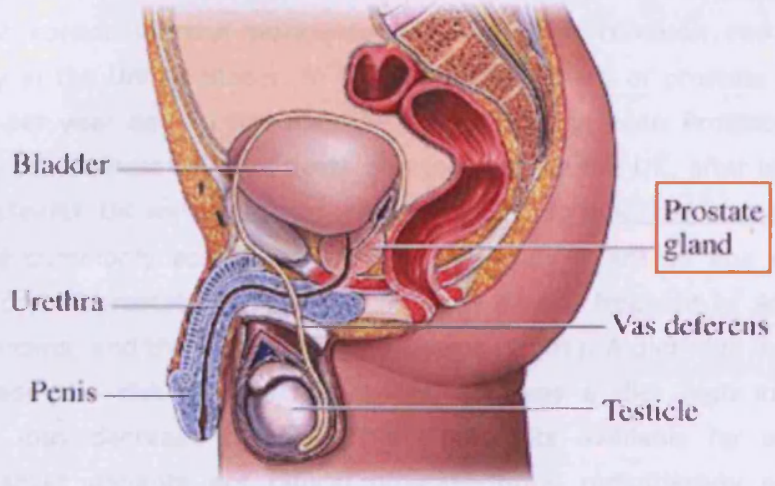

Figure 1: Anatomy of the male reproductive system (picture from http://www.liv.ac.uk/researchintelligence/issue21/images/prostate.jpg). The prostate gland is located below the bladder and in front of the rectum.

2. Pathologies of the prostate

The three most common problems occurring in the prostate are inflammation (prostatitis), enlargement (BPH), and cancer (PCa). The symptoms of an unhealthy prostate (a simple inflammation, a BPH or a cancer) are a need to urinate frequently, especially at night; difficulty starting urination or holding back

urine; inability to urinate; weak or interrupted flow of urine; painful or burning urination, and difficulty in having an erection; painful ejaculation; blood in urine or semen or frequent pain and stiffness in the lower back, hips, or upper thighs. Prostatitis is an inflammation of the prostate gland that may or may not be caused by an acute or recurrent infection. Benign prostatic hyperplasia (BPH) is an abnormal growth of normal prostate cells ending in an enlargement of the gland, squeezing the urethra, which may gradually lead to bladder and/or kidney damage. BPH is not cancerous and does not increase the risk of prostate cancer. Prostate cancers are classical adenocarcinomas, made up of epithelial cells with varying degrees of glandular architecture. High grade prostate intraepithelial neoplasia (PIN) is considered the precursor of a majority of invasive prostate adenocarcinomas (Haggman et al., 1997). BPH and PCa have different origins within the gland, the peripheral zone is the most frequent site of cancer and the transition zone is the almost exclusive site of BPH (McNeal, 1981b; Colombo et al., 2001).

3. Prostate cancer: risk factors, treatments, staging and grading

Prostate cancer has become a major public health issue. It is the third commonest cancer in men worldwide and the most common non-cutaneous malignancy in the United States. In the UK, 32.000 cases of prostate cancer are diagnosed per year and 10.000 men die from PCa each year. Prostate cancer is the second commonest cause of death due to cancer in the UK, after lung cancer. (Cancer Research UK website: http://info.cancerresearchuk.org/cancerstats). The risk factors commonly associated with prostate cancer are an age over 50, a family history of prostate cancer, the ethnicity (more frequent in African than white Americans, and the diet (Hsing and Devesa, 2001). A diet high in animal fat may increase the risk of prostate cancer, whereas a diet high in fruit and vegetables may decrease the risk. The treatments available for early stage prostate cancer patients are radical prostatectomy, radiotherapy or watchful waiting. For late stage prostate cancer, i.e. PCa that has started invading other organs (metastases), the treatments available are androgen ablation therapy and chemotherapy. The majority of advanced stage PCa patients have developed bone lesions, causing morbidity (Jacobs, 1983; Lange and Vessela, 1998). Localised prostate cancer detected at an early stage is curable, whereas treatments for advanced prostate cancer are not curative.

An accurate assessment of the clinical stage and grade of prostate tumours is crucial for patients outcome. The stage refers to the extent and spread of the

disease, while the grade refers to the nature (aggressiveness) of the particular tumour (table 1). The currently used TNM staging system (UICC 1997) for prostate cancer is based on the old system proposed by Schroder in 1992 (Schroder et al., 1992). There are 4 different stages of prostate cancer, pT1 (organ confined, not palpable), pT2 (organ confined, palpable), pT3 (extracapsular spread), and pT4 (local organs invaded). The presence of regional lymph nodes (N) and distant metastases (M) are also assessed. The grading system currently used for prostate cancer had first been proposed in 1966 by Donald F. Gleason, hence its name (Gleason, 1966). The Gleason score (GSC) is a pathologic classification only, based on the premise that poorly differentiated tumours are more aggressive and unpredictable than well-differentiated tumours. Pathologists look for a primary predominant pattern, and a secondary or lesser pattern (Gleason grades), and each is given a score from 1 to 5. Scores for primary and secondary patterns are added together to achieve the Gleason score for the tumour. Scores can range from 2 (uniformly well differentiated 1+1) to 10 (diffusely anaplastic 5+5). The higher the Gleason score, the more aggressive is the tumour and the worse is the prognosis (Gleason, 1992).

Pathological staging of primary tumour (pT)		Staging by presence of distant metastases (M)	
pT2	Organ confined	MX	Presence of distant metastases cannot be assessed
T2a	Unilateral		
T2b	Bilateral	M0	No distant metastases
pT3	Extraprostatic extension	M1	Distant metastases
T3a	Extraprostatic extension	M1a	Non regional lymph nodes metastases
T3b	Seminal vesicle invasion	M1b	Bone metastases
pT4	Invasion of bladder, and rectum	M1c	Other sites metastases
Staging by regional lymph node involvement (N)		Gleason score (GSC)	
NX	Regional lymph nodes cannot be assessed	2-4	2.1% risk of developing metastases
			5.4% risk of developing metastases
N0	No regional lymph nodes	4-5	13.5% risk of developing metastases
N1	Metastasis in regional lymph nodes	7-10	More aggressive neoplasms with seminal vesicles extension, and/or metastases spread

Table 1: Staging and grading of prostate tumours. The stage of the tumour (pT) refers to the extent and spread of the disease, while the grade refers to the nature (aggressiveness) of the particular tumour. The presence of regional lymph nodes (N) and distant metastases (M) is also assessed.

4. Molecular biology and genetics of prostate cancer

Prostate cancer develops from a lesion in the epithelial layer of the peripheral zone of the gland to become an invasive tumour that spreads within the prostate

and subsequently acquires the potential to metastasise to distant sites, most often the lymph node and bone. The molecular biology of PCa and its progression is characterised by aberrant activity of several regulatory pathways (for a review see Quinn et al, 2005), which can be grouped broadly into androgen receptor signalling (AR mutation and/or amplification), signal transduction (family of EGF receptors), cell cycle regulation (c-Myc amplification, increased $p16^{INK4A}$, decreased $p27^{KIP1}$, decrease or loss of pRb, increased proliferation index), apoptosis (increased apoptotic index, p53 and Bcl-2), cell adhesion and cohesion (reduced E-cadherin and catenins, increased metalloproteinases and chondroitin sulphate), and angiogenesis (increased VEGF, VEGF receptors, nitric oxid).

Moreover, chromosomal alterations are commonly observed in PCa, and the characteristic patterns of chromosome abnormalities can be considered as indicative of stages of PCa progression (for a review see Bova and Isaacs, 1996; Bate-Shen and Shen, 2000). Prostate cancer lesions are heterogeneous and of multifocal nature. Allelic losses on chromosomes 1, 3, 7q, 8p, 10q, 11, 13q, 16q, 17q, and 18q have been commonly reported. Despite their significance for prostate carcinogenesis, no single candidate tumour suppressor gene has been definitely assigned a role in cancer progression. Several candidate have been implicated, such as proteins RB, p53, PTEN, NKX3.1, KLF6 (Narla et al., 2001), and ETS transcription factors (ERG and ETV1) (Tomlins et al., 2005). However, none of these has been shown to be mutated in a large percentage of prostate cancer specimens and reports are conflicting. In addition, although chromosome gains appear to be less frequent than chromosome losses, gains at 3, 8q and 7 have been reported (Sattler et al., 1999; Alcaraz et al., 1994; Bandyk et al., 1994; Van Den Berg et al., 1995).

Section 2: Theories of cancer progression

For the last 50 years, the prevailing explanatory theory for cancer transformation has been the somatic mutation theory (SMT), which is a molecular-based theory, i.e. a reductionist theory according to which all complex cancer phenomena can be reduced to simple molecular events (Curtis HJ., 1965). The premise of the molecular-based theory (SMT) is that the default state of all cells is quiescence (G0 state). The somatic mutation or molecular-based theory of cancer defines cancer as a genetic disease of cell proliferation. Tumourigenesis is a long multistep process. Each step reflecting a genetic alteration that confers a growth advantage to the cell (each step defines a premalignant state). Only when

a cell has accumulated 4 to 6 genetic alterations (at the minimum) does it develop into an invasive cancer (for reviews see Renan, 1993; Tomlinson et al, 1996; Boland et al., 1999). Another less "in-vogue" and indeed very controversial theory (Blagosklonny, 2005) is the original tissue-organisation-field theory (TOFT), or tissue-based theory (Soto and Sonneschein, 2005). This theory was first suggested at the end of the 19th century by Boll, Conheim, and Ribbert, and was subsequently forgotten after the introduction of molecular biology tools. The premise of this tissue-based theory is that the default state of all cells is proliferation. The tissue-based theory of cancer defines cancer as a problem of tissue organisation and communication. Cancer probably arise from a combination of both molecular-based mutations and tissue-miscommunications.

In the following chapter, the molecular based theory will be discussed in details as most points described here will be referred to in the results and discussions chapter.

1. Genetic alterations

a. Oncogenes, tumour suppressor genes and stability genes

The genetic alterations encountered in a cancer cell occur within three categories of genes, oncogenes, tumour suppressor genes and stability genes. Oncogenes are genes that become constitutively active when they are mutated, or active under conditions in which the wild type gene is not. Oncogene activation can result from chromosomal translocations, gene amplifications, or subtle intragenic mutations affecting crucial residues (regulating the activity of the gene product). An activating somatic mutation in one allele of an oncogene is generally sufficient to confer a selective growth advantage to the cell bearing it. There are more than a hundred oncogenes identified, and they all show a dominant gain-of-function mutation. Tumour suppressor genes are genes that show a reduced activity when they are mutated. Tumour suppressor gene inactivation can result from missense mutations at crucial residues (regulating the activity of the gene product), mutations resulting in a truncated protein, deletions or insertions, or epigenetic silencing. Mutations in both the maternal and paternal alleles of a tumour suppressor gene are generally required to confer a selective advantage to the cell. There are more than 30 tumour suppressor genes identified, and they all show a recessive loss-of-function mutation. Stability genes are genes involved in DNA repair (MMR mismatch repair, NER nucleotide excision repair, and BER base excision repair), mitotic recombination, and chromosomal segregation. When they

are mutated, on both alleles, they become inactivated and mutations in other genes (oncogenes, tumour suppressor genes) occur at higher rates. Inactivation of stability genes therefore increase genetic instability, which is a trait found in many cancer cells.

b. The nine cancer gene pathways

Interestingly, most cancer-associated mutations are affecting a few limited number of cellular regulatory pathways, or cancer gene pathways. Within each cancer gene pathway the same exclusivity principle applies. Namely, one and only one gene is generally mutated per cancer pathway in any single tumour, as if mutating any of the genes of the pathway had similar functional effects and therefore gives no selective advantage (for a review see Vogelstein and Kinzler, 2004). Nine cancer gene pathways have thus been described (figure 2). The retinoblastoma protein (RB) and p53 tumour suppressor protein (P53) pathways are intertwined and regulate cell cycle progression/arrest. The apoptosis pathway controls programmed cell death. The receptor tyrosine kinase (RTK) and SMAD pathways are mitogenic signalling pathways, which transduce growth factors signals into transcriptional activation of genes mainly involved in cell growth/proliferation. The phosphoinositide 3 kinase (PI3K) pathway is the survival-promoting pathway. The glioma-associated oncogene (GLI) pathway induces cell cycle progression. GLI proteins, which are members of the Kruppel zinc finger family, are direct effectors of the sonic hedgehog signalling. The adenomatous polyposis coil (APC) pathway regulates the Wnt-regulated β-catenin degradation, which regulates signal transduction and cadherin mediated cell/cell adhesion (Miller et al., 1996). The APC pathway also regulates cytoskeletal proteins involved in cell migration, cell adhesion and mitosis (Nathke, 2004, and 2005). The hypoxia inducible factor-1 (HIF1) pathway is activated by oxygen deprivation to trigger an overexpression of glycolytic enzymes and angiogenic factors. Each of the cancer gene pathway described eventually leads to activation of the HIF1 pathway, which promotes angiogenesis, and therefore survival of the cancer cells. All solid tumours (95% of all tumours), among which prostate cancer, achieve angiogenesis.

These cancer gene signalling pathways have been thoroughly studied over the past decades as detailed in figure 3. Interestingly, the sonic hedgehog signalling pathway has recently been linked to prostate cancer abnormal expansion (Sanchez et al., PNAS, 2004).

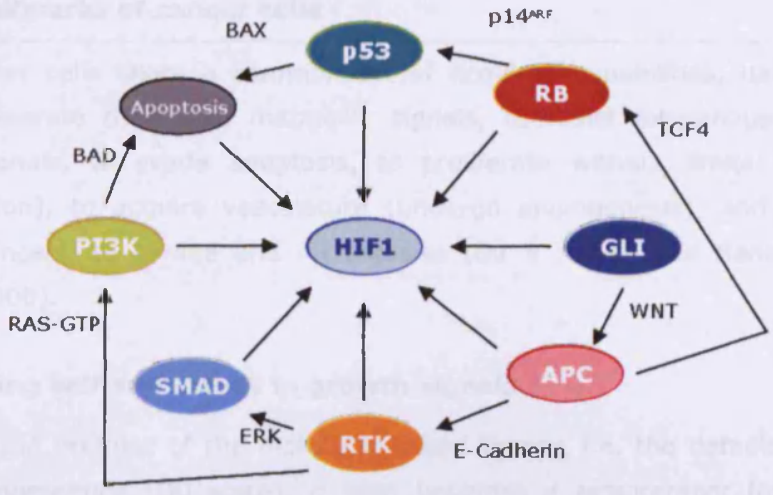

Figure 2: The nine cancer gene pathways (picture from Vogelstein and Kinzler, 2004). p53: p53 tumour suppressor gene. RB: retinoblastoma. GLI: glioma-associated oncogene. APC: adenomatous polyposis coli. RTK: receptor tyrosine kinase. PI3K: phosphatidyl-inositol-3 kinase. Apoptosis: programmed cell death, HIF1: hypoxia-inducible factor 1.

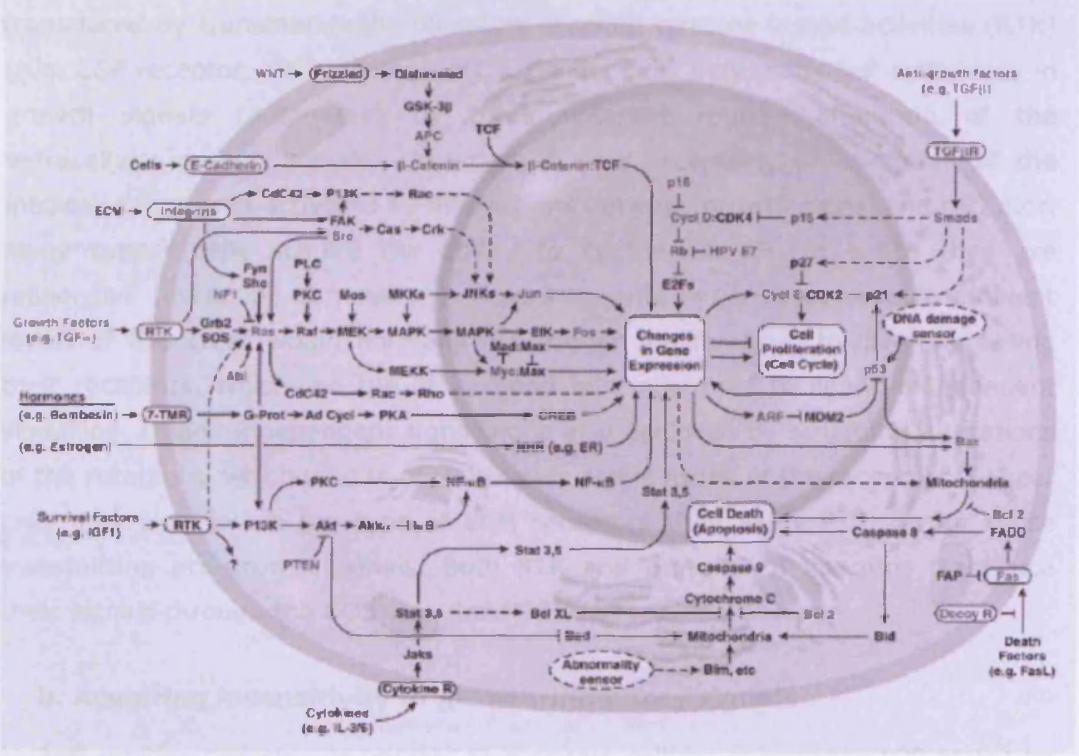

Figure 3: Integrated circuits of the cell (picture from Hanahan and Weinberg, 2000). In bold are the genes known to be functionally altered in cancer.

2. The hallmarks of cancer cells

Most cancer cells share a common set of acquired capabilities, namely the ability to generate their own mitogenic signals, to resist exogenous growth-inhibitory signals, to evade apoptosis, to proliferate without limits (undergo immortalisation), to acquire vasculature (undergo angiogenesis), and in more advanced cancers, to invade and metastasise (for a review see Hanahan and Weinberg, 2000).

a. Acquiring self sufficiency in growth signals

Following the premise of the molecular-based theory, i.e. the default state of all cells is quiescence (G0 state), it then becomes a requirement for normal epithelial cells to be able to respond to mitogenic growth signals in order to evolve to an active profilerative state (G1/S-G2/M phases of the cell cycle). Mitogenic signals, such as diffusible growth factors (GFs), extracellular matrix (ECM) components, and cell-to-cell adhesion/interaction molecules are transduced by transmembrane receptors carrying tyrosine kinase activities (RTK) (e.g. EGF receptor, MET receptor, etc.). Cancer cells may reach self-sufficiency in growth signals (autonomy) by three different routes: alteration of the extracellular growth signals, alteration of their receptors, or alteration of the intracellular circuits activated by interactions between growth signal and receptor. Many cancer cells acquire the ability to synthesise GFs to which they are responsive (autocrine stimulation). Others become hyper-responsive to ambient levels of GFs (that would normally not trigger proliferation) by overexpressing their receptors, which, on the other hand may also lead to ligand-independent signalling. Ligand-independent signalling is also achieved by structural alterations of the receptors, which lead to constitutively active forms of the receptors. Cancer cells may also switch the type of ECM receptors they express to favour those transmitting pro-growth signals. Both RTK and pro-growth integrins transduce their signals through the SOS-Ras-Raf-MAPK intracellular cascade.

b. Acquiring insensitivity to growth-inhibitory signals

Anti-proliferative signals operate to maintain cellular quiescence (G0 state) by blocking cell proliferation, either by preventing the transition of quiescent cells into the G1/S phase of the cell cycle, or by inducing cell differentiation, i.e. entering the postmitotic phase. Both these events are under the control of the retinoblastoma protein (RB), which was the first tumour suppressor identified. Protein RB is on the one hand, a negative regulator of the cell cycle that

Bcl-W) apoptotic proteins. The ultimate effectors of apoptosis include an array of intracellular proteases, the cysteine aspartyl-specific proteases or CASPASES, which cleave cellular substrates, leading to biochemical and morphological changes that are characteristic of apoptosis (Kumar, 2007). Besides these proteotypic caspase-dependent apoptosis pathways, there are also less well-defined cell death pathways that do not require CASPASES activation (Borner and Monney, 1999; Sperandio et al., 2000). Survival signals are conveyed by IGF1,2/IGFR-1 (Insulin Growth Factor-1 or -2/Insulin Growth Factor Receptor-1) and IL3/IL3R (Interleukin3/Interleukin3 Receptor), whereas death signals are conveyed by FAS/FASR (FAS Receptor) and TNFα/TNFR-1 (Tumour Necrosis Factor alpha/Tumour Necrosis Factor Receptor-1). Abrogation of adherence-based survival signals (cell/matrix and cell/cell interactions) elicits apoptosis. Cancer cells may therefore escape apoptosis by modifying their integrin repertoire that will also allow them to impair contact with the underlying basement membrane.

d. Acquiring unlimited proliferative potential (resistance to senescence)

The acquired disruptions of cell-to-cell signalling (independence to growth signals, insensitivity to anti-growth signals, and resistance to apoptosis) are not sufficient to ensure expansive tumour growth. Mammalian cells are indeed governed by yet another program, called senescence that limits their aberrant multiplication (for reviews see Hayflick, 1997 and 2003; Stewart and Weinberg, 2006). Cells that have reached their finite replicative potential enter senescence. Replicative generations are counted by the 50 to 100 base pair (bp) loss of telomeric DNA from the ends of each chromosome. The telomeres, protective ends of chromosomes, are composed of several thousand repeats of a short 6bp sequence element (TTAGGG). To ensure chromosomal stability, telomeres are protected from homologous recombinations and from the DNA repair machinerie by shelterin. Shelterin is a complex of six telomere-specific proteins (TRF1/2, TIN2, TPP1, POT1 and Rap1) that determine the structure of telomeres terminus (T-loops allowing distinction from sites of DNA damage) and control the synthesis of telomeric DNA by the telomerase enzyme (for a review see De Lange, 2005). The telomerase enzyme adds hexanucleotide repeats onto the ends of telomeric DNA to maintain a certain length. In normal cells, the telomerase enzyme is inactive and a progressive erosion of telomeres naturally occurs through successive cycles of replication, which is attributed to the inability of DNA polymerases to completely replicate the 3'ends of chromosomal DNA during each S phase. The loss of telomeres is translated into a loss of ability to protect

chromosomes from end-to-end fusions. Telomeres erosion below a certain length trigger the crisis state, which is characterised by a strong chromosomal instability (karyotypic disarray) inevitably resulting in cell death. Ongoing maintenance of telomeres is therefore a prerequisite for cell immortalisation (indefinite proliferation), which permits unlimited multiplication of descendant cells (replicative immortality), a hallmark of cancer. Cancer cells may avoid senescence by maintaining telomeres at a length above the critical threshold. Telomeres maintenance is mainly achieved by reactivating (upregulating the expression of) the telomerase enzyme. Telomere maintenance may also be achieved by a telomerase-independent mechanism, termed alternative lengthening of telomeres or ALT (Bryan et al., 1995; Henson et al., 2002).

e. Acquiring sustained angiogenesis (VEGF secretion)

Tumours cannot grow to a size greater than 2mm in diameter unless they succeed in acquiring access to the circulatory system. Indeed, oxygen and nutrients supplied by the vasculature are crucial for cell function and survival, obligating virtually all cells in a tissue to reside within 100μm of a capillary blood vessel. Initially, proliferating cancer cells lack angiogenic ability, therefore they cannot promote the growth of new blood vessels (neoangiogenesis). Tumour cells acquire access to the circulatory system by achieving the angiogenic switch from vascular quiescence, by secreting pro-angiogenic factors and by down-regulating the expression of anti-angiogenic factors (Bergers et al., 2003). Pro-angiogenic factors secreted by cancer cells are mainly vascular endothelial growth factors (VEGFs) and fibroblast growth factors (FGFs), while anti-angiogenic factors would be represented by thrombospondin-1 (TSP-1) and β-interferon (β-IFN). Angiogenic factors receptors, which are tyrosine kinase receptors, are displayed by endothelial cells. HIF1α, which plays a major role in the response of tumours to hypoxia, is mainly responsible for the angiogenic switch (Semenza, 2000; Diaz-Gonzalez et al., 2005). Integrin signalling also contributes to acquiring sustained angiogenesis. Quiescent vessels express one class of integrins, whereas sprouting capillaries express another (αVβ3, and β1-integrins, Sheppard, 2002). Thus, there are pro- and anti-angiogenic integrins, like there are pro- and anti-growth integrins, and pro- and anti-apoptotic integrins.

The process of new blood vessel formation (neo-angiogenesis) is thus essential for the growth and metastatic propagation of cancer and is therefore a feature of many cancers, including prostate cancer, where quantification of microvessel density correlates with disease stage and outcome (Weidner et al., 1993; Jackson

et al., 1997). In prostate cancer, gene expression of angiogenic factors, such as VEGF, correlates with the metastatic potential of prostate cancer cells (Aalinkeel et al., 2004).

3. Metastasis, and the invasive growth program

Cancer cells have thus to reach the circulation to eventually metastasise new sites (figure 4). Metastatic dissemination occurs when the cancer cells spread from the primary tumour site (figure 4.1), invade the surrounding tissue (figure 4.2), and reach the circulation for intravasation (figure 4.3). As a primary tumour grows, it needs to develop a blood supply that can support its metabolic needs. The new blood vessels can provide an escape route by which cancer cells leave the primary tumour site and enter the circulation. Cancer cells are also able to enter existing blood vessels and lymphatic vessels. The cells need to survive in the circulation (apoptosis-resistance, change of integrins repertoire) until they can extravasate at a new site (figure 4.4). Once in the new site, the cancer cells must initiate and maintain growth to form micrometastases (figure 4.4). This growth must be sustained by the development of new blood vessels in order for a macroscopic tumour to form (figure 4.5).

The first step in metastasis is the detachment of cancer cells from the primary tumour and the gain of motility, i.e. acquiring invasive capabilities. The invasive growth program is a complex biological program that instruct cells to dissociate, migrate, degrade the surrounding matrix, proliferate and survive (for reviews see Trusolino and Comoglio, 2002; Comoglio and Trusolino, 2002; Gentile and Comoglio, 2004). This program is an essential mechanism for embryonic development, tissue morphogenesis, and wound healing, that is aberrantly implemented for cancer dissemination and metastasis. The hepatocyte growth factor (or scatter factor) HGF, through its specific receptor MET, fully controls the coordinated regulation of the invasive growth program. Other cytokines and growth factors can be responsible for parts of the program. For example, HGF can down-regulate the transcription of E-cadherins, as shown in the prostate cancer cell line derived from a brain metastasis DU145 (Miura et al., 2001), or stimulate their proteolytic cleavage by matrix metalloproteinases (MMP), as shown in the prostate cancer cell line derived from a lymph node metastasis LNCaP (Davies et al., 2001), which triggers the destabilisation of the adherens junctions maintaining the normal attachment of epithelial cells within a tissue (scattering). Intercellular adhesions are held by cadherins, which are connected to the cytoskeleton by catenins. Additionally, HGF can disrupt the structural integrity of

adherens junctions by increasing β-catenins phosphorylation (Davies et al., 1999). In all cases, HGF weakens carcinoma cells aggregation and facilitates their dissociation and scattering.

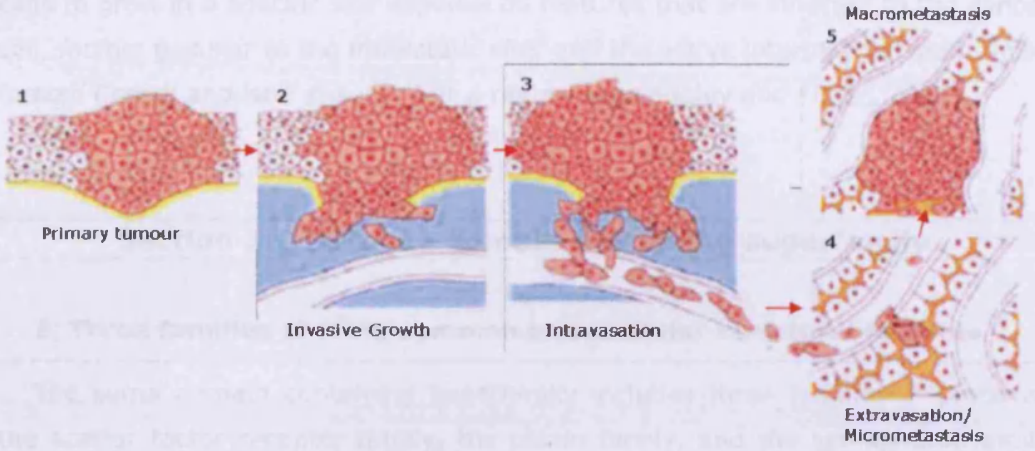

Figure 4: Stages of tumour metastasis (picture from Mol et al., 2007). 1. Stage of primary tumour (cancer cells are highlighted in red). 2. Invasive growth: cancer cells detach from the primary tumour and start to invade the surrounding tissue. 2. Intravasation: migratory cancer cells reach the nearest blood vessel and intravasate into the blood stream. 4. Extravasation: travelling cancer cells escape the vessel and start to invade secondary tissues and micrometastasis of single cells develops. 5. Macrometastasis: a secondary tumour develops from the micrometastasis.

Stromal invasion by cancer cells is another crucial step for metastasis. Cancer cells that have spread from the primary tumour site have to start to recognise ECM molecules that are present in the stromal compartment through which they invade. HGF can also strongly influence apoptosis resistance and adaptation to a new environment, both by up regulating the transcription of certain integrins and by stimulating their aggregation at actin-rich adhesive sites, without modifying the number of integrin molecules at the membrane (Trusolino et al., 1998 and 2000). Such positive regulation of integrin synthesis allows survival of cancer cells and migration within stroma. HGF can also enhance the expression of a large number of matrix metalloproteinases (MMPs) and stimulate the conversion of their precursors into active enzymes (Rosenthal et al., 1998; Monvoisin et al., 2002; Park et al., 2003). At the leading edge of migrating cells, MMPs interact with integrins to localise and concentrate the extracellular matrix digestion (Brooks et al., 1996; Hofmann et al., 2000). Additionally, some MMPs can selectively cleave ECM ligands to reveal cryptic domains that display chemotactic properties and facilitate cell migration (Giannelli et al., 1997). Matrix metalloproteinases can also have a significant effect on the ability of cancer cells to grow in a secondary site (for a review see Chambers and Matrisian, 1997).

Overexpression of MMPs has been reported in prostate cancer (Aalinkeel et al., 2004; Morgia et al., 2005).

Metastases can show an organ-specific pattern of spread. For example, breast and prostate tumours preferentially metastasise to the bone. The ability of cancer cells to grow in a specific site depends on features that are inherent to the cancer cell, factors peculiar to the metastatic site, and the active interplay between these factors ('seed' and 'soil' theory) (for a review see Langley and Fidler, 2007).

Section 3: The sema domain containing superfamily

1. Three families sharing common extracellular structural features

The sema domain containing superfamily includes three families of proteins, the scatter factor receptor family, the plexin family, and the semaphorin family (figure 5). All three protein families share similar extracellular structural features, namely a sema domain, one or more copies of a small cystin-rich domain (CRD) located immediately C-terminal of the sema domain, and at least one immunoglobulin-like domain (Ig-like domain). Those three extracellular domains have been involved in protein/protein or protein/ligand interactions.

a. The sema domain

The sema domain was first described by Kolodkin and colleagues in 1993 (Kolodkin et al., 1993). It is a conserved extracellular stretch of approximately 500 amino acids (aa), whose three-dimensional crystal structure is a variant of the seven blade β-propeller fold (figure 6) (Antipenko et al., 2003; Love et al., 2003; Gherardi et al., 2003; Stamos et al., 2004). The β-propeller is a very widely used protein fold topology that consists of multiple (4 to 8, typically 7) four-stranded, twisted β sheets, formed sequentially and packed face to face around a central axis. The sema domain is the largest known variant of the β-propeller fold with 500aa. Most seven blade β-propellers contain approximately 400aa, 438aa in the larger propeller of αV-integrin. The extra sequence found in the sema domain produces several long loops and a long insertion (shown in red on figure 6) (Gherardi et al., 2004). Throughout evolution, the β-propeller fold has been extensively adapted to protein/ligand binding and catalysis.

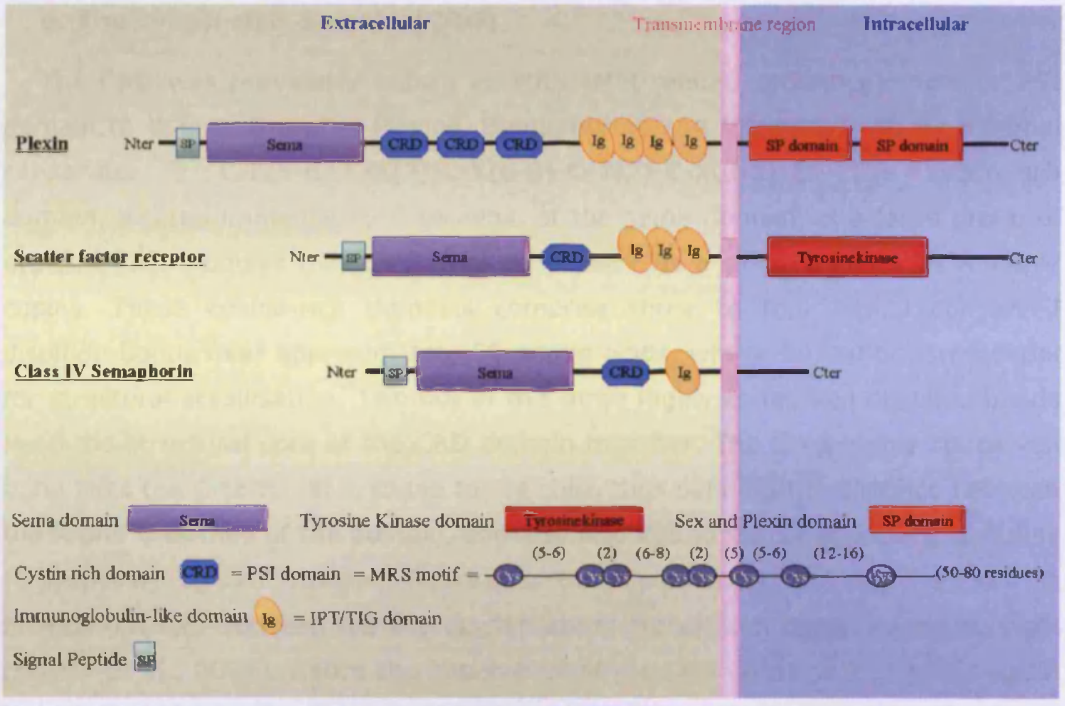

Figure 5: The sema domain containing superfamily contains three members: semaphorins, plexins, and scatter factor receptors. They are characterized by the presence of amino-terminal special features, such as the sema domain (a stretch of 500 amino acids approximately), cystin-rich regions (CRD), and immunoglobulin-like motifs (Ig).

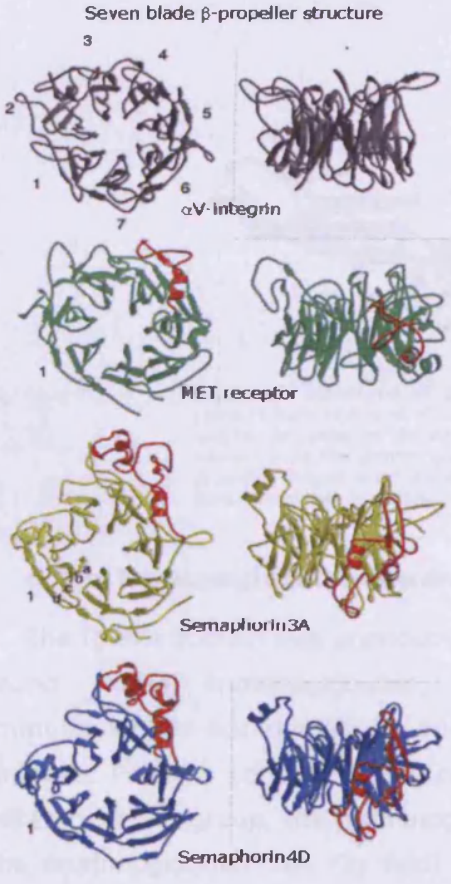

Figure 6: Structure of the sema domain (picture from Gherardi et al., 2004). Ribbon diagrams of the seven-blade β-propellers of αV-integrin (in grey) (PDB code 1l5g), MET receptor (in green) (PDB code 1shy), Semaphorin3A protein (in yellow) (PDB code 1q47), and Semaphorin4D protein (in blue) (PDB code 1olz). The left panels show views of the domains along the pseudo-sevenfold axes. Right panels show the same domains tilted by 908 degrees around the horizontal axis to show the top and bottom faces of the domains. The insertion/extrusion typical of the sema domains of Semaphorins 3A, 4D and MET is shown in red

b. The cystin-rich domain (CRD)

The CRD was previously known as MRS (Met-related sequence) motif or PSI domain (a domain found in Plexins, Semaphorins and Integrins), whose minimal consensus is C-X(5-6)-C-X(2)-C-X(6-8)-C-X(2)-C-X(3-5)-C. The cystin-rich domain, located immediately C-terminal of the sema domain, is a large group of cysteine rich modules that can either be present as a single copy or as multiple copies. These cosine-rich domains comprise three to four highly conserved disulfide bonds over approximately 50 amino acids, whose formation is essential for structural stabilisation. Two out of the three highly conserved disulfide bonds keep the structural core of the CRD domain together. The third highly conserved bond links the C-terminal cysteine to the core, thus defining the distance between the N and C termini of the domain, and also orientating the neighbouring domains (β-propeller, Ig-like domain, figure 7). In semaphorins, the CRD domain is providing a link between the β-propeller ligand recognition domain and the stalk (Kozlov et al., 2004). Hence the importance of the CRD domains for the biological function of the sema domain. Mutations in these regions modulate the sema domain biological activity (Behar et al., 1999).

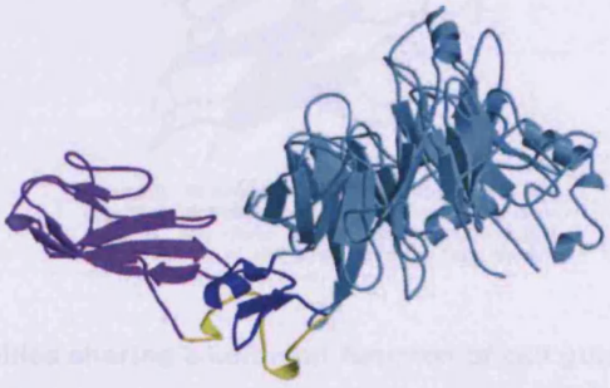

Figure 7: Structure of the CRD domain of Semaphorin4D (picture from Kozlov et al., 2004). The CRD domain (in blue) likely orients the adjacent domains for proper ligand binding The CRD domain links the Immunoglobulin-like domain (in purple) with the propeller-shaped sema domain (in cyan). Variable part of the CRD domain is shown in yellow.

c. The immunoglobulin-like domain (Ig-like domain)

The Ig-like domain was previously known as IPT repeat or TIG domain (repeats found within immunoglobulins, plexins and transcription factors). The immunoglobulin-like domain is one of the most widespread domains among animals. Proteins containing one or more Ig-like domains are part of a wider heterogeneous group, the immunoglobulin superfamily, built on a common fold, the immunoglobulin fold (Ig fold), whose structural characteristic is this of a

Greek-key β-barrel or a sandwich of two β-sheets (Figure 8) (for a review see Halaby and Mornon, 1998). The superfamily can be divided into discrete structural sets by the number and length of the β-strands. The two major types of Ig-like domains are the constant C type (subtypes C1 to C4, Fn3, and H) and the variable V type, containing an extra loop (for reviews see Bork et al., 1994; Halaby et al., 1999). The I type is an intermediate between the C1 and V types (Gerstein and Altman, 1995). Proteins containing domains of the C1 and V sets are mostly molecules of the vertebrate immune system, whereas those from the I set are mainly cell surface-adhesion proteins, as well as intracellular muscle proteins. The Ig-like domain of MET is of the E type, which is found earlier in bacterial enzymes, as well as in transcription factors of the NF-κB/REL/dorsal family. Preliminary analyses (unpublished data) suggest that the Ig-like domain of class 3 semaphorins is of the I type (Gherardi et al., 2003). Proteins with Ig-like domains are mostly involved in cell adhesion and pattern recognition.

Figure 8: Structure of the immunoglobulin-like (Ig-like) domain (from the protein data bank website: http://www.rcsb.org/pdb/home/home.do). Ig-like domain of the muscle protein Titin, module m5 (PDB code 1ncu), I set.

d. Three families sharing a common function of cell guidance

Because of their structural homology, scatter factor receptors, plexins and semaphorins share a common role in mediating cell guidance cues (Artigiani et al., 1999). Semaphorins belongs to the larger family of neuronal guidance factors, also comprising the ephrins, netrins and slits families (for a review see Dickson, 2002). Indeed, the formation of a functional neuronal network requires proper targeting of axons, which is accomplished by sensing a variety of extracellular cues (guidance factors) in the local environment. Neuronal growth cones, located at the tip of the growing axons, are highly motile structures that respond to guidance cues by selectively altering the stability of the actin cytoskeleton and microtubules. Guidance receptors transduce their signal through activation of Rho guanosine triphosphatases or Rho GTPases in order to mediate

axonal retraction or attraction (for reviews see Huber et al., 2003). Plexins, as semaphorin receptors, mediate axon and cell guidance. Stimulation of plexin receptors by their ligands, semaphorins, also leads to a cascade of small cytoplasmic GTPases activation, including p190-Rho-GAP and PDZ-Rho-GEF, resulting in the reorganisation of cytoskeletal structures and therefore neurons and cell migration or motility. Scatter factor HGF also activates Rho GTPases, such as Rac1, RhoA, and cdc42, to induce scattering, as shown in the prostate cancer cell line derived from a brain metastasis DU145 (Wells et al., 2005) and in other cell types (Royal et al., 2000; Miao et al., 2003). HGF triggers a variety of cellular responses ranging from cell scattering (motility) and proliferation to branching morphogenesis, invasive growth, and angiogenesis, through the specific receptor MET, which is a tyrosine-kinase receptor (for reviews see Vande Woude et al., 1997, Zhang and Vande Woude, 2003, Gao and Vande Woude, 2005, Furge et al, 2000, Tamagnone and Comoglio, 1997, Comoglio et al., 1999, Comoglio and Boccaccio, 2001). Additionally, those signalling pathways are able to interplay, as when plexin receptors interact with scatter factor receptors to induce invasive growth (Giordano et al., 2002, Conrotto et al., 2004). For example, scatter factor receptor MET interacts with all three class B plexins, but not A or D plexins. PlexinB1 and MET interaction is ligand-independent, but activation of PlexinB1 upon ligand binding then stimulates the tyrosine kinase activity of MET, which enhances invasive growth (Giordano et al., 2002).

In the following section, focus will mainly be brought on the prototypes for each family (scatter factor receptors; plexins; and semaphorins); looking at their structures, signalling pathways, biological effects in vitro and in vivo, at physiological and pathological levels.

2. The scatter factor receptor family

a. General features

The proto-oncogenes c-Met, Ron and c-Sea are the three members of the scatter factor receptor family (figure 9). These proto-oncogenes respectively encode the single-pass cell membrane glycoproteins MET, RON and SEA, which are receptors for scatter factors (SFs) also called Plasminogen-Related Growth Factors (PRGFs) (for a review see Comoglio et al., 1999). Scatter factor 1 (SF1), or PRGF-1, is the hepatocyte growth factor HGF that specifically binds the scatter factor receptor MET. Scatter factor 2 (SF2), or PRGF-2, is the macrophage stimulating protein MSP that specifically binds the scatter factor receptor RON.

HGF and MET are the prototypes of the scatter factor and scatter factor receptor families.

Met homologues are found in vertebrates, including mice, rats, chicks, frogs and puffer fish, but none were found in invertebrates (neither in *Drosophila melanogaster* nor in *Caenorhabditis elegans)*. HGF and MET expression starts during embryogenesis predominantly in developing epithelial organs (lung, pancreas, kidney, intestine, and salivary gland), and transiently in skeletal muscle and neuronal cells. Particularly, MET receptor is expressed at the surface of epithelial cells while HGF is secreted by mesenchymal cells in close vicinity (Sonnenberg et al., 1993). This specific distribution between HGF and its receptor indicates a paracrine mode of action.

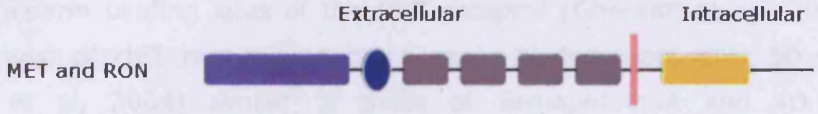

Figure 9: Domain architecture of the scatter factor receptor family members (picture from Gherardi et al., 2004). The N-terminal sema domain is in purple, followed by one CRD repeat (cystin-rich domains) in blue, and four immunoglobulin-like domains in grey. The C-terminal moiety is intracellular and contains a tyrosine kinase domain (in orange). The cellular membrane is in pink.

b. Structure of scatter factor HGF

The human gene encoding HGF spans approximately 70kDa on chromosome 7q11.1-21 and consists of 18 exons (Saccone et al., 1992; Seki et al., 1991). HGF is a large molecule (approximately 100kDa) that shares structural homology (approximately 40%) with plasminogen, an enzyme of the blood coagulation cascade, and has a similar mechanism of activation (Donate et al., 1994). HGF is secreted as a single chain precursor (pro-HGF) that is activated in the extracellular environment by specific proteases (e.g. uPA and tPA) releasing two subunits (α and β), joined by disulfide bonds. The α chain (heavy) of HGF has a molecular mass around 60kDa and contains four typical Kringle domains, which are cysteine-rich double-looped structures presenting protein/protein interaction properties, a receptor binding site, short sequence folded in a hairpin loop and located at the N-terminal extremity, and a heparin binding site. The β chain (light) of HGF weighs approximately 30kDa and is closely related to the catalytic domain of serine proteases. However, HGF has lost the catalytic serine protease activity during evolution, when the serine residue that forms the catalytic triad necessary for the catalytic activity of serine proteases was substituted with a tyrosine (Lokker et al., 1992). Although HGF is a soluble molecule normally found in serum, it also naturally accumulates, bound to sulphated glycosaminoglycans

(GAGs) such as heparan-sulphate, in the extracellular matrix and in basement membranes (Kobayashi et al., 1994).

c. Structure of scatter factor receptor MET

The human Met gene spans more than 120kb on chromosome 7q21-q31 and consists of 21 exons (Liu, 1998). The primary Met transcript produces a 150kDa polypeptide that is partially glycosylated into a 170kDa-precursor protein. After further glycosylation, MET precursor is cleaved by furin protease into a 50kDa extracellular α-chain and a 140kDa transmembrane β-chain, linked via disulfide bonds (Komada et al., 1993). The α-chain of MET receptor is extracellular, heavily glycosylated and spans approximately 310 residues. The α-chain and the first 212 extracellular residues of the β-chain represent the ligand binding (sema domain) and the heparin binding sites of the MET receptor (Gherardi et al., 2003). The sema domain of MET receptor adopts a seven-bladed β-propeller 3D structure (Stamos et al, 2004) similar to those of Semaphorin3A and 4D proteins (Antipenko et al., 2003 and Love et al., 2003). The sema domain of MET receptor is a ligand binding domain, which also plays a critical role in ligand dependent and independent receptor dimerisation and activation (autophosphorylation and transducers phosphorylation) (Kong-Beltran, 2004). The intracellular part of the β-chain of MET receptor tyrosine kinase comprises a tyrosine kinase domain, whose crystal structure has been published (Schiering et al., 2003, Bolanos-Garcia, 2005), a tyrosine autophosphorylation site and a multifunctional docking site, whose consensus sequence is Y^{1349}VHVNATY^{1356}VNV (Ponzetto et al., 1994). The multisubstrate-docking site is responsible for much of MET receptor signal transduction (Komada and Kitamura, 1993; Zhu et al., 1994).

d. HGF/MET signalling pathways

Upon ligand binding, MET receptor undergoes dimerisation and autophosphorylation of two specific tyrosine residues, Y^{1234} and Y^{1235} located within the activation loop of the tyrosine kinase domain (figure 10). This autophosphorylation activates the intrinsic kinase activity of MET receptor leading to transphosphorylation of the two tyrosine residues Y^{1349} and Y^{1356} located within the multisubstrate docking site, thus allowing binding and phosphorylation of adapter proteins and signal transducers that contain Src homology 2 and 3 domains (SH2 and SH3), phosphotyrosine binding domains (PTB) and MET binding domains (MBD). Mutational analysis shows that Y^{1349} and Y^{1356} mediate the interaction with Shc, Src and Gab1, while Y^{1356} alone mediates recruitment of

Grb2, PI3K, PLC-γ, SHP2 (for reviews see Furge et al., 2000; Bolanos-Garcia, 2005).

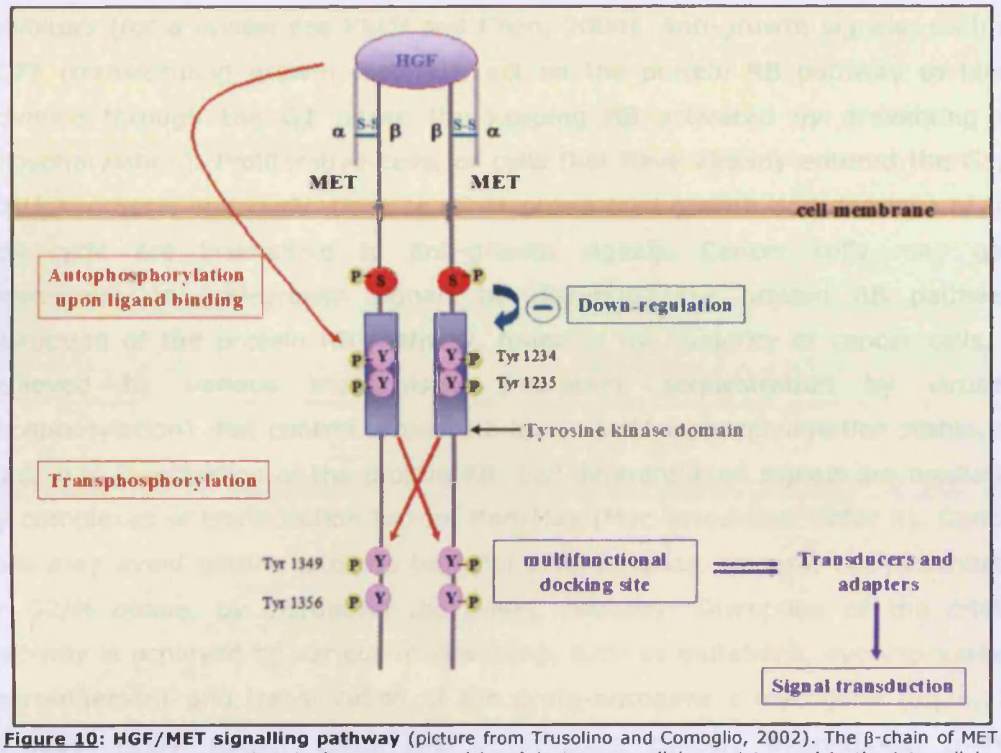

Figure 10: HGF/MET signalling pathway (picture from Trusolino and Comoglio, 2002). The β-chain of MET receptor contains a sema domain (not represented here) in its extracellular moiety, and in the intracellular moiety a tyrosine kinase domain, a tyrosine autophosphorylation site and a multifunctional docking site, which consensus sequence is Y1349VNVXXXY1356VHV. When bound to its specific ligand HGF, MET receptor undergoes dimerisation and autophosphorylation of two specific tyrosines of the tyrosine kinase domain. Once activated by phosphorylation, the tyrosine kinase domain of each monomer phosphorylates the two tyrosines of the multifunctional docking site of each other monomer (transphosphorylation). The activated docking site subsequently binds several transducers and/or adapters

e. HGF/MET biological effects

HGF/MET signalling induces mitogenic (growth/proliferation, protection against apoptosis), motogenic (dissociation/scattering, motility/migration, acquisition of polarity, ECM invasion) and morphogenic (branching morphogenesis, tubule formation) responses *in vitro*, and during embryonal development (figure 11). *In vivo*, HGF/MET signalling plays a role in growth, wound healing, tissue regeneration, invasion and tumour metastasis, and finally angiogenesis (for a review see Maulik et al., 2002).

HGF is the only growth factor able to elicit the full complex genetic programs of branching morphogenesis and invasive growth (for a review see Zhang and Vande Woude, 2003). The morphogenetic branching program is a differentiation program in which groups of cells proliferate, migrate and differentiate to form a connected series of tubules arranged like the branches of a tree. Such paracrine

represses the expression of genes essential for cell growth/proliferation (for reviews see Giacinti and Giordano, 2006; Macaluso et al., 2006), and on the other hand, a positive regulator of cell differentiation that counteracts differentiation inhibitors (for a review see Khidr and Chen, 2006). Anti-growth signals, such as TGFβ (transforming growth factor-β), act on the protein RB pathway to block advance through the G1 phase (by keeping RB activated by preventing its phosphorylation). Proliferative cells, or cells that have already entered the G1/S (DNA synthesis and replication) or G2/M phase (cell growth and division) of the cell cycle are insensitive to anti-growth signals. Cancer cells may gain insensitivity to anti-growth signals by disrupting the protein RB pathway. Disruption of the protein RB pathway, found in the majority of cancer cells, is achieved by various mechanisms (mutation, sequestration by viruses, phosphorylation) that control protein RB levels and/or phosphorylation status, all leading to inactivation of the protein RB. Cell differentiation signals are mediated by complexes of transcription factors Mad/Max (Myc associated factor X). Cancer cells may avoid getting into the terminal differentiation process, i.e. postmitotic or G2/M phase, by disrupting the c-MYC pathway. Disruption of the c-MYC pathway is achieved by various mechanisms, such as mutations, overexpression, rearrangement and translocation of the proto-oncogene c-myc gene (8q24.12-q24.13). Many cancer cells, like in prostate cancer, overexpress c-MYC oncoprotein (Jenkins et al., 1997), which impairs cell differentiation by shifting the balance of transcription factors back to Myc/Max complexes, thus promoting cell growth. Integrins and other cell adhesion molecules also send anti-growth signals to the cells. However, it is very likely that these adherence-based anti-growth signals impinge on the protein RB circuit.

c. Acquiring resistance to programmed cell death (apoptosis)

Cells have an intrinsic mechanism of self destruction called programmed cell death or apoptosis. Normally, an excessive proliferation/growth at inappropriate sites induces apoptosis in the affected cells. The ability of cancer cells to expand in number is therefore determined not only by the rate of proliferation but also by their ability to acquire resistance to apoptosis. The apoptotic program is a multistep program that leads to cellular membrane disruption, cytosol extrusion, chromosome fragmentation, and degradation of the nucleus. Many of the signals that elicit apoptosis converge on the mitochondria (for a review see Gogvadze and Orrenius, 2006), which respond by releasing cytochrome C (Cyt-C), and other pro-apoptotic proteins. This release is controlled by members of the Bcl-2 family, which includes both pro- (Bax, Bak, Bid, Bim) and anti- (Bcl-2, Bcl-XL,

signalling between epithelial cells and mesenchymal cells is vital to embryogenesis and contributes to kidney and mammary gland formation, migration and development of muscle and neuronal precursors, and liver and placenta development (Bladt et al., 1995; Schmidt et al., 1995; Niemann et al., 1998). The invasive growth program (as mentioned in the previous section, 3. Metastasis) is a complex biological program that instruct cells to dissociate, migrate, degrade the surrounding matrix, proliferate and survive (for reviews see Trusolino and Comoglio, 2002; Comoglio and Trusolino, 2002; Gentile and Comoglio, 2004). The invasive growth program is an essential mechanism for embryonic development, tissue morphogenesis, and wound healing.

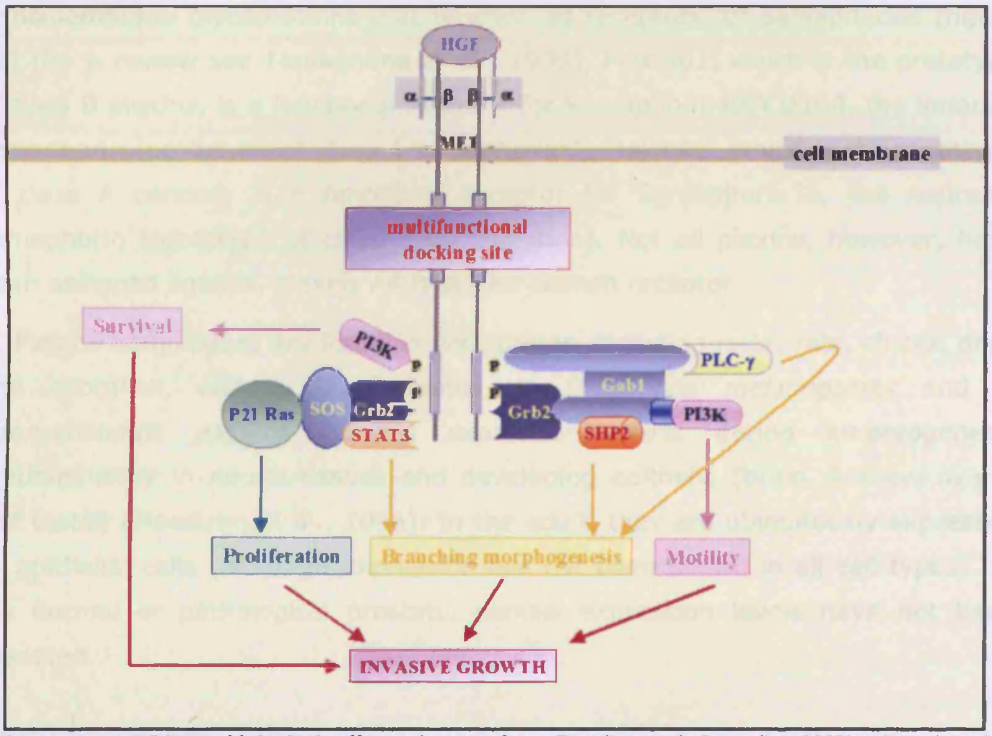

Figure 11: HGF/MET biological effects (picture from Trusolino and Comoglio, 2002). Upon ligand stimulation, MET receptor acts via a two-phosphotyrosine docking site to activate multiple intracellular transducers and signalling pathways. Phosphatidylinositol 3 kinase (PI3K)-dependent signals result in promotion of cell motility and survival. The superactivation of the Grb2-SOS-Ras cascade leads to uncontrolled proliferation and oncogenic transformation. Sustained recruitment of the phospholipase C-γ (PLC-γ) and the protein tyrosine phosphatase SHP2, as well as the integrity of the signal transducers and activators of transcription (STAT) pathway, are required for MET receptor's morphogenetic activity

In normal prostate, HGF is secreted by stromal cells while epithelial cells express the receptor MET (Humphrey et al., 1995). Scatter factor receptor MET has been reported to be overexpressed in PIN, carcinoma and metastasis (Pisters et al., 1995). However, attempts to link HGF/MET signalling pathway to the metastatic abilities of prostate tumour cells have not yet been successful *in vivo*. Nevertheless, inhibition of HGF/MET signalling pathway reduces *in vitro* invasion

and migration of two prostate cancer cell lines derived from a brain (DU145) and bone (PC3) metastases (Davies et al., 2004).

3. The plexin family

a. General features

The plexin family is a homogenous family of at least nine members, which have been subdivided into four classes on the basis of sequence similarity, namely class A plexins (A1 to A4), class B plexins (B1 to B3), PlexinC1 and PlexinD1 (see nomenclature table below). Plexin genes encode single transmembrane glycoproteins that function as receptors for semaphorins (figure 12) (for a review see Tamagnone et al., 1999). PlexinB1, which is the prototype of class B plexins, is a functional receptor for Semaphorin4D/CD100, the immune semaphorin (prototype of class 4 semaphorins). PlexinA1, which is the prototype of class A plexins, is a functional receptor for Semaphorin3A, the neuronal semaphorin (prototype of class 3 semaphorins). Not all plexins, however, have been assigned ligands, plexins A4 is still an orphan receptor.

Plexins homologues are found in vertebrates, including mice, rats, chicks, dogs and zebrafish, and in invertebrates, in *Drosophila melanogaster* and in *Caenorhabditis elegans*. Plexins expression starts during embryogenesis predominantly in neural tissues and developing epithelia (brain, kidney, ovary, and testis) (Maestrini et al., 1996). In the adult, they are ubiquitously expressed by epithelial cells (although expression has not been shown in all cell types). In the normal or pathological prostate, plexins expression levels have not been assessed.

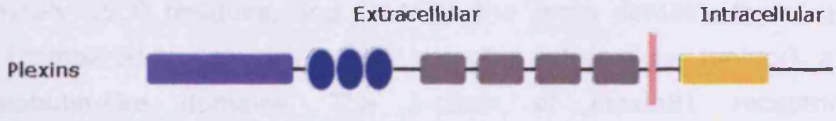

Figure 12: Domain architecture of the plexin family members (picture from Gherardi et al., 2004) The N-terminal sema domain is in purple, followed by three CRD repeats (cystin-rich domains) in blue, and four immunoglobulin-like domains in grey. The C-terminal moiety is intracellular and contains two highly conserved sex and plexin (SP) domains (in orange) that lack a catalytic activity (represented here in one domain). The cellular membrane is in pink.

b. Plexin nomenclature

Plexin nomenclature is summarised in table 2.

Accepted denomination	Other known denomination				chromosomal location (in humans)
In-/Vertebrates	**Human**			**Clones**	
PlexinA1	Plexin a1 PLEXIN A1	PLEXIN 1 PLXN1	NOV		3q21-qter
PlexinA2	Plexin a2 PLEXIN A2	PLEXIN 2 PLXN2	OCT		Chr 1
PlexinA3	Plexin a3 PLEXIN A3	PLEXIN 4 PLXN4	SEX		Xq28
PlexinA4	Plexin a4 PLEXIN A4				Chr 7
PlexinB1	Plexin b1 PLEXIN B1	PLEXIN 5 PLXN5	SEP	KIAA0407	3p21.31
PlexinB2	Plexin b2 PLEXIN B2			MM1 KIAA0315	22q13.31-q13.33
PlexinB3	Plexin b3 PLEXIN B3	PLEXIN 6 PLXN6			Xq28
PlexinD1	Plexin d1 PLEXIN D1				Chr 3
Viral		**Vaccinia Virus (VV)**			
PlexinC1	Plexin c1 PLEXIN C1 VESPR	A39R			Chr12

Table 2: Plexin nomenclature and chromosomal location in humans.

c. Structure of PlexinB1 receptor

Class B plexins (at least, PlexinB1 and B2) are the closest homologues to scatter factor receptors, i.e. MET, the prototype of the scatter factor receptor family. PlexinB1 is the prototype of class B plexins. The human plexin b1 gene spans approximately 26kb on chromosome 3p21.31 and consists of 32 exons. The primary plexin b1 transcript produces a 300kDa polypeptide that is partially glycosylated. PlexinB1 precursor, like MET precursor, is cleaved by furin protease into a 200kDa extracellular α-chain and a 100kDa transmembrane β-chain (Artigiani et al., 2003). The α-chain of PlexinB1 receptor is extracellular, spans approximately 1500 residues, and contains the sema domain, three cystin-rich domains (compared to only one in MET receptor extracellular moiety), and three immunoglobulin-like domains. The β-chain of PlexinB1 receptor spans approximately 620aa, with a transmembrane domain of approximately 18aa. The cytoplasmic moiety of the β-chain of PlexinB1 exhibits two well-conserved domains among plexin receptors. Those two domains were formerly known as SP domains (Sex and Plexin domains), as they were first identified in the SEX proteins family, now the plexin family (see nomenclature table). Those two SP domains, now known as C1 and C2 domains (Castellani and Rougon, 2002), were first defined as two homologous regions of approximately 320 and 150 amino acids, separated by a divergent insert of approximately 70 residues, showing no

kinase activity (Maestrini et al., 1996). The C1 and C2 domains share sequence similarity with the GAP domain of the Ras family-specific GTPase activating proteins, especially R-Ras-GAP (Rohm et al., 2000a). However, in plexins intracellular region, this GAP homology domain is divided into two by an unrelated linker region, which shows a CRIB (Cdc42/Rac-Interactive Binding)-like motif. The CRIB-like motif is a small GTPase binding motif, therefore mainly binding the small GTPases Cdc42 and Rac, but also binding other small GTPases, such as Rho and Rnd1 (Kruger et al., 2005; Oinuma et al., 2004a).

d. PlexinB1/Semaphorin4D signalling pathway

Stimulation of PlexinB1 by its ligand Semaphorin4D regulates the activity of small cytoplasmic GTPases, such as R-Ras, Rac and Rho (figure 13). The cytoplasmic domain of plexins has two highly conserved domains denoted C1 and C2, which have weak homology to Ras-GAPs (GTPase activating proteins). The C1 and C2 domains of PlexinB1 interact to form an inactive conformation (figure 13a). Rnd1 binds to the linker region between these domains and disrupts this inactive conformation (figure 13b). R-Ras can then bind to regions of both domains of PlexinB1 (Oinuma et al., 2003 and 2004b). The binding of R-RasGTP is dependent on Rnd1 binding and disruption of the closed conformation. In the absence of receptor clustering by Semaphorin4D, binding of R-RasGTP to PlexinB1 suppresses the basal GTPase activity of R-Ras and traps it in its active form (figure 13c). The R-Ras-GAP activity of PlexinB1 is activated upon receptor clustering resulting in inactivation of R-Ras (figure 13d) (Oinuma et al., 2004a). PlexinB1 also binds RacGTP and sequesters it from its downstream signalling partners such as PAK (Vikis et al., 2002). PlexinB1 controls the activation state of Rho via PDZ-Rho-GEF and LARG which bind to the C-terminal end of PlexinB1 (Swiercz et al., 2002), and by activating p190-Rho-GAP (Barberis et al., 2005).

Stimulation of PlexinB1 by its ligand Semaphorin4D also activates tyrosine kinase cascades through interaction with receptor tyrosine kinases MET (Giordano et al., 2002; Conrotto et al., 2004) and ErbB2 (Swiercz et al., 2004). PlexinB1 interacts with these receptors via its extracellular domain (figure 14). Activation of PlexinB1 results in activation of the tyrosine kinase activity of both MET and ErbB2, resulting in the phosphorylation of PlexinB1 and MET or ErbB2. PlexinB1 also promotes the activation of tyrosine kinase cascades in endothelial cells via PYK2 and Src (Basile et al., 2005), resulting in phosphorylation of PlexinB1 and the p85 regulatory subunit of phosphoinositide 3 kinase (PI3K).

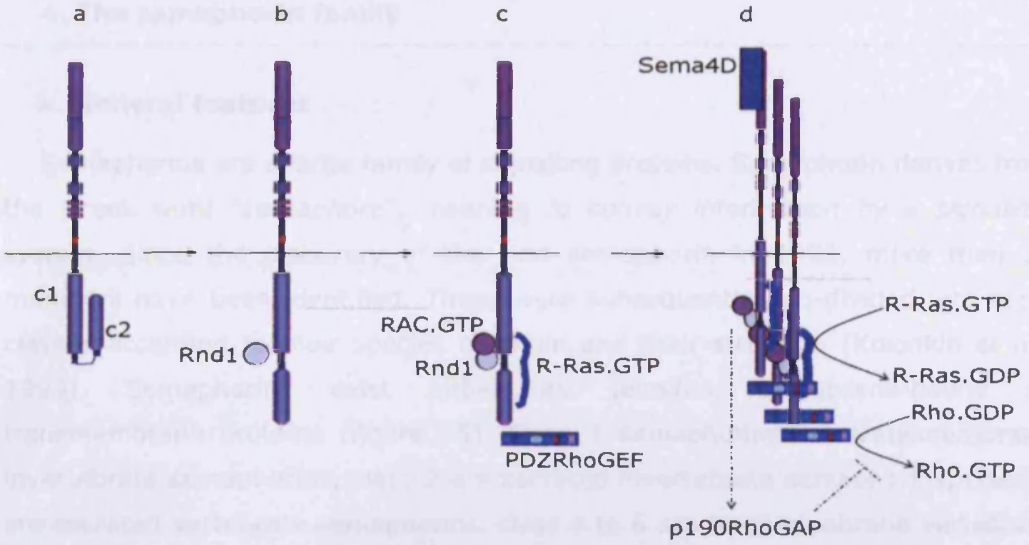

Figure 13: PlexinB1/Semaphorin4D signalling pathway via small GTPases (picture from M. Williamson). **a.** In the absence of ligand binding or receptor clustering the C1 and C2 domains of the cytoplasmic domains of PlexinB1 interact to form a closed inactive conformation. **b.** The closed secondary structure is disrupted upon Rnd1 binding. **c.** This allows the binding of R-RasGTP to regions in the C1 and C2 domains. RacGTP also binds to a region between the C1 and C2 domains and PDZ-Rho-GEF binds to the C-terminal end of the cytoplasmic domain (the dependence of RacGTP or PDZ-Rho-GEF on Rnd1 binding has not been shown). At this stage the basal GTPase activity of R-Ras is inhibited by PlexinB1 binding and so R-Ras remains in its active state. **d.** Upon receptor clustering as a result of ligand binding or overexpression, the R-RasGAP activity of PlexinB1 is activated resulting in the conversion of R-RasGTP to R-RasGDP. PDZ-Rho-GEF is also activated resulting in RhoA activation and MAPK pathway activation. p190-Rho-GAP is also activated, which inactivates RhoA.

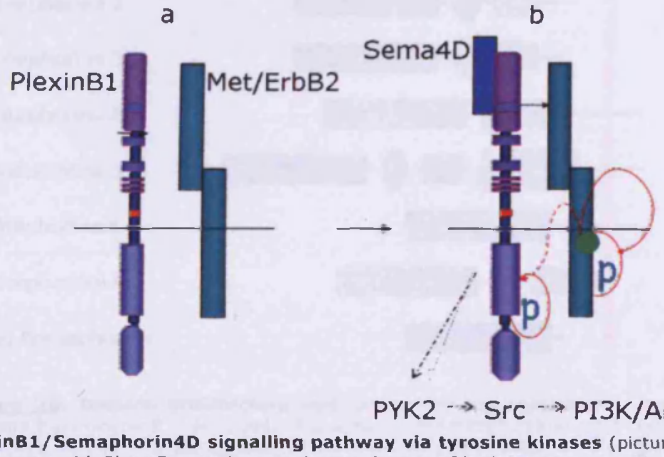

Figure 14: PlexinB1/Semaphorin4D signalling pathway via tyrosine kinases (picture from M. Williamson). **a.** Met and ErbB2 interact with PlexinB1 via the cytoplasmic domain of both receptors. **b.** Upon receptor clustering as a result of ligand binding (Semaphorin4D) or overexpression, Met/ErbB2 is activated, resulting in activation of the tyrosine kinase activity of c-Met/ErbB2 and tyrosine phosphorylation of both Met/ErbB2 and PlexinB1. PI3K is also activated via PYK2 and Src upon PlexinB1 activation.

e. PlexinB1/Semaphorin4D biological effects

Activation of plexins, either by ligand binding or overexpression, regulates the activity of small cytoplasmic GTPases and tyrosine kinases, resulting in the reorganisation of cytoskeletal structures and subsequent cell adhesion, migration, and motility, and invasive growth (for a review see Kumanogoh and Kikutani, 2004).

4. The semaphorin family

a. General features

Semaphorins are a large family of signalling proteins. Semaphorin derives from the Greek word "*semaphore*", meaning *to convey information by a signalling system*. Since the discovery of the first semaphorin in 1992, more than 30 members have been identified. These were subsequently sub-divided into eight classes according to their species of origin and their structure (Kolodkin et al., 1993). Semaphorins exist either as secreted, membrane-bound or transmembrane proteins (figure 15). Class 1 semaphorins are transmembrane invertebrate semaphorins, class 2 are secreted invertebrate semaphorins, class 3 are secreted vertebrate semaphorins, class 4 to 6 are transmembrane vertebrate semaphorins, class 7 are membrane-bound vertebrate semaphorins, and class 8 are secreted viral semaphorins.

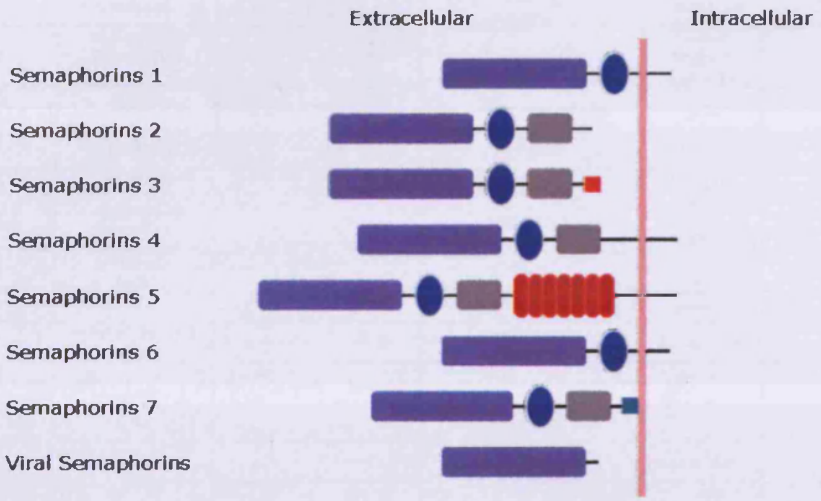

Figure 15: Domain architecture and classes of the semaphorin family members (picture from Gherardi et al., 2004). Semaphorins are classified into eight classes, namely the animal (1–7) and viral semaphorins. The viral semaphorin shown in the figure only contains the sema domain, and corresponds to the product of reading frames present in vaccinia and variola viruses. Other viral semaphorins, such as that of the fowlpox virus (UniProt accession code Q9J5F6), contain the CRD repeat (cystin-rich domain). The Sema domain is in purple, the CRD repeat in blue, the Ig-like domain in grey, the thrombospondin repeats in dark red, the basic motif in bright ref, the GPI anchor in green, and the cellular membrane in pink.

Semaphorins homologues are found in vertebrates, including mice, rats, chicks, dogs and zebrafish, and in invertebrates, such as *Grasshopper, Drosophila Melanogaster* and *Caenorhabditis Elegans*. Semaphorins expression starts during embryogenesis, predominantly in neural and vascular tissues. In the normal or pathological prostate, expression profiles of semaphorins have not been assessed.

Accepted denomination	Other known denomination				Human Chromosomal Location
Invertebrates	**Grasshopper (SAM)**	***Drosophila Melanogaster(DME)***	***Caenorhabdbitis. Elegans (CEL)***		
Sema-1a	G-Sema I	D-Sema I	Ce-Sema I Ce-Sema-1a Smp-1	T-Sema I Fasciculin IV	2L (29E2-29E3)
Sema-1b		D-Sema III	Ce-Sema-1b Smp-2	Sema III	2R (54D4-54D5)
Sema-2a	G-Sema II	D-Sema II	Ce-Sema II	Sema II	2R (53C6-53C7)
Vertebrates	**Human (H-, HSA)**	**Chick (C-, GGA)**	**Mouse (M-, MMU)**	**Rat (RNO, R-) Zebrafish (Z)** ...	
SEMA3A	Sema 3 H-Sema I SEMA III SEMA1 SEMAL SEMAD	C-Collapsin-1 Collapsin-1 Coll-1 COLL-1	M-SemD	R-Sema III Sema-Z1a	7p12.1
SEMA3B	H-Sema V H-Sema A SEMAA		M-SemA	Sema5 ? LUCA-1 ?	3p21.3
SEMA3C	H-Sema E SEMAE	COLL-3 C-Coll-3	M-SemE		7q21-q31
SEMA3D		COLL-2 C-Coll-2		Sema-Z2	7q21.11
SEMA3E	SEMAH	COLL-5 C-Coll-5	M-Sema H M-Sema K	KIAA0331	7q21.11
SEMA3F	H-Sema IV Sema III/F H-Sema3F		M-Sema IV	SemaK Sema4 Sema IV	3p21.3
SEMA3G	Sem2				3p21.1
SEMA4A	SEMAB		M-SemB		1q22
SEMA4B	SEMAC		M-SemC	KIAA1745	15q25
SEMA4C	SEMAI SEMAF		M-Sema F	Sema f Semac11 KIAA1739	2q11.2
SEMA4D	SEMAJ CD100	COLL-4 C-Coll-4	M-Sema G		9q22-q31
SEMA4E				Sema-Z7	?
SEMA4F	SEMAM SEMAW H-Sema W		m-Sema M M-Sema W	R-Sema W	2p13.1
SEMA4G				KIAA1619	10q24.32
SEMA5A	SEMAF		M-SemF		5p15.2
SEMA5B	SEMAG		M-SemG M-SemB	KIAA1445	3q21.1
SEMA5C				D-Sema5C	?
SEMA6A	SEMAQ		M-Sema VIa	KIAA1368	5q23.1
SEMA6B	SEMAZ SEMAN		M-Sema VIb	R-Sema Z	19p13.3
SEMA6C	SEMAY		M-Sema Y	R-Sema Y	1q21.2
SEMA6D				KIAA1479	15q21.1
SEMA7A	SEMAL H-Sema L H-Sema K1 CD108		M-Sema L M-Sema K1	CDw108	15q22.3-q23
Viral	**Vaccinia Virus (VV)**				
SEMAVA	Vaccinia sema A39R	Variola sema			
SEMAVB	AHVsema				

Table 3: Semaphorin nomenclature and chromosomal location in humans (according to the Semaphorin Nomenclature Committee).

b. Semaphorin nomenclature

Semaphorin nomenclature is complex and confusing. Table 3 gives a summary of the current denomination of semaphorins in various species, as well as their chromosomic location when known.

c. Class 3 of secreted semaphorins and Semaphorin3E

There are 7 members in the human class 3 semaphorin family of secreted proteins, namely Semaphorin3A to 3G. They contain an average of about 750 amino-acids and weigh approximately 85 KDa. They exhibit an N-terminal sema domain, an immunoglobulin-like domain, and a C-terminal basic domain (figure 16). Although secreted semaphorins are diffusible signals, they are probably tethered to the cell surface and extracellular matrix by the basic charged sequence of their C-terminal moiety, which exhibits binding properties. The amino-terminal extremity of class 3 semaphorins is involved in the receptor specificity and biological activity of semaphorins (Feiner et al., 1997; Koppel et al., 1997). Semaphorin3A is the prototype of this family of secreted proteins.

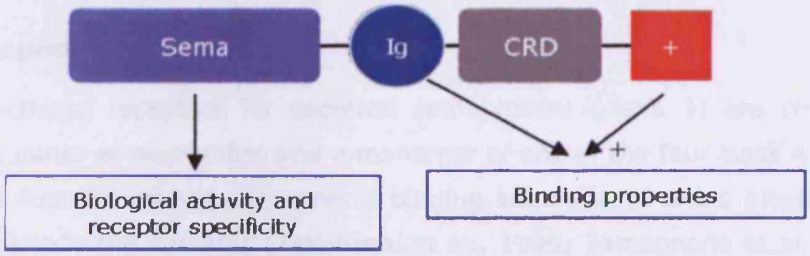

Figure 16: Secreted semaphorins structure and function. Secreted semaphorins (class 3) contain an N-terminal extremity, a sema domain (Sema, in purple), a CRD domain (in grey), an immunoglobulin-like domain (Ig, in blue), and a basic (+) C-terminal extremity (in red). The Sema domain confers biological activity and receptor specificity, while the C-terminal extremity confers binding properties to secreted semaphorins.

Class 3 semaphorins exist in monomeric, dimeric and processed forms. Indeed, class 3 semaphorins (3A, 3B, 3C, and 3E) are known to dimerise and undergo proteolytic processing by furin and furin-like convertase (Adams et al., 1997; Klosterman et al., 1998; Koppel et al., 1998). The furin-dependent proteolytic processing of Semaphorin3A, 3B and 3C has been shown to determine their repulsive potency (Adams et al., 1997), and this of Semaphorin3E converts its repelling signal into an inducer of invasive growth (Christensen et al., 2005). The semaphorin 3e gene spans more than 285kb on chromosome 7q21.11 and consists of 17 exons. Its mRNA is 6474bp long and encodes a protein of 775aa. The KIAA0331 clone of semaphorin 3e gene encodes a protein of 814 aa and

weigh approximately 90KDa. Semaphorin3E protein is also known as SemaH, or Collapsin-5 in chicks, and m-Sema-H or m-Sema-K in mice.

d. Class 4 of transmembrane semaphorins and Semaphorin4D

Class 4 semaphorins are transmembrane proteins exhibiting an N-terminal sema domain, an immunoglobulin-like domain, and a single-pass domain. There are 7 members in the human class 4 semaphorin family, namely Semaphorin4A to 4G. Semaphorin4D, also known as CD100, is the prototype of this yet uncharacterised family. Semaphorin4D/CD100 protein is known as the immune semaphorin because of its role in controlling immune and inflammatory responses (for reviews see Kumanogoh and Kikutani, 2003; Takegahara et al., 2005). Semaphorin4D can be found either as a membrane bound or as a soluble protein, suggesting that it might also function as a receptor to induce a bi-directional signalling (Tamagnone et al., 1999). The semaphorin 4d gene spans more than 102kb on chromosome 9q22-q31 and consists of 14 exons. Its mRNA is 4675bp long and encodes a protein of 862aa. The transmembrane form of Semaphorin4D weighs approximately 150kDa, while the soluble version weighs 120kDa.

e. Semaphorin receptors

The functional receptors for secreted semaphorins (class 3) are complexes including a dimer of neuropilins and a monomer of one of the four class A plexins. Neuropilins function as the semaphorin binding subunits, whereas plexins serve as signal transducing subunits (Takahashi et al., 1999; Tamagnone et al., 1999). Neuropilins are considered essential co-receptors for secreted semaphorins, as these would not directly bind plexins (Kolodkin et al, 1997; Chen et al., 1998). The growth repelling activities of class 3 semaphorins are associated with the neuropilin-binding capacity of their full-length, dimeric forms (Miao et al., 1999; Kessler et al., 2004; Bielenberg et al., 2004). For example, the active receptor for Semaphorin3A is a complex made of a dimer of Neuropilin1 and a monomer of PlexinA1 (Takahashi et al., 1999). Semaphorin3A binds Neuropilin1 but not Neuropilin2 (Chen et al., 1997; He and Tessier-Lavigne, 1997; Kolodkin et al., 1997), whereas Semaphorin3B, 3C and 3F bind to both neuropilins (1 and 2) (Takahashi et al., 1998). Semaphorin3C binds to PlexinA2 and PlexinD1 (Kolodkin et al., 1997; Gitler et al., 2004). Although, it had previously been shown that the chick Semaphorin3E was able to bind Neuropilin1 (Feiner et al., 1997), a more recent study has shown that Semaphorin3E directly binds to PlexinD1 (class D plexin), independently of neuropilins (Gu et al., 2005).

Semaphorins	Receptors
Sema-1a	Plexin A
Sema-1b	Plexin A
Sema-2a	?
SEMA3A	NP1 & PlexinA1 or PlexinA2 or PlexinA3
SEMA3B	NP1-NP2 & VEGFR2
SEMA3C	NP1- NP2 & Plexin A1 or PlexinA2 or PlexinD1 or PlexinB1
SEMA3D	NP1
SEMA3E	NP1? PlexinD1
SEMA3F	NP1- NP2 & PlexinA1 or PlexinA3
SEMA4A	Tim-2
SEMA4B	?
SEMA4C	PlexinB2
SEMA4D	PlexinB1
SEMA4E	?
SEMA4F	?
SEMA5A	PlexinB3
SEMA5B	?
SEMA5C	?
SEMA6A	Plexin?
SEMA6B	?
SEMA6C	?
SEMA6D	Plexin A1 & VEGFR-2 & OTK
SEMA7A	PlexinC1
SEMAVA	PlexinC1
SEMAVB	PlexinC1

Table 4: Semaphorins and receptors, plexins and neuropilins. NP (1/2): Neuropilin1/2. VEGFR-2: vascular endothelial growth factor receptor-2. OTK: off track receptor.

In contrast, membrane-associated semaphorins (class 4 to 7 semaphorins) bind directly to plexin receptors, and do not interact with neuropilins. Their functional receptor is a monomere of plexin. For example, PlexinB1 is the functional receptor for Semaphorin4D in non-lymphoid tissues (Giordano et al., 2002), Semaphorin6D binds to PlexinA1 (Toyofuku et al., 2004), and Semaphorin7A to PlexinC1 (Tamagnone et al., 1999). A soluble version of Semaphorin4D has been found in various cellular types. This soluble Semaphorin4D protein acts through PlexinC1 on human monocytes and through PlexinB1 on immature dendritic cells (Chabbert-de Ponnat et al., 2005). The functional receptor for Semaphorin4D in lymphoid tissues is CD72 (Kumanogoh et al., 2000).

f. Neuropilins structure and functions

At least eight members have been characterised in the neuropilin family. Neuropilins are single spanning transmembrane proteins. Their extracellular moiety contains two N-terminal domains similar to complement binding domains called CUB domains, two coagulation factor V/VIII homology domains, and a MAM (Meprin/A5/Mu-phosphatase) domain (figure 17). The intracellular moiety of neuropilins is a short cytoplasmic tail of about 40 amino acids that contains a PDZ domain-binding motif.

Neuropilins are widely expressed in all phyla, except in flies. Particularly, they are expressed at the surface of neuronal cells, endothelial cells of capillaries and blood vessels, and in mesenchymal cells surrounding blood vessels.

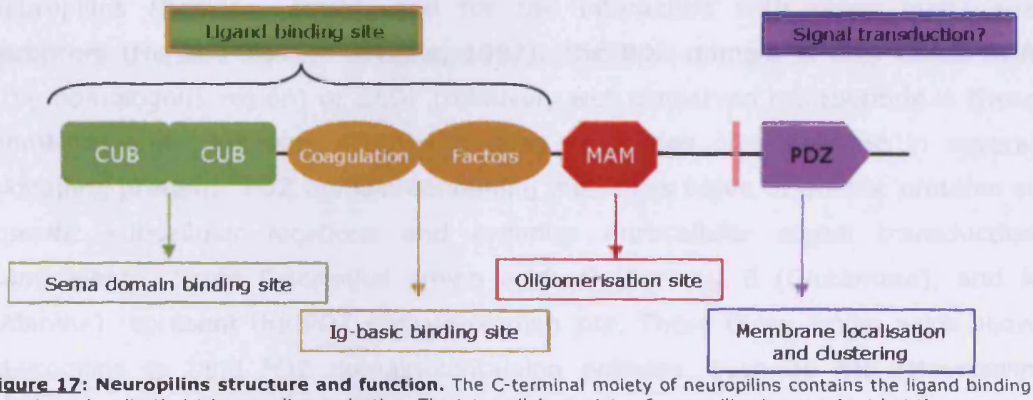

Figure 17: Neuropilins structure and function. The C-terminal moiety of neuropilins contains the ligand binding domain and a site that triggers oligomerisation. The intracellular moiety of neuropilins is very short but the presence of a PDZ domain may confer neuropilins a role in signal transduction. CUB: complement binding domain, MAM: meprin/A5/Mu-phosphatase domain, Ig: immunoglobulin.

Neuropilin 1 and 2 genes span respectively 120kb on chromosome 10p12 and 112 kb on chromosome 2q34 (Rossignol et al., 1999). Neuropilin 1 consists of 17 exons and weighs approximately 140KDa, whereas neuropilin 2 contains 18 exons or 17 exons if alternatively spliced (Rossignol et al., 2000). Despite similar domain structures, the overall homology between these two neuropilins is only 44%. In fact, both neuropilins are expressed in several tissue-specific splice forms that differ by their C-terminal moiety. At least three isoforms of Neuropilin1 (Np1, s12Np1, and s11Np1) and five isoforms of Neuropilin2 (Np2a(17), Np2a(22), Np2b(0), Np2b(5), and s9Np2) are generated by alternative splicing. The alternative splicing occurs in the linker regions, which are located between the coagulation factor-homology and MAM domains as well as between the MAM and transmembrane domains. Some neuropilin isoforms are soluble. They correspond to truncated N-terminal neuropilin regions, lacking the transmembrane and cytoplasmic domains. The soluble neuropilin isoforms may

play a role of natural inhibitors (Rossignol et al., 2000). In fact, transmembrane neuropilins and soluble neuropilins perform opposite functions, the first acting as receptors and the latter as receptor antagonists (Gagnon et al., 2000).

The CUB domain, of approximately 110 residues, contains four conserved cysteines that form two disulfide bridges. The structure of the CUB domain has been predicted to be a β-barrel similar to that of immunoglobulins. The CUB and coagulation factor homology domains represent the ligand-binding site. CUB binds to the sema domain and the coagulation factor homology domain binds to the immunoglobulin-like domain and the basic C-terminal tail of secreted semaphorins. The MAM domain, of approximately 170 amino acids, also contains four cysteines that probably form disulfide bridges. This domain is thought to have an adhesive function, and is involved in the oligomerisation process of neuropilins (Roskies, 1998), and for the interaction with other membrane receptors (He and Tessier-Lavigne, 1997). The PDZ domain is also called DHR (Dlg homologous region) or GLGF (relatively well conserved tetrapeptide in these domains) and possesses different binding properties and is found in several signalling proteins. PDZ domain-containing molecules serve to anchor proteins at specific subcellular locations and organise intracellular signal transduction components. Three C-terminal amino acids S (Serine), E (Glutamate), and A (Alanine) represent the PDZ domain-binding site. These three amino acids allow neuropilins to bind PDZ domain-containing proteins, such as NIP (Neuropilin Interacting Protein). NIP protein might participate in the regulation of neuropilin signalling as a molecular adapter that couples neuropilins to membrane trafficking machinery, as is the case in dynamic axon growth cones (Kornau et al., 1997). Soluble neuropilins, missing the last three SEA-COOH amino acids, might not interact with NIP but with other adapters. Also, NIP protein could act positively to link neuropilins to signalling molecules or to the cytoskeleton in order to permit clustering, and/or it could act as an inhibitory protein to mask critical regions of neuropilins that interact with other signalling molecules or receptors. Therefore, PDZ domain-binding sites are responsible for neuropilins localisation and clustering, and eventually signal transduction (Cai and Reed, 1999).

Neuropilins are functionally active when they form either homodimers or heterodimers. They are co-receptors for class 3 semaphorins and for selected isoforms of the angiogenic vascular endothelial growth factor, those containing a heparin-binding domain ($VEGF_{165, 145}$) (Serini et al., 2003; Torres-Vasquez, 2004; Soker et al., 1998). Neuropilins form complexes with plexins, VEGFs receptors and with adhesion molecules such as L1-CAM (Castellani et al., 2000).

Consequently, neuropilins are involved in many biological processes, such as axonal guidance (via semaphorin interactions), angiogenesis (via VEGF interactions), cell adhesion (via the coagulation factor domains and L1-CAM interactions), tumourigenesis and tumour progression (for a review see Guttmann-Raviv et al., 2006).

g. Semaphorins functions

Semaphorins are chemotactic guidance cues playing crucial roles orchestrating cellular movement. Semaphorins were first identified in the nervous system for their role in neuronal cell migration and axon guidance. Since their first identification in the early 90s' in the developing nervous system, semaphorins have been reported to be expressed in many other tissues and organs, including the immune and vascular systems, where they play major roles (for reviews see Bismuth and Boumsell, 2002; Moretti et al., 2006; Eichmann et al., 2005).

Class 3 of secreted semaphorins are known to act on nerves as repulsive or attractive cues. For example, Semaphorin3A, which is essential for the correct wiring of the peripheral nervous system (PNS), functions as an axonal repellent for motoneurons, sympathetic ganglion neurons, and a subset of sensory neurons. Semaphorin3B and 3C repel sympathetic ganglion neurons, but not DRG (dorsal root ganglion) neurons, unlike Semaphorin3A (Takahashi et al., 1998). Additionally, Semaphorin3C attracts cortical axons (Pascual et al., 2005; Bagnard et al., 2000). Semaphorin3E inhibits growing retinal axons (Steinbach et al., 2002) while it stimulates neurite outgrowth of PC12 cells, to the same extent as NGF (Sakai et al., 1999). A Semaphorin3E mutation (S703L) has been found in a patient with CHARGE syndrome, which is characterised by nerve dysfunction, cardiac defects, and growth retardation (Lalani et al., 2004).

Class 3 of secreted semaphorins are known to act on endothelial cells as repulsive or attractive cues. For example, Semaphorin3A inhibits endothelial cell adhesion and migration through integrin inhibition, thus controlling vascular morphogenesis (Serini et al., 2003). Semaphorin3F is also an inhibitor of angiogenesis inhibiting $VEGF_{165}$- and bFGF-induced angiogenesis (Kessler et al., 2004). Semaphorin3C, which is required for normal cardiovascular patterning, stimulates endothelial cell proliferation and survival and enhances their adhesion by increasing integrin activity, to the same extent as VEGF-A. Semaphorin3C also induces endothelial cell directional migration by stimulating integrin phosphorylation, and tube formation by stimulating $VEGF_{120}$ secretion via neuropilin/plexin signalling, like VEGF-A, and contrary to Semaphorin3A (Banu et

al., 2006). Interestingly, Semaphorin3A and $VEGF_{165}$ compete for Neuropilin1 binding (Bachelder et al., 2003). Semaphorin3E, through its specific PlexinD1 receptor, restricts vessel growth and branching to intersomitic regions, thus controlling endothelial cells positioning and the patterning of developing vasculature during embryogenesis (Gu et al., 2005). PlexinD1 is a receptor for secreted Semaphorin3C and 3E that is expressed by endothelial cells and is critical for vascular development (Gitler et al., 2004; Torres-Vasquez, 2004).

Some semaphorins play major roles in the immune system, such as transmembrane Semaphorin4D protein (CD100), Semaphorin7A, and secreted Semaphorin3A, by regulating humoral and cellular immune responses, as well as the inflammatory response (Shi et al., 2000; Czopik et al., 2006; Suzuki et al., 2007; Lepelletier et al., 2006). The soluble version of the transmembrane Semaphorin4D protein inhibits immune cell migration (Delaire et al., 2001).

Recently, semaphorins have been implicated in tumourigenesis, tumour cell migration, invasive growth, and angiogenesis (Neufeld et al., 2005; Pan et al., 2007; Serini et al., 2003; for reviews see Hinck, 2004; Chedotal et al., 2005 and 2007; Suchting et al., 2006). Semaphorin3B and 3F are tumour suppressors, whose genes are located on chromosome 3p21.3, which is frequently lost (LOH) in prostate cancer (Dahiya et al., 1997). Semaphorin3F is also a potent metastasis inhibitor that is markedly down regulated in highly metastatic melanoma tumour cells (Kessler et al., 2004; Bielenberg et al., 2004). Particularly, Semaphorin3F inhibits the formation of metastases in the lymph node and lung. Semaphorin3C is overexpressed in ovarian tumour cell lines with invasive and metastatic behaviour (Yamada et al., 1997; Christensen et al., 1998; Neufeld et al., 2005). Semaphorin3E expression positively correlates with the metastatic ability of breast cancer cells, and its paracrine stimulation promotes metastasis growth in the lung (Christensen et al., 1998 and 2005). Semaphorin3E, when truncated at its C-terminal moiety by furin(-like) convertase, mediates tumour-endothelial cells interaction, stimulating lung endothelial cells migration via Erk1/2 activation and thus contributing to a local angiogenic response, which contributes to metastasis to the lung (Christensen et al., 2005). Semaphorin4D is also able to control invasive growth and tumour angiogenesis, because of the association of its receptor PlexinB1 with the MET receptor, which when stimulated by its ligand HGF controls invasive growth, and because Semaphorin4D stimulates endothelial cell migration (Giordano et al., 2002; Conrotto et al., 2004; Basile et al., 2006).

AIMS and OBJECTIVES

Semaphorins control the migration of nerve, immune, and endothelial cells, and are increasingly implicated in tumour cell migration and invasion. The aims of this thesis were therefore to investigate whether semaphorins also play a role in normal and/or tumour cell migration in prostate and whether semaphorin signalling is involved in the development of diseases of the prostate (BPH, PCa, metastasis) by influencing cellular movement.

Because the expression of semaphorins and their receptors, plexins and neuropilins, had not been assessed in normal or diseased prostate before, we first needed to establish whether semaphorins and their receptors were synthesised by prostate cells. To study their expression profiles, 10 prostate cell lines were grown to approximately 80% confluence, and total RNA was extracted at three consecutive passages for each cell line. The presence of semaphorins, plexins, and neuropilins genes was detected by RT-PCRs using specific primers.

After establishing that normal and diseased prostate cell lines express semaphorins and receptors, we needed to understand what could regulate their expression in diseased prostate. We hypothesised that semaphorin expression is switched on in cancer in response to hypoxia. Expression of semaphorins in response to regions of hypoxia in a tumour may activate plexin receptors on endothelial cells promoting their migration and enhancing angiogenesis. Regions of hypoxia are frequent in cancers and HIF1α, a transcription factor whose degradation is inhibited as a response to hypoxia, is overexpressed in prostate primary tumours and regional and distant lymph node and bone metastases, compared to normal prostate tissue (Du et al., 2003; Hao et al., 2004). HIF1α is mainly responsible for the angiogenic switch (Semenza, 2000; Diaz-Gonzalez et al., 2005) thus promoting an increase in VEGF expression and angiogenesis, the formation of new blood vessels bringing oxygen and nutrients that are essential for the survival of the cancer cells and for the growth and metastatic propagation of cancer. In prostate cancer, the quantification of microvessel density and the gene expression of angiogenic factors (such as VEGF) have been correlated with the metastatic potential of prostate cancer cells (Weidner et al., 1993; Jackson et al., 1997; Aalinkeel et al., 2004).

The regulation of semaphorins expression by oxygen deprivation had not been investigated before. In order to investigate the expression profiles of semaphorins following hypoxic conditions, normal and primary tumour prostate cell lines as

well as one colon carcinoma cell line were cultured in hypoxic incubators. After 24h and 48h, total RNA was extracted and RT-PCRs were performed using specific primers for secreted semaphorins.

The expression of the semaphorin 3e gene, one of the least studied secreted semaphorins at the time (2001), had been positively correlated with the metastatic ability of breast cancer cells (Christensen et al., 1998). Four years later, the same group confirmed their results and showed that semaphorin 3e paracrine stimulation promoted metastasis growth in the lung (Christensen et al., 2005). Moreover, RT-PCR experiments from results chapter 1 of this thesis showed that semaphorin 3e expression was ubiquitous in all the prostate cell lines tested, with variation in expression according to the cell type. To quantify semaphorin 3e expression in normal and diseased prostate, real-time RT-PCR experiments using specific primers and probes were performed. To understand the role of Semaphorin3E in normal and diseased prostate, the protein had to be produced in vitro, as it is not commercially available (unlike Semaphorin3A). To produce Semaphorin3E protein, its complete cDNA sequence was amplified by PCR using primers with specific sites for 2 restriction enzymes, and ligated into a mammalian expression vector. The recombinant vector containing the transgene was subsequently used to transform Cos-7 cells. After 72h, the medium was collected, concentrated, and the amount of secreted Semaphorin3E protein was measured. The secreted Semaphorin3E protein was thus available for further experiments.

Prior to investigating the roles of Semaphorin3E on cell migration in prostate cells which are not easily transfectable, preliminary experiments about its role at large were performed in easily transfectable cellular systems (Cos, NIH and HEK cells). Results published by other groups showed that Semaphorin3A and 3F inhibited β1-integrin-mediated adhesion of endothelial cell and tumour cell on fibronectin respectively, while Semaphorin3C stimulated endothelial cell adhesion by increasing β1-integrin activity, suggesting a role for secreted semaphorins in regulating integrin-mediated cell adhesion (Serini et al., 2003; Bielenberg et al., 2004; Banu et al., 2006). Cell adhesion is a phenotype involved in cell migration and metastasis and the role of Semaphorin3E in cell adhesion had not previously been determined. To determine if Semaphorin3E protein has an affect on cell adhesion, adhesion assays were performed in the presence of Semaphorin3E. In addition the effect of Semaphorin3E protein on β1-integrin activity and focal adhesion formation was determined using immunocytochemistry. It is only with the publication of Semaphorin3E functional receptor, PlexinD1 (Gu et al., 2005),

that it was possible to elucidate the role of Semaphorin3E with these preliminary experiments. Further experiments using prostate cells are needed to investigate the role of Semaphorin3E specifically in the prostate and prostate cancer.

In parallel, Dr. Williamson (my supervisor) discovered that the plexin b1 gene is mutated in prostate cancer and metastasis (Wong et al., 2007). In an attempt to understand the biological effects of these mutations on cell movement, migration assay experiments were performed, in presence or absence of ligand, Semaphorin4D.

The aims of the thesis were therefore to:

1. Determine if semaphorins and their receptors are expressed in prostate cell lines and tissue.
2. Determine if expression of semaphorins is regulated by hypoxia in normal and cancer prostate cell lines.
3. Determine the effect of Semaphorin3E protein on cell adhesion and β1-integrin activity.
4. Determine the effect of mutations found in the plexin b1 gene in prostate cancer on cell motility.

CHAPTER 2: MATERIALS AND METHODS

LIST OF MANUFACTURERS CONTACT DETAILS

Applied Biosystems: http://www3.appliedbiosystems.com/AB_Home/index.htm, 850 Lincoln Centre Drive, Foster City, CA 94404, USA.

ATCC: http://www.lgcpromochem-atcc.com/, LGC Standards, Queens Road, Teddington, Middlesex, TW11 0LY, UK.

Autogen Bioclear: http://www.autogenbioclear.com/, Holly Ditch Farm, Mile Elm, Calne, Wiltshire, SN11 0PY, UK.

Billups Rothenberg: http://www.brincubator.com/, PO Box 977, Del Mar, CA 92014-0977, USA.

Biogene Ltd: http://www.biogene.com/index.cfm, BioGene House, 6 The Business Centre, Harvard Way, Kimbolton, Cambs PE28 0NJ, United Kingdom

Cambrex: www.cambrex.com,Cambrex Corporation, 1 Meadowlands Plaza, East Rutherford, New Jersey 07073.

Chemicon International: www.chemicon.com, 28820 Single OAk Drive, Temecula, CA 92590.

Clontech: www.clontech.com, Clontech Laboratories, Inc., 1290 Terra Bella Ave., Mountain View, CA 94043, USA.

Costar/Corning Incorporated: http://www.scienceproducts.corning.com, Corning, NY 144831, USA.

Eppendorf: http://www.eppendorf.co.uk/int/?l=3, Endurance House, Vision Park, Chivers Way, Histon, Cambridge, CB24 9ZR, UK.

Gibco, Invitrogen: http://www.invitrogen.com/site/us/en/home.html, Invitrogen Ltd, 3 Fountain Drive, Inchinnan Business Park, Paisley, UK, PA4 9RF.

Jackson ImmunoResearch Laboratories, Inc.: www.jacksonimmuno.com, 872W. Baltimore Pike, P.O. Box 9, West Grove, PA 19390.

Labtech international: http://www.labtech.co.uk/, 1 Acorn house, The Broyle Ringmer, East Sussex, BN8 5NN.

Leec Ltd: http://www.leec.co.uk/web/LEEC/index.cfm, Private road 7, Colwick Industrial Estate, Nottingham, NG42AJ, UK.

Millipore: http://www.millipore.com/, Suite 3 & 5, Building 6, Croxley Green Business Park, Watford, Hertfordshire. WD18 8YH.

New Brunswick Scientific: http://www.nbsc.com/, PO Box 4005, Edison, NJ 08818-4005, USA.

Nunc: http://www.nuncbrand.com/en/default.aspx, 75 Panorama, Creek Drive, Rochester, NY, 14625-2385.

Pierce: http://www.piercenet.com/, PO Box 117, Rockford, IL 61105, USA.

Qiagen: http://www1.qiagen.com/Default.aspx?, QIAGEN House, Fleming Way, Crawley, West Sussex, RH10 9NQ.

Pierce: http://www.piercenet.com/, PO Box 117, Rockford, IL 61105 USA.

R&D Systems: http://www.rndsystems.com/, 19 Barton Lane, Abingdon Science Park, Abingdon, OX14 3NB, UK.

Santa Cruz Biotechnology: http://www.scbt.com/, Santa Cruz Biotechnology, Inc. 2145 Delaware Avenue Santa Cruz, CA. 95060 U.S.A.

Sigma: www.sigma.com, 3050 Spruce Street, Saint Louis, Missouri 63103 USA.

Sorvall : http://www.thermo.com/com/cda/home/1,,,00.html, hermo Fisher Scientific Inc., 81 Wyman Street, Waltham, MA 02454, USA.

Stratagene: http://www.stratagene.com/homepage/default.aspx, 11011 N. Torrey Pines Road, La Jolla, CA 92037, USA.

Vector Labs: http://www.vectorlabs.com/uk/default.asp, 3 Accent Park, Bakewell Road Orton Southgate, Peterborough, PE2 6XS, England

Section 1: Materials

1. Cellular biology materials

All the cell lines cited below were genotyped, maintained and catalogued by Professor Masters (email: jmasters@ucl.ac.uk). Cells were typed by short tandem repeat profiling (Masters et al., 2001). Only stocks that had been genotyped were used for experiments. All prostate cell lines were maintained in culture in a humidified incubator at 36.5°C, 21% O_2, 5% CO_2 (LEEC). The cells were cultured in flasks (Nunc). When confluency was reached, the cells were rinsed with PBS (Gibco), and trypsinised for re-seeding at a 1/5 density (Trypsin 2.5g/L, Gibco). The culture medium was typically changed every two-three days.

a. Prostate cell lines

The matched non-neoplastic ("normal") and primary tumour derived cell lines were isolated from a patient with localised prostate carcinoma and were subsequently immortalised by the HPV virus (Bright et al., 1997). From patient number 1542 were isolated non-neoplastic ("normal") epithelial cells 1542NPTX (abbreviated 42N), non-neoplastic ("normal") stromal cells 1542FTX (42F) and primary tumour cells 1542CPTX (42C). From patient number 1532 were isolated non-neoplastic ("normal") epithelial cells 1542NPTX (32N), non-neoplastic ("normal") stromal cells 1532FTX (32F) and primary tumour cells 1532CPTX (32C). Matched non-neoplastic ("normal") and primary tumour derived cell lines were grown in keratinocyte-SFM medium (Gibco), supplemented by 2.5μg of recombinant epidermal growth factor (rEGF), 15mg of bovine pituitary extract (BPE), and 8% foetal calf serum (FCS, Gibco).

The BPH derived cell lines were isolated from a patient diagnosed with benign prostate hyperplasia and are of epithelial (Pre2.8) or stromal (S2.13) origins (Daly-Burns et al., 2007). They were immortalised by a temperature sensitive SV40 virus construct. BPH-derived epithelial cells were grown in PREGM medium (Cambrex), with supplements. BPH-derived stromal cells were grown in RPMI1640 medium (Gibco), supplemented by 8% FCS (Gibco).

The PCa metastasis derived cell lines, which spontaneously immortalised, were isolated from metastases to the brain (DU145), the lymph nodes (LNCaP), or the bone (PC3). They were grown in RPMI1640 medium (Gibco), supplemented by 8% FCS and L-Glutamine (2mM, Gibco). Among the three metastases derived cell lines, PC3 and DU145 are able to form tumours when injected to immuno-suppressed animals. LNCaP cells do not form tumours in nude mice, unless co-

injected with fibroblasts or a matrix containing adhesion factors. LNCaP cell line was isolated from lymph node metastasis of a patient diagnosed with prostate cancer (Horoszewicz et al., 1980 and 1983). LNCaP cells are androgen-sensitive cells, although they do express a mutated version of the androgen receptor (AR). LNCaP cells are tumourigenic in mice, but not metastatic. DU145 cell line was isolated from brain metastasis of a 69-year-old patient with moderately differentiated prostate cancer (Stone et al., 1978 and Mickey et al., 1980). DU145 cells are androgen-insensitive cells, as they do not express the androgen receptor. DU145 cells are tumourigenic in mice but not metastatic. PC3 cell line was isolated from bone metastasis of a 62-year-old patient with undifferentiated prostate cancer (Kaighn et al., 1978 and 1979). PC3 cells are androgen-insensitive cells since they do not express the androgen receptor. They are highly tumourigenic and metastatic in mice.

Cell lines	Passages
LNCaP	26 / 27 / 28
DU145	74 / 75 / 76
PC3	29 / 30 / 31
1542CPTX (42C)	67 / 68 / 69
1542NPTX (42N)	49 / 50 / 51
1542FTX (42F)	23 / 24 / 25
Pre2.8	52 / 54 / 57
S2.13	62 / 63 / 64

Table 5: Prostate cell lines passages at which total RNA was extracted for RT-PCR.

b. Other cells in culture

The colon carcinoma cell line HT29 (obtained from ATCC) was grown in McCoy's medium (Gibco) with 8% FCS (Gibco).

The monkey kidney Cos-1 and Cos-7 cells (obtained from ATCC) were grown in RPMI1640 medium (Gibco) supplemented by 8% FCS and L-Glutamine (2mM, Gibco).

The mouse fibroblast NIH3T3 cells (obtained from ATCC) were grown in DMEM medium (Gibco), supplemented by 8% FCS and L-Glutamine (2mM, Gibco).

The human embryonic kidney HEK293 cells (obtained from ATCC) were grown in DMEM medium supplemented by 8% NCS (Labtech International) and L-Glutamine (2mM, Gibco).

c. Paired non-neoplastic and carcinoma prostate tissue samples

Paired clinical samples from 6 patients with prostate cancer were kindly provided by Helmut Klocker from the University of Innsbruck, Austria (table 6). For each patient, they provided us with a malignant and non-neoplastic sample (total RNA extracts, extracted from laser capture microdissected fresh frozen prostate tissue). Patients presented no regional lymph node metastasis (N0), clinical stages ranging from confined tumours (pT2) to tumours that have extended through the prostatic capsule (pT3a); i.e. tumours confined within the prostate but involving both lobes (2c) and tumours with extra capsular extension (3a), Gleason scores (GSC) between 5 and 7. Unfortunately, distant metastasis could not be assessed (MX) (table 6). The Gleason grade defines the grade of the malignancy (ranges from 2 to 10) and illustrates the architectural changes of the cancer. The Gleason score is the sum of the 2 highest grades. A Gleason score between 5-7 defines well-moderately differentiated tumours. The higher the Gleason score the more severe and less differentiated the cancer is. Poorly differentiated tumours have lost their ability to form gland-like structures. These tumours are the most aggressive and are most likely associated with capsular infiltration, seminal vesicles extension, and/or metastatic spread.

Sample number	Prostate weight (g)	pT	N	M	R	GSP	GSC
1-2	37	3a	0	X	0	3+2	5
3-4	40	2c	0	X	1	3+3	6
5-6	47	2c	0	X	0	3+3	6
7-8	34	3a	0	X	1	3+3	6
9-10	20	2c	0	X	1	3+2	5
11-12	45	2c	0	X	0	3+4	7

Table 6: Histological data of the paired non-neoplastic/carcinoma prostate tissue samples (H. Klocker). The 6 paired carcinoma/non-neoplastic tissue samples are originating from patients with well or moderately differentiated tumours (GSC 5-7), confined within the prostate, either involving both lobes (2c) or with extra capsular extension (3a), presenting however no regional lymph node metastases (N:0), and whose distant metastases could not be assessed (M:X). pT: tumour stage, R: recurrence, GSP: Gleason grade, GSC: Gleason score.

2. Molecular biology materials

a. Plasmid DNAs

KIAA0331/pBLUESCRIPT II SK(+) phagemid was kindly provided by Tanaka (KIAA0331 clone DKFZp566H0824 in pAMP1 from RZPD). This phagemid contains the complete coding sequence of semaphorin 3e gene with the 5' and 3' untranslated regions (UTR). Semaphorin 3e insert was amplified from this

plasmid using specific primers containing restriction enzyme sites (5'KpnI-forward primer and 3'NotI-reverse primer, refer to page 63).

The expression vector pEF6/Myc-His-version B (Invitrogen) contains the T7 primer, the restriction enzyme sites 5'KpnI and 3'NotI, a Myc epitope and a 6xHis-Tag (figure 18). This expression vector was used for the cloning of semaphorin 3e insert.

PlexinA1/VSV and Neuropilin1/HA plasmids DNA were kindly provided by S. Strittmaker in pcDNA3.1 vectors (Takahashi and Strittmatter, 2001). These plasmids were used to transfect cells that were subsequently used in immunohistochemistry experiments and adhesion assays in presence or absence of Semaphorin 3A or 3E proteins.

PlexinB1 plasmid DNA was kindly provided by A. Hall (Driessens et al., 2001) in a pCDNA3 vector.

AP-Semaphorin4D-GST plasmid was kindly provided by L.Tamagnone (Tamagnone et al., 1999) in an APtag-1 vector.

PlexinD1/pBKVSV plasmid was kindly provided by A. Puschel (Rohm et al., 2000b). This phagemid vector pBK (Stratagene, Kanamycin^r) contains plexin d1 cDNA and a VSV-Tag that has been introduced between the signal peptide and the plexin d1 coding sequence. This plasmid was used to transfect cells that were subsequently used for immunohistochemistry experiments and adhesion assays in presence or absence of Semaphorin3A or 3E proteins.

All the above cited plasmids were amplified in Max Efficiency® DH5α™-competent cells (refer to page 65), and purified using the Maxi Purification kit (refer to page 65). Mammalian cells were transfected with each plasmid using Lipofectamine™2000 (refer to page 67).

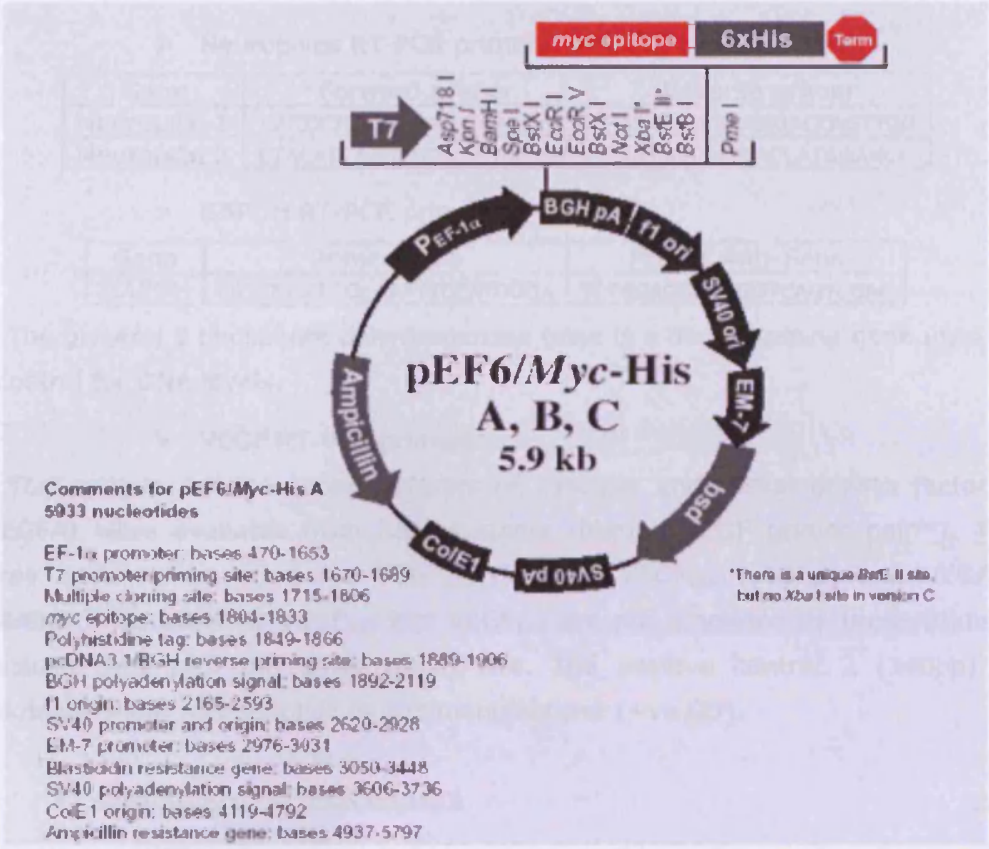

Figure 18: Plasmid pEF6/Myc-His (version B, Invitrogen).

b. Primers and probes

- Primers for RT-PCR

All PCR primers were designed manually and synthesised by Invitrogen. Primers were used at a concentration of 10pmol/μL.

➢ Semaphorins RT-PCR primers:

Gene	Forward primer	Reverse primer
Semaphorin 3a	ACTGGCTATTTCAGCAATGGAGC	AACTTGTTCACAGAACTCATCC
Semaphorin 3b	GACTTTCAGCCTGGAGCGAAC	CTCTGTTCGGAGACTTGGACG
Semaphorin 3c	CAAGACCTCTGAATACTTCAGCC	GTACCATCTGGGATGACATGTGC
Semaphorin 3e	GGGCACATTATCACCTTGCTCC	CTCATCGTCATGCTCAGTGCGG
Semaphorin 3f	CTCCGTGTTCCGAGGCTCTGC	TAGCGCCCGTCGCCTGCATCC
Semaphorin 4d	GGTCTTCGCTGTGAACGCAC	AAGTAGACCCTGTCATCCTC

➢ Plexins RT-PCR primers:

Gene	Forward primer	Reverse primer
Plexin a1	GGGACGCCAGCTCCGTGCGTGC	CTTCAGCTCCAACAGGCCAGTGG
Plexin a2	GTGTATTGGCGAGTGTAAGCCAG	AGCTGGGTCTCAGATACGGTGAC
Plexin a3	CGGCAGCGTGGCCTCGCTCAC	GGAGGATGATGCGAGTCATGCG
Plexin b1	GCTGGGCTGTCTGCAAGTGGCAG	GGGAAGATATGGAGCCAGAACCTG
Plexin b3	CAGTGGCAGTCACCTCTATGTCC	GACCTGCCAGGCCTTCGACCTG

➢ Neuropilins RT-PCR primers:

Gene	Forward primer	Reverse primer
Neuropilin 1	CCTCCTGTTGTGTCTTCAGGGC	GAGCGCTCTGCAGACCAGTTGG
Neuropilin 2	CTACATCAAGTTCACACTCCGAC	CCATTGTCATCACCATGGAGCC

➢ GAPDH RT-PCR primers:

Gene	Primer Sens	Primer Anti-Sens
GAPDH	CCACCCATGGCAAATTCCATGGCA	TCTAGACGGCAGGTCAGTCCAC

The glycerol 3 phosphate dehydrogenase gene is a housekeeping gene used as a control for DNA levels.

➢ VEGF RT-PCR primers:

The primers for the three isoforms of vascular endothelial growth factor A (VEGFA) were available from R&D systems (human VEGF primer pair™). The three isoforms amplified are $VEGF_{206}$ (567bp), $VEGF_{189}$ (516bp) and $VEGF_{165}$ (444bp). The isoforms $VEGF_{121}$ and $VEGF_{145}$ are not amplified by these primers because they lack the lower target site. The positive control 2 (340bp) of unknown origin was supplied by the manufacturer (+ve Ctr).

- Quantitative RT-PCR primers

Quantitative PCR primers were designed using Primer Express® software and synthesised by Invitrogen. Primers and probes were chosen on two consecutive exons (in order to selectively amplify the cDNA and not contaminating genomic DNA), which do not show any alternative splicing. The probes are overlapping the two exons.

➢ Semaphorin 3e qRT-PCR primers and probe:

Semaphorin 3e gene	Sequence
Forward primer-Exon 16	CAGAAAGGACGTGAGACAAGAAA
Reverse primer-Exon 17	ACCAAGGTCCATCTTAACCACTCT
Probe/FAM dye	TCATCTGTCTTCACCTCCT

➢ Plexin b1 qRT-PCR primers and probe:

Plexin b1 gene	Sequence
Forward primer-Exon 30	CAAGGCCATCCCTGAGATCTAC
Reverse primer-Exon 31	AACAGGTCATCCACGAACTTCTG
Probe/FAM dye	CCATGAAGGGCACCC

- Sequencing and cloning primers

The same PCR primers than those used for RT-PCR were used for sequencing purposes at a concentration of 4pmol/μL. The sequencing primers used for the

cloning of semaphorin 3e gene were designed manually and synthesised by Invitrogen.

- Semaphorin 3e cloning and sequencing primers:

Semaphorin 3e	Sequence
5'KpnI-forward primer	CGCGCGGGTACCGCATGGCATCCGCGGGC
3'NotI-reverse primer	CGCGCGGCGGCCGCGAGGAGTCCAGCGTGT

pEF6-*Sema3e*-Myc/His	Sequence
P1-T7 promoter/priming site	TAATACGACTCACTATAGGG
P2-Sema3e-Exon 1-reverse primer	CATCCAGCAGCATTGTATGG
P3-Sema3e-Exon 17-forward primer	AATTCTTGCAGCTGATCGGT
P4-BGH-Reverse priming site	TAGAAGGCACAGTCGAGG

c. Antibodies and Semaphorin3A protein

The conditions used for each antibody (concentration and dilution) have previously been optimised by me or other people in the laboratory. The dilutions cited below are optimal for each antibody.

The ICα2 antibody is an in-house rabbit anti-PlexinB1 antibody, which was kindly provided by S. Giordano (Giordano et al., 2002). This antibody was used for western blotting at a 1/500 dilution, using a secondary mouse anti-rabbit antibody HRP (horseradish peroxidase)-conjugated at a 1/1500 dilution (Autogen). The size of the expected band is 100kDa.

The c-Myc antibody (9E10: sc-40) is a mouse anti-Myc antibody (Santa Cruz Biotechnology, Inc), which was used for western blotting at a dilution 1/600 to detect the Myc epitope of the recombinant Semaphorin3E protein produced. The secondary antibody, a goat anti-mouse antibody HRP-conjugated was used at a 1/1000 dilution (Autogen). The size of the expected band is approximately 90KDa.

The MAB2079Z antibody is a mouse monoclonal anti-human β1-integrins antibody, which is specific for active conformations of human β1-integrins (Chemicon International). This antibody was used for indirect immunofluorescence at a 1/200 dilution.

The V9131 antibody is a mouse monoclonal anti-vinculin antibody (Sigma), which was used for indirect immunofluorescence at a 1/400 dilution.

The V4888 antibody is a rabbit anti-VSV antibody (Sigma), which was used for indirect immunofluorescence at a 1/00 dilution.

The HA-probe (Y-11:sc805) is a rabbit polyclonal anti-HA IgG antibody (Santa Cruz Biotechnology, Inc), which was used for indirect immunofluorescence at a 1/00 dilution.

All the other secondary antibodies used are from Jackson ImmunoResearch Laboratories, Inc.: fluorescein (FITC)-conjugated polyclonal rabbit anti-mouse antibody, rhodamine (TRITC)-conjugated donkey anti-mouse antibody, TRITC-conjugated goat anti-rabbit antibody, fluorescein (FITC)-conjugated donkey anti-goat antibody, and fluorescein (FITC)-conjugated donkey anti-rabbit antibody. All secondary antibodies were used at a 1/100 dilution for indirect immunofluorescence.

Phalloidin TRITC-conjugated (Sigma) to stain actin microfilaments in red (8.3µL/2.3mL). The mounting medium with DAPI (Vector labs) was used to stain nuclei in blue.

Recombinant human semaphorin-3A/Fc chimera (R&D systems) is the Semaphorin3A protein used for biological assays such as adhesion assays. A working stock solution of 100µg/mL in 0.1% BSA was prepared.

Section 2: Methods

1. General methods

a. Bacterial transformation and plasmid DNA (maxi, mini) preparations

Competent E.Coli strains, Max Efficiency DH5α™ (Invitrogen), were transformed by heat-shock with double-stranded circular plasmid DNA: 50µL of competent cells and an aliquot of plasmid DNA (e.g. Semaphorin3E, PlexinB1, PlexinA1, Neuropilin1, PlexinD1, Semaphorin4D expression vectors) were thawed on ice for few minutes. 1µL of plasmid DNA (10ng/mL) was added to the 50µL of competent cells, and incubated on ice for 30 minutes. Cells were then heat-shocked in a water bath at 42°C for 45 seconds and immediately placed on ice for 2 minutes before adding 450µL of S.O.C medium (S.O.C medium: S.O.B. medium, 1M MgCl2, 20mL Glucose 1M. S.O.B medium: 20g bacto-tryptone, 5g bacto-yeast extract, 0.5g NaCl, 2.5mL KCl 1M, deionised H2O to 1L, pH adjusted to 7 with NaOH 100µL, autoclave.). Transformed cells were incubated in a shaking incubator at 225rpm for 1h at 37°C to allow expression of antibiotic resistance. Transformed cells were then diluted 1:10 and 1:100 with S.O.C medium and

spread on LB (Luria Bertani broth: 10g tryptone, 5g yeast extract, 10g NaCl, deionised H2O to 1L, adjust pH to 7 with 5N NaOH, autoclave) /Ampicillin (final concentration 100μg/mL) plates for incubation overnight at 37°C (turned upside-down).

The following day, single colonies were isolated with a pipette tip and used to inoculate a starter culture of 5ml of LB/Ampicillin broth which was incubated for approximately 8h in a shaking incubator at 300rpm (Innova 4300, New Brunswick Scientific) and 37°C. Glycerol stocks of positively transformed bacteria were stored at -80°C (0.85mL starter culture, 0.15mL glycerol). The rest of the starter culture was diluted 1/500 and used to inoculate 100mL of selective LB medium (overnight in a shaking incubator at 300rpm) for (low copy) plasmid DNA preparations. Bacterial cells were harvested by centrifugation at 6000g in Sorvall SuperT21 (SL250T rotor) for 15 minutes at 4°C. Supernatant was removed by inverting the tubes and bacterial pellets were resuspended in 4mL of Buffer P1/RNase A by vortexing (Maxi Kit, Qiagen). Then 4mL of Buffer P2 were added and mixed by thoroughly inverting the tubes. After 5 minutes incubation at room temperature, 4mL of buffer P3 were added and mixed by gently inverting the tubes. After 15 minutes incubation on ice, the precipitated material was centrifuged at 20000g for 30 minutes at 4°C and the supernatant containing the plasmid DNA was recentrifuged for 15 minutes at 4°C at 20000g. Supernatant was applied to an equilibrated QIAGEN-tip100 column, subsequently washed with 2x10mL of Buffer QC to eliminate all contaminants (RNA, proteins, and low-molecular impurities). The plasmid DNA was eluted with 5 mL Buffer QF. The protocol for plasmid DNA preparation is based on a modified alkaline lysis procedure (Buffer P1, P2), and on the binding of the plasmid DNA to an anion-exchange resin (QIAGEN-tip) under appropriate low salt and pH conditions (Buffer QC, QF). Eluted plasmid DNA is then concentrated and desalted by isopropanol precipitation, by adding 3.5mL of isopropanol (0.7 volume) to the eluted DNA, mixing, and centrifugating at 15000g for 30 minutes at 4°C. DNA pellets were washed with 2mL 70% ethanol, and centrifuged at 15000g for 10 minutes. Supernatants were carefully removed, the pellets air-dried for 5 minutes, and redissolved in 200μL of TE buffer (10mM Tris-Cl, pH7.5, 1mM EDTA).

b. Digestion by restriction enzymes, DNA precipitation and purification

The reaction used for enzymatic digestion (NotI, KpnI) of DNA (e.g. semaphorin 3e cloning) was the following:

DNA	20μg
Enzyme	20U
Buffer 10X	1/10 final volume
dH2O	to final volume
Final volume	20μL

The mixture was left 2h at least or overnight at 37°C and heated at 65°C for 5 minutes to inactivate the enzyme. DNA was precipitated in between 2 digestions because the enzymes buffers were not compatibles (enzymes from New England Biolabs).

DNA precipitation (e.g. in between two digestions by different restriction enzymes) was obtained by adding 0,1 volume of 3M sodium acetate (NaAc), pH 5.2 and 2 volumes of 95% ethanol to one volume of DNA sample. The mixture was left 15 minutes on ice before centrifugation at maximum speed (16100g, Eppendorf centrifuge) for 25 minutes. The supernatant was decanted and the pelleted DNA washed with ice-cold 70% ethanol before being centrifuged 10 minutes and decanted. Pelleted DNA was air-dried and resuspended in an appropriate volume buffer or deionised water.

DNA purification was performed directly from the agarose gel using the QIAquick Gel Extraction Kit (Qiagen). The DNA fragment to purify was excised from the agarose gel with a clean scalpel, weighted, and incubated in 3 volumes of Buffer QG at 50°C for 10 minutes (until the gel has completely dissolved). After adding 1 gel volume of isopropanol, the mixture was applied to the QIAquick column and the column centrifuged for 1 minute. The bound DNA was washed by adding 0.75mL of Buffer PE to the column and centrifuging 1 minute. Finally, the DNA was eluted by adding 50μL of Buffer EB to the column and centrifuging 1 minute at maximum speed. Sample concentration was estimated using a spectrophotometer.

c. Cell transfection

Cells were transfected using Lipofectamine™ 2000, 1mg/ml (Invitrogen). 24h prior to the transfection, cells were plated in T80 flasks in growth medium at a high density in order to obtain about 90% confluency on the day of transfection. To obtain optimal transfection efficiency, plasmid DNA and Lipofectamine™ 2000 reagent were diluted in Opti-MEM® Reduced Serum Medium (Invitrogen). 24μg of plasmid DNA (PlexinA1, Neuropilin1, Semaphorin3E plasmids, etc.) and 60μL of Lipofectamine™ 2000 were diluted in 1.5mL of Opti-MEM® medium respectively. After 5 minutes incubation at room temperature the diluted plasmid DNA was

combined to the diluted Lipofectamine™ reagent and mixed gently. The solution was incubated for 20 minutes at room temperature to allow the formation of DNA-Lipofectamine™ 2000 complexes. Finally, the mixture was added to the cells in culture. After 48h incubation, the cells were ready to assess for transgene expression.

2. Expression profiling of semaphorins, plexins, neuropilins, and VEGFs in normoxic and hypoxic conditions in prostate cell lines and tissues

a. Cell culture under normoxic and hypoxic conditions

Cell culture under normoxic conditions was performed in our laboratory using a humidified incubator at 36.5°C, 21% O_2, 5% CO_2 (LEEC). Cell culture under hypoxic conditions was performed at the Rayne Institute (University College London, Shakib et al., 2005), using a specific humidified incubator at 36.5°C, 1% O_2, 5% CO_2, 94%N_2 (Billups Rothenberg Modulator Incubator, ICN-Flow). The gas was circulated at 2 bar pressure at 10L/min flow for 20 minutes at room temperature and the chamber was sealed. The medium pO_2 fell within 20 minutes and was maintained for the duration of the experiment.

Normal and primary tumour prostate cells, as well as colon cancer cells were transported on ice to the Rayne Institute. Cells were plated in flasks (Nunc) and allowed to grow to 90% confluency in a normoxic incubator. Subsequently, the flasks (3 T175 flasks per cell line) were incubated in an adjacent hypoxic incubator for 24h and 48h. After 24h under hypoxic conditions, the medium had already changed colour (from red to yellow) and many dead cells were in suspension. Total RNA from each flask was extracted using the RNAeasy® Mini Kit (Qiagen, refer to page 68), and transported on dry ice back to the laboratory, where it was stored and used for further experiments.

b. Total RNA extractions

All RNA extractions were carried out using the RNAse-Free DNAse protocol of the RNAeasy® Mini Kit (Qiagen). Cells were trypsinised, pelleted, and homogenised by adding 600µL of buffer RLT and vortexing until complete homogenisation. The homogenised lysate was directly passed onto the QIAshredder column, and centrifuged for 2 minutes at maximum speed (16100g=13200rpm, Eppendorf centrifuge 5415D). One volume (600µL) of 70% ethanol was added to the homogenised lysate (supernatant), well mixed, and applied to an RNAeasy mini spin column to allow total RNA to bind to the column.

After centrifugating 15 seconds at 8000g (9300rpm), contaminants were washed away by adding 700μL of buffer RW1, centrifugating for further 15 seconds at 8000g (9300rpm), and 500μL of buffer RPE, centrifugating for 15 seconds at 8000g (9300rpm). 500 more μL of buffer RPE were pipetted onto the column, and centrifuged for 2 minutes at maximum speed to dry the RNAeasy membrane (9300rpm). Total RNA was eluted from the column by adding 30μL of RNase-free water directly onto the RNAeasy column, and centrifugating for 1 minute at 8000g (9300rpm).

c. Reverse Transcriptase Polymerase Chain Reaction: RT-PCR

First strand cDNA was synthesised from total RNA by incubating the following mixture at 70°C for 10 minutes and then quick chilling on ice:

Oligo $(dT)_{12-18}$ (500μg/mL)	1μl	(Invitrogen)
Total RNA	5μg	
dH_2O	12μl	

The same amount of total RNA was used for each RT-PCR reaction. The following components were then added to the mixture and incubated at 42°C for 2 minutes:

5x first strand buffer	4μl
0.1M DTT (dithiothreitol)	2μl
10mM dNTP Mix	1μl

dNTP is deoxy-nucleoside 5'-triphosphate; contains 10mM each of dATP, dGTP, dCTP and dTTP. SUPERSCRIPT™ RNAse II H^- Reverse Transcriptase (Invitrogen) is added to the mixture and incubated at 42°C for 50 minutes, and then heated at 70°C for 15 minutes to inactivate the reactions.

Control samples with no reverse transcriptase enzyme (control no RT), no DNA (control no DNA), as well as GAPDH controls have been performed for each experiment. All polymerase chain reactions (PCRs) have been performed on a Perkin Elmer Thermal Cycler and all products run on an ethidium bromide stained agarose gel electrophoresis (0.8-2%) and visualised by UV transillumination. Controls with no RT enzyme or no DNA were negative, and GAPDH expression levels were similar, showing approximately equal levels of total RNA between samples (results not always shown). Quantification of each PCR product (band intensity) has been performed using GeneTools software. Standard paired T-tests statistical analysis has been performed using Excel software (refer page 81).

Normoxic conditions:

Profiling experiments under normoxic conditions have been performed in triplicate, on three consecutive RNA extractions (from three different passages) for each of the 10 prostate cell lines. The results presented are normalised means with standard errors of the mean (SEM). Normalisation was performed for each gene (semaphorins, plexins, neuropilins) against expression values obtained in the non-neoplastic "normal" epithelial prostate cell line 1542NPTX, abbreviated 42N (value=1). Example: the value obtained for semaphorin 3e band intensity in cell line 42C (1542CPTX) was divided by the value obtained for the same gene in cell line 42N, used as a reference for normal expression. The value obtained for the same gene in cell line 42F (1542FT) was also divided by the value obtained in cell line 42N, etc. The same applies for the other cell lines and the other genes. Standard paired T-tests statistical analysis has been performed using Excel software (refer to page 81).

At least one PCR product of each primer pair (refer to page 62) was sequenced (University of Dundee). Sequences were compared to the reference sequence for each gene on the NCBI website (http://www.ncbi.nlm.nih.gov/), using the BLAST tool and each was found to be correct (see Appendix 1, page 179).

VEGFA isoforms:

Each RT-PCR for vascular endothelial growth factor A isoforms has been performed twice, giving the same results. The results presented are representative. The presence of mRNA for the three VEGF-A isoforms has also been assessed in RNA extracted from total prostate (commercially available from Clontech). The aim was to determine which isoforms were present for each cell type and therefore statistical analysis was not applicable.

Hypoxic conditions:

Each RT-PCR has been performed in triplicate, giving the same results. The results presented are representative (means of three repeats, with standard error of the mean (SEM). Normalisation was performed for each semaphorins gene against expression values obtained in the non-neoplastic "normal" epithelial prostate cell line 1542NPTX (42N=1), or against expression values obtained in the matched primary tumour prostate cell line 1542CPTX (42C=1), or against expression values obtained in the colon cancer cell line HT29 (HT29=1). Standard paired T-tests statistical analysis has been performed using Excel software (refer to page 81). The hypoxia-induced transcriptional activation of vascular endothelial growth factor VEGFA in the colon cancer cell line HT29 (Ellis et al., 1998) was used as a positive control. The VEGF primers used are the human VEGF primer pair™ (specific for all three VEGFA isoforms: $VEGF_{165}$, $VEGF_{189}$, and $VEGF_{206}$).

However, the percentage of agarose gel electrophoresis used here (0.8%) prevents visualising all isoforms.

d. Quantitative polymerase chain reaction: real-time PCR (qRT-PCR)

Primers and probes have been designed using Primer Express® software following manufacturer's instructions. Semaphorin 3e specific primers and probe span exons 16 to 17, where no alternative splicing has been detected (data not shown). Plexin b1 specific primers and probe span exons 31 to 32. Each step has been optimised as suggested in the manual. Each qRT-PCR has been performed in triplicate, using β1-actin as internal control, with ABI PRISM® 7700 Sequence Detection System (Applied Biosystems). The results have been transformed and normalised as follows:

1. ΔCT=Average CT β1actin–Average CT sample
2. Relative ΔCT=40-ΔCT
3. $\Delta\Delta CT=2^{\text{-Relative CT}}$
4. Remove baseline=ΔΔCT sample÷ΔΔCT β1actin

The results presented are normalised means of three independent repeats, with standard error of the mean (SEM). Another normalisation has been performed for each gene (semaphorin 3e, plexin b1) against expression values obtained in normal epithelial prostate cells (1542NPTX, abbreviated 42N, value=1). Standard paired T-tests statistical analysis has been performed using GraphPad software (refer to page 81).

e. Screening for the presence of HIF-responsive elements (HRE)

The consensus sequence of HIF-responsive elements (HRE) is RCGTG, where R is A or G (Wenger et al., 2005). In order to search for the presence of HREs within the promoter regions of secreted semaphorin genes, the sequence of their promoters (promoter + first intron) was extracted form the NCBI database (http://www.ncbi.nlm.nih.gov/) and consensus sequences were screened using the word search tool from Word software.

3. PlexinB1 mutations, Semaphorin4D production and migration assays

a. PlexinB1 mutations: site-directed mutagenesis and stable transfection (Magali Williamson and John Masters)

Three of the most frequently found changes of plexin b1 gene in prostate cancers and metastases were introduced into a cDNA clone of plexin b1 by *in vitro* site-directed mutagenesis (experiments performed by my colleagues, Wong et al., 2007). The three mutations are single nucleotide changes: mutation A5359G, mutation A5653G, and mutation T5714C. NIH3T3 and Cos-1 cells were transfected (Lipofectamine™2000, Invitrogen) with wild-type plexin b1 expression vector *pcDNA3-WT-plxb1*, with mutant plexin b1 expression vectors *pcDNA3-plxb1-A5359G*, *pcDNA3-plxb1-A5653G*, and *pcDNA3-plxb1-T5714C*, and with the expression vector only *pcDNA3*. The cells were selected for the presence of the transgene using geneticin (G418, Gibco). Expression of wild-type and mutants forms of PlexinB1 was checked by RT-PCR (M. Williamson, personal communication). Stable cell lines expressing vector only, wild-type PlexinB1 protein (WT-PlxB1), and the three mutant forms of PlexinB1 protein have thus been established in the laboratory and I used them in the following experiments.

b. Migration assays in modified Boyden chambers

Technique optimisation and primary results:

Migration assays were performed in modified Boyden chambers, which are polycarbonate filters with pores of 8μm diameter (Transwell®, Costar). The under surface of the membrane was coated with fibronectin (50μl at 10μg/ml in PBS (0.1% solution, Sigma), left to dry for approximately 2 hours and rinsed in PBS. Cells stably transfected with wild type or mutants plexin b1 expression vector were grown to near confluency, harvested using a non-enzymatic cell dissociation solution (Sigma) and counted with a haemocytometer. $4x10^4$ cells were resuspended in medium completed with 0.1% NCS (Labtech International), and were added to the upper chamber and allowed to migrate for 3h at 37°C. After migration, the inside of each filter was wiped off with a cotton bud. The cells that have migrated through the filters adhere to the lower side of the Boyden chamber, coated with fibronectin. The attached cells were then rinsed in PBS, fixed in paraformaldehyde 4% for 10 minutes, rinsed in PBS, stained with haematoxylin 4% for 10 minutes, and rinsed with tap water. Finally, the cells that have migrated through the filter were counted (means of 4 to 5 random fields) using a microscope (objective x20).

Optimisation of the technique has been performed on the number of transfected cells to plate in the upper chamber ($1x10^4$, $4x10^4$, $1x10^5$), on the time of incubation at 37°C (2h, 3h, 4h, 6h, 12h), on the presence or absence of serum in the medium (8% NCS or 0.1% NCS), and finally, on the concentration of

Semaphorin4D ligand to add in the lower chamber (0-200ng/mL). Experiments were performed in triplicate and repeated three times. Results have been normalised to the level of migration encountered by the cells transfected by the vector only (vector=100%). ANOVA statistical analysis has been performed using GraphPad software (refer to page 81).

Effects of PlexinB1 mutant forms on cell migration:

Three experiments were performed in triplicate. Four to five random fields were counted per Transwell using a microscope. The results presented are the number of cells counted per cm^2. Results have been normalised to the level of migration encountered by the cells transfected by the vector only (vector=1). ANOVA statistical analysis has been performed using GraphPad software (refer to page 81).

c. Production and quantification of Semaphorin4D protein

Cos-1 cells were transfected with the AP-Sema4D-GST plasmid (refer to page 67). After 72h, the medium was collected, and the concentration of protein was assessed using the AP Assay Reagent A 2X (Biogene Ltd.). Five µL of medium, 45µL of water, and 50µL of AP reagent were mixed in a tube and incubated 10 minutes at 37°C. To stop the reaction, 100µL of NaOH 0.5M were added. Prior to measuring absorbance at 405nm, 800µL of water were added to obtain a final volume of 1mL. AP enzyme catalyses the following reaction: PNPP⇔PNP+P (PNPP=p-Nitrophenyl Phosphate). PNP appears yellow at an optical density of 405nm. The optical density was measured using a spectrophotometer. Concentration of Semaphorin4D protein (Q_{Sema4D} in µg/mL) was calculated as follow:

c_{Sema4D} in mol/L=$OD_{405nm} \div l.c$; c=concentration Sema4D; l=cuvette length=1cm

Extinction coefficient of para-nitrophenol at 405nm: $\varepsilon_{PNP}=18.380 M^{-1}cm^{-1}$

c_{Sema4D} in mol/mL/min=$c_{Sema4D} \div N$ with N=incubation time (min) at 37°C

c_{Sema4D} in mol/min or unit (U)=c_{Sema4D} in mol/mL/min÷volume (mL)=A_{enzyme}

Q_{Sema4D} in µg/mL=$A_{enzyme} \div A_{specific}$ (A= activity of the AP enzyme)

Specific activity of AP enzyme: $A_{specific}$ =1500U/mg

4. Semaphorin3E cloning, immunocytology, and adhesion assays

a. Semaphorin 3e cloning into pEF6/Myc-His mammalian expression vector

Semaphorin 3e gene was PCR-amplified from the phagemid KIAA0331/pBLUESCRIPTIISK(+) using the Pfu DNA polymerase (Stratagene) and forward and reverse primers specifically designed to contain KpnI and NotI restriction enzymes sites, respectively (refer to page 63). The PCR reaction was:

Semaphorin 3e DNA	2μg
Buffer 10X	1/10 of the final volume
dNTP Mix (2mM)	5μL
Forward primer	2μL
Reverse primer	2μL
dH_2O	30μL
Pfu enzyme	1U
Final volume	50μL

PCR conditions were 2 minutes at 95°C, 15 cycles at 1 minute at 95°C, 1 minute at 60°C, and 1.30 minutes at 74°C, and 7 minutes at 74°C and 4°C. PCR products were subsequently digested by KpnI (GGTAC/C) and NotI (GC/GGCCGC) restriction enzymes (Invitrogen, refer to page 66). As those two restriction enzymes are not diluted in the same reaction buffer, DNA was ethanol precipitated in between the two reactions (refer to page 67). The semaphorin 3e insert was then purified from an agarose gel electrophoresis using the QIAquick Gel Extraction Kit (Qiagen, refer to page 67). The mammalian expression vector pEF6/Myc-His-version B (Invitrogen) was also digested by KpnI and NotI enzymes and dephosphorylated by the CIAP enzyme, calf intestinal alkaline phosphatase (GibcoBRL). CIAP enzymatic reaction was as follows:

DNA 5' overhang ends	1pmol
Dephosphorylation Buffer 10X	4μL
CIAP enxyme in Dilution Buffer	0.01U
dH20	to 39μL

Incubation was performed at 37°C for 30 minutes, and the CIAP enzyme was heat inactivated at 65°C for 15 minutes. The digested semaphorin 3e insert and dephosphorylated expression vector were then ligated using the T4-DNA Ligase (Invitrogen). Ligation reaction was as follows (3:1 ratio insert:vector):

Vector ends	30fmol
Insert ends	90fmol
Ligase Buffer 5X	4μL
T4 DNA Ligase	0.1U
dH20	to 20μL

The solution was incubated for an hour at room temperature. The ligation reaction was diluted 5 fold prior to transform *Escherichia Coli* host strains (refer to page 65). The presence of the insert was checked in several colonies by PCR using semaphorin 3e primers (refer to page 63), which allowed the elimination of false positive colonies. Colonies containing the recombinant vector were grown up in LB browth and the plasmid DNA purified using the Plasmid Mini Kit (Qiagen, refer to page 65). RT-PCRs were performed using the P1-T7 and P4-BGH primers located respectively at the 5' and 3' ends of the multiple cloning site of pEF6 vector, and P2 and P3 primers located respectively within the first and last exons of semaphorin 3e gene (refer to page 63).

RT-PCR were performed using sequencing primers (refer to page 63) and PCR products were sent to the University of Dundee for sequencing. Sequencing of these PCR products (vector-Sema3e) as well as of the whole insert DNA (semaphorin 3e) using overlapping primers (Invitrogen) allowed us to confirm that semaphorin 3e cDNA had been inserted in frame and with no mutations. Expression vectors containing the correct sequence of semaphorin 3e complete coding sequence were then transformed into bacteria and grown in LB/Ampicillin (final concentration 100μg/mL) broth and the plasmid DNA purified using the Plasmid Maxi kit (Qiagen, refer to page 65).

b. Production and purification of Semaphorin 3E protein

Three T175 flasks of mammalian Cos-7 cells were subsequently transfected with the recombinant expression vector pEF6-*Sema3e*-Myc/His using Lipofectamine™2000 (Invitrogen, refer to page 67). After 48h incubation at 37°C, 150μL of a cocktail of protease inhibitor (Sigma P8340, containing Apoptinin, Bestatin, E-64, Leupeptin, Pepstatin A) was added to the medium to avoid the degradation of the recombinant protein, and was also added 20μL of a furin protease inhibitor (Clontech, decanoyl-RVKR-chloromethylketone). After 72h, the medium was collected, and concentrated using an Amicon Ultra 15 Centrifugal Filter Device Ultracel-PL 30 (Millipore), i.e. up to 15mL of collected medium at a time was added to the filter device (regenerated cellulose) and centrifuged at 4000g for 20 minutes using swinging bucket rotors. The retentate volume (~200μL) was immediately removed from the filter and collected. The presence of the recombinant protein was checked by western blotting (refer to page 134) from the concentrated fraction, which was stored in aliquots at -80°C. Semaphorin 3E protein is a secreted protein. Western blotting using the anti-Myc

antibody allowed its detection in the concentrated collected media (refer to pages 64 and 76).

Semaphorin3E protein was detected using a nickel column, which specifically binds 6xHis-Tags (BD TALON® Resin, Clontech, following manufacturer's instructions). Small scale purification under denaturing conditions was initially performed (all at 4°C unless stated otherwise). One mL of concentrated conditioned medium was centrifuged at 14000rpm for 2 minutes, and the pellet was re-suspended in 0.5mL of Denaturing Equilibration (DE) Buffer (pH 8.0). The solution was centrifuged for further 5 minutes to pellet insoluble debris and transferred to a tube containing 50µL of prewashed TALON®Resin. After 10 minutes agitation at room temperature, the sample was centrifuged at 14000rpm for 1 minute to pellet protein/resin complexes. One mL of DE Buffer was added to wash the complexes, and the resin was pelleted at 14000rpm for another minute. After a second wash, the 6x-His tagged Semaphorin3E protein was eluted by adding 50µL of Elution Buffer, vortexing and centrifugating briefly. Another elution was performed by adding 50µL of EDTA (pH8.0), which removes bound metal from the resin, vortexing and centrifugating briefly. The supernatant contains the protein. Protein concentration was measured using the Lowry method (Sigma) and estimated by western blotting (results not shown). Purification of the recombinant protein under native conditions using the large scale purification protocol failed (results not shown). This might be due to an inaccessible tag under native conditions, or a protease cleavage, which cuts off the tag. However, to test the effects of Semaphorin3E protein, it is not necessary to have it purified and it was therefore used as such.

c. Protein extraction and Lowry Protein Assay

One mL of RIPA buffer [150mM NaCl, 10%Nonidet P-40 (NP-40, nonionic detergent), 0,5% sodium deoxycholate (DOC, ionic detergent), 0,1% sodium dodecylsulfate (SDS, ionic detergent), and tris, pH 8.0, 50mM] containing 100µL of cocktail of proatease inhibitors [Sigma P8340, Aproptinin 80µM (inhibitor of serine proteases), Leupeptin 2mM (inhibitor of serine and cysteine proteases)], Bestsatin 4mM (inhibitor of aminopeptidases), Pepstatin A 1,5mM (inhibitor of acid proteases), E-64 1,4mM (inhibitor of cysteine proteases)] was used to lyse confluent cells in culture (T80 flask) and precipitate proteins (30 minutes on ice with occasional rocking of the plate). The lysates obtained were pre-cleared by centrifugation at 10000rpm for 5 minutes at 4°C. Protein concentrations were normalised using the Lowry Protein Assay kit (Sigma). A series of BSA (Bovine

Serum Albumin) standard was prepared as follows: In tube 1 was added 125µL of BSA (2mg/mL) and 375µL of water, which gives a 500µL solution of BSA at 0.5mg/mL. In tubes 2 to 6, 200µL of water was added. A two fold dilution series was made by transferring 200µL from tube 1 into tube 2, mix, and then transfer 200µL from tube 2 into tube 3, mix, and etc. The test samples were prepared by mixing 10µL of cell lysate and 190µL of water. A 200µL water tube was used as a blank. One mL of Lowry reagent (Folin-Ciocalteu) was then added to each tube in a defined order and at 20 seconds intervals. Solution were mixed well (vortex) and after 10 minutes, 100µL of yellow stop solution (diluted 2 fold in water) was added to each tube in the same order and at 20 seconds intervals. After vortexing, the solutions were left at room temperature for 30 minutes. The optical density of each sample was measured at 750nm, using the water control as a blank. A graph was drown of BSA concentration versus OD, and the concentration in proteins of test samples were determined using the graph. Cell lysate is 20X diluted.

d. Western blotting

Electrophoresis on denaturing (SDS) polyacrylamide gels (PAGE) is used for analytical separation of proteins, based upon molecular weight. Polyacrylamide gels were made by the free radical-induced polymerisation of acrylamide and N,N'-methyenebisacrylamide The formation of free radicals (obtained from the chemical decomposition of ammonium persulfate $S_2O_8^{2-}$ $2SO_4^-$) is catalysed by TEMED (N,N,N',N'-tetramethylenediamine). Polymerised gels are porous and the size of the pores is controlled by the proportion of polyacrylamide and its degree of cross-linking. Higher percentage gels are used to resolve smaller proteins.

Resolving gel:

	13% gel	10% gel	8% gel	6% gel
H_2O	3mL	3.9mL	4.6mL	5.3mL
30% acrylamide (TOXIC)	4.3mL	3.4mL	2.7mL	2.0mL
1.5M Tris pH8.8	2.5mL	2.5mL	2.5mL	2.5mL
10% SDS	100µL	100µL	100µL	100µL
10% ammonium persulphate (APS)	100µL	100µL	100µL	100µL
N,N,N',N'-Tetramethylethylenediamine (TEMED)	8µL	8µL	8µL	8µL

Stacking gel:

H_2O	3mL
30% acrylamide (TOXIC)	670µL
1M Tris pH6.8	250µL
10% SDS	40µL
10% ammonium persulphate (APS)	40µL
N,N,N',N'-Tetramethylethylenediamine (TEMED)	6µL

The Mini-PROTEAN II system (Bio-Rad) was used. The glass plates were washed and rinsed with ethanol until they are completely clean. The glass plates with spacers were assembled and snapped into the casting slot of the casting stand. The resolving gel was then prepared using freshly made 10% APS, and adding the TEMED just before the pouring as the gel polymerise quickly. Approximately 7mL of resolving gel was poured into each glass plate assemblies, and overlayed with water to make the top of the gel in a straight line. The water was removed once the gel had polymerised. The stacking gel (2mL) was then poured and the well formers was inserted between the glass plates and left to polymerise before being removed.

Protein samples were denatured in 2X Laemmli buffer [100mM Tris-HCl, pH 8.0, 2% β-mercaptoethanol, 4% SDS, 0,2% bromophenol blue dye, 20% glycerol], and boiled for 10 minutes at 98°C before being resolved by SDS-PAGE. Sodium dodecylsulfate (SDS) is an anionic detergent that break disulfide bonds and negatively charge proteins. Forty μg of denatured proteins (in SDS-PAGE loading buffer) were loaded per lane, and resolved at 100 Volts in SDS-PAGE running buffer for 1h to 2h, depending on protein size.

SDS-PAGE loading buffer (stored at 4°C):

Deionised water	4.0 mL
0.5 M Tris-HCl, pH 6.8	1.0 mL
Glycerol	0.8 mL
10% (w/v) SDS	1.6 mL
2-mercaptoethanol	0.4 mL
1% (w/v) bromophenol blue	0.2 mL

SDS-PAGE running buffer 5X:

Tris base	7.5g
Glycine	36g
SDS	2.5g
Deionised water	500mL

Proteins were then electrophorically transferred from the resolution gel to an Immobilon™-P Polyvinylindene Difluoride Membranes (PVDF, Sigma-Aldrich). The membrane was pre-wet in 100% methanol for 15 seconds and then 1X transfer buffer. Prior to use, Whatmann paper and scouring pads were also soaked in transfer buffer 1X.

Transfer buffer 10X (stored at 4°C):

Tris base	150g
Glycine	720g
Deionised water	10L

Glass plates were cleaved leaving the gel on the large plate. The stacking gel removed, the gel was briefly rinsed in transfer buffer. The membrane was apposed to the gel, excluding air bubbles. The wet Whatmann paper was put on the membrane and inverted on the wet scouring pad. The glass was then removed and another wet Whatmann paper and scouring pad were apposed to the gel. The gel and membrane in sandwich were placed in a cassette and then in a tank containing 1X transfer buffer, and a magnetic stirrer. Electrophoresis was run at 40V overnight at 4°C (the negative charge on the side of the gel and the positive charge on the side of the nitrocellulose membrane).

The membrane (or blot) was blocked for an hour with 5% dry milk (marvel) in PBS/Tween-20 0.1% (rocking, room temperature) to saturate non-specific protein binding sites in order to diminish the background staining. The blots were then incubated rocking for an hour at room temperature or overnight at 4°C with specific primary antibodies in 1% marvel/PBS (e.g. anti-Myc antibody 1/600 dilution, anti-IC2 antibody 1/500 dilution). The blots were then washed 3 times in PBS/Tween-20 0.1% and PBS, and incubated an additional hour with HRP-conjugated secondary antibodies in 1% marvel/PBS (e.g. HRP-conjugated goat anti-mouse antibody 1/1000 dilution, HRP-conjugated mouse anti-rabbit antibody 1/1500 dilution). After four washes in PBS/Tween-20 0.1% and PBS, the proteins were visualised by chemiluminescence (ECL), using super signal west Pico chemiluminescence substrate (Pierce). Membranes were then wrapped in Saran film, and in a dark room, a hyperfilm was apposed for chromogenic detection. Each exposed hyperfilm was immersed in developer, then fixer, for 2 to 3 minutes, and finally rinsed in water. Each band detected represents a protein.

e. Immunocytochemistry and immunostaining

Cos-7 cells were transfected with PlexinA1 and Neuropilin-1, and PlexinD1 expression vectors using Lipofectamine™2000 (Invitrogen) (refer to page 67). Fourty eight hours after transfection, cells were trypsinised and plated on coverslips placed in 24 well plates to achieve approximately 60% confluence the next day. Transfected cells were incubated for further 30 minutes at 37°C, with or without Semaphorin3A protein (4μg/mL) and Semaphorin3E (~4μg/mL). Experiments using Semaphorin3A protein were performed in serum free DMEM medium (DMEM/SF), while experiments using Semaphorin3E conditioned medium were performed in DMEM medium containing 3.2% FBS (DMEM/3.2%). Cells were gently washed with PBS twice (to remove PBS the plates were inverted onto a towel), and fixed on ice with paraformaldehyde 4% during 10 minutes. PFA was freshly prepared, made in PBS, heated in a water bath at 65°C to dissolve and

cooled at 4°C. Cells were then washed twice with PBS and immunostained. Blocking solution (2% horse serum in PBS) was added and put on a shaker for 20 minutes. The blocking solution removed, the cells were then incubated for 30 minutes at room temperature on a shaker with the primary antibody (dilution 1/100, except when mentioned otherwise). After three washes with PBS for 5 minutes each, on a shaker, the cells were incubated another 30 minutes with the secondary antibody (dilution 1/100) on a shaker at room temperature, covering with silver foil. Cells were washed three times in PBS and on a shaker and with silver foil cover. on a slide and the coverslips were mounted inverted onto the slide where a drop of vectastain DAPI conjugated (VectorLabs) was added. Coverslips were secured by putting nail varnish around the edge. Cells were observed under a microscope at 40X and 100X objective. Coverslips were done in triplicate, and the experiment was repeated twice giving the same results.

Controls with no primary antibody were performed for each condition and each experiment (results not always shown). Immunostaining was performed using phalloidin-TRITC-conjugated (8.3μL/2.3mL) to stain actin microfilaments in red, the primary monoclonal mouse antibody directed against active conformations of human β1 integrins (dilution 1/200), or the primary mouse monoclonal anti-vinculin antibody (dilution 1/400), or the primary mouse anti-Myc antibody, or the primary rabbit anti-VSV antibody, or the primary rabbit anti-HA antibody, and the secondary polyclonal rabbit anti-mouse FITC-conjugated antibody to stain in green, or the secondary donkey anti-mouse TRITC-conjugated antibody, or the secondary goat anti-rabbit TRITC-conjugated antibody to stain in red (refer to page 64).

f. Adhesion assay

Human embryonic kidney cells (HEK293 cells) were transfected with PlexinA1 and Neuropilin1 expression vectors, PlexinD1 expression vector, and sterile water (mock transfection) using Lipofectamine™2000 (Invitrogen) (refer to page 67). Adhesion assays were performed using the lid of a 96 well plate (Nunc), on which three different substrates (matrices) were coated (final concentration 20μg/mL). 80μL of each matrix, fibronectin, poly-L-Lysine, and PBS (negative control to check the cells do not adhere directly to the tissue culture plate) were applied to 3 wells of the lid of a 96 well plate. The lid was then carefully placed in a humidified chamber and left overnight at 4°C. The following day, each drop of matrix was aspirated, and the lid was flooded three times in PBS. The lid was dried by aspirating gently, before blocking at 37°C in the humidified chamber for

3h using a PBS solution containing 1% BSA. The lid was then washed three times in PBS and dried by aspiration. Cells at 70% confluence, fed the day before, were spin down and re-suspended in Optimem medium (Gibco) only. A solution of 10^4 cells/80µL drop was prepared. Sixty µL of cells were plated and incubated at 37°C in the humidified chamber for 10 minutes and 30 minutes in absence or presence of ligand Semaphorin3A (4µg/mL) or Semaphorin3E (~4µg/mL in conditioned medium). After three PBS washes, the lid was dried by aspiration. Unattached cells were washed off with PBS. Cells were then fixed for 20 minutes at room temperature with 4% paraformaldehyde, washed three times in PBS, and stained with 1% methylene blue for 1h at room temperature. The lid was washed twice in distilled water and left to dry overnight. The absorbance was measured on a plate reader. Each experiment was performed in triplicate and the results presented are the mean of three independent repeats with standard errors of the mean (SEM). ANOVA statistical analysis has been performed using GraphPad software (refer to page 81).

5. Statistical analysis

a. Mean and Standard Error of the Mean (SEM)

Experimental results of *in vitro* assays presented in this thesis were calculated as means of three independent repeats (n=3) with standard error of the mean (± SEM). The SEM is a measure of how far a sample mean is likely to be from the true population mean. The SEM is calculated by this equation: $SEM=SD/\sqrt{n}$, n=number of replicates. The standard deviation (SD) quantifies variability. $SD=\sqrt{[\Sigma(y_i-y_{mean})^2/N-1]}$, y_i=value i, y_{mean}=average, N=sample size. The SD quantifies scatter, i.e. how much the values vary from one another. With *in vitro* system with no biological variability, the scatter can only result from experimental imprecision, which is why we chose to present the data as means ± SEM. The SEM quantifies how accurately the mean was assessed. Mean, SD and SEM were calculated using Excel or GraphPad software.

ANOVA and T-tests statistical analysis are used routinely in many fields of science because they work well even if the sample distribution is only approximately Gaussian, which is the case of many kinds of biological data following a bell-shaped distribution. In this thesis, we assume that we have sampled data from populations that follow a Gaussian bell-shaped distribution and therefore used standard paired T-tests and ANOVA statistical analysis to measure the significance of the differences observed.

b. Paired T-test

Paired T-tests allow the comparison of two paired groups. Paired groups means that we are comparing two columns of matched data, i.e. repeated experiments. Paired T-tests calculate the difference between each set of pairs, and analyzes that list of differences. Two-tail pvalue were selected as they are usually more appropriate. Therefore, standard paired, two-tail T-test statistical analysis have been applied in this thesis using Excel or GraphPad software when comparing two groups for the same variable, for example the (q)RT-PCRs. Because of the small number of repeats (n=3), an effect was considered statistically significant at pvalue inferior to 0.05 (depicted as * in graphic presentations).

c. Analysis of Variance (two-way ANOVA)

Standard statistical two-way analysis of variance (two-way ANOVA) allows the comparison of three or more groups with data categorized in two ways. The two-way ANOVA determines how a response is affected by two factors, by comparing the differences among group means with the pooled standard deviations of the groups. Two-way ANOVA compares the means.

Two-way ANOVA has been applied using GraphPad software when testing the effects of 2 different conditions (± serum and ± Semaphorin4D) on the migration of cells (Cos or NIH3T3 cells transfected with wild-type or mutant forms of PlexinB1), or when testing the effects of different proteins (Semaphorin3E and Semaphorin3A) on the adhesion of cells transfected with different receptors (PlexinA1/Neuropilin1 and with PlexinD1) on different substrates (Poly-L-Lysine, fibronectin). An effect was considered statistically significant at pvalue inferior to 0.001.

CHAPTER 3: RESULTS

Section 1: Expression profiling of semaphorins and their receptors in prostate cell lines and hypoxia-induced regulation of secreted semaphorins gene expression

Semaphorins are chemotactic guidance cues playing crucial roles orchestrating cellular movement. Since their first identification in the early 90s' in the developing nervous system, semaphorins have been reported to be expressed in many other tissues and organs, including the immune and vascular systems, where they play major roles (for reviews see Bismuth and Boumsell, 2002; Moretti et al., 2006; Eichmann et al., 2005). Recently, semaphorins have also been implicated in tumour cell migration and invasion, and in tumour angiogenesis by controlling integrin function (Serini et al., 2003; for reviews see Neufeld et al., 2005; Chedotal, 2007; Pan et al., 2007).

Plexins and neuropilins are high affinity receptors for semaphorins. Plexins are guidance receptors, signalling through interaction with small GTPases (Rho, Rac, Ras). Neuropilins are also co-receptors for vascular endothelial growth factors (VEGF-A isoforms), which control angiogenesis (Neufeld et al., 2002; Chen et al., 2005). There are few studies which highlight the importance of neuropilins and VEGFs in prostate cancer tissues and cell lines, by showing variation in expression levels of these molecules in tumour angiogenesis (Latil et al., 2000; Miao et al., 2000). However, there are no studies at present showing the presence of secreted semaphorins and their receptors, in normal or diseased prostate. The aim of this chapter is therefore to study the distribution of semaphorins and their receptors in prostate cell lines.

Most human cancers become life threatening as a result of metastasis, and although it is well documented that prostate cancer preferentially metastasises to the bone (Bubendorf et al., 2000; Rubin et al., 2000), it is still unclear how and why it occurs. The scatter factor receptor MET, a member of the sema domain containing superfamily which controls the invasive growth program, has been reported to be overexpressed in prostate cancer (Pisters et al., 1995). However, attempts to link HGF/MET signalling to the metastatic abilities of prostate tumour cells have not yet been successful. The receptor for the chemokine CXCL12, CXCR4 has also been reported to be overexpressed in cells derived from prostate cancer metastases (Araya et al., 2004). CXCR4 controls the homing of breast tumour cells to the bone (Kang et al., 2003). None of the theories suggested, however, is sufficient on its own

to explain the progression of prostate cancer and spread to other organs (Tantivejkul et al., 2004; Yin et al., 2005).

Moreover, regions of decreased oxygenation are frequent within solid tumours, and the transcription factor HIF1 (hypoxia inducible factor 1) is a key mediator of hypoxic responses. Under normoxic conditions HIF1α (the subunit regulating HIF1 transcriptional activity) is subject to ubiquitination and proteosomal degradation, which are inhibited under hypoxic conditions (Semenza, 2001). Overexpression of HIF1α has been detected in many invasive cancers as well as in their regional and distant metastases, whereas normal tissues and non-invasive benign tumours do not overexpress HIF1α (Zhong et al., 1999). In prostate, HIF1α has been reported to be overexpressed in high-grade PIN, primary tumours and regional and distant lymph node and bone metastases, whereas normal prostate tissue and benign hyperplasic tissue (BPH) do not overexpress HIF1α (Du et al., 2003; Hao et al., 2004). HIF1 activates the transcription of genes promoting tumour cell growth (glucose transporters and glycolytic enzymes), adhesion, migration, and organ specific metastasis (CXCR4 receptor), invasion (scatter factor receptor MET), and vasculature remodelling and neoangiogenesis (VEGF-As) (Pennacchietti et al., 2003, Staller et al., 2003; Kang et al., 2003 ; Ferrara et al., 2003). To date there are no studies showing that the transcription of secreted semaphorin genes is regulated by hypoxia in cancer and metastases. The aim of this chapter is to study the effects of hypoxia on secreted semaphorins gene expression.

In order to investigate the possible roles of semaphorin signalling in normal prostate homeostasis, prostate cancer progression, metastasis and angiogenesis, the expression profiles of secreted semaphorins and their receptors, plexins and neuropilins, as well as those of vascular endothelial growth factor (VEGF-A isoforms) have been studied by RT-PCR in prostate cell lines derived from a benign hyperplasic (BPH) epithelia (Pre2.8) and stroma (S2.13), a primary tumour (1542CPTX or 42C), the matched non-neoplastic epithelium (1542NPTX or 42N) and stroma (1542FT or 42F) and a metastasis to the bone (PC3), the brain (DU145) and the lymph node (LNCaP). RT-PCR products were verified by sequencing (refer to page 70); all were the correct sequence (see Appendix 1). Also, in order to assess whether hypoxia controls the transcription of secreted semaphorin genes, their expression profiles have been studied in matched non-neoplastic and primary tumour derived prostate cell lines and in a colon cancer cell line following hypoxic conditions. The same

amount of RNA was used for all reactions and GAPDH control was used to ensure equal amounts of RNA was analysed between samples.

1. Expression profiles of semaphorins in 10 prostate cell lines following normoxic conditions

The presence of messenger RNA for secreted semaphorins 3a, 3b, 3c, 3e, 3f, and for transmembrane semaphorin 4d have been assayed by RT-PCR in 10 prostate cell lines. Figure 19 is the presentation of one representative agarose gel.

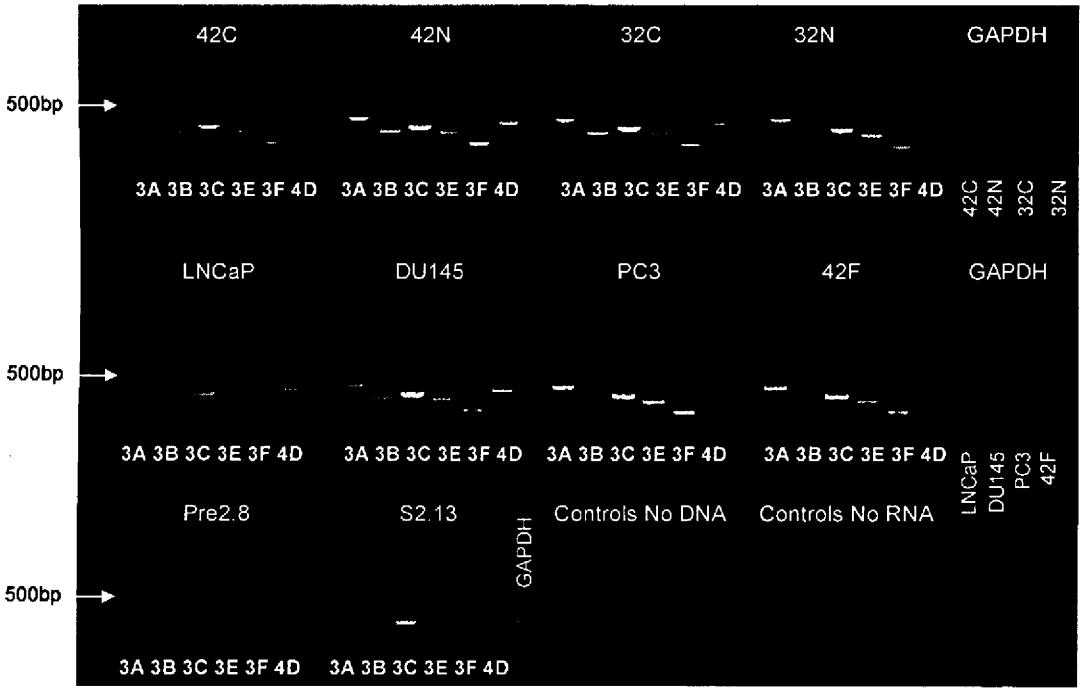

Figure 19: Semaphorins mRNA expression profiles (RT-PCR) in 10 prostate cell lines, derived from primary tumours (1542CPTX or 42C, and 1532CPTX or 32C), the matched non-neoplastic "normal" epithelia (1542NPTX or 42N and 1532NPTX or 32N) and stroma (1542FTX or 42F), metastases to the lymph node (LNCaP), the brain (DU145) and the bone (PC3), and benign hyperplastic epithelia (Pre2.8) and stroma (S2.13). The Glycerol-3-phosphate dehydrogenase (GAPDH) housekeeping gene shows approximately equal levels of total RNA between samples.

RT-PCRs were performed in triplicate, on three different RNA extractions (from three consecutive passages) for each of the 10 prostate cell lines. The results presented below are normalised means with standard errors of the mean (SEM). Band intensities for each gene, obtained using the Syngene software, have moreover been normalised to the expression levels found in the non-neoplastic ("normal") prostate epithelial cell line (42N=1). Expression levels found in the non-neoplastic prostate epithelial cell line 1542NPTX (42N) were chosen as a reference of normal expression throughout. These non-neoplastic ("normal") cells were isolated from a

normal area of the prostate of a patient with localised carcinoma (Bright et al., 1997). Standard T-test statistical analysis was applied using Excel software (*: significant=<0.05). The expression levels obtained for semaphorin 4d are the results of one triplicate experiment; no statistical analysis was applicable. Moreover, semaphorin 4d PCR product was not sequenced, and thus it will not be discussed in this thesis.

The results in figure 19 (summarised in table 7) show that messenger RNA for semaphorins 3a, 3b, 3c, 3e, 3f, and 4d are ubiquitously synthesised, although at various levels, in the 10 prostate cell lines tested.

Origin	Matched non-neoplastic ("normal")		Matched primary tumour	Benign hyperplastic prostate (BPH)		Metastasis to the		
Derived cell line	Epithelia (1542NPTX or 42N)	Stroma (1542FTX or 42F)	Epithelia (1542CPTX or 42C)	Epithelia (Pre2.8)	Stroma (S2.13)	Lymph node (LNCaP)	Brain (DU145)	Bone (PC3)
Semaphorin 3a	1	1.3±0.2	0.4±0.1	0.4±0.2	0.7±0.1	0	0.6±0.3	1±0.4
Semaphorin 3b	1	1±0.3	0.5±0.1	0.3±0.3	0.7±0.3	0.1±0.2	0.5±0.3	0.3±0.2
Semaphorin 3c	1	1.3±0.1	0.7±0.1	0.8±0.4	1±0.2	0.3±0.2	0.7±0.3	0.7±0.3
Semaphorin 3e	1	1.3±0.1	1±0.4	1±0.4	0.7±0.1	0.1±0.2	0.6±0.2	1.1±0.4
Semaphorin 3f	1	0.7±0.1	0.6±0.2	0.7±0.2	0.6±0.05	0.6±0.1	0.8±0.1	1±0.3
Semaphorin 4d	1	0.4	0.4	0.5	0.6	0.9	1	0.2
Neuropilin1	1	1.6±0.1	0.8±0.2	0.3±0.1	0.5±0.2	0.8±0.1	1.1±0.3	1.5±0.05
Neuropilin2	1	1.3±0.1	0.3±0.2	0.3±0.1	0.5	0.1±0.05	0.6±0.1	0.7±0.1
Plexina1	1	0.6±0.07	0.3±0.2	0.2±0.2	0.3±0.3	0.1±0.05	0.6±0.05	1.1±0.2
Plexina2	1	0.2±0.1	0.5±0.2	0.3±0.1	0.3±0.2	0.1±0.05	0.4±0.2	0.5±0.2
Plexina3	1	0.3±0.2	0.5±0.2	0.3±0.1	0.4±0.1	0.4±0.05	1±0.2	0.8±0.3
Plexinb1	1	0.2±0.07	0.9±0.2	0.5±0.1	0.3±0.1	0.5±0.1	0.8±0.2	0.7±0.05
Plexinb3	1	0.4±0.1	0.9±0.3	0.5±0.05	1	0.9±0.3	1.2±0.05	1.9±0.1

Table 7: Fold change in semaphorins and their receptors, plexins and neuropilins, gene expression in 8 prostate cell lines (RT-PCR). Expression levels found in the non-neoplastic ("normal") prostate epithelial cell line 1542NPTX (42N) were chosen as a reference of normal expression (expression=1, grey colour). The results presented are normalised mean (to 42N expression levels) with standard error of the mean (± SEM). The green colour indicates a significant decrease in expression level; the stronger the shading the stronger the decrease. The red colour indicates a significant increase in expression level; the stronger the shading the stronger the increase. When the increase or decrease was not significant, or when there was no change in expression level or when no statistical analysis was performed, no colour was applied.

The results in figure 20 show that in the fibroblast cell line 1542FTX (42F) derived from non-neoplastic ("normal") prostate, mRNA expression levels of secreted semaphorins 3a, 3c, and 3e are increased by 1.3 fold, while those of semaphorin 3f are decreased by 0.7 fold, compared to the levels found in the epithelial counterpart (42N). Semaphorin 3b mRNA expression levels are not changed. The results suggest that expression levels of most secreted semaphorins are higher in cells of stromal origin than of epithelial origin in non-neoplastic ("normal") prostate.

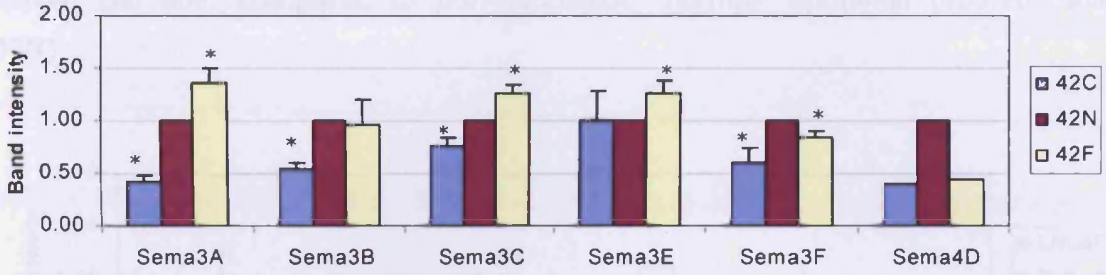

Figure 20: Semaphorins mRNA expression profiles (RT-PCR) in prostate cell lines derived from a primary tumour (1542CPTX or 42C, blue) and the matched non-neoplastic ("normal") epithelia (1542NPTX or 42N, purple) and stroma (1542FTX or 42F, yellow). Results are normalised mean (to 42N expression levels) of tree independent experiments with standard error of the mean (SEM). Standard T- test has been applied (*: significant change :< 0.05).

In the prostate primary tumour derived epithelial cell line 1542CPTX (42C), mRNA expression levels of semaphorins 3a, 3b, 3c, and 3f, are decreased by 1.4 to 2 fold, compared to expression levels found in the "normal" prostate cell lines of epithelial (42N) and stromal (42F) origins (figure 20). In contrast, semaphorin 3e mRNA expression levels in the primary tumour derived cell line (42C) are not changed compared to non-neoplastic "normal" epithelial levels (42N). The results suggest that expression levels of most secreted semaphorins are decreased in the primary tumour cell line, except those of semaphorin 3e, which remain similar to expression levels found in the non-neoplastic "normal" prostate epithelial cell line.

The results in figure 21 shows that in the prostate cancer cell line derived from a lymph node metastasis (LNCaP), mRNA expression levels of all secreted semaphorins are strongly decreased, compared to non-neoplastic "normal" epithelial levels (42N). Expression levels of semaphorins 3f and 3c mRNA are decreased by respectively 1.6 and 3 fold, and those of semaphorins 3b and 3e are decreased by 10 fold. No mRNA could be detected for semaphorin 3a. The results suggest that expression levels of secreted semaphorins are strongly decreased in the prostate cancer cell line derived

from a lymph node metastasis, compared to "normal" epithelial (42N) and stromal (42F) levels.

In the prostate cancer cell line derived from a brain metastasis (DU145), mRNA expression levels of transmembrane semaphorin 4d are similar to that found in the non-neoplastic "normal" epithelial cell line 42N (figure 21); while expression levels of secreted semaphorins are decreased by 1.25 to 2 fold (although it is not always significant). The results suggest that expression levels of secreted semaphorins are decreased in the brain metastasis derived cell line, like in the lymph node metastasis derived cell line, compared to non-neoplastic "normal" epithelial prostate levels (42N).

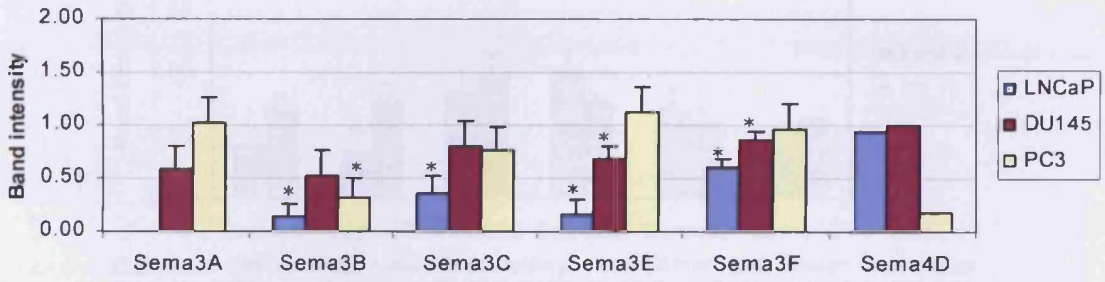

Figure 21: Semaphorins mRNA expression profiles (RT-PCRs) in prostate cancer cell lines derived from a lymph node metastasis (LNCaP), a brain metastasis (DU145), and a bone metastasis (PC3). Results are normalised mean (to 42N expression levels) of three independent experiments with standard error of the mean (SEM). Standard T- test has been applied (*: significant change :< 0.05).

In the prostate cancer cell line derived from a bone metastasis (PC3), mRNA expression levels of semaphorins 3a, 3e and 3f remain similar to non-neoplastic "normal" epithelial levels (42N), while those of semaphorin 3c are decreased by 1.4 fold and those of semaphorin 3b are strongly decreased by 3 fold (figure 21). The results suggest that in the bone metastasis derived cell line, expression levels of semaphorins 3a, 3e and 3f, unlike the other semaphorins, remain similar to non-neoplastic "normal" epithelial levels (42N).

The results in figure 22 show that in the prostate epithelial cell line (Pre2.8) derived from benign prostate hyperplasia (BPH), mRNA expression levels of semaphorins 3a, 3b, an 3f are decreased by 1.2 to 3 fold, compared to non-neoplastic "normal" epithelial expression levels (42N). In contrast, expression levels of semaphorins 3c and 3e remain equal to "normal" epithelial levels (42N). The results suggest that expression levels of semaphorins, except those of semaphorins

3c and 3e, are decreased in the epithelial cell line derived from BPH, compared to the epithelial cell line derived from non-neoplastic "normal" prostate.

In the prostate stromal cell line derived from BPH (S2.13), mRNA expression levels of semaphorins 3a, 3b, 3e, and 3f are decreased by 1.4 to 1.6 fold, compared to the levels found in the non-neoplastic "normal" epithelial cell line 42N, while those of secreted semaphorin 3c remain similar to 42N levels (figure 22). The results suggest that expression levels of semaphorins, except those of semaphorin 3c, are decreased in the stromal cell line derived from BPH, compared to the epithelial and stromal cell lines derived from non-neoplastic "normal" prostate.

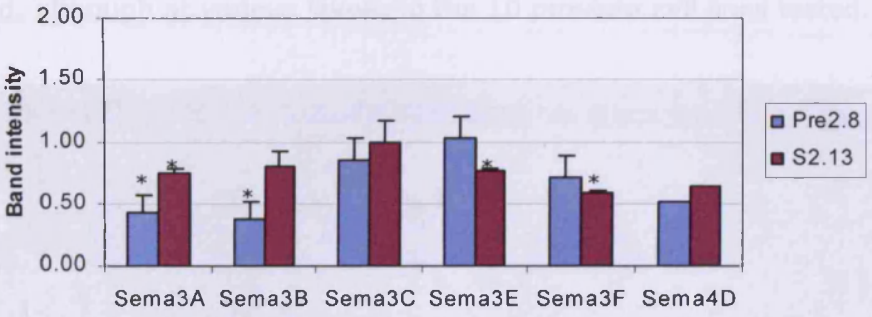

Figure 22: Semaphorins mRNA expression profiles (RT-PCR) in benign hyperplasic prostate (BPH) cell lines of epithelial origin (Pre2.8) and stromal origin (S2.13). Results are normalised mean (to 42N expression levels) of three independent experiments with standard error of the mean (SEM). Standard T- test has been applied (*: significant change :< 0.05).

The results in figure 22 also show that semaphorins mRNA expression profiles in the stromal cell line (S2.13) derived from BPH tend to be higher than in the epithelial counterpart (Pre2.8), like in the cell lines derived from non-neoplastic "normal" prostate, except for semaphorins 3e and 3f, which are more highly expressed in BPH derived epithelial cells than in their stromal counterpart.

2. Expression profiles of plexins and neuropilins in 10 prostate cell lines following normoxic conditions

Plexins and neuropilins are high affinity receptors for semaphorins. The mRNA expression profiles of plexins a1, a2, a3, b1 and b3 and neuropilins 1 and 2 have been assayed by RT-PCR in 10 prostate cell lines. Figure 23 is the presentation of one representative agarose gel.

RT-PCRs were performed in triplicate, on three consecutive RNA extractions (from three different passages) for each of the 10 prostate cell lines. The results presented below are normalised means with standard errors of the mean (SEM). Thus, band intensities have been normalised for each gene to the expression levels found in the non-neoplastic ("normal") prostate epithelial cell line (42N=1). Expression levels found in the non-neoplastic "normal" prostate epithelial cell line 1542NPTX (42N) were chosen as a reference of normal expression throughout. Standard T-test statistical analysis was applied using Excel software (*: significant=<0.05).

The results in figure 23 (summarised in table 7) show that messenger RNA for neuropilins 1 and 2, and for plexins a1, a2, a3, b1 and b3 are ubiquitously synthesised, although at various levels, in the 10 prostate cell lines tested.

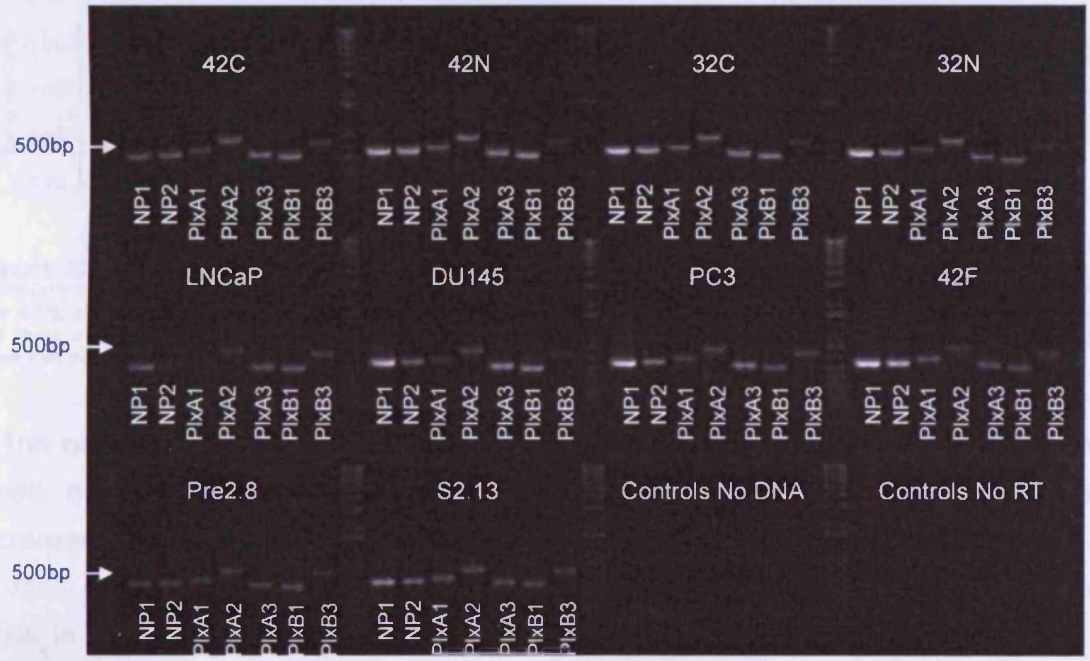

Figure 23: Plexins and neuropilins mRNA expression profiles (RT-PCR) in 10 prostate cell lines, derived from primary tumours (1542CPTX or 42C, and 1532CPTX or 32C), the matched non-neoplastic "normal" epithelia (1542NPTX or 42N and 1532NPTX or 32N) and stroma (1542FTX or 42F), metastases to the lymph node (LNCaP), the brain (DU145) and the bone (PC3), and benign hyperplasic epithelia (Pre2.8) and stroma (S2.13). NP: neuropilin; Plx: plexin.

The results in figure 24 show that in the fibroblast cell line derived from non-neoplastic "normal" prostate (42F), mRNA expression levels of neuropilins 1 and 2 are increased by 1.4 and 1.6 fold, while those of plexins class A (a1, a2, a3) and class B (b1, b3) are decreased by 1.6 to 5 fold, compared to the levels found in the epithelial counterpart (42N). The results suggest that, like semaphorins, neuropilins expression levels are higher in cells of stromal origin than of epithelial origin in non-

neoplastic "normal" prostate, whereas the contrary is observed for plexins expression levels, which are higher in normal epithelial cells than in stromal cells.

In the prostate primary tumour derived epithelial cell line (42C), mRNA expression levels of neuropilin 2 are decreased by 5 fold (figure 24), compared to "normal" epithelial levels (42N). Expression levels of plexins class A (a1, a2, a3) are also decreased by 2 to 3 fold, while those of class B (b1, b3) remain equal to "normal" levels (42N), and those of neuropilin 1 are not significantly changed. The results suggest that, unlike those of class B plexins, mRNA expression levels of class A plexins and neuropilin 2 are decreased in the prostate primary tumour derived cell line, compared to non-neoplastic derived cell line.

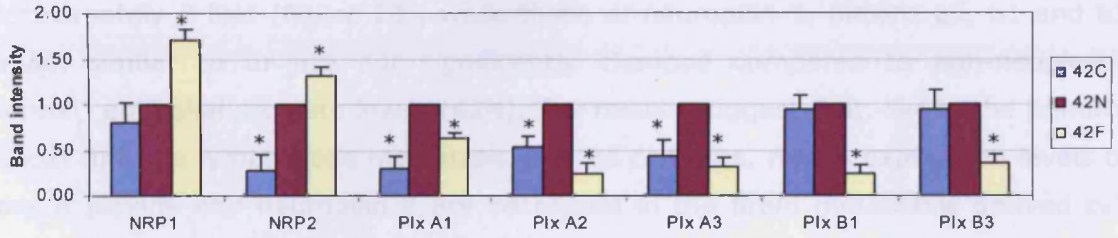

Figure 24: Plexins and neuropilins mRNA expression profiles (RT-PCR) in prostate cell lines derived from a primary tumour (1542CPTX or 42C, blue) and the matched non-neoplastic ("normal") epithelia (1542NPTX or 42N, purple) and stroma (1542FTX or 42F, yellow). Results are normalised means (to 42N expression levels) of three independent experiments with standard error of the mean (SEM). NRP: neuropilin; Plx: plexin. Standard T-test has been applied (*: significant change :< 0.05).

The results in figure 25 show that in the prostate cancer cell line derived from a lymph node metastasis (LNCaP), mRNA expression levels of neuropilin 2 are decreased by 10 fold, those of class A plexins (a1, a2, a3) are decreased by 2.5 to 10 fold, and those of plexin b1 are decreased by 2 fold, compared to expression levels in 42N cells. In contrast, mRNA expression levels of plexin b3 are similar to "normal" expression levels (42N), and primary tumour levels (42C), and those of neuropilin 1 are not significantly changed. The results suggest that, like in the primary tumour cell line, mRNA expression levels of class A plexins and neuropilin 2 are decreased in the lymph node metastasis derived cell line, compared to non-neoplastic "normal" prostate epithelial levels (42N).

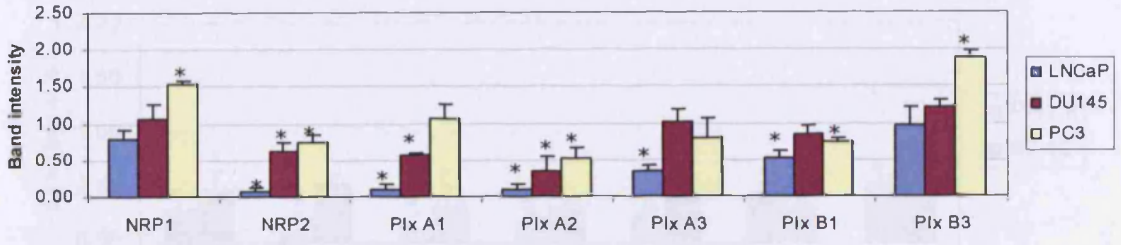

Figure 25: Plexins and neuropilins mRNA expression profiles (RT-PCR) in prostate cancer cell lines derived from a lymph node metastasis (LNCaP), a brain metastasis (DU145), and a bone metastasis (PC3). Results are normalised means (to 42N expression levels) of three independent experiments with standard error of the mean (SEM). NRP: neuropilin; Plx: plexin. Standard T- test has been applied (*: significant change :< 0.05).

In the prostate cancer cell line derived from a brain metastasis (DU145), mRNA expression levels of neuropilin 2 and plexins a1 and a2 are decreased by approximately 2 fold (figure 25), while those of neuropilin 1, plexins a3, b1 and b3 remain similar to or are not significantly changed compared to non-neoplastic "normal" epithelial prostate levels (42N). The results suggest that, like in the primary tumour and the lymph node metastasis derived cell lines, mRNA expression levels of class A plexins and neuropilin 2 are decreased in the brain metastasis derived cell line, compared to non-neoplastic "normal" levels (42N), except for plexin a3, whose levels are unchanged.

In the prostate cancer cell line derived from a bone metastasis (PC3), mRNA expression levels of neuropilin 1 are increased by 1.5 fold (figure 25), while those of neuropilin 2 are decreased by 1.4 fold, compared to non-neoplastic "normal" levels (42N). Plexins a2 and b1 mRNA expression levels are also decreased by 1.2 to 1.5 fold, while those of plexin a1 and a3 remain "normal", and those of plexin b3 are increased by 1.9 fold compared to the levels found in non-neoplastic "normal" epithelial cells (42N). The results suggest that in the bone metastasis derived cell line, like in the cell lines derived from a primary tumour, a lymph node and a brain metastases, neuropilin 2 and plexin a2 mRNA expression levels are decreased, compared to non-neoplastic "normal" epithelial levels. Interestingly, plexin a1 mRNA expression levels remain "normal", and those of plexin a3 are not significantly changed. Moreover, neuropilin 1 and plexin b3 expression levels are increased in the bone metastasis derived cell line, compared to the other metastases derived cell lines (lymph node and brain), the primary tumour and the matched non-neoplastic "normal" epithelial cell lines.

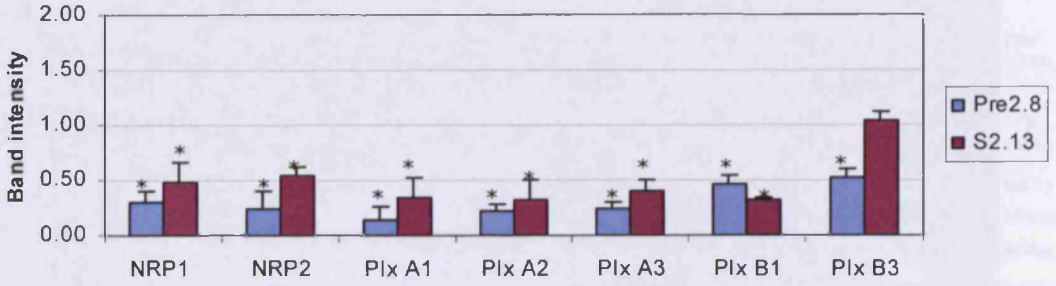

Figure 26: Plexins and neuropilins mRNA expression profiles (RT-PCR) in benign hyperplasic prostate (BPH) cell lines of epithelial origin (Pre2.8) and stromal origin (S2.13). Results are normalised means (to 42N expression levels) of three independent experiments with standard error of the mean (SEM). NRP: neuropilin; Plx: plexin. Standard T- test has been applied (*: significant change :< 0.05).

The results in figure 26 show that in the prostate epithelial cell line (Pre2.8) derived from benign prostate hyperplasia (BPH), as well as in the stromal counterpart (S2.13), mRNA expression levels of all plexins and neuropilins are strongly decreased by 2 to 5 fold, compared to non-neoplastic "normal" epithelial levels (42N), except for plexin b3, whose levels remain similar to "normal" levels in S2.13 cells. In contrast to the levels found in stromal cells from non-neoplastic "normal" prostate (42F), where expression levels of both neuropilins are increased by 1.5 fold, they are decreased by 2 fold in the BPH derived stromal cell line. Inversely, plexin b3 mRNA levels are strongly decreased in the stromal cell line derived from non-neoplastic "normal" prostate (42F), while they remain similar to 42N levels in the stromal cell line derived from BPH (S2.13). The results suggest that plexins and neuropilins mRNA expression profiles are strongly decreased in both epithelial and stromal cell lines derived from BPH.

3. Expression profiles of vascular endothelial growth factor (VEGF-A isoforms) in 10 prostate cell lines following normoxic conditions

The presence of mRNA for three isoforms of vascular endothelial growth factor A, $vegf_{206}$, $vegf_{189}$ and $vegf_{165}$, have been assayed by RT-PCR, in 10 prostate cell lines. Figure 27 is the presentation of one representative agarose gel. Band intensities were not measured as the aim of this experiment was to identify the different vegf isoforms present in prostate cell lines, as well as to see if vegf was expressed in prostate cancer cell lines before we could use it as a control in subsequent hypoxia experiments.

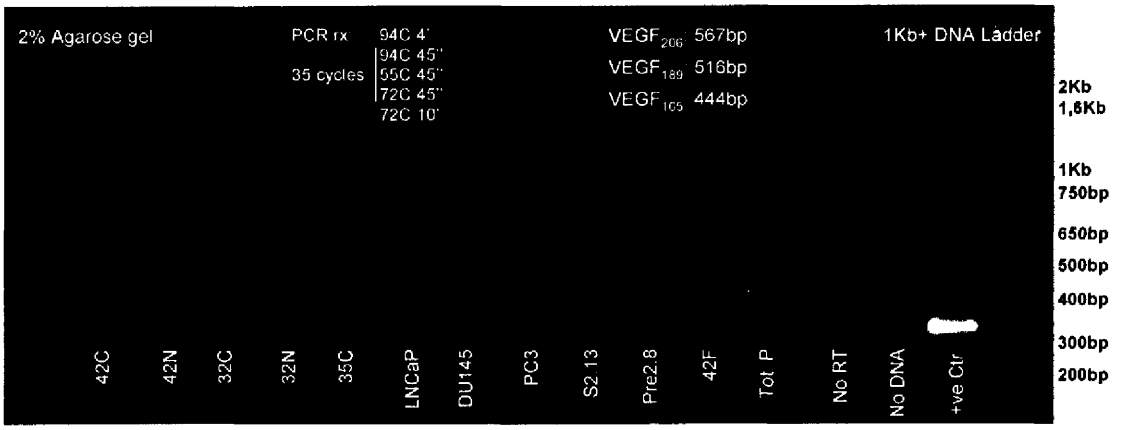

Figure 27: Vascular endothelial growth factor A isoforms mRNA expression profiles (RT-PCR) in 10 prostate cell lines, derived from primary tumours (1542CPTX or 42C, and 1532CPTX or 32C), the matched non-neoplastic ("normal") epithelia (1542NPTX or 42N and 1532NPTX or 32N) and stroma (1542FTX or 42F), metastases to the lymph node (LNCaP), the brain (DU145) and the bone (PC3), and benign hyperplasic epithelia (Pre2.8) and stroma (S2.13), as well as in total RNA prostate extract (Tot.P) and in a positive control provided by the manufacturer (+ve).

The results in figure 27 show that messenger RNA for vascular endothelial growth factor isoform $VEGF_{206}$ is undetectable in the 10 prostate cell lines tested, which is consistent with the expression profile found in total prostate RNA extract. In contrast, the other two vascular endothelial growth factor A isoforms, $VEGF_{165}$ and $VEGF_{189}$, are synthesised by most prostate cell lines, although at various levels. Nine out of the 10 prostate cell lines tested synthesise mRNA for the predominant isoform of vascular endothelial growth factor $VEGF_{165}$, and 6 out of 10 synthesise mRNA for the other isoform $VEGF_{189}$. Noticeably, in the prostate cancer cell line derived from a brain metastasis (DU145), no messenger RNA for VEGF-A isoforms is detected.

Stromal cells, whether from non-neoplastic "normal" prostate (42F) or benign prostate hyperplasia (BPH) (S2.13) do not synthesise mRNA for $VEGF_{189}$ isoform, but do synthesise mRNA for the predominant isoform, $VEGF_{165}$, although at much lower levels than in their respective epithelial counterparts (42N and Pre2.8). BPH derived epithelial cells (Pre2.8) only synthesise mRNA for the predominant $VEGF_{165}$ isoform, whereas non-neoplastic "normal" epithelial cells (42N) express mRNA for both $VEGF_{165}$ and $VEGF_{189}$ isoforms.

Both prostate cell lines derived from two primary tumours (42C and 32C) and their matched non-neoplastic "normal" epithelia (42N and 32N) express both $VEGF_{165}$ and $VEGF_{189}$ isoforms of vascular endothelial growth factor-A. The predominant isoform in the primary tumour cell lines is $VEGF_{165}$, while it is $VEGF_{189}$ in the matched non-neoplastic "normal" epithelial cell lines.

Both $VEGF_{165}$ and $VEGF_{189}$ isoforms are detected in the lymph node metastasis (LNCaP) and bone metastasis (PC3) derived cell lines, and in both cases, $VEGF_{165}$ is the predominant isoform. No messenger RNA, for any of the three isoforms of VEGF tested, is detectable in the prostate cancer cell line derived from a brain metastasis (DU145).

The results suggest that the 10 prostate cell lines tested synthesise mRNA for vascular endothelial growth factor-A, except the cell line derived from a brain metastasis. In all the cell lines tested, the predominant isoform of vascular endothelial growth factor-A detected is $VEGF_{165}$, except in the non-neoplastic "normal" epithelial cell lines, where the predominant isoform is $VEGF_{189}$. Additionally, benign hyperplastic prostate epithelial and stromal cell lines synthesise mRNA only for the predominant isoform $VEGF_{165}$. Also, non-neoplastic "normal" stromal prostate cells synthesise messenger RNA only for $VEGF_{165}$, while their epithelial counterpart synthesise mRNA for the predominant isoform and also for $VEGF_{189}$ isoform. Finally, both isoforms $VEGF_{165}$ and $VEGF_{189}$ are synthesised by cells derived from a prostate primary tumour, a lymph node and a bone metastases.

4. Search for HIF-responsive elements (HRE) within the promoter regions of secreted semaphorin genes

In order to assess the susceptibility of secreted semaphorin genes to hypoxia, their genomic sequences have been screened for the presence of HIF-responsive elements (HRE), whose consensus sequence is RCGTG (where R=A or G). A single HRE is necessary but not sufficient to efficiently activate gene transcription in response to hypoxia. A fully functional HRE thus usually contains neighbouring DNA sites for additional transcription factors, which may confer tissue-restricted activity to the HRE. Tandemly arrayed HREs can also form functional HIF responsive elements (for a review see Wenger et al., 2005). Screened promoter sequences were obtained from the NCBI website (refer to page 71).

The results in table 8 show that the vegf promoter region contains many HRE motifs, 10 in total, among which only one of them has been shown to be functional (Wenger et al., 2005). Equally, secreted semaphorin genes contain several HRE motifs, although their functionality also needs to be confirmed. Surprisingly, among secreted semaphorins, only one gene, semaphorin 3d, does not exhibit any HIF responsive elements in the promoter region. The semaphorin 3f gene possesses four

HRE, semaphorins 3b and 3c genes five, and semaphorins 3a and 3e genes seven. Interestingly, semaphorin 3e gene presents two tandemly arrayed HRE, which may form functional HIF1 responsive elements. These preliminary results raise the possibility that most secreted semaphorins may be sensitive to hypoxia-induced HIF1-dependent transcriptional activation.

Gene Name	HREs number and location						Intron 1	
	5'Flanking		5'UTR + Exon		Intron 1		Total length	Length screened
	gcgtg	acgtc	gcgtg	acgtc	gcgtg	acgtc		
Sema3a	3	0	0	0	3	1	19800bp	All
Sema3b	2	0	0	0	2	1	777bp	All
Sema3c	2	3	0	0	0	0	2000bp	All
Sema3d	0	0	0	0	0	0	?	All
Sema3e	0	2	1	0	0	0	158,153bp	4900bp
					4	0		30,900bp
Sema3f	0	3	0	0	1	0	?	All
Vegf	2	2	2	0	4	0	3028bp	All

Table 8: Number and location of HIF responsive elements (HREs) within secreted semaphorins (Sema3) and vascular endothelial growth factor (Vegf) genes. HRE consensus sequence is RCGTG (Wenger et al., 2005). The promoter regions screened ranged from 3,000bp upstream of the transcription start site, to exon 1, which includes the 5'UTR, and intron 1. UTR: untranslated region. Sequences were obtained from NCBI, and screened using the search tool from Word software.

5. Expression profiles of secreted semaphorins and vascular endothelial growth factor (VEGF) in prostate and colon cell lines following hypoxia for 24h and 48h

The matched prostate primary tumour derived cell line 42C, and its non-neoplastic "normal" counterpart, the epithelial cell line 42N, as well as the colon cancer cell line HT29 have been incubated in a hypoxic incubator for 24h and 48h. Subsequently, mRNA expression profiles of secreted semaphorins 3a, 3b, 3c, 3e, and 3f have been assayed by RT-PCR. Presented data (figure 28) are the results of one representative RT-PCR. RT-PCRs were performed in triplicate, and repeated three times. The results presented below are normalised means with standard errors of the mean (SEM). Thus, band intensities have been normalised for each gene to the expression levels found in the non-neoplastic ("normal") prostate epithelial cell line at 0h (42N/0h=1), or for figure 32 to the levels found in the primary tumour cell line at 0h (42C/0h=1), and for figure 33 to the levels found in the colon cancer cell line at 0h (HT29/0h=1). Standard T-Test statistical analysis was applied using Excel software (*: significant=<0.05).

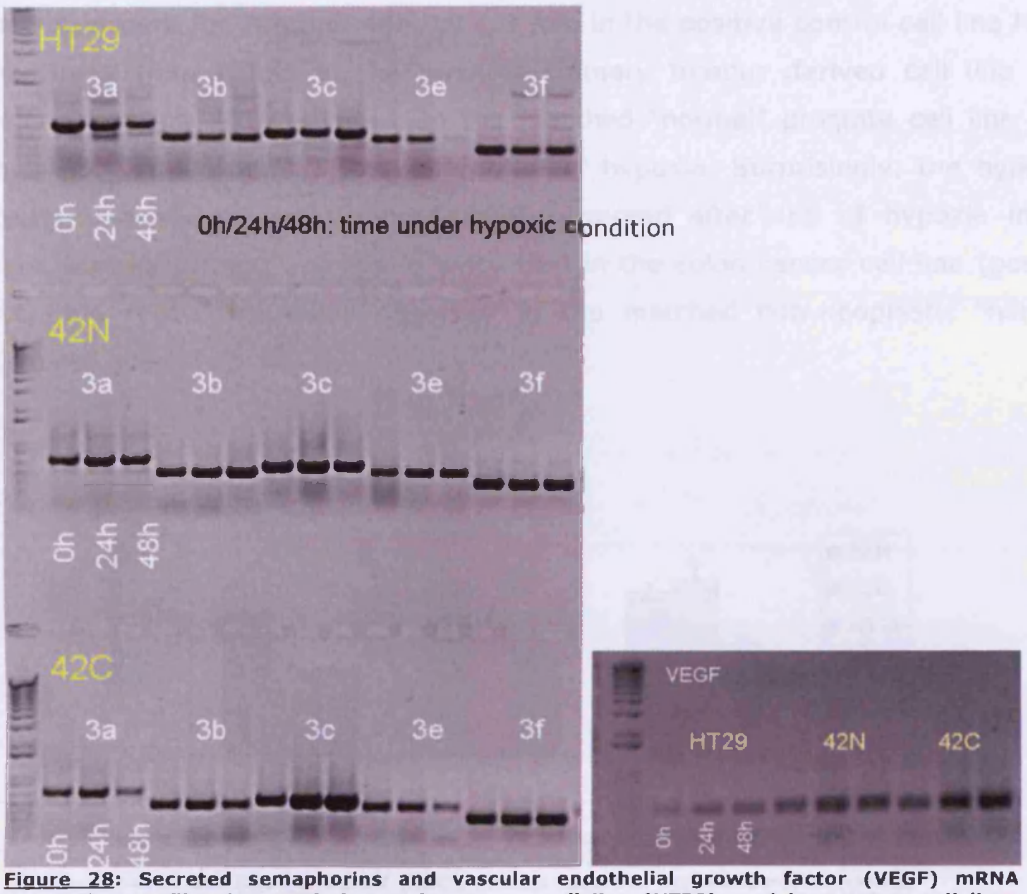

Figure 28: Secreted semaphorins and vascular endothelial growth factor (VEGF) mRNA expression profiles (RT-PCR), in a colon cancer cell line (HT29), and in prostate cell lines derived from a primary tumour (1542CPTX or 42C), and the matched non-neoplastic "normal" epithelia (1542NPTX or 42N), following hypoxia for 24h and 48h.

The results in figure 28 show that, in the colon cancer cell line HT29, the levels of vascular endothelial growth factor (VEGF) mRNA increases after 24h and 48h of hypoxic conditions as expected, providing a positive control. The results also show that mRNA for secreted semaphorins 3a, 3b, 3c, 3e, and 3f are synthesised, in HT29 cells, at much higher levels than those of VEGF, which is also observed in the prostate cell lines (42N and 42C). Generally, the results suggest that VEGF and secreted semaphorin expression levels are largely regulated by hypoxic conditions.

a. Expression profile of VEGF in prostate and colon cell lines following hypoxia for 24h and 48h

The results in figure 29 and 30 (summarised in table 9) show that in normoxic conditions, VEGF mRNA expression levels are identical in both prostate and colon cancer cell lines and significantly lower than in the non-neoplastic "normal" prostate cell line (42N). VEGF mRNA expression levels progressively increase, following

hypoxic treatment for 24h and 48h, by 1.3 fold in the positive control cell line HT29, and by more than 2 fold in the prostate primary tumour derived cell line 42C, whereas there is a slight increase in the matched "normal" prostate cell line 42N, which is not significant (1.1 fold) after 48h of hypoxia. Surprisingly, the hypoxia-induced transcriptional activation of VEGF observed after 48h of hypoxia in the prostate primary tumour cell line is twice that in the colon cancer cell line (positive control) and reach the levels observed in the matched non-neoplastic "normal" prostate cell line.

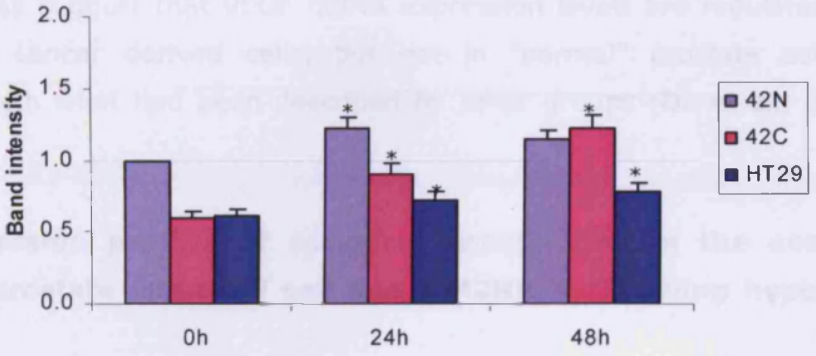

Figure 29: Vascular endothelial growth factor (VEGF) mRNA expression profiles (RT-PCR) in the colon cancer cell line HT29, the prostate primary tumour cell line 1542CPTX (42C), and its matched non-neoplastic "normal" prostate epithelial cell line 1542NPTX (42N), in normoxic conditions (0h), and following hypoxia for 24h or 48h. Results are mean of three independent experiments with standard error of the mean (SEM). Results were normalised to the levels found in the non-neoplastic ("normal") prostate epithelial cell line at 0h (42N/0h=1). Standard T-test has been applied over time for each cell line (*: significant change :< 0.05).

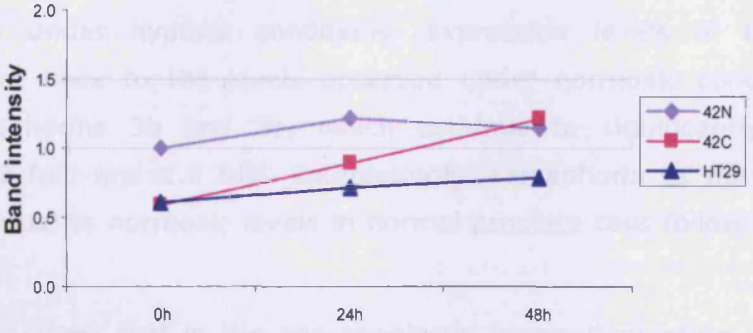

Figure 30: VEGF mRNA expression profiles (RT-PCR) in the colon cancer cell line HT29, the prostate primary tumour cell line 1542CPTX (42C), and its matched non-neoplastic "normal" prostate epithelial cell line 1542NPTX (42N), in normoxic conditions (0h), and following hypoxia for 24h or 48h. Results were normalised to the levels found in the non-neoplastic ("normal") prostate epithelial cell line at 0h (42N/0h=1).

VEGF	Hypoxia	
Cell line	**24h**	**48h**
HT29	1.2	1.3
42N	1.2	1.1
42C	1.5	2.1

Table 9: Fold change in VEGF mRNA expression levels (RT-PCR) in the colon cancer cell line HT29, the prostate primary tumour cell line 42C, and its matched non-neoplastic "normal" prostate epithelial cell line 42N, after 24h and 48h of hypoxia.

The results suggest that VEGF mRNA expression levels are regulated by hypoxia in prostate cancer derived cells, but not in "normal" prostate cells, which is consistent with what had been described by other groups (Du et al., 2003; Hao et al., 2004).

b. Expression profiles of secreted semaphorins in the non-neoplastic "normal" prostate epithelial cell line 1542NPTX following hypoxia for 24h and 48h

The results in figure 31 (summarised in table 10) show that mRNA expression levels of secreted semaphorins are regulated by hypoxia in the non-neoplastic "normal" prostate epithelial cell line. The results show that after 24h of hypoxia, mRNA expression levels of secreted semaphorins 3a, 3b, 3c, 3e and 3f are significantly increased by 1.2 to 1.4 fold, compared to normoxic levels (0h). Over a period of 48h under hypoxic conditions, expression levels of most secreted semaphorins are back to the levels observed under normoxic conditions, except those of semaphorins 3b and 3e, which continue to significantly increase by respectively 1.6 fold and 1.3 fold. Interestingly, semaphorin 3f mRNA expression levels remain equal to normoxic levels in normal prostate cells following hypoxia for 24h and 48h.

The results suggest that in the non-neoplastic "normal" prostate epithelial cells, gene expression of secreted semaphorins is either not regulated by hypoxia (semaphorin 3f), or is regulated by hypoxia, either progressively and positively (semaphorins 3b and 3e), or following a biphasic pattern (semaphorins 3a and 3c).

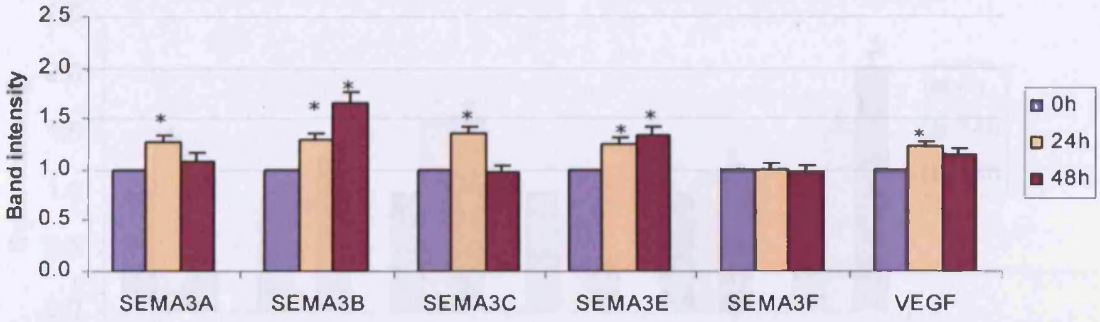

Figure 31: Expression profiles of secreted semaphorins (RT-PCR) in the non-neoplastic "normal" prostate epithelial cell line 1542NPTX (42N), in normoxic conditions (0h), and following hypoxia for 24h or 48h. Results are mean of three independent experiments with standard error of the mean (SEM). Results were normalised to the levels found in the non-neoplastic ("normal") prostate epithelial cell line at 0h (42N/0h=1) Standard T-test has been applied for each semaphorin (*: significant change :< 0.05).

Cell line	42N	
Hypoxia	**24h**	**48h**
Sema3a	1.3	1.1
Sema3b	1.3	1.65
Sema3c	1.4	1.0
Sema3e	1.25	1.3
Sema3f	1.0	0.98
VEGF	1.2	1.1

Table 10: Fold change in secreted semaphorins expression levels in the non-neoplastic "normal" prostate epithelial cell line 42N, after 24h and 48h of hypoxia.

c. Expression profiles of secreted semaphorins in the prostate primary tumour cell line 1542CPTX following hypoxia for 24h and 48h

The results in figure 32 (summarised in table 11) show that mRNA expression levels of secreted semaphorins are strongly regulated by hypoxia in the prostate primary tumour cell line. The results show that after 24h of hypoxia, mRNA expression levels of secreted semaphorins 3a and 3c are significantly increased by 1.4 and 1.6 fold, compared to normoxic levels (0h), while those of semaphorins 3b and 3e are decreased by 1.1 and 1.3 fold respectively. Like in the non-neoplastic "normal" prostate epithelial cell line, in the matched primary tumour cell line, expression levels of semaphorin 3f are not significantly changed at 24h of hypoxia, compared to normoxic levels. However, after 48h of hypoxia, expression levels of semaphorins 3b, 3c, and 3f are significantly increased by 1.3, 1.6 and 1.2 fold respectively, while those of semaphorins 3a and 3e are significantly decreased by 2 and 3 fold respectively.

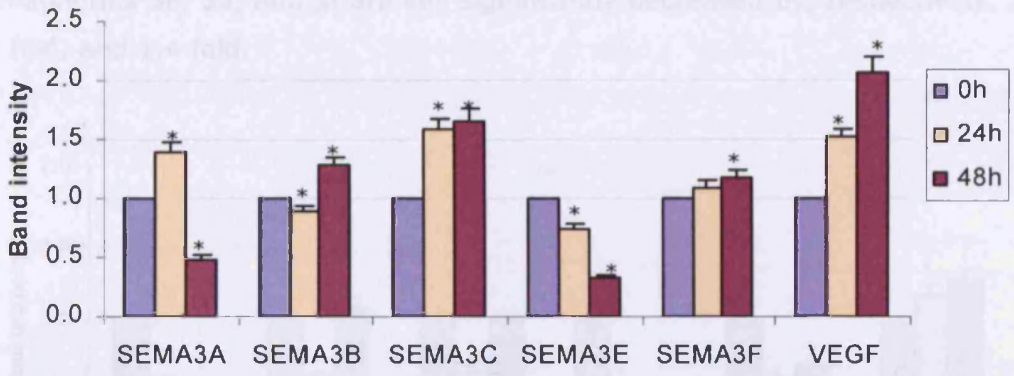

Figure 32: Expression profiles of secreted semaphorins (RT-PCR) in the prostate primary tumour cell line 1542CPTX (42C), in normoxic conditions (0h), and following hypoxia for 24h or 48h. Results are mean of three independent experiments with standard error of the mean (SEM). Results were normalised to the levels found in the prostate primary tumour cell line at 0h (42C/0h=1) Standard T-test has been applied for each semaphorin (*: significant change :< 0.05)

Cell line	42C	
Hypoxia	**24h**	**48h**
Sema3a	1.4	0.5
Sema3b	0.9	1.3
Sema3c	1.6	1.65
Sema3e	0.75	0.3
Sema3f	1.1	1.2
VEGF	1.5	2.1

Table 11: Fold change in secreted semaphorins expression levels in the prostate primary tumour cell line 42C, after 24h and 48h of hypoxia.

The results suggest that in prostate primary tumour derived cells following hypoxia, semaphorins expression levels are strongly regulated either progressively and positively (semaphorins 3c and 3f), or progressively and negatively (semaphorin 3e) or following a biphasic pattern (semaphorins 3a and 3b). The results also demonstrate that in the prostate primary tumour cells, semaphorins are regulated by hypoxia in a different fashion than in the non-neoplastic "normal" prostate cells.

d. Expression profiles of secreted semaphorins in the colon cancer cell line HT29 following hypoxia for 24h and 48h

The results in figure 33 (summarised in table 12) show that mRNA expression levels of secreted semaphorins are also strongly regulated by hypoxia in the colon cancer cell line. The results show that after 24h of hypoxia, mRNA expression levels of all the secreted semaphorins tested are significantly decreased by 1.4 to 1.6 fold, compared to normoxic conditions. Over a 48h period of hypoxia, the expression levels of secreted semaphorins 3b and 3c are back to normoxic levels, while those of

semaphorins 3e, 3a, and 3f are still significantly decreased by, respectively, 2.5 fold, 25 fold, and 1.4 fold.

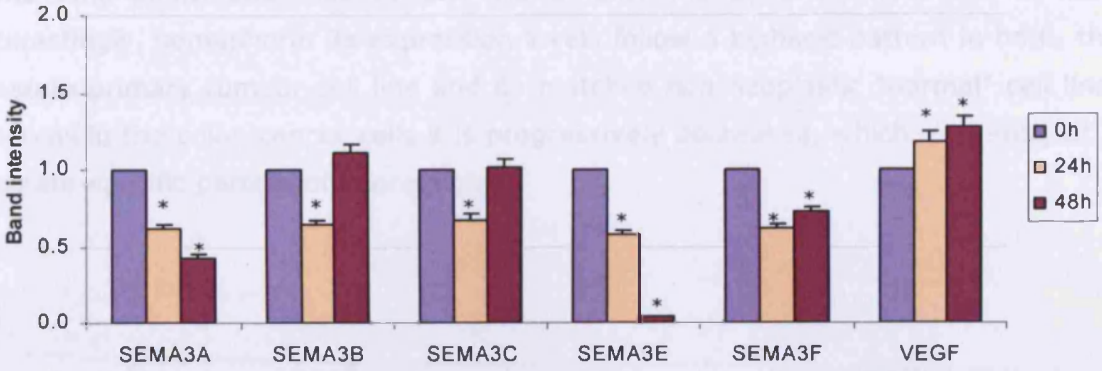

Figure 33: Expression profiles of secreted semaphorins (RT-PCR) in the colon cancer cell line HT29, in normoxic conditions (0h), and following hypoxia for 24h or 48h. Results are mean of three independent experiments with standard error of the mean (SEM). Results were normalised to the levels found in the colon cancer cell line at 0h (HT29/0h=1) Standard T-test has been applied for each semaphorin (*: significant change :< 0.05)

Cell line	HT29	
Hypoxia	**24h**	**48h**
Sema3a	0.6	0.4
Sema3b	0.6	1.1
Sema3c	0.7	1.0
Sema3e	0.6	0.04
Sema3f	0.6	0.7
VEGF	1.2	1.3

Table 12: Fold change in secreted semaphorins expression levels in the colon cancer cell line HT29, after 24h and 48h of hypoxia.

These results suggest that, after 24h of hypoxia, the expression levels of all the secreted semaphorins tested are decreased in the colon cancer cells, whereas they are increased in the "normal" prostate cells. Additionally, in colon cancer cells, like in prostate primary tumour cells, expression levels of semaphorins 3a and 3e are strongly and progressively (for semaphorin 3e) decreased by hypoxia.

e. Expression profile of semaphorin 3a in prostate and colon cell lines following hypoxia for 24h and 48h

The results in figures 34 and 35 show that in normoxic conditions, expression levels of semaphorin 3a are twice lower in the prostate primary tumour cell line (42C), while they are 1.3 times higher in the colon cancer cell line (HT29) than in the

non-neoplastic "normal" epithelial prostate cell line. In both cancer derived cell lines following hypoxia for 24h and 48h, expression levels of semaphorin 3a are significantly decreased, compared to non-neoplastic "normal" prostate levels at the same time point, and thus by 1.7 fold at 24h and by 2 or more fold at 48h. Interestingly, semaphorin 3a expression levels follow a biphasic pattern in both, the prostate primary tumour cell line and its matched non-neoplastic "normal" cell line, whereas in the colon cancer cells it is progressively decreased, which may suggest a prostate-specific pattern of expression.

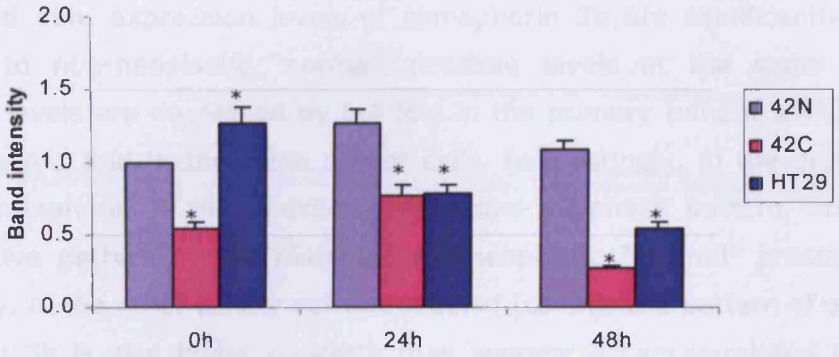

Figure 34: Secreted semaphorin 3a expression profiles (RT-PCR) in the colon cancer cell line HT29, the prostate primary tumour cell line 1542CPTX (42C), and its matched non-neoplastic "normal" prostate epithelial cell line 1542NPTX (42N), in normoxic conditions (0h), and following hypoxia for 24h or 48h. Results are mean of three independent experiments with standard error of the mean (SEM). Results were normalised to the levels found in the non-neoplastic ("normal") prostate epithelial cell line at 0h (42N/0h=1). Standard T-test has been applied for each time point (*: significant change :< 0.05).

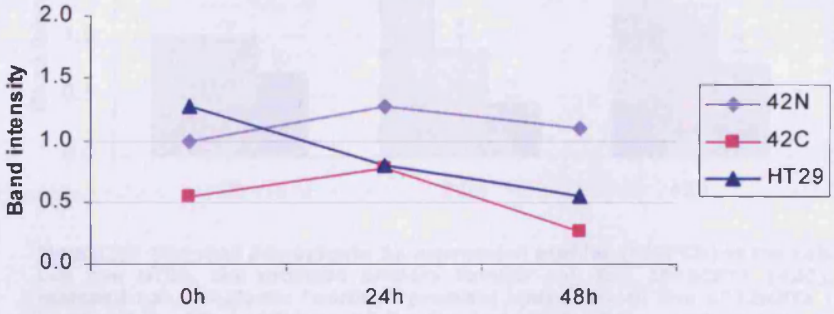

Figure 35: Secreted semaphorin 3a expression profiles (RT-PCR) in the colon cancer cell line HT29, the prostate primary tumour cell line 1542CPTX (42C), and its matched non-neoplastic "normal" prostate epithelial cell line 1542NPTX (42N), in normoxic conditions (0h), and following hypoxia for 24h or 48h. Results were normalised to the levels found in the non-neoplastic ("normal") prostate epithelial cell line at 0h (42N/0h=1).

The results suggest that semaphorin 3a mRNA expression levels are regulated by hypoxia in the same manner in the matched "normal" and primary tumour prostate cells. In the prostate and colon cancer cell lines following hypoxia for 48h, expression

levels of semaphorin 3a are decreased, while they are unchanged in the non-neoplastic "normal" prostate cell line.

f. Expression profile of semaphorin 3b in prostate and colon cell lines following hypoxia for 24h and 48h

The results in figures 36 and 37 show that in normoxic conditions, semaphorin 3b mRNA expression levels are identical in the matched non-neoplastic "normal" and primary tumour prostate cell lines, while they are decreased by 1.4 fold in the colon cancer cell line. In both cancer derived cell lines (42C and HT29) following hypoxia for 24h and 48h, expression levels of semaphorin 3b are significantly decreased, compared to non-neoplastic "normal" prostate levels at the same time point. Expression levels are decreased by 1.4 fold in the primary tumour derived cells and by more than 2 fold in the colon cancer cells. Interestingly, in the prostate cancer cell line, semaphorin 3b mRNA expression follows a biphasic pattern, while it follows a progressive pattern in the matched non-neoplastic "normal" prostate cell line. Additionally, in the other cancer cell line studied (colon), the pattern of expression of semaphorin 3b is also biphasic, which may suggest a cancer-related behaviour of semaphorin 3b transcription.

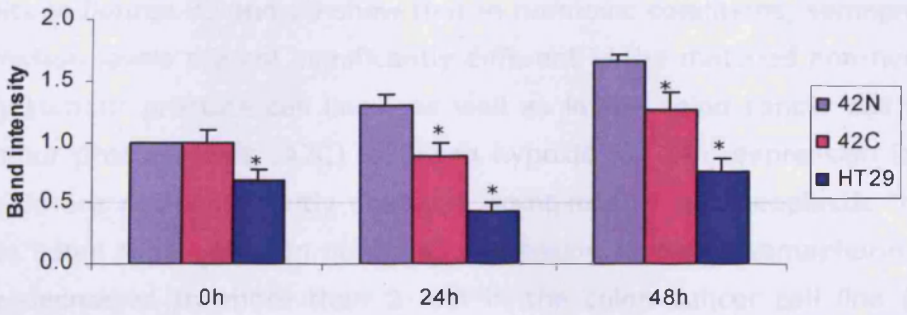

Figure 36: Secreted semaphorin 3b expression profiles (RT-PCR) in the colon cancer cell line HT29, the prostate primary tumour cell line 1542CPTX (42C), and its matched non-neoplastic "normal" prostate epithelial cell line 1542NPTX (42N), in normoxic conditions (0h), and following hypoxia for 24h or 48h. Results are mean of three independent experiments with standard error of the mean (SEM). Results were normalised to the levels found in the non-neoplastic ("normal") prostate epithelial cell line at 0h (42N/0h=1). Standard T-test has been applied for each time point (*: significant change :< 0.05).

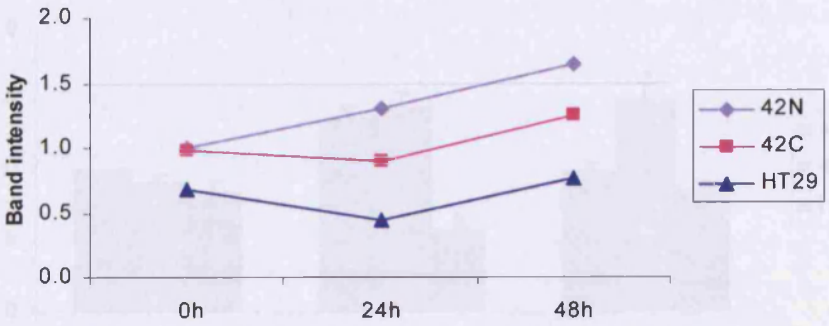

Figure 37: Secreted semaphorin 3b expression profiles (RT-PCR) in the colon cancer cell line HT29, the prostate primary tumour cell line 1542CPTX (42C), and its matched non-neoplastic "normal" prostate epithelial cell line 1542NPTX (42N), in normoxic conditions (0h), and following hypoxia for 24h or 48h. Results were normalised to the levels found in the non-neoplastic ("normal") prostate epithelial cell line at 0h (42N/0h=1).

The results suggest that semaphorin 3b mRNA expression levels are regulated by hypoxia in both prostate primary tumour cells and non-neoplastic "normal" prostate cells, and that after 48h of hypoxia, semaphorin 3b mRNA expression levels in the cancer cells are decreased, compared to the levels in non-neoplastic "normal" prostate cells.

g. Expression profile of semaphorin 3c in prostate and colon cell lines following hypoxia for 24h and 48h

The results in figures 38 and 39 show that in normoxic conditions, semaphorin 3c mRNA expression levels are not significantly different in the matched non-neoplastic and primary tumour prostate cell lines, as well as in the colon cancer cell line. In primary tumour prostate cells (42C) following hypoxia for 24h, expression levels of semaphorin 3c are not significantly changed, compared to non-neoplastic "normal" levels at the same time point. In contrast, expression levels of semaphorin 3c are significantly decreased by more than 2 fold in the colon cancer cell line (HT29), compared to non-neoplastic "normal" prostate levels at the same time point. Inversely, In primary tumour prostate cells following hypoxia for 48h, expression levels of semaphorin 3c are significantly increased by 1.5 fold, while they are not significantly changed in the colon cancer cells, compared to the levels found in the non-neoplastic "normal" prostate cells at the same time point. Interestingly, in the primary tumour prostate cells, semaphorin 3c expression is progressively regulated by hypoxia, whereas in non-neoplastic "normal" prostate cells and in colon cancer cells, its expression follows a biphasic pattern.

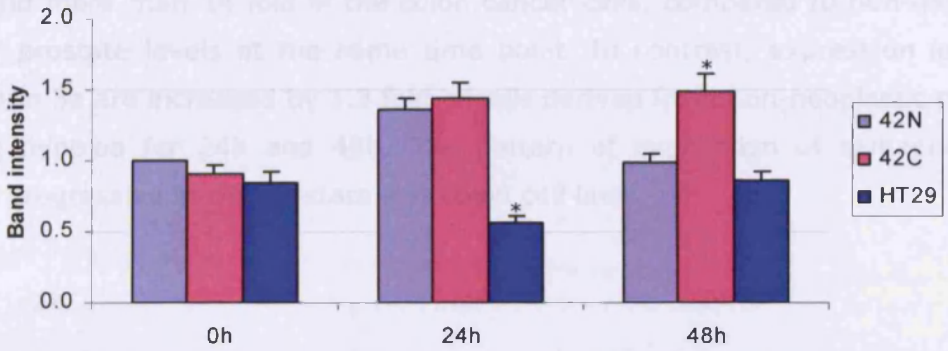

Figure 38: Secreted semaphorin 3c expression profiles (RT-PCR) in the colon cancer cell line HT29, the prostate primary tumour cell line 1542CPTX (42C), and its matched non-neoplastic "normal" prostate epithelial cell line 1542NPTX (42N), in normoxic conditions (0h), and following hypoxia for 24h or 48h. Results are mean of three independent experiments with standard error of the mean (SEM). Results were normalised to the levels found in the non-neoplastic ("normal") prostate epithelial cell line at 0h (42N/0h=1). Standard T-test has been applied for each time point (*: significant change :< 0.05).

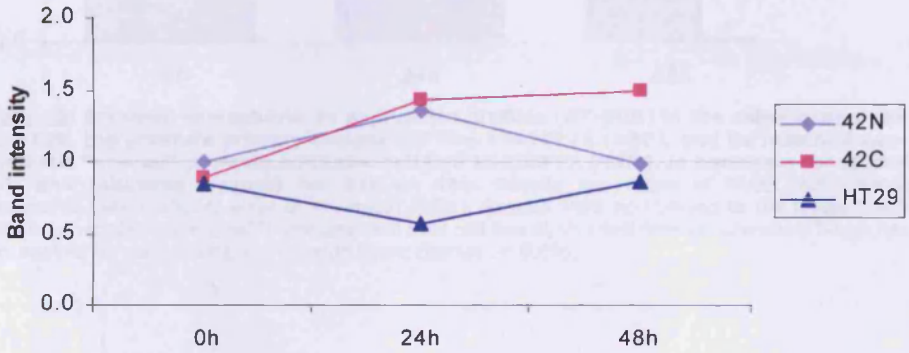

Figure 39: Secreted semaphorin 3c expression profiles (RT-PCR) in the colon cancer cell line HT29, the prostate primary tumour cell line 1542CPTX (42C), and its matched non-neoplastic "normal" prostate epithelial cell line 1542NPTX (42N), in normoxic conditions (0h), and following hypoxia for 24h or 48h. Results were normalised to the levels found in the non-neoplastic ("normal") prostate epithelial cell line at 0h (42N/0h=1).

The results suggest that the pattern of expression of semaphorin 3c mRNA in prostate cells following hypoxia for 48h is progressively increased in primary tumour cells, while it is unchanged in "normal" cells (and in colon cancer cells), which may suggest a prostate cancer-related behaviour of semaphorin 3c transcription.

h. Expression profile of semaphorin 3e in prostate and colon cell lines following hypoxia for 24h and 48h

The results in figures 40 and 41 show that in normoxic conditions, semaphorin 3e mRNA expression levels are not significantly different in the matched non-neoplastic and primary tumour prostate cell lines, and in the colon cancer cell line (HT29). In prostate and colon cancer cells following hypoxia for 24h and 48h, expression levels of semaphorin 3e are strongly decreased by 1.5 and 3.5 fold in the prostate cells and

by 2.5 and more than 14 fold in the colon cancer cells, compared to non-neoplastic "normal" prostate levels at the same time point. In contrast, expression levels of semaphorin 3e are increased by 1.3 fold in cells derived from non-neoplastic prostate following hypoxia for 24h and 48h. The pattern of expression of semaphorin 3e mRNA is progressive in the prostate and colon cell lines.

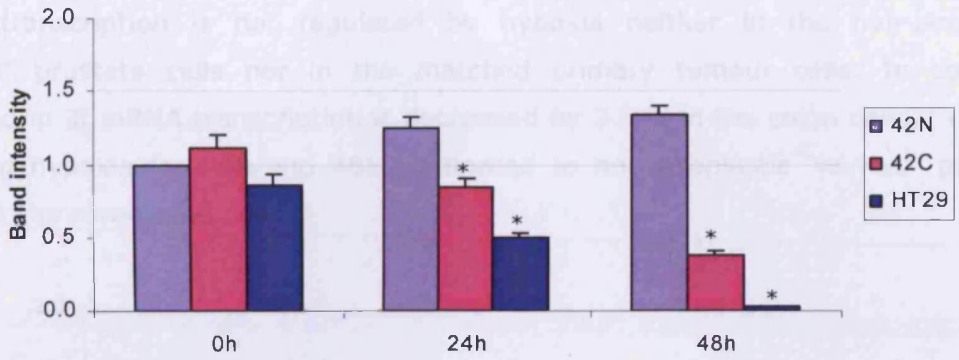

Figure 40: Secreted semaphorin 3e expression profiles (RT-PCR) in the colon cancer cell line HT29, the prostate primary tumour cell line 1542CPTX (42C), and its matched non-neoplastic "normal" prostate epithelial cell line 1542NPTX (42N), in normoxic conditions (0h), and following hypoxia for 24h or 48h. Results are mean of three independent experiments with standard error of the mean (SEM). Results were normalised to the levels found in the non-neoplastic ("normal") prostate epithelial cell line at 0h (42N/0h=1). Standard T-test has been applied for each time point (*: significant change :< 0.05).

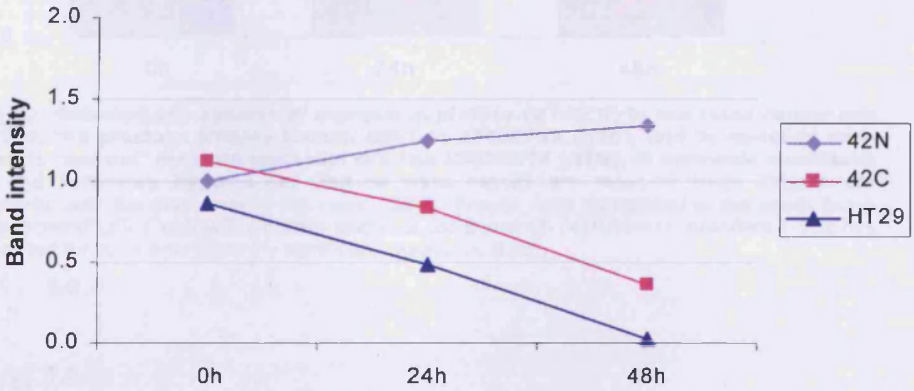

Figure 41: Secreted semaphorin 3e expression profiles (RT-PCR) in the colon cancer cell line HT29, the prostate primary tumour cell line 1542CPTX (42C), and its matched non-neoplastic "normal" prostate epithelial cell line 1542NPTX (42N), in normoxic conditions (0h), and following hypoxia for 24h or 48h. Results were normalised to the levels found in the non-neoplastic ("normal") prostate epithelial cell line at 0h (42N/0h=1).

The results suggest that hypoxia turns off semaphorin 3e transcription in both prostate and colon cancer cell lines, while it slightly increases its transcription in the cells derived from non-neoplastic "normal" prostate after 48h of hypoxia. The results may suggest that there is a cancer-related behaviour of semaphorin 3e transcription.

i. Expression profile of semaphorin 3f in prostate and colon cell lines following hypoxia for 24h and 48h

The results in figures 42 and 43 show that in normoxic conditions semaphorin 3f mRNA expression levels are not significantly different in the matched non-neoplastic and primary tumour prostate cells, while it is decreased in the colon cancer cells compared to non-neoplastic "normal" prostate levels. Interestingly, semaphorin 3f mRNA transcription is not regulated by hypoxia neither in the non-neoplastic "normal" prostate cells nor in the matched primary tumour cells. In contrast, semaphorin 3f mRNA transcription is decreased by 2 fold in the colon cancer cell line following hypoxia for 24h and 48h, compared to non-neoplastic "normal" prostate levels at the same time point.

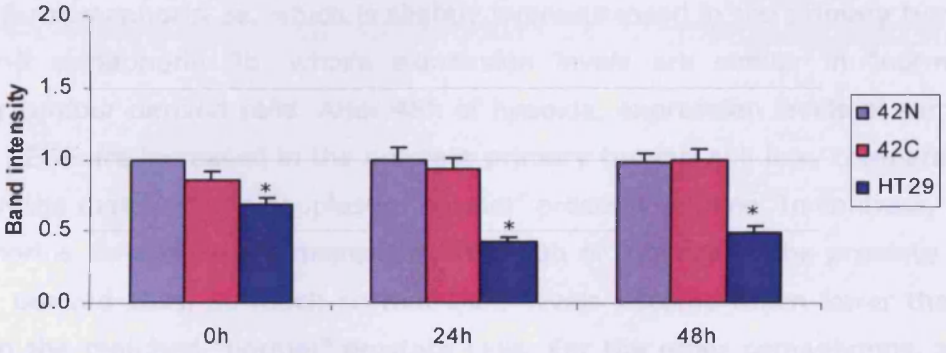

Figure 42: Secreted semaphorin 3f expression profiles (RT-PCR) in the colon cancer cell line HT29, the prostate primary tumour cell line 1542CPTX (42C), and its matched non-neoplastic "normal" prostate epithelial cell line 1542NPTX (42N), in normoxic conditions (0h), and following hypoxia for 24h or 48h. Results are mean of three independent experiments with standard error of the mean (SEM). Results were normalised to the levels found in the non-neoplastic ("normal") prostate epithelial cell line at 0h (42N/0h=1). Standard T-test has been applied for each time point (*: significant change :< 0.05).

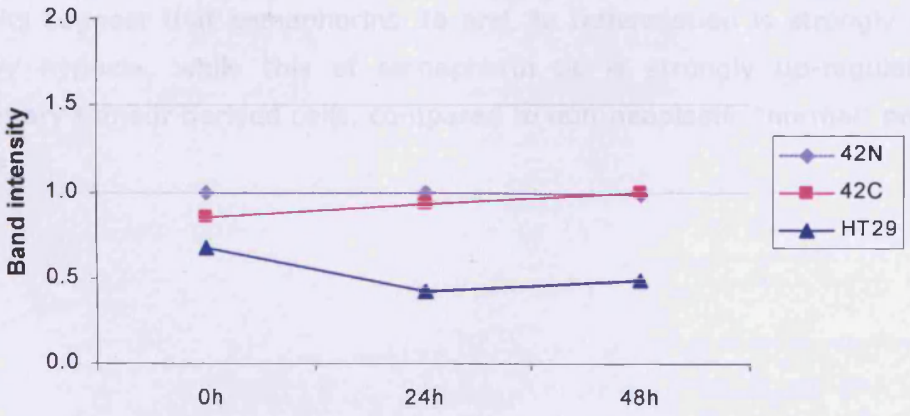

Figure 43: Secreted semaphorin 3f expression profiles (RT-PCR) in the colon cancer cell line HT29, the prostate primary tumour cell line 1542CPTX (42C), and its matched non-neoplastic "normal" prostate epithelial cell line 1542NPTX (42N), in normoxic conditions (0h), and following hypoxia for 24h or 48h. Results were normalised to the levels found in the non-neoplastic ("normal") prostate epithelial cell line at 0h (42N/0h=1).

The results suggest that hypoxia does not regulate semaphorin 3f transcription in in the matched non-neoplastic "normal" prostate cells and primary tumour cells, whereas its expression is progressively regulated by hypoxia over a 48h period in colon cancer derived cells.

j. Relative expression levels of secreted semaphorin genes in the prostate primary tumour cell line 1542CPTX following hypoxia for 24h and 48h, compared to the matched non-neoplastic cell line 1542NPTX

The results in figure 44 confirm the results obtained under normoxic conditions, which have been discussed previously. Namely, mRNA expression profiles of secreted semaphorins are reduced in the prostate primary tumour derived cell line 42C, compared to the matched non-neoplastic "normal" prostate derived cell line 42N, except for semaphorin 3e, which is slightly overexpressed in the primary tumour cell line, and semaphorin 3b, whose expression levels are similar in "normal" and primary tumour derived cells. After 48h of hypoxia, expression levels of semaphorin 3c and VEGF are increased in the prostate primary tumour cell line, compared to the levels in the matched non-neoplastic "normal" prostate cell line. In contrast, those of semaphorins 3a and 3e are decreased after 48h of hypoxia in the prostate primary tumour derived cells, so much so that their levels become much lower than those found in the matched "normal" prostate cells. For the other semaphorins, although their expression levels are variable, they remain expressed at higher levels in the non-neoplastic "normal" prostate derived cell line than in the matched primary tumour derived cell line following hypoxia.

The results suggest that semaphorins 3a and 3e transcription is strongly down-regulated by hypoxia, while this of semaphorin 3c is strongly up-regulated in prostate primary tumour derived cells, compared to non-neoplastic "normal" prostate derived cells.

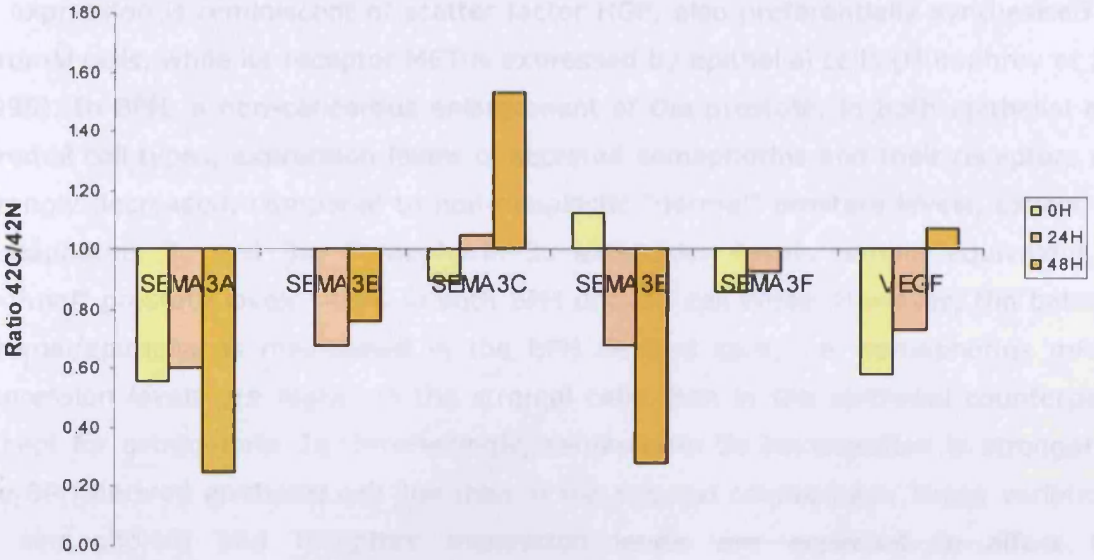

Figure 44: Relative expression levels of secreted semaphorin genes in the prostate primary tumour cell line 1542CPTX (42C), compared to the matched non-neoplastic cell line 1542NPTX (42N), following hypoxia for 24h and 48h.

6. Discussion

In this section, we report the first expression profiles study of semaphorins and their receptors, as well as vascular endothelial growth factors (VEGF-A isoforms), in cell lines derived from non-neoplastic "normal" prostate, benign prostate hyperplasia (BPH), prostate primary tumour, and metastases to the bone, the brain, and the lymph node.

The results show that messenger RNA for secreted and transmembrane semaphorins (3a, 3b, 3c, 3e, 3f, and 4d), as well as for their high affinity receptors, plexins (a1, a2, a3, b1, and b3) and neuropilins (np1 and np2) are widely expressed, although at various levels, in epithelial and stromal cells derived from a non-neoplastic "normal" prostate (42N and 42F), epithelial and stromal cells derived from a benign prostate hyperplasia (Pre2.8 and S2.13), epithelial cells derived from a prostate primary tumour (42C), and epithelial cells derived from metastases to the lymph node (LNCaP), the brain (DU145), and the bone (PC3).

Particularly, the results accentuate the differences in expression levels between stromal and epithelial cell types in non-neoplastic "normal" prostate and benign hyperplasic prostate (BPH). In non-neoplastic "normal" prostate, class 3 (secreted) semaphorins and neuropilin receptors are preferentially synthesised by stromal cells, while epithelial cells preferentially synthesise mRNA for plexin receptors. This pattern

of expression is reminiscent of scatter factor HGF, also preferentially synthesised by stromal cells, while its receptor MET is expressed by epithelial cells (Humphrey et al., 1995). In BPH, a non-cancerous enlargement of the prostate, in both epithelial and stromal cell types, expression levels of secreted semaphorins and their receptors are strongly decreased, compared to non-neoplastic "normal" prostate levels, except for semaphorins 3c and 3e. Semaphorin 3c expression levels remain equivalent to "normal" prostate levels (42N) in both BPH derived cell types. However, the balance stromal/epithelial is maintained in the BPH derived cells; i.e. semaphorins mRNA expression levels are higher in the stromal cells than in the epithelial counterpart, except for semaphorin 3e. Interestingly, semaphorin 3e transcription is stronger in the BPH derived epithelial cell line than in the stromal counterpart. These variations in semaphorins and receptors expression levels are expected to affect the interactions between stromal and epithelial cells of the prostate, which will most probably reflect on the architecture of the tissue. Further experiments, such as co-culture experiments, are necessary to investigate this further.

The results also highlight the differences in expression levels between cells derived from a primary tumour, three metastases and non-neoplastic "normal" prostate. They show that in the prostate cell lines derived from a primary tumour and two of the three metastases (brain and lymph node), the transcription of secreted semaphorins, class A plexins and neuropilin 2 are strongly decreased, while this of neuropilin 1 and plexin b3 remain "normal".

Noticeably, plexin b3 expression levels are comparable to or stronger than normal epithelial prostate levels in derived cells from the primary tumour, the three metastases, and the stromal BPH. Plexin b3 expression levels are only significantly reduced in stromal cells derived from normal prostate and in epithelial cells derived from BPH. It is only recently that PlexinB3 ligand Semaphorin5A has been identified (Artigiani et al., 2005). These results may suggest important roles for Semaphorin5A signalling in prostate carcinogenesis and metastasis. It would be interesting to determine semaphorin 5a expression profile in prostate cell lines and tissue.

Interestingly, in the prostate cells derived from a bone metastasis, the mRNA expression levels of semaphorins 3a, 3e, 3f, plexins a1 and a3 remain similar to non-neoplastic levels, and those of neuropilin 1 are increased, compared to the primary tumour or the other metastases derived cells. Semaphorin3A and 3F proteins bind to both PlexinA1 and A3 receptors, and to both Neuropilins with varying affinities. These

results suggest an autocrine type of regulation of Semaphorin3A and/or 3F signalling pathway in cells derived from prostate cancer metastases to the bone. Additionally, in the prostate cells derived from a bone metastasis, the mRNA expression levels of semaphorin 3b, the other tumour suppressor semaphorin, are strongly decreased compared to non-neoplastic "normal" levels, which may indicate distinct roles for Semaphorin3B and 3F proteins in prostate cancer and metastasis.

At the time these experiments were performed, the receptor for Semaphorin3E protein was still unknown. It was generally accepted that secreted semaphorin receptors were a complex made of a homo- or hetero-dimer of neuropilins and a monomer of class A plexin (mostly plexin a1); and that the specificity of semaphorin signalling depended on the combination of neuropilins and plexin present. It would now be interesting to evaluate plexin d1 mRNA expression levels in the 10 prostate cell lines to check whether there may be an autocrine regulation of Semaphorin3E signalling in prostate cancer and metastases. Moreover, semaphorin 3e expression levels also remain "normal" in the prostate primary tumour cell line and in the BPH derived epithelial cells, whereas all the other secreted semaphorins are strongly downregulated. An overexpression of semaphorin 3e, which is known mainly as a repellent cue, has also been reported in metastatic cell lines derived from mice mammary carcinoma (Christensen et al., 1998). Altogether, these results may suggest an important role for Semaphorin3E protein in prostate cancer progression and metastasis.

Altogether, these expression profiling results suggest an autocrine or paracrine type of semaphorin signalling in prostate, as most cell lines express the ligands and their receptors. However, it is still unclear what controls semaphorin expression. As intratumoral hypoxia is frequently found in advanced cancers, and hypoxia inducible factor-1α is markedly overexpressed in prostate cancers and metastases (Zhong et al., 1999), we sought to determine whether secreted semaphorin mRNA expression levels would be regulated by hypoxia in prostate cell lines. First, secreted semaphorins promoter regions were screened for the presence of HIF-responsive elements (HREs). The results show that all secreted semaphorins, but semaphorin 3d promoter, exibit 4 to 7 HREs. Interestingly, semaphorin 3e promoter presents two tandemly arrayed HREs, which can also form functional HIF responsive elements (Wenger et al., 2005). These preliminary results suggest that most secreted semaphorins may be sensitive to hypoxia-induced HIF1-dependent transcriptional activation.

Expression profiling experiments demonstrate that, overall, the expression of secreted semaphorins is hypoxia-regulated, and together with the demonstration of HRE, suggest that semaphorin regulation may be dependent on HIF1. Cancer-specific and tissue-specific patterns of expression following hypoxia can be observed. For example, a tissue-specific behaviour (prostate vs. colon) exists for semaphorin 3f, whose mRNA expression levels are unchanged in the cells derived from non-neoplastic "normal" prostate, and the matched primary tumour, compared to normoxic levels, while they are strongly decreased in the colon cancer cells, following hypoxia for 48h. In contrast, a cancer-specific expression pattern is observed for semaphorin 3e, whose transcription is strongly and progressively down-regulated in both cancer cells (prostate and colon) following hypoxia, compared to normoxic levels, and contrary to the transcriptional activation seen in the non-neoplastic "normal" prostate cells. Altogether, these results suggest that a prostate cancer-specific expression pattern of secreted semaphorins may be detectable after 48h of hypoxia, which can be defined in this case (1542CPTX and 1542NPTX cells), by a strong transcriptional activation of semaphorin 3c, and a strong transcriptional inhibition of semaphorins 3a and 3e. Similarly, a colon cancer-specific expression pattern of secreted semaphorins after 48h of hypoxia may be detected, which can be defined, in the HT29 cells, by a strong transcriptional inhibition of semaphorins 3a and 3e, and also 3f.

Of particular interest is the transcriptional behaviour of secreted semaphorin 3e in the cancer cells following hypoxia, which may be the result of an indirect inhibition (HIF could increase the expression of an inhibitor of semaphorin 3e transcription). To our knowledge, this study is the first study reporting an hypoxia-induced transcriptional inhibition. Further experiments are necessary nonetheless to confirm those results. Future work would include semaphorin promoter reporter constructs in order to study the effects of the presence and absence of HIF1α on the reporter expression.

Finally, these expression profiling results suggest that all secreted semaphorins may play roles in normal prostate homeostasis as well as in prostate cancer transformation, progression and maybe neo-angiogenesis, as all secreted semaphorins and their receptors are synthesised by prostate cell lines, and as secreted semaphorin genes expression is regulated by hypoxia, which is frequently encountered in intratumoral areas, and defined as a trigger for neo-angiogenesis.

However, there are limitations to this study, which need to be addressed by further work. It would be of interest to assess the distribution of semaphorins and receptors in more prostate cell lines, and to perform immunohistochemistry experiments of secreted semaphorin proteins in prostate tissues, which would involve developing antibodies to some of the semaphorins, as not all of them are commercially available. Further experiments to study the roles of semaphorins in prostate would include *in vivo* experiments to look at the effect on tumour formation in mice, using normal prostate cell lines stably transfected and overexpressing Semaphorin3A, 3C or 3E proteins for example.

Section 2: Role of PlexinB1 mutations and PlexinB1/Semaphorin4D signalling in prostate cancer and metastases

PlexinB1 is the functional receptor for transmembrane semaphorin 4D in non lymphoid tissues (nervous system), while it is CD72 in lymphoid tissues (immune system). Semaphorin4D signalling has been extensively studied in the immune system where it has been shown to regulate humoral and cellular immune responses, as well as the inflammatory response. In the nervous system, Semaphorin4D signalling, through PlexinB1, regulates axonal growth cone guidance. Semaphorin4D signalling, through PlexinB1, has also been implicated in invasive growth, through interaction with the scatter factor receptor MET (Giordano et al., 2002), and recently in angiogenesis (Basile et al., 2006). However, at present, there are no studies showing the roles of PlexinB1/Semaphorin4D signalling in normal and diseased prostate.

Previous work in the laboratory has identified 13 somatic missense mutations in the cytoplasmic domain of plexin b1 gene. Mutations were found in 89% (8/9) of prostate cancer bone metastases, 41% (7/17) of lymph node metastases and 46% (41/89) of primary cancers. Over 40% of prostate cancers contained the same mutation, A5653G. Overexpression of the PlexinB1 protein was found in the majority of primary tumours (Wong et al., 2007). Three mutations were studied here, two of the most common mutations found in prostate cancer A5653G and T5714C and the one found in LNCaP (A5359G). These three mutations are single nucleotide changes. The nucleotide change A5653G leads to a Thr1795Ala amino acid change, which has been identified in 38 primary tumours and 9 metastases. The nucleotide change T5714C leads to a Leu1815Pro amino acid change, which has been identified in 2 primary tumours and 3 metastases. And finally, the nucleotide change A5359G leads to a Thr 1697 Ala amino acid change, which is heterozygous in LNCaP cells.

The high frequency of mutation and overexpression of PlexinB1 suggests that PlexinB1 has a role in prostate cancer progression. A higher frequency of mutations was found in the metastases suggesting that the mutations may contribute to invasion and metastasis. An increase in cell motility is a phenotype associated with invasion and metastasis. PlexinB1 has been shown to affect cell migration (Barberis et al., 2004; Basile et al., 2005; Oinuma et al., 2006). To test the hypothesis that the mutations found in plexin b1 gene have an effect on cell migration, transwell migration assays were performed in the presence and absence of Semaphorin4D

ligand. Plexin b1 expression levels were assessed in prostate cell lines and tissues by quantitative RT-PCR. Those of semaphorin 4d were assessed by RT-PCR in the previous chapter.

1. Quantitative expression levels of plexin b1 in prostate cell lines and tissues

Plexin b1 mRNA expression levels have been quantified by real-time RT-PCR (qRT-PCR) in 8 prostate cell lines previously described, as well as in six paired non-neoplastic and carcinoma prostate tissue samples, originating from patients with well and moderately differentiated tumours, confined within the prostate, and with no regional lymph node metastases detected. Quantitative RT-PCRs were performed in triplicate, and on three different RNA extractions (from three consecutive passages). The results presented are normalised means (refer to page 71) with standard errors of the mean (SEM). Normalisation has also been performed to the expression levels found in the non-neoplastic ("normal") prostate epithelial cell line (42N=1), used as a reference. Standard T-test statistical analysis has been applied using GraphPad software.

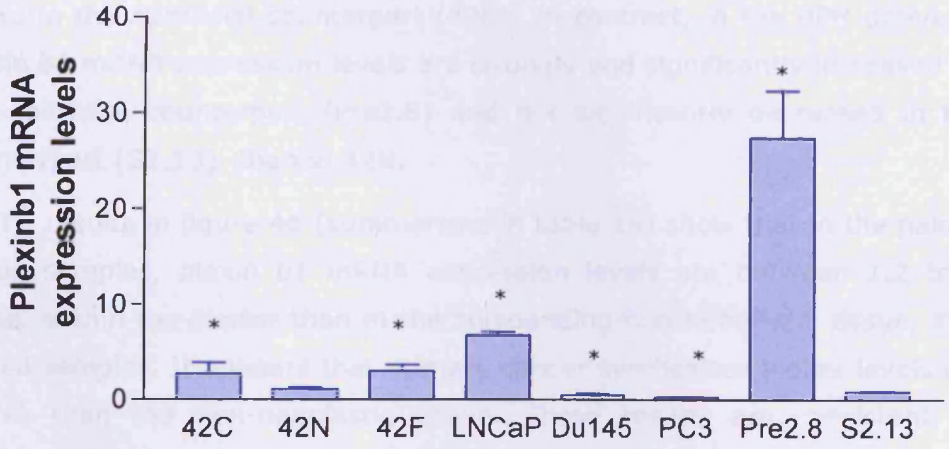

Figure 45: Plexin b1 mRNA expression profiles (qRT-PCR) in 8 prostate cell lines, derived from a primary tumour (1542CPTX or 42C), the matched non-neoplastic "normal" epithelia (1542NPTX or 42N) and stroma (1542FTX or 42F), metastases to the lymph node (LNCaP), the brain (DU145) and the bone (PC3), and benign hyperplasic epithelia (Pre2.8) and stroma (S2.13). Results are mean of three replicates, normalised to 42N expression levels, with standard error of the mean (SEM). Standard T- test has been applied (*: significant change :< 0.05).

Cell lines	Relative expression levels
42C	2.7
42N	1
42F	3.0
LNCaP	6.75
Du145	0.5
PC3	0.3
Pre2.8	27.3
S2.13	0.9

Table 13: Relative expression levels of plexin b1 mRNA (qRT-PCR) in 8 prostate cell lines.

The results in figure 45 (summarised in table 13) show that plexin b1 mRNA expression levels are significantly higher in the prostate primary tumour derived cell line (42C), compared to the levels found in the matched non-neoplastic "normal" counterpart (42N). Additionally, plexin b1 mRNA levels are also strongly (more than 6 fold) and significantly increased in the cell line derived from a lymph node metastasis (LNCaP), while they are significantly decreased in the other two cell lines derived from the brain (DU145) and the bone (PC3) metastases, compared to the levels in non-neoplastic "normal" prostate cell line (42N). Results show that plexin b1 mRNA expression levels are significantly increased (3 fold) in the stromal cell line (42F) derived from the non-neoplastic "normal" prostate, compared to the levels found in the epithelial counterpart (42N). In contrast, in the BPH derived cell lines, plexin b1 mRNA expression levels are strongly and significantly increased (27 fold) in the epithelial counterpart (Pre2.8) and not significantly decreased in the stromal counterpart (S2.13), than in 42N.

The results in figure 46 (summarised in table 14) show that in the paired prostate tissue samples, plexin b1 mRNA expression levels are between 1.2 to 2.7 times higher within the cancer than in the surrounding non-neoplastic tissue, in 5 out of 6 paired samples. It appears that primary cancer synthesises higher levels of plexin b1 mRNA than the non-neoplastic tissue. These results are consistent with those obtained with the cell lines (i.e. plexin b1 mRNA expression levels are on average 3 times higher in the primary tumour derived cells than in the matched non-neoplastic prostate epithelial cells). However, no association could be established between plexin b1 mRNA expression profile and the stage or Gleason score of the tumour.

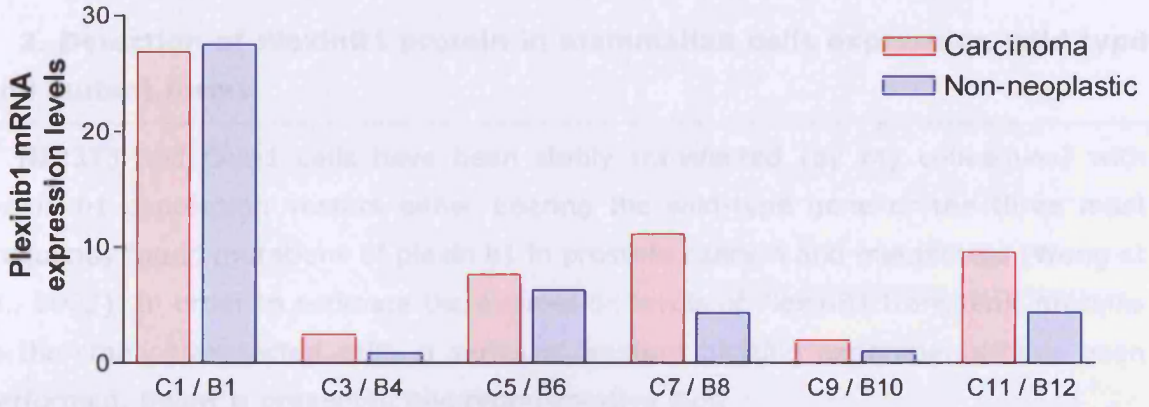

Figure 46: Plexin b1 mRNA expression profiles (qRT-PCR) in 6 paired non-neoplastic/carcinoma prostate tissue samples. Results are mean of three replicates from one experiment. No statistical analysis has been applied.

Tissue sample	Relative expression levels	pT	GSC
C1 B2	27.0 27.5	3a	5
C3 B4	2.5 0.9	2c	6
C5 B6	7.7 6.3	2c	6
C7 B8	11.2 4.3	3a	6
C9 B10	2.0 1.0	2c	5
C11 B12	9.6 4.4	2c	7

Table 14: Relative expression levels of plexin b1 mRNA (qRT-PCR) in 6 paired prostate tissue samples. Tumour stage (pT) and Gleason score (GSC) are listed. A Gleason grade between 5 and 7 describes well and moderately differentiated tumours. Tumours are either confined within the prostate but involving both lobes (2c) or with extracapsular extension (3a).

Surprisingly, the results obtained with the quantitative RT-PCR technique do not match the results obtained with the semi-quantitative RT-PCR method (refer to figures on pages 92 and 93). As quantitative RT-PCR results are more accurate, ideally, the expression levels for all semaphorins should be quantitated by this method. However, unfortunately this was prohibitively expensive to do. The variation in expression levels for plexin b1 mRNA in between RT-PCR and real time PCRs may be explained by the fact that the primers used for both techniques are different and not located at the same region of plexin b1 gene. It is possible that the regions are spliced differently, which would explain the difference in expression pattern seen.

2. Detection of PlexinB1 protein in mammalian cells expressing wild type and mutant forms

NIH3T3 and Cos-1 cells have been stably transfected (by my colleagues) with plexin b1 expression vectors either bearing the wild-type gene or the three most frequently found mutations of plexin b1 in prostate cancers and metastases (Wong et al., 2007). In order to estimate the expression levels of PlexinB1 transgenic proteins in the stably transfected cells, a series of western blotting experiments have been performed. Below is presented one representative blot.

Figure 47: Western blot of wild-type and mutant forms of PlexinB1 protein in stably transfected NIH3T3 cells. V: vector control, WT: wild-type PlexinB1, D: A5359G mutant form of PlexinB1, F: A45 mutant form of PlexinB1, G: T5714C mutant form of PlexinB1, T: NIH3T3 untransfected cells. HT: HT29 cells, positive control. IC2α antibody provided by L. Tamagnone (Artigiani et al., 2003). Expected band at approximately 100KDa.

The results in figure 47 show that the polyclonal anti-PlexinB1 antibody supplied by L. Tamagnone (Artigiani et al., 2003) stains many non-specific bands in addition to the approximately 100kDa band of interest (truncated form of PlexinB1, transmembrane β-chain, after cleavage by proprotein convertase). A band of the correct size is found in the positive control HT29 cells (HT) and is absent from the negative controls (expression vector only (V) and untransfected cells (T)). This band is also present in the NIH3T3 stable cells, which suggest that the stable cell lines express PlexinB1 protein.

These results, together with the RT-PCR results (M. Williamson, personal communication), show that the stable clones express wild-type and mutant forms of PlexinB1, therefore they were used for the following migration experiments.

3. Migration assays in modified Boyden chambers

a. Technique optimisation and primary results

To assess whether any of the selected single nucleotide mutations of plexin b1 gene has any effect on cell movement, migration assays have been performed in modified Boyden Chambers. The technique was optimised according to the number of cells in the upper chamber, the time of incubation at 37°C, and the presence or absence of serum. The best results were obtained when plating $4x10^4$ cells in the upper chamber with an incubation time of 3h at 37°C. Up to 10^5 cells could be plated in the upper chamber, but it was harder to count the cells because they clumped at the periphery and in the centre of the filter.

In order to measure the effects of serum concentration in the incubating medium, Cos-1 and NIH3T3 cells stably transfected with vector only, wild-type PlexinB1, and mutants T5714C-PlexinB1 and A5359G-PlexinB1 respectively, have been incubated in completed medium (8% serum), and in medium containing 0.1% serum. The results in figure 48 and 49 show that serum concentration has no significant effect on Cos-1 cell migration (p value=0.353), whereas a high concentration of serum has a significant effect on NIH3T3 cell migration (p value<0.001), which migrate faster in complete medium. All later experiments have therefore been performed using NIH3T3 cells and medium containing 0.1% serum.

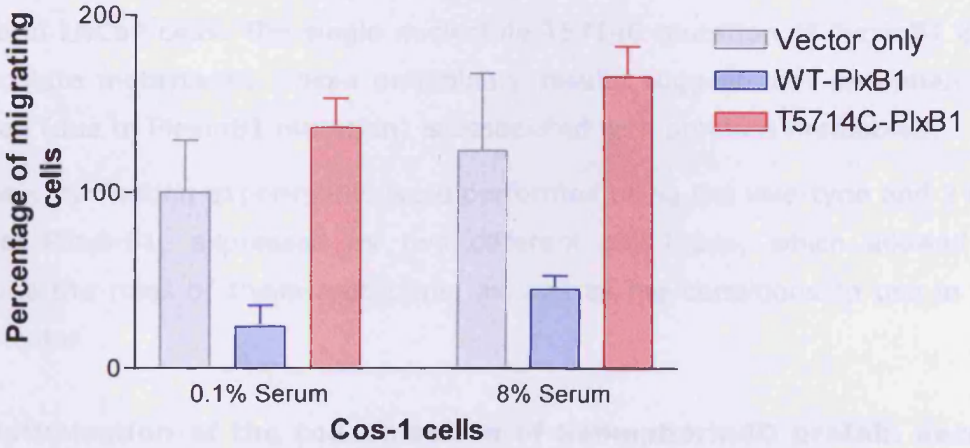

Figure 48: Migration assay of Cos-1 cells stably transfected with pcDNA3 vector only, wild-type PlexinB1 (WT-PlxB1) and mutant T5714C-PlexinB1. Presence of serum (RPMI1640 medium completed with 8% FBS) or absence of serum (0.1% FBS) has no significant effect on cell migration. The effect of T5714C mutation is significant in Cos-1 cells, P value=0.0019. Results are mean of three independent experiments with standard error of the mean (SEM). ANOVA statistical analysis has been applied using GraphPad software, which showed that the effects of serum are not significant (p value = 0.353), while the effects of mutation are significant (p value < 0.001).

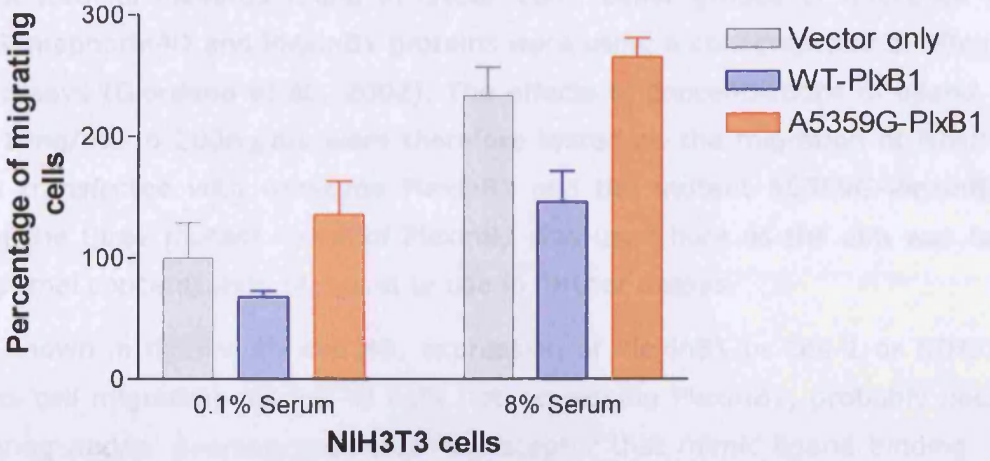

Figure 49: Migration assay of NIH3T3 cells stably transfected with pcDNA3 vector only, wild-type PlexinB1 (WT-PlxB1) and mutant A5359G-PlexinB1. The presence of serum (DMEM medium completed with 8% NCS) has a significant effect on cell migration. The effect of A5359G mutation is significant in NIH3T3 cells, P value=0.0044. Results are mean of three independent experiments with standard error of the mean (SEM). ANOVA statistical analysis has been applied using GraphPad software, which showed that the effects of serum and mutation are significant (p values < 0.001).

The results show that in Cos-1 stably transfected cells (figure 48), like in NIH3T3 stably transfected cells (figure 49), overexpression of wild-type PlexinB1 inhibits cell migration. It has previously been shown that overexpression of PlexinB1 protein mimics ligand binding, which explains why there is an effect on migration in the absence of ligand (Giordano et al., 2002). In contrast, an overexpression of mutants T5714C-PlexinB1 and A5359G-PlexinB1 prevents the expected inhibition of migration, thus bringing the percentage of migrating cells to slightly higher levels than control levels (vector only). The single nucleotide A5359G mutation of PlexinB1 is found in LNCaP cells. The single nucleotide T5714C mutation of PlexinB1 is found in 3 prostate metastases. These preliminary results suggest that an enhanced cell migration (due to PlexinB1 mutation) is associated with prostate metastasis.

These optimisation experiments were performed using the wild-type and 2 mutant forms of PlexinB1, expressed by two different cell types, which allowed us to determine the roles of these mutations, as well as the conditions to use in further experiments.

b. Optimisation of the concentration of Semaphorin4D protein necessary to detect an effect on cell migration

In order to determine the concentration of Semaphorin4D ligand to use for further experiments, optimisation assays were performed using wild-type PlexinB1 and one

mutant form of PlexinB1 found in LNCaP cells. Other groups of reference working with Semaphorin4D and PlexinB1 proteins were using a concentration of 50ng/mL for their assays (Giordano et al., 2002). The effects of concentrations of ligand varying from 10ng/mL to 200ng/mL were therefore tested on the migration of NIH3T3 cells stably transfected with wild-type PlexinB1 and the mutant A5359G-PlexinB1. Only one of the three mutant forms of PlexinB1 was used here as the aim was to define the optimal concentration of ligand to use in further assays.

As shown in figures 48 and 49, expression of PlexinB1 in Cos-1 or NIH3T3 cells inhibits cell migration relative to cells not expressing PlexinB1, probably because of clustering and/or overexpression of the receptor that mimic ligand binding. Figures 50 and 51 show that addition of 10 or 25ng/mL of Semaphorin4D ligand further inhibits cell migration. At 50ng/mL, the cell migration of cells expressing wild-type PlexinB1 is at a rate similar to that seen in the absence of Semaphorin4D protein. Figure 49 shows that migration of NIH3T3 cells expressing mutant A5359G-PlexinB1 is enhanced relative to cells expressing no PlexinB1 or wild-type PlexinB1. As figure 50 shows, migration is also further reduced following addition of 10 or 25ng/mL of Semaphorin4D protein but increased following addition of 50ng/mL relative to that seen in the absence of Semaphorin4D protein.

Other concentrations of Semaphorin4D protein were tested (results not shown), which showed that migration was further increased using 100ng/mL of ligand, while at 200ng/mL, migration was slighly decreased for both the wild-type and the mutant form A5359G-PlexinB1, compared to 100ng/mL. At 200ng/mL of Semaphorin4D, the migration of the mutant form of PlexinB1 was still enhanced compared to the wild type.

Because cell migration was increased when using a concentration of Semaphorin4D equal or superior to 50ng/mL, and as other groups of reference were using this same concentration, 50ng/mL of ligand were then used to subsequently test the effects of the three mutations on cell motility, in presence or absence of ligand.

Altogether, these results suggest that Semaphorin4D ligand has a biphasic effect on PlexinB1 signalling. Mutation of PlexinB1 and addition of a high concentration of Semaphorin4D ligand (50ng/mL) synergise to enhance cell migration.

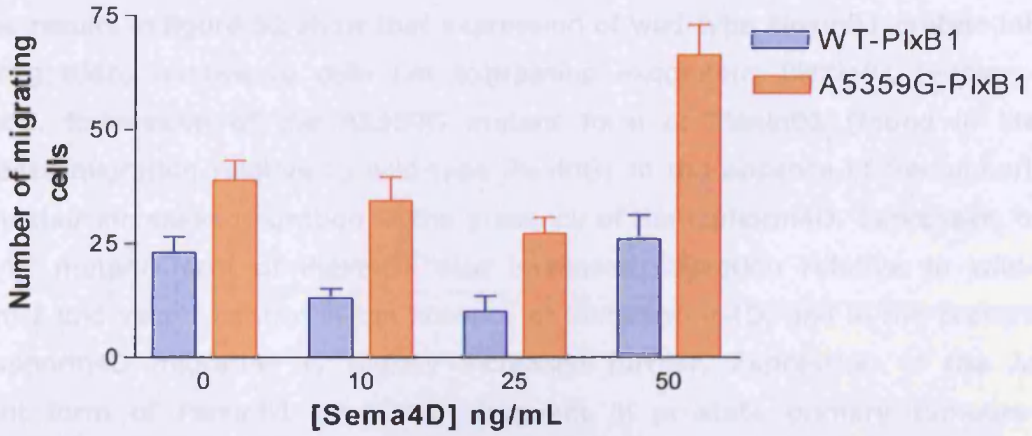

Figure 50: Effect of different concentrations of Semaphorin4D on cell migration. NIH3T3 cells stably transfected with wild-type PlexinB1 (WT-PlxB1) and mutant A5359G-PlexinB1. Various concentrations of Sema4D ligand were tested (0 to 50ng/mL). The mutation A5359G of PlexinB1 has no effect on ligand binding. Concentrations of Sema4D≤50ng/mL further inhibit cell migration, whereas a concentration of 50ng/mL increases cell migration adding to the effects of mutation A5359G of PlexinB1. Results are mean of three independent experiments with standard error of the mean (SEM). ANOVA statistical analysis has been applied using GraphPad software, which showed that the effects of the mutation and of the presence of ligand in the medium are significant (p values < 0.001).

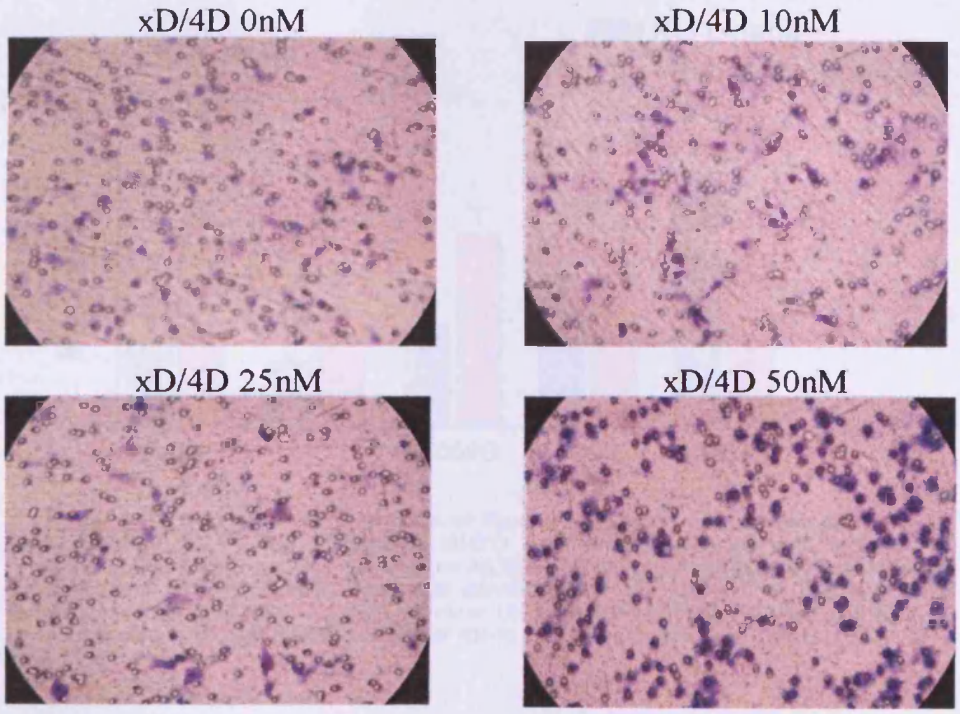

Figure 51: Effect of different concentrations of Semaphorin4D protein on the migration of NIH3T3 cells stably transfected with A5359G-PlexinB1 mutant (xD). Concentrations of 0ng/mL, 10ng/mL, 25ng/mL and 50ng/mL of Sema4D ligand were tested. Four random fields were counted under a microscope at magnification

4. Effects of three mutations of PlexinB1 on cell migration

Three replicated migration assay experiments have then been performed to measure the effects of plexin b1 mutations on cell movement.

The results in figure 52 show that expression of wild-type PlexinB1 protein inhibits cell migration, relative to cells not expressing exogenous PlexinB1 (vector only, control). Expression of the A5359G mutant form of PlexinB1 (found in LNCaP) increases migration relative to wild-type PlexinB1 in the absence of Semaphorin4D, and further increases migration in the presence of Semaphorin4D. Expression of the T5714C mutant form of PlexinB1 also increases migration relative to wild-type PlexinB1 and vector control in the absence of Semaphorin4D, and in the presence of Semaphorin4D migration is slightly increased further. Expression of the A5653 mutant form of PlexinB1 (the most frequent in prostate primary tumours and metastases) strongly increases migration relative to wild-type PlexinB1 and vector control in the absence of Semaphorin4D, and in the presence of 50ng/mL of Semaphorin4D migration is reduced but still increased relative to wild-type PlexinB1 and vector control.

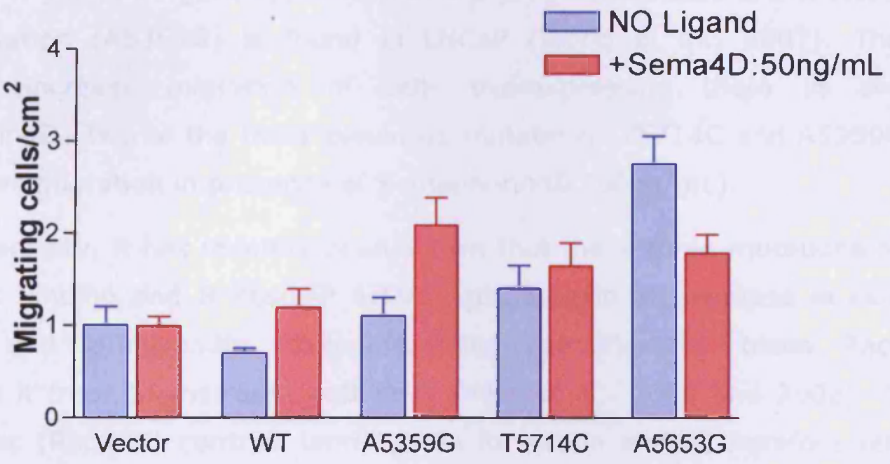

Figure 52: Effect of three mutations of PlexinB1 protein and presence of ligand Semaphorin4D on cell migration. NIH3T3 cells stably transfected with wild-type PlexinB1 (WT-PlxB1) and PlexinB1 mutants A5359G, T5714C and A5653G. A concentration of 50ng/mL of Semaphorin4D ligand was added. Results are mean of three independent experiments with standard error of the mean (SEM). ANOVA statistical analysis has been applied, which showed that the effects of ligand and mutation are significant (p values < 0.001).

5. Discussion

In this section, we report the first study of PlexinB1 and Semaphorin4D signalling in prostate cells and together the results suggest that PlexinB1 has a role in prostate cancer.

We show by quantitative RT-PCR that plexin b1 mRNA is overexpressed in a prostate primary tumour cell line and a bone metastasis derived cell line and that overexpression in NIH3T3 cells of wild-type PlexinB1, activated either by clustering or low concentrations of Semaphorin4D, inhibits cell migration, whereas high Semaphorin4D concentrations (50ng/mL in this model) increase cell migration. Two other groups confirmed that PlexinB1 activation inhibits cell migration in NIH3T3 and Cos-7 cells (Barberis et al., 2004; Oinuma et al., 2006). However, two other groups have shown that PlexinB1 activation can increase cell migration in MLP29 cells and in endothelial cells (Giordano et al., 2002; Basile et al., 2005). The effect of activation of PlexinB1 on cell migration therefore appears to be dependent on cell type and the signalling pathways expressed.

We also report that the three mutant forms of PlexinB1 tested have an effect on cell migration. Two mutations (A5653G and T5714C) are the most frequent mutations of plexin b1 gene found in prostate primary tumours and metastases. The other mutation (A5359G) is found in LNCaP (Wong et al., 2007). These three mutations increase migration of cells overexpressing them in absence of Semaphorin4D. Two of the three plexin b1 mutations (T5714C and A5359G) further increase cell migration in presence of Semaphorin4D (50ng/mL).

In the laboratory, it has recently been shown that these three mutations hinder Rac and R-Ras binding and R-RasGAP activity resulting in an increase in cell motility, adhesion and lamellipodia extension. Wild-type PlexinB1 binds RacGTP and sequesters it from downstream pathways (Vikis et al., 2000 and 2002). The active form of Rac (RacGTP) controls lamellipodia formation and is therefore required for cell migration. Thus, wild-type PlexinB1 protein prevents lamellipodia formation and subsequent cell migration by sequestering the active form of Rac. The mutant forms of PlexinB1 do not bind RacGTP (O. Wong, personal communication), so expression of the mutant forms of PlexinB1 would be predicted to enhance cell migration relative to the wild-type form. The increase in migration of cells expressing mutant forms of PlexinB1 relative to wild-type PlexinB1 is therefore consistent with a loss of RacGTP binding and is consistent with the results presented. Oinuma and colleagues have shown that wild-type PlexinB1 binds R-RasGTP and acts as a GTPase activating protein (GAP), resulting in the conversion of R-RasGTP to its inactive GDP bound form (Oinuma et al., 2004). They have recently shown that R-RasGTP activates integrins (Oinuma et al., 2006). Integrin activation is required for cell migration and inhibition of R-Ras inhibits migration. Mutant forms of PlexinB1 do not bind R-RasGTP

(Wong et al., 2007), and therefore do not inactivate R-Ras and do not inhibit the R-Ras/integrin pathway. This finding explains the loss of inhibitory function of the mutant forms of PlexinB1 but not the gain of function (i.e. does not explain the increase of migration over vector control). Further experiments to explain gain of function are required.

Section 3: Cloning of semaphorin 3e gene and roles of Semaphorin3E protein on cell phenotype and behaviour

Until a recent and important finding (Gu et al., 2005), little was known of Semaphorin3E protein, its receptor and its role. This group recently identified PlexinD1 as a functional receptor for Semaphorin3E protein in endothelial cells, inducing the inhibition of vessels formation and repulsion of surrounding vessels. Before this finding, it was thought that, like all secreted semaphorins (class 3), the receptor for Semaphorin3E would be a complex made of a class A plexin and a dimer of neuropilins. This theory had never been proved, but it had been shown that Semaphorin3E protein binds to Neuropilin1 (Feiner et al., 1997). Gu and colleagues, however, demonstrate that Semaphorin3E protein does not bind to neuropilins (1 or 2), but directly to class D PlexinD1.

We have shown in section 1 of this chapter that semaphorin 3e mRNA is synthesised by many prostate cell lines. Semaphorin 3e mRNA is expressed in the cell lines derived from two primary tumours and the matched non-neoplastic "normal" prostate epithelia and stroma (with a higher expression in the stromal cells than in the epithelial counterpart). Semaphorin 3e mRNA is expressed in three cell lines derived from metastases, with a strong expression in the bone metastasis derived cells. Semaphorin 3e mRNA is also expressed in cells derived from benign hyperplasic prostate (BPH), with a strong expression in the epithelial cell line compared to the matched stromal cell line. We have also shown that semaphorin 3e expression was under the control of hypoxia in one of the matched primary tumour and non-neoplastic "normal" cell lines, as well as in one colon cancer cell line. Semaphorin 3e mRNA expression levels were increased by hypoxia in the "normal" prostate epithelial cells, while they were strongly decreased in the matched primary tumour cells and in the colon cancer cell line.

We studied semaphorin 3e mRNA expression profile in six paired non-neoplastic and carcinoma prostate tissue samples by real-time RT-PCR (qRT-PCR), with the aim of determining if semaphorin 3e gene is differentially expressed in prostate cancer. The complete coding sequence of semaphorin 3e gene was cloned into a mammalian expression vector and the protein produced. Subsequently, the effects of Semaphorin3E protein on cell behaviour and phenotype were studied by means of immunostaining and adhesion assays.

1. Quantitative expression levels of semaphorin 3e mRNA in prostate cell lines and tissues

Semaphorin 3e mRNA expression levels have been quantified by real-time RT-PCR (qRT-PCR) in 8 prostate cell lines and six tissue samples previously described. Quantitative RT-PCRs were performed in triplicate, and on three different RNA extractions (from three consecutive passages). The results presented are normalised means (refer to page 71) with standard errors of the mean (SEM). Normalisation has also been performed to the expression levels found in the non-neoplastic ("normal") prostate epithelial cell line (42N=1), used as a reference. Standard T-test statistical analysis has been applied using GraphPad software.

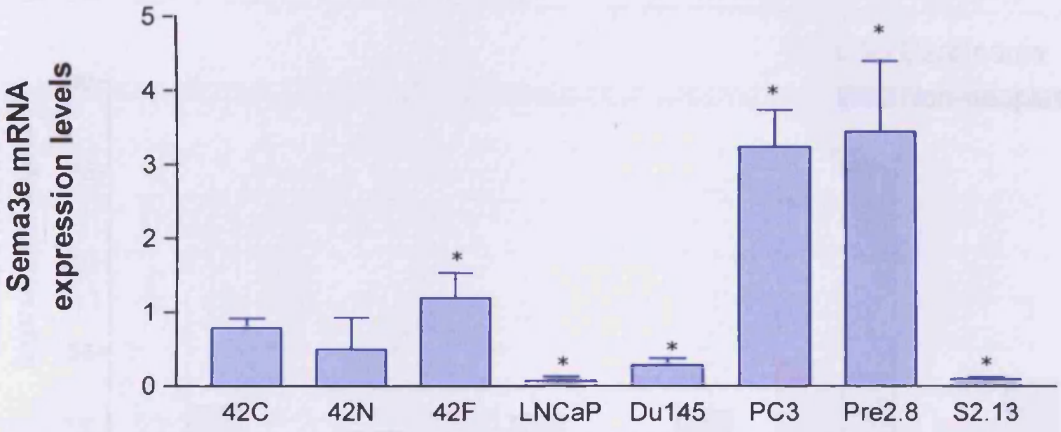

Figure 53: Semaphorin 3e mRNA expression profiles (qRT-PCR) in 8 prostate cell lines, derived from a primary tumour (1542CPTX or 42C), the matched non-neoplastic "normal" epithelia (1542NPTX or 42N) and stroma (1542FTX or 42F), metastases to the lymph node (LNCaP), the brain (DU145) and the bone (PC3), and benign hyperplastic epithelia (Pre2.8) and stroma (S2.13). Results are mean of three replicates normalised to 42N expression levels, with standard error of the mean (SEM). Standard T- test has been applied (*: significant change :< 0.05).

Cell lines	Relative expression levels
42C	0.8
42N	1
42F	1.2
LNCaP	0.1
Du145	0.3
PC3	3.2
Pre2.8	3.4
S2.13	0.1

Table 15: Relative expression levels of semaphorin 3e mRNA (qRT-PCR) in 8 prostate cell lines.

The results in figure 53 (summarised in table 15) show the same trend as the RT-PCR results detailed in section 1 of this chapter (refer to pages 88 to 90).

Semaphorin 3e mRNA expression levels are slightly higher in the stromal cells derived from normal prostate (42F) compared to the levels observed in epithelial cells (42N). The results also confirm that there is no significant difference in the levels of expression of semaphorin 3e between primary tumour derived prostate cells (42C) and the matched non-neoplastic "normal" cells (42N). Also, the results show that semaphorin 3e expression levels are extremely low (10 fold decrease) in a cell line derived from a lymph node metastasis (LNCaP) and in stromal cells derived from BPH (S2.13), very low (more than 3 fold decrease) in cells derived from a brain metastasis (DU145) whereas they are strongly increased (more than 3 fold) in cells derived from a bone metastasis (PC3) and in epithelial cells derived from BPH (Pre2.8).

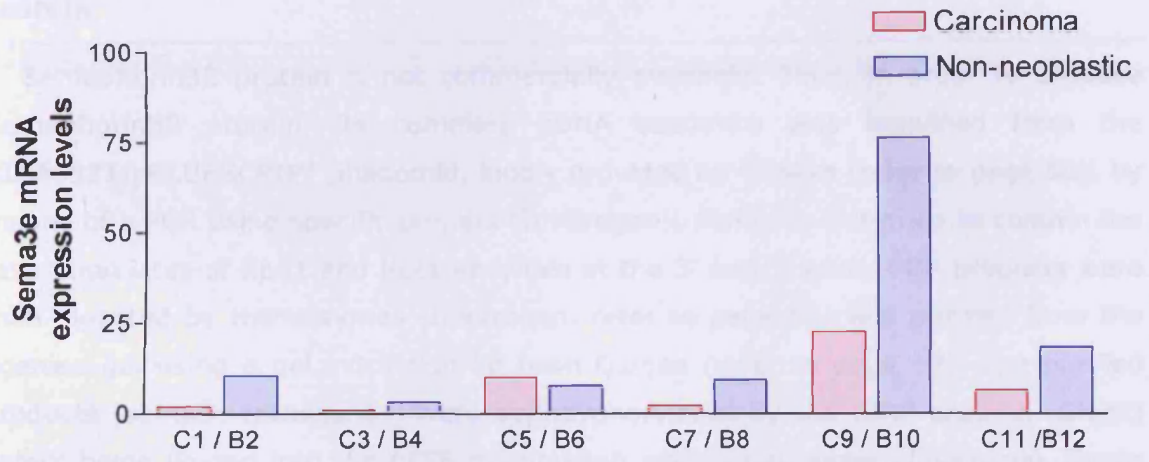

Figure 54: Semaphorin 3e mRNA expression profiles (qRT-PCR) in 6 paired non-neoplastic/carcinoma prostate tissue samples. Results are mean of three replicates from one experiment. No statistical analysis has been applied.

Tissue Sample	Relative expression levels	pT	GSC
C1 B2	2.1 10.5	3a	5
C3 B4	1.1 3.1	2c	6
C5 B6	10.2 7.7	2c	6
C7 B8	2.3 9.4	3a	6
C9 B10	22.6 76.2	2c	5
C11 B12	6.7 18.3	2c	7

Table 16: Relative expression levels of semaphorin 3e mRNA (qRT-PCR) in 6 paired prostate tissue samples. Tumour stage (pT) and Gleason score (GSC) are listed. A Gleason grade between 5 and 7 describes well and moderately differentiated tumours. Tumours are either confined within the prostate but involving both lobes (2c) or with extracapsular extension (3a).

The results in figure 54 and table 16 show that semaphorin 3e mRNA expression levels are 3 to 5 times higher in non-neoplastic tissue, compared to the carcinoma counterpart, and thus in 5 out of 6 paired samples. This may reflect the higher proportion of stromal cells seen in normal prostate tissue compared to cancer, as higher semaphorin 3e expression was found qRT-PCR and RT-PCR in the stromal cell line (42F). These tissue samples are paired non-neoplastic and cancer regions of well and moderately differentiated prostate tumours with no regional lymph node metastases. However, no association was seen between semaphorin 3e mRNA expression profile and the stage or Gleason score of the tumour.

2. Cloning of semaphorin 3e gene and production of Semaphorin3E protein

Semaphorin3E protein is not commercially available. Thus, in order to produce Semaphorin3E protein, its complete cDNA sequence was amplified from the KIAA0331/pBLUESCRIPT phagemid, kindly provided by Tanaka (refer to page 60), by means of a PCR using specific primers (Invitrogen), manually designed to contain the restriction sites of Kpn1 and Not1 enzymes at the 3′ and 5′ ends. PCR products were then digested by the enzymes (Invitrogen, refer to page 56) and purified from the agarose gel using a gel extraction kit from Qiagen (refer to page 57). The purified products (sema3e transgenes) were dephosphorylated by the CIAP enzyme (Gibco) before being ligated into the pEF6 mammalian expression vector (Invitrogen, figure 55) using the T4 DNA ligase (Invitrogen) (refer to pages 73 to 75).

The recombinant vector containing the transgene, pEF6-*Sema3e*-Myc/His was subsequently used to transform *Escherichia Coli* host strains (refer to page 65). The presence of the insert was checked in several colonies by PCR using the specific semaphorin 3e primers in order to eliminate false positives (figure 56). The insertion of the transgene was further checked by PCR in two of those positive colonies (figure 58), using primers located at the overlap transgene-vector (P1, P2, P3, P4, Invitrogen, refer to page 63) (figure 57). The cloned semaphorin 3e complete coding sequence was then verified by sequencing using specific and overlapping primers. The sequence of the transgene was checked using BLAST tool from the NCBI website (http://www.ncbi.nlm.nih.gov/). No mutations had been inserted during the cloning (figure 59).

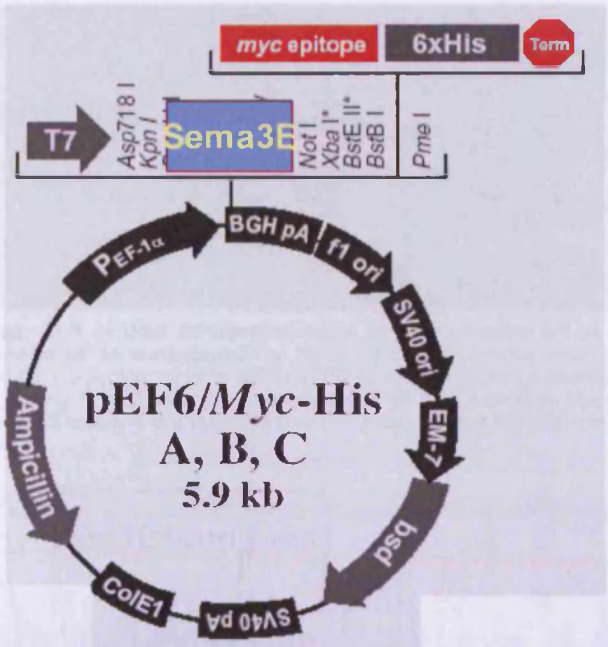

Figure 55: Schematic representation of the mammalian expression vector pEF6/Myc-His (version B, Invitrogen), **with semaphorin 3e gene inserted between KpnI and NotI sites.**

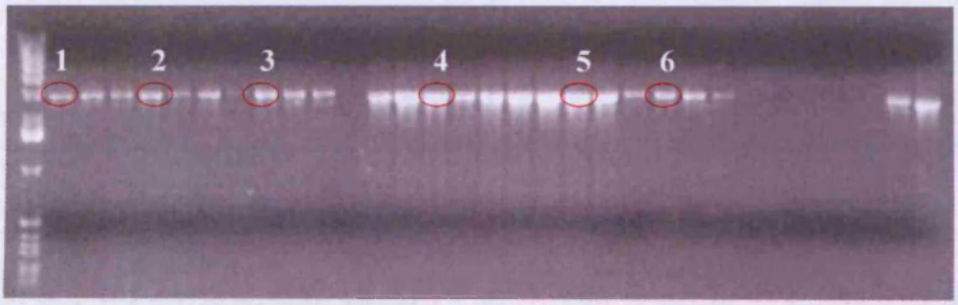

Figure 56: Direct PCR of E.Coli colonies transformed with pEF6-Sema3e-Myc-His. Some colonies (for example 1 to 6) are positive for the presence of the transgene (Semaphorin 3e), and some are negative.

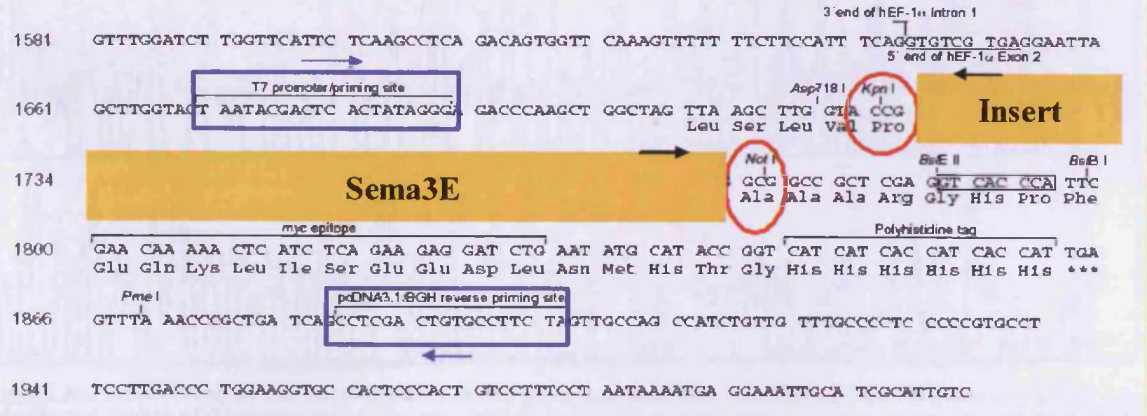

Figure 57: Schematic representation of the multiple cloning site of pEF6-Sema3e-Myc-His. In purple, the forward T7 promoter/priming site primer (P1-T7) and the reverse BGH-reverse priming site (P4-BGH). The black arrows represent the reverse P2-Sema3e primer located within exon 1 of semaphorin 3e gene, and the forward P3-Sema3e primer located in exon 17.

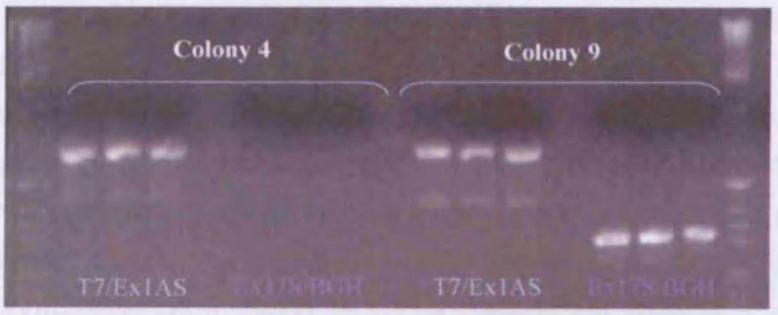

Figure 58: PCR of DNA minipreparations of two positive E.Coli colonies for semaphorin 3e transgene. The following sets of primers were used: P1-T7/P2-Exon1 (expected band at 650bp), P3-Exon17/P4-BGH (expected band at 310bp). Colony 9 is a true positive (presence of both bands at the expected size), whereas colony 4 is a false positive (only one band at the expected size).

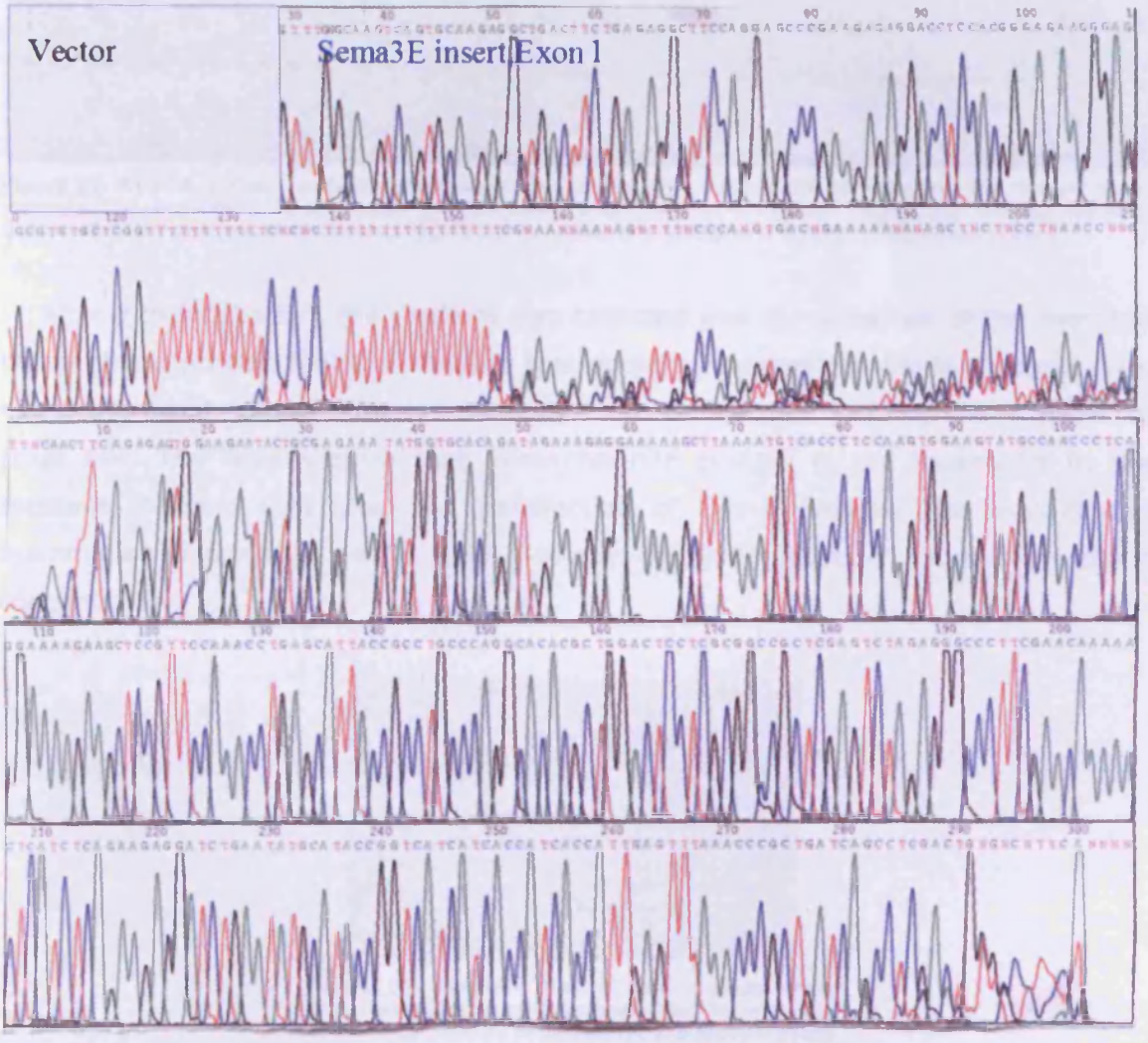

Figure 59: Sequencing of the recombinant vector pEF6-Sema3e-Myc-His. The plasmid DNA was sequenced using the forward primer P1-T7-promoter/priming site, located at the 5'end of the vector and the reverse primer P2-Sema3e-Exon1, located within the first exon of the semaphorin 3e gene.

Cos-7 cells were then transfected with the recombinant mammalian expression vector pEF6-*Sema3e*-Myc/His to produce the protein. Several Cos colonies were checked for the presence of the transgene (figure 60). A positive colony was chosen for subsequent protein production. The recombinant Semaphorin3E protein is coupled to a Myc epitope and a His-Tag, which allow its detection and purification on a nickel column. Untransfected and mock transfected Cos-7 cells do not endogenously synthesise semaphorin 3e mRNA (results not shown).

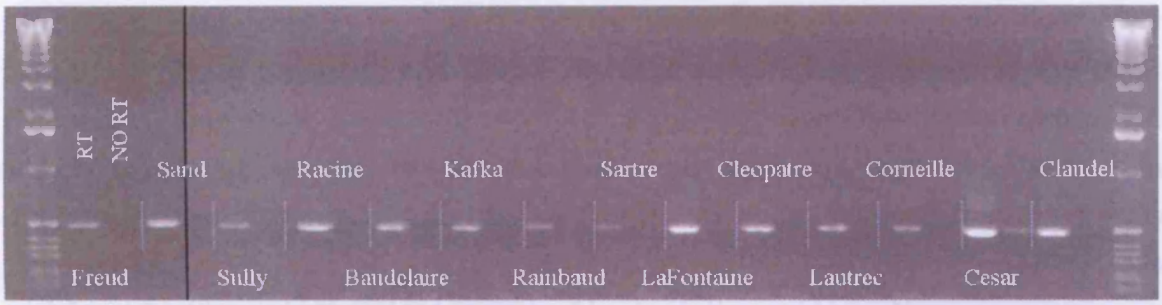

Figure 60: RT-PCR of Cos-7 cells transfected with the expression vector pEF6-Sema3e-Myc-His. Several clones expressed the semaphorin 3e transgene. For each clone, a control with no reverse transcriptase enzyme has been performed. Cos-7 cells and mock transfected cells do not express any semaphorin 3e mRNA (resultsnot shown).

After 72h incubation, the medium was collected and the presence of the secreted recombinant protein Sema3E-Myc/His was detected by western blotting (figure 61), using the 9E10 mouse anti-Myc antibody from Santa Cruz Biotechnology (refer to page 64). The results show that Semaphorin3E protein is not detectable in the medium collected 72h after the transfection of Cos-7 cells by the recombinant mammalian expression vector pEF6-*Sema3e*-Myc/His (figure 61, lane D) without concentration.

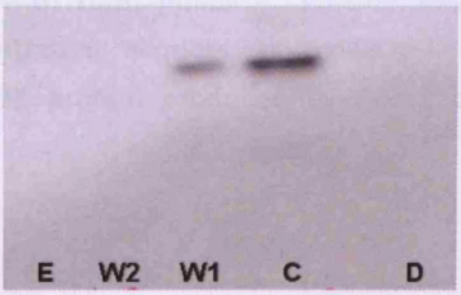

Figure 61: Western blot of the medium from transfected Cos-7 cells; detection of the presence of the recombinant Sema3E-Myc-His protein using Myc antibody. Medium was concentrated by ultra-filtration. C: concentrated fraction after ultra-filtration, E: eluted fraction, W1 and W2: fractions collected after the first (W1) and second (W2) washes. D: medium not concentrated.

In order to detect the recombinant protein produced by the transfected Cos cells, the medium had to be concentrated by ultrafiltration (Amicon Ultra Centrifugal Filter Device PL30, Millipore, refer to page 75). The results show that the presence of the recombinant Sema3E-Myc/His protein was then detectable in the concentrated fraction of the collected medium (figure 61, lane C).

It has been shown that the activity of class 3 semaphorins is modulated by furin (Adams et al., 1997; Christensen et al., 2005). Furin is a proprotein convertase which has been shown to cleave various latent precursor proteins into their biologically active products, and whose cleavage recognition sequence is RX(K/R)R (figure 62). Importantly, the putative furin recognition sequence of Semaphorin3E protein is located between the sema domain and the immunoglobulin-like domain (figure 62). The presence of furin protease in the medium of transfected Cos-7 cells could eliminate the Myc epitope and His-Tag of the recombinant Sema3E-Myc/His protein, which are both added at the 3'end of the protein, thus preventing its detection by western blotting. At first, we thought that the protein was undetectable in the collected medium because of a probable cleavage by furin protease. Thus, in parallel, the recombinant protein was re-expressed in Cos-7 cells treated by an inhibitor of the furin protease (decanoyl-RVKR-chloromethylketone, Clontech, refer to page 75).

The results confirm that furin proprotein convertase cleaves the recombinant Sema3E-Myc/His protein, as we detect more protein in the medium treated with furin inhibitor than in the medium not treated with the inhibitor (figure 63). Also, the presence of the recombinant protein is undetectable in non-concentrated fraction, whether treated or not with furin inhibitor. Further experiments were therefore performed using concentrated aliquots of collected medium containing the recombinant Semaphorin3E protein produced by Cos-7 cells in presence of furin protease inhibitor.

MASAGHITLLLWGYLLELWTGGHTADTTHPRLRLSHKELLNLN
RTSIFHSPFGFLDLHTMLLDEYQERLFVGGRDLVYSLSLERISDGY
KEIHWPSTALKMEECIMKGKDAGECANYVRVLHHYNRTHLLTC
GTGAFDPVCAFIRVGYHLEDPLFHLESPRSERGRGRCPFDPSSSFIS
TLIGSELFAGLYSDYWSRDAAIFRSMGRLAHIRTEHDDERLLKEPK
FVGSYMIPDNEDRDDNKVYFFFTEKALEAENNAHAIYTRVGRLCV
NDVGGQRILVNKWSTFLKARLVCSVPGMNGIDTYFDELEDVFLLP
TRDHKNPVIFGLFNTTSNIFRGHAICVYHMSSIRAAFNGPYAHKEG
PEYHWSVYEGKVPYPRPGSCASKVNGGRYGTTKDYPDDAIRFARS
HPLMYQAIKPAHKKPILVKTDGKYNLKQIAVDRVEAEDGQYDVLF
IGTDNGIVLKVITIYNQEMESMEEVILEELQIFKDPVPIISMEISSKRQ
QLYIGSASAVAQVRFHHCDMYGSACADCCLARDPYCAWDGISCSR
YYPTGTHAKRRFRRQDVRHGNAAQQCFGQQFVGDALDKTEEHLA
YGIENNSTLLECTPRSLQAKVIWFVQKGRETRKEEVKTDDRVVKM
DLGLLFLRLHKSDAGTYFCQTVEHSFVHTVRKITLEVVEEEKVEDM
FNKDDEEDRHHRMPCPAQSSISQGAKPWYKEFLQLIGYSNFQRVEE
YCEKVWCTDRKRKKLKMSPSKWKYANPQEKKLRSKPEHYRLPRH
TLDS

Figure 62: The furin protease recognition sequence of Semaphorin3E protein. The sema domain of Semaphorin3E protein is highlighted in yellow, and spans 300 amino acids (241-540), the immunoglobulin domain is highlighted in pink and spans 90 amino acids (647-736). The furin protease cleavage recognition sequence is located between these two domains, in red (consensus sequence is RX(K/R)R).

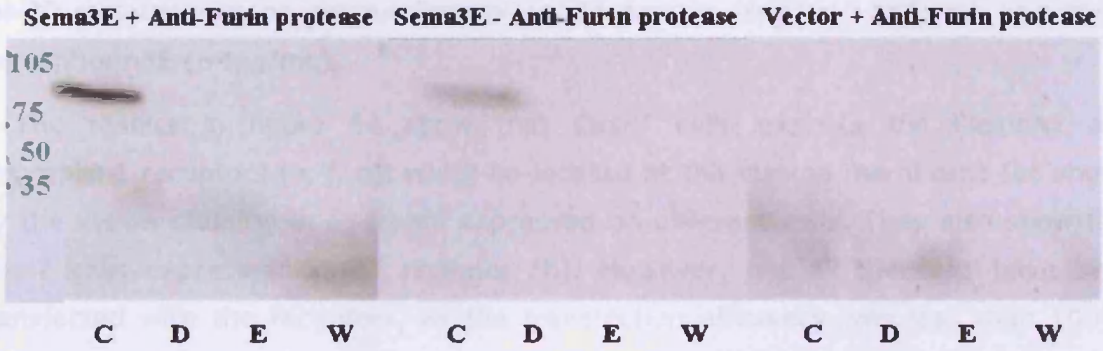

Figure 63: Western blot of the medium of Cos-7 cells transfected with the expression vector pEF6-Sema3e-Myc-His or the vector only, and treated or not treated with furin inhibitor. Medium was concentrated by ultra-filtration. C: concentrated fraction after ultra-filtration, D: medium not filtered, i.e. not concentrated, E: eluted fraction, W: fraction collected after the first wash. The control Vector – Anti-furin protease is also negative (not shown).

Altogether, these results show that semaphorin 3e cloning and production were successful. In contrast, purification of the protein using a nickel column was unsuccessful, probably because the His tag was cleaved or hidden (refer to pages 75 and 76). However, to test the effects of Semaphorin3E protein, it is not necessary to have it purified on a nickel column and it was therefore concentrated but not purified. Protein concentration was measured using the Lowry method (Sigma, refer to page 76) and estimated by western blotting (refer to page 77), using the anti-Myc antibody (Santa Cruz Biotechnology, refer to page 64) (results not shown).

3. Effects of Semaphorin3A and Semaphorin3E on the morphology and interactions of Cos-7 cells overexpressing PlexinA1 and Neuropilin1 receptors or PlexinD1 receptor

a. Actin microfilament distribution in Cos-7 cells overexpressing PlexinA1 and Neuropilin1 receptors or PlexinD1 receptor

To test the effects of Semaphorin3E protein on cell phenotype and behaviour, Cos-7 cells have been transfected with expression vectors for PlexinA1/Myc and Neuropilin1/HA (Semaphorin3A receptors), or PlexinD1/VSV (Semaphorin3E receptor). Their expression was verified 48h after transfection by immunostaining using primary antibodies against their tags (Myc, HA or VSV) and secondary antibodies conjugated with fluorescent green (FITC) or red (TRITC) dyes (refer to pages 64 and 79). Actin microfilaments were stained with phalloidin conjugated to a red dye (TRITC) and nuclei were stained in blue (DAPI). Cells were further treated for 30 minutes with or without Semaphorin3A protein (4μg/mL) and with or without Semaphorin3E (~4μg/mL).

The results in figure 64 show that Cos-7 cells express the PlexinA1 and Neuropilin1 receptors (e, f, g), which co-localise at the plasma membrane (as shown by the yellow staining in e) or are expressed on different cells. They also show that Cos-7 cells express PlexinD1 receptor (h). However, not all the cells have been transfected with the receptors, as the transfection efficiency was less than 100%. Nonetheless, RT-PCR showed that Cos-7 cells endogenously express high levels of all three receptors (results not shown). Therefore, even if all cells are not transfected, we can still expect to see some effect with Semaphorin3A and Semaphorin3E proteins.

The results in figure 65 show that actin microfilament distribution is different between Cos-7 cells transfected with PlexinD1 receptor and those transfected with PlexinA1 and Neuropilin1 receptors. No stress fibers are observed in the cells transfected with PlexinD1 receptor (g, h), whereas the cells transfected with PlexinA1 and Neuropilin1 present stress fibers (e, f). Addition of the ligands, Semaphorin3A (a, b) or Semaphorin3E (c) inhibits the formation of stress fibers in cells transfected with PlexinA1 and Neuropilin1, which suggest that Semaphorin3E may bind Neuropilin1 in our cellular system, as shown by Feiner and colleagues (Feiner et al.,

1997). Addition of Semaphorin3E protein (d) does not induce stress fibers formation in cells transfected with PlexinD1.

Altogether these results suggest that an overexpression of Semaphorin3A receptors, PlexinA1 and Neuropilin1, lead to stress fibers formation, which is inhibited by addition of its specific ligand, Semaphorin3A, but as well by Semaphorin3E. In contrast, cell transfected by Semaphorin3E specific receptor, PlexinD1, do not show any stress fiber formation, which may suggest that stress fiber formation is activated by Neuropilins rather than Plexins.

b. Effects of Semaphorin3A and Semaphorin3E on β1-integrin activation in Cos-7 cells overexpressing PlexinA1 and Neuropilin1 receptors or PlexinD1 receptor

The effects of Semaphorin3A and Semaphorin3E proteins in cells overexpressing the receptors PlexinA1 and Neuropilin1, or PlexinD1 were also visualised by immunostaining using an antibody directed against active conformations of human β1-integrin. Cell adhesion is mediated by integrins, which are transmembrane receptors interacting with the extracellular matrix. For instance, α5β1-integrin is the typical fibronectin receptor involved in matrix attachment (Wu et al., 1993; Zhang et al., 1993; Danen et al., 2002).

The results in figure 66 show that Cos-7 cells overexpressing PlexinA1 and Neuropilin1 receptors stain for active β1-integrin (d, e) in the cytoplasm. When treated with Semaphorin3E (b) or Semaphorin3A (a), these cells still stain for active β1-integrin. However, a sparse distribution of the cells is observed when treated with Semaphorin3A, which would support the claim that Semaphorin3A protein inhibits β1-integrin adhesion, as shown by Serini and colleagues (Serini et al., 2003). The effect of Semaphorin3A protein on active conformations of β1-integrins is less obvious under a microscope at a 40X magnification (figure 67, a and d). The results in figure 66 also show that Cos-7 cells overexpressing PlexinD1 receptor stain for active β1-integrin (f), but treatment with Semaphorin3E strongly inhibits active β1-integrin staining (c). Even at a 40X magnification (figure 67, c and f), the effect of Semaphorin3E protein on β1-integrins is visible, which suggests that the inhibitory effect of Semaphorin3E is stronger than the inhibitory effect observed with Semaphorin3A.

Altogether, these results confirm that PlexinA1 and Neuropilin1 receptors are not functional receptors for Semaphorin3E protein, as no effect is observed in cells overexpressing PlexinA1 and Neuropilin1 receptors and treated by Semaphorin3E. In contrast, PlexinA1 and Neuropilin1 are functional receptors for Semaphorin3A in Cos cells. The results confirm that PlexinD1 is a functional receptor for Semaphorin3E in Cos cells, which suggest that it might be the case in many other cellular systems, as already shown in endothelial cells by Gu and colleagues (Gu et al., 2005). The results also show that Semaphorin3E protein strongly reduces active β1-integrins immunostaining of cells overexpressing its functional receptor PlexinD1, suggesting that Semaphorin3E inhibits cell-matrix adhesion, more strongly than Semaphorin3A does.

c. Effects of Semaphorin3A and Semaphorin3E on vinculin in Cos-7 cells overexpressing PlexinA1 and Neuropilin1 receptors or PlexinD1 receptor

The effects of Semaphorin3A and Semaphorin3E proteins in cells overexpressing the receptors PlexinA1 and Neuropilin1, or PlexinD1 were visualised by immunostaining using an antibody directed against vinculin. Vinculin is an actin-binding protein that links integrins to the actin cytoskeleton, modulating focal adhesion (FA) structure and function. Vinculin is ubiquitously expressed and is traditionally used as a marker for focal adhesion formation, which has a punctate appearance by immunostaining (Zamir and Geiger, 2001).

The results in figure 68 indicate that Cos-7 cells overexpressing plexinA1 and Neuropilin1 receptors do not stain for vinculin at focal adhesions (e, f, g) because the marked typical punctate staining is detectable only when the cells were treated with Semaphorin3A protein (a, b). The results also show that Semaphorin3E protein does not lead to the formation of focal adhesions by Cos-7 cells overexpressing PlexinA1 and Neuropilin1 receptors (c), whereas it does in Cos-7 cells overexpressing PlexinD1 receptor (d). Altogether, these results show that activation of PlexinA1 and Neuropilin1 receptors by Semaphorin3A ligand, and activation of PlexinD1 receptor by Semaphorin3E ligand activate vinculin-mediated formation of focal adhesions.

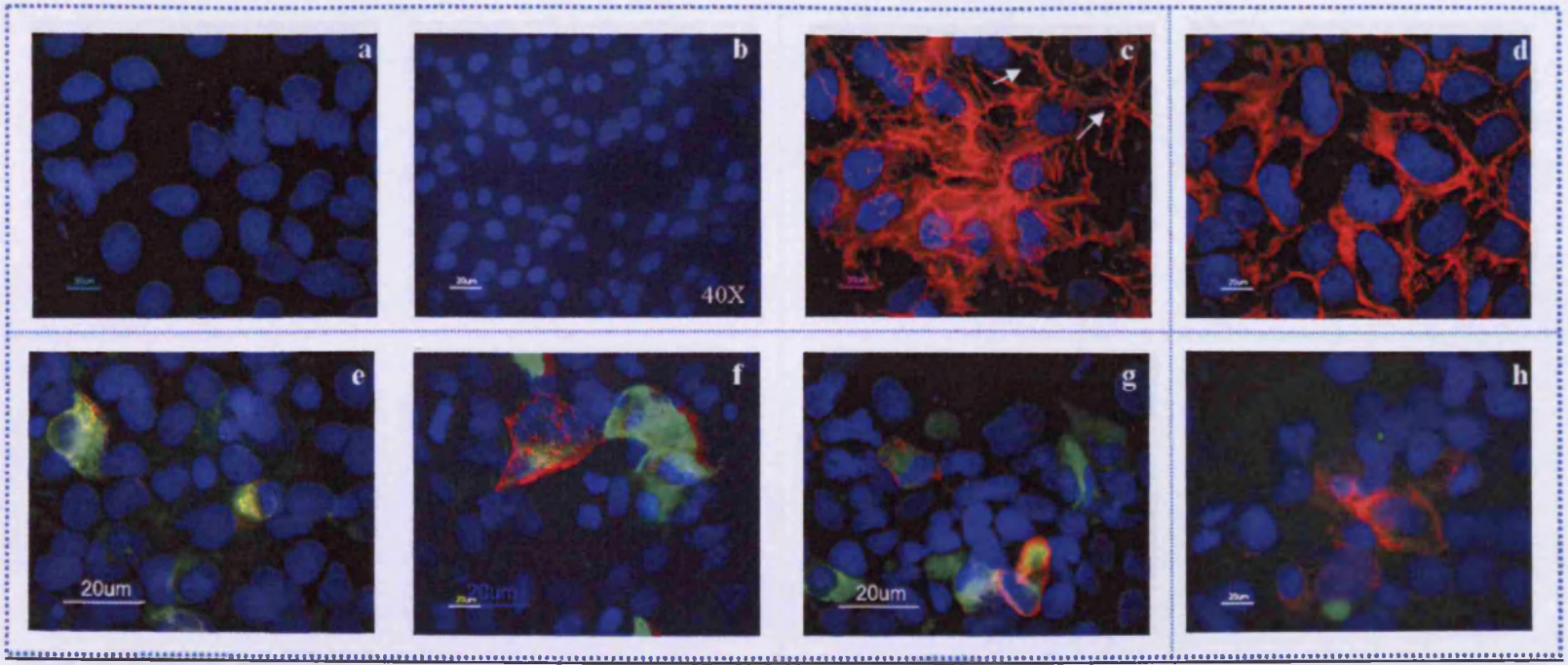

Figure 64: Immunostaining of Cos-7 cells transfected with semaphorin receptors PlexinA1/Myc and Neuropilin1/HA (a, c, e, f, and g) or PlexinD1/VSV (b, d, h) (100X magnification). ***a:*** no primary antibody, secondary rabbit anti-mouse FITC-conjugated. ***b***: no primary antibody, secondary goat anti-rabbit TRITC-conjugated. ***c, d***: phalloidin-TRITC-conjugated. Arrows point at stress fibers. ***e, f, g:*** primary mouse anti-Myc and rabbit anti-HA antibodies and secondary rabbit anti-mouse FITC-conjugated and goat anti-rabbit TRITC-conjugated. ***h:*** primary rabbit anti-VSV antibodies and secondary goat anti-rabbit TRITC-conjugated.

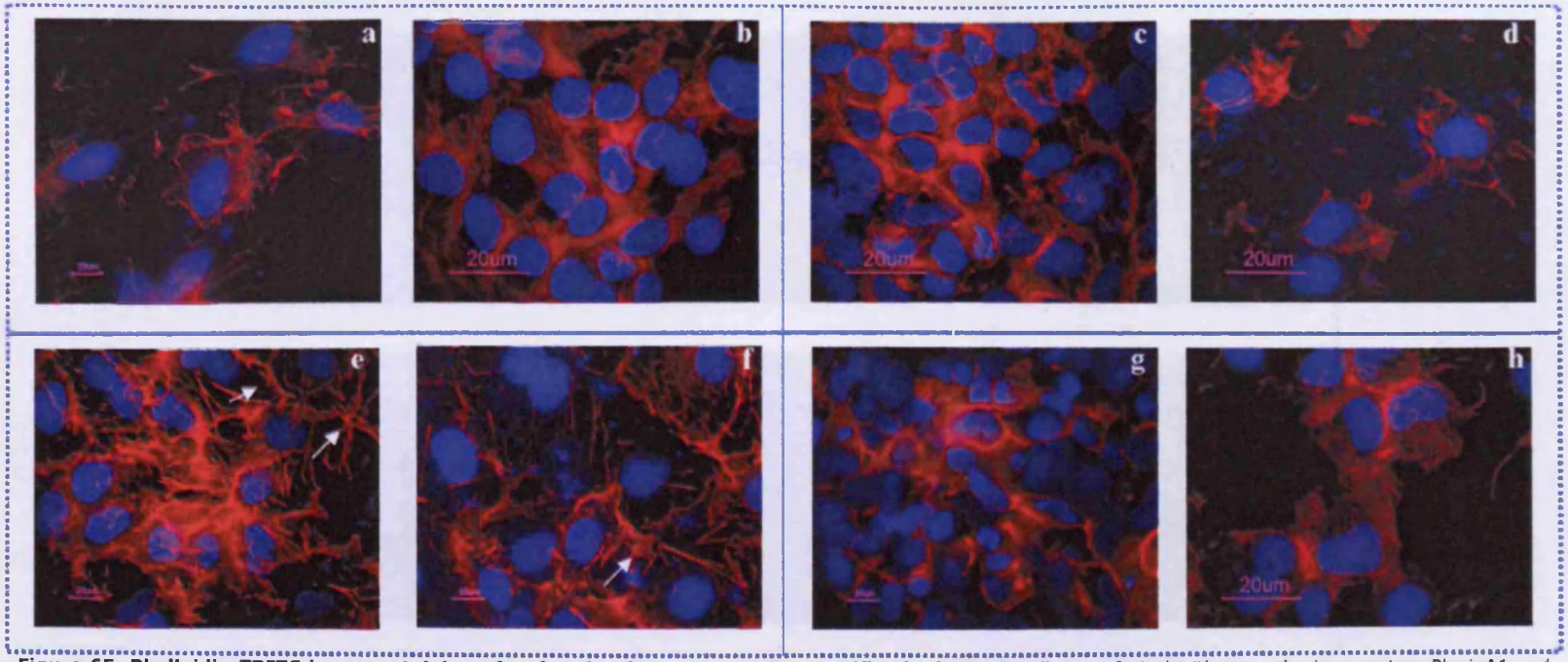

Figure 65: Phalloidin-TRITC immunostaining of actin microfilaments (100X magnification). Cos-7 cells transfected with semaphorin receptors PlexinA1 and Neuropilin1 (a, b, c, e, f) or PlexinD1 (d, g, h) and treated with Semaphorin3A protein (a, b) or Semaphorin3E protein (c, d). Cos-7 cells overexpressing PlexinA1 and Neuropilin1 receptors present stress fibers (arrows, e, f), but none when they have been treated with Semaphorin3A (a, b) or Semaphorin3E (c). Cos-7 cells overexpressing PlexinD1 do not present stress fibers, whether treated (d) or not treated with Semaphorin3E (g, h).

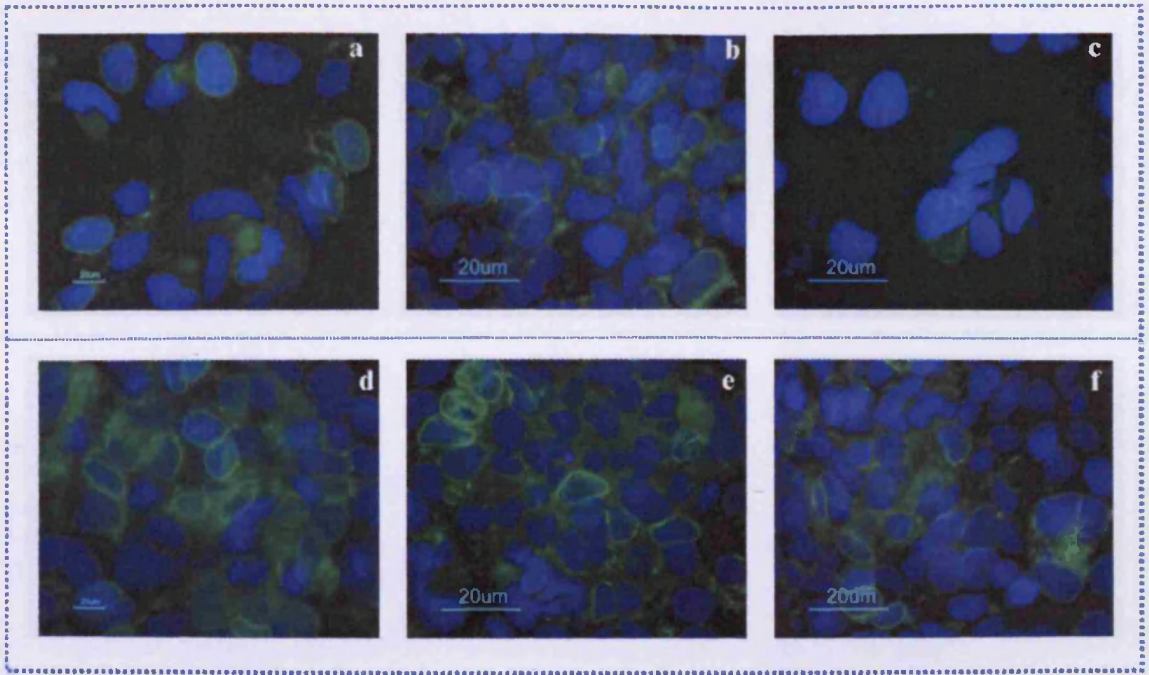

Figure 66: Immunostaining of β1-integrin active conformations (100X magnification). Cos-7 cells transfected with semaphorin receptors PlexinA1 and Neuropilin1 (a, b, d, e) or PlexinD1 (c, f) and treated with Semaphorin3A (a) or Semaphorin3E (b, c) proteins. Cells expressing receptors PlexinA1 and Neuropilin1 receptors stain for active β1-integrin whether untreated (d, e) or treated with Semaphorin3A (a) or Semaphorin3E protein (b). Cells expressing PlexinD1 receptor stain for active β1-integrin when untreated (f) whereas treatment with Semaphorin3E protein (c) strongly inhibits β1-integrin immunostaining

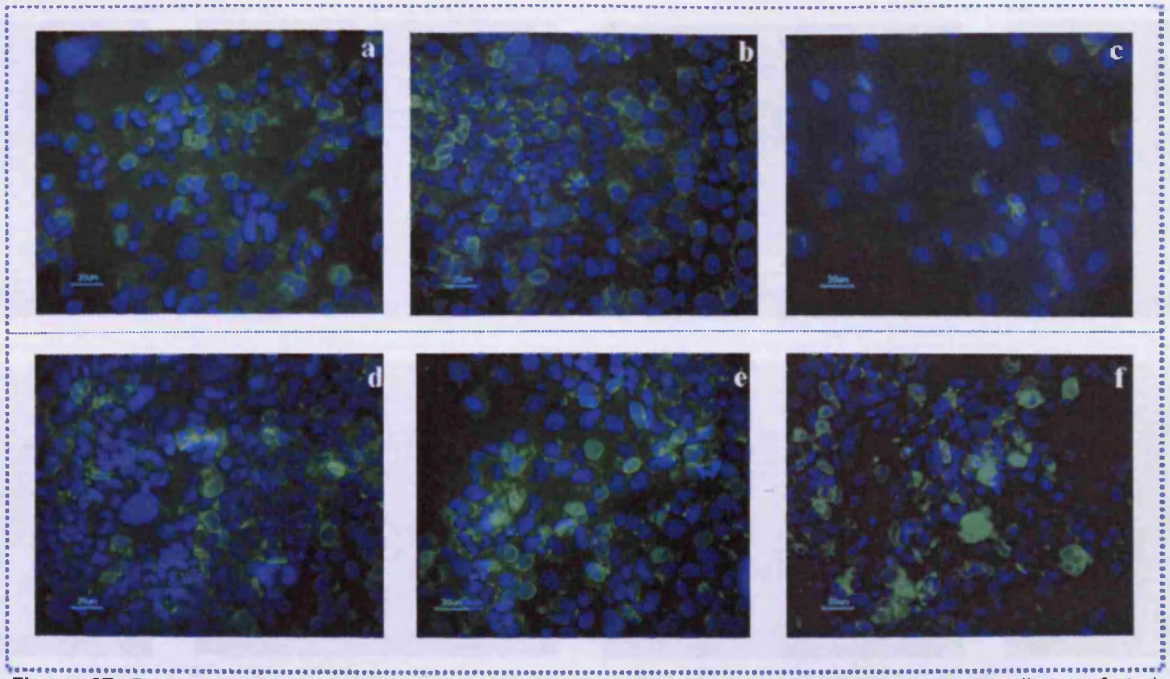

Figure 67: Immunostaining of β1-integrin active conformations (40X magnification). Cos-7 cells transfected with semaphorin receptors PlexinA1 and Neuropilin1 (a, b, d, e) or PlexinD1 (c, f) and treated with Semaphorin3A (a) or Semaphorin3E (b, c) proteins. Cells expressing receptors PlexinA1 and Neuropilin1 receptors stain for active β1-integrin whether untreated (d, e) or treated with Semaphorin3A (a) or Semaphorin3E protein (b). Cells expressing PlexinD1 receptor stain for active β1-integrin when untreated (f), whereas treatment with Semaphorin3E protein (c) inhibits β1-integrin immunostaining.

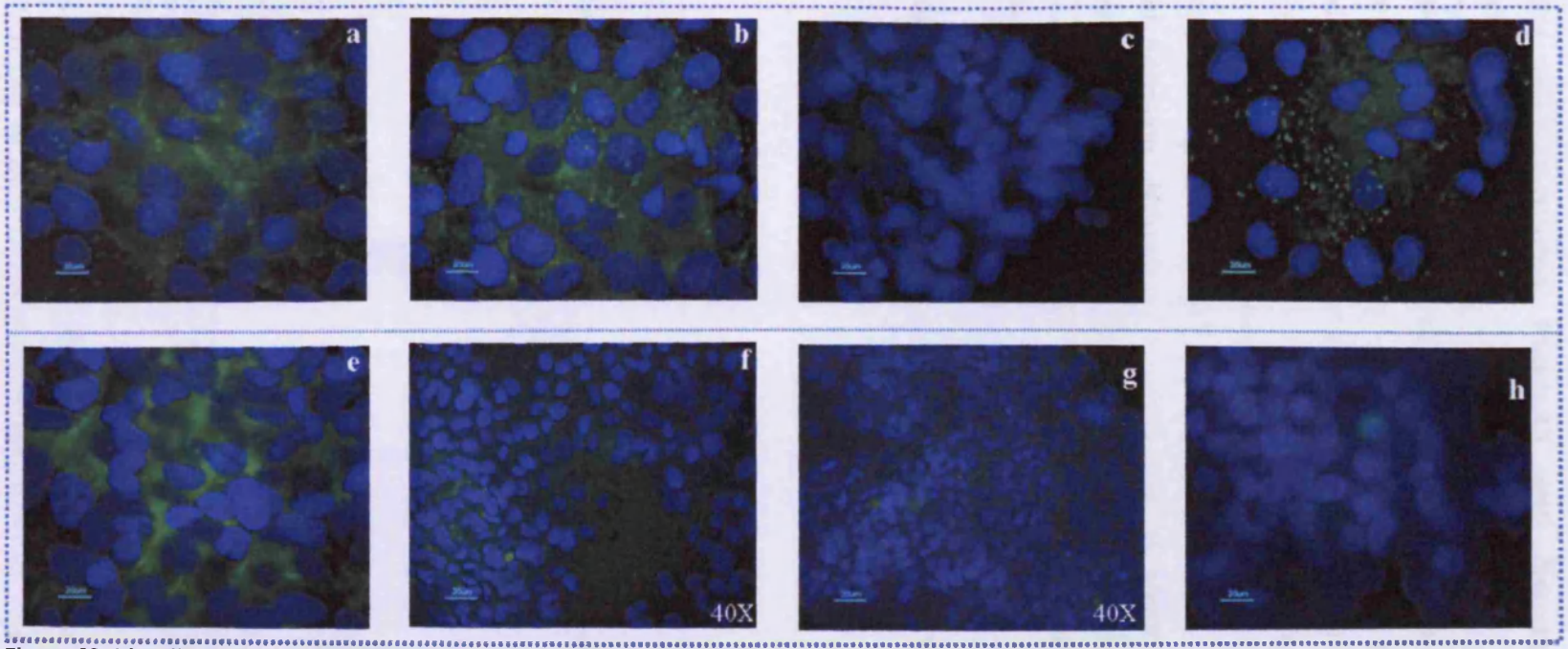

Figure 68: Vinculin immunostaining (100X or 40 X magnifications). Cos-7 cells transfected with semaphorin receptors PlexinA1 and Neuropilin1 (a, b, c, e, f, g) or PlexinD1 (d, h) and treated with Semaphorin3A (a, b) and Semaphorin3E proteins c, d). Cells expressing receptors PlexinA1 and Neuropilin1 (e, f, g) and treated with Semaphorin3E protein (c) do not stain for vinculin, whereas those treated with Semaphorin3A (a, b) do (dotted staining). Cells expressing PlexinD1 receptor do not stain for vinculin (h) unless treated with Semaphorin3E protein (d) (punctate staining).

4. Effects of Semaphorin3A and Semaphorin3E on cell adhesion of HEK293 cells overexpressing PlexinA1 and Neuropilin1 receptors or PlexinD1 receptor

The adhesion of cells overexpressing PlexinA1 and Neuropilin1 receptors, and PlexinD1 receptor was tested on two different substrates, over time (10 and 30 minutes), and in presence or absence of ligands (refer to pages 59, 67, and 80). HEK293 cells were chosen and this assay was optimised by us. Adhesion assays were performed on the lid of a 96 well plate (refer to page 80), coated with fibronectin, which mediates an integrin based adhesion, or poly-L-lysine, which mediates a non-integrin based adhesion. Adhesion was measured by absorbance (methylene blue staining of adhered cells) on a plate reader. Assays were performed in triplicate, and repeated three times independently. ANOVA statistical analysis has been applied using GraphPad software.

a. Effect of matrix and time on cell adhesion of HEK293 cells

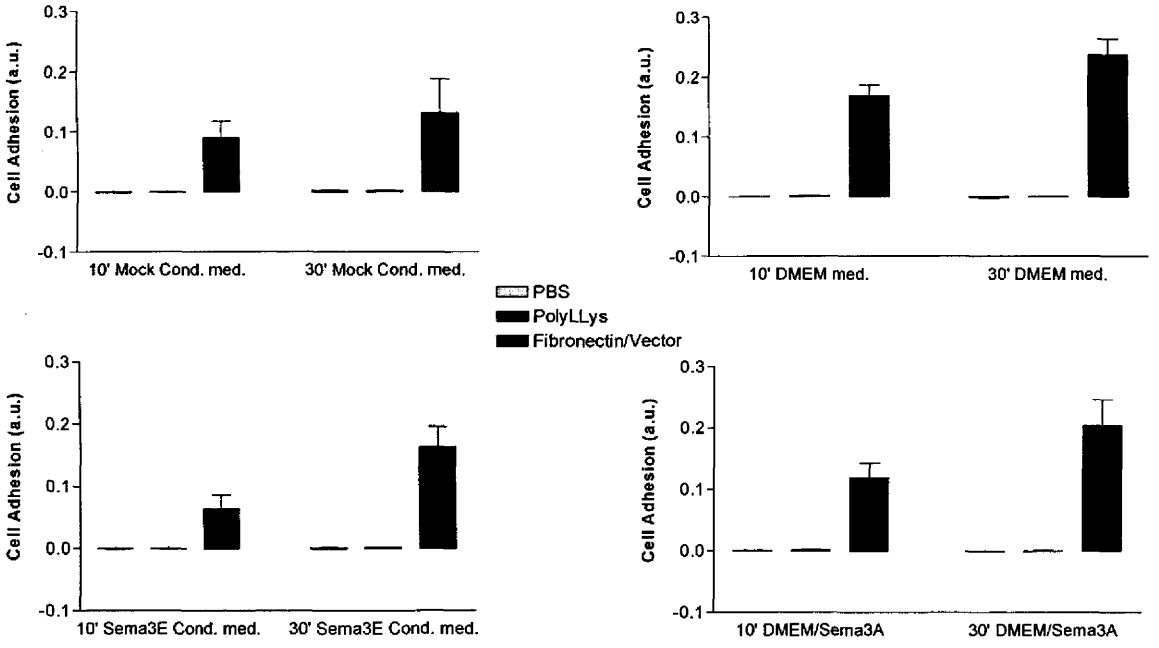

Figure 69: Adhesion assay on two different substrates, poly-L-lysine and fibronectin. HEK293 cells transfected with the control vector pcDNA3. Results are mean of three independent experiments, with standard error of the mean (SEM). ANOVA statistical analysis has been applied, which showed that the effects of matrices and time are significant (p value < 0.001).

The results in figure 69 show that HEK293 cells mock transfected do not adhere to the plastic (PBS) nor to poly-L-lysine substrate, whether in presence (lower panels) or absence (top panels) of ligands, Semaphorin3A (right panels) or 3E (left panels).

Similarly, cells overexpressing PlexinA1 and Neuropilin1 receptors, or PlexinD1 receptor do not adhere to plastic (PBS) nor to poly-L-lysine substrate whether in the presence or absence of ligands (results not shown).

In contrast, HEK293 cells mock transfected adhere to fibronectin in presence (lower panels) or absence (top panels) of ligands, Semaphorin3A (right panels) or 3E (left panels), which suggest that HEK293 cells endogenously express the integrins which bind to fibronectin and that cell adhesion is mediated by integrins. Additionally, a significant increase in cell adhesion is observed over time (p value <0.001), which suggest that cell adhesion increases with time with or without ligand.

b. Effect of Semaphorin3A and Semaphorin3E on cell adhesion of HEK293 cells overexpressing PlexinA1 and Neuropilin1 receptors or PlexinD1 receptor

The results presented are normalised means with standard errors of the mean (SEM) (refer to page 81). Normalisation has been performed to the absorbance found in the mock transfected cells untreated by ligand (Mock=1).

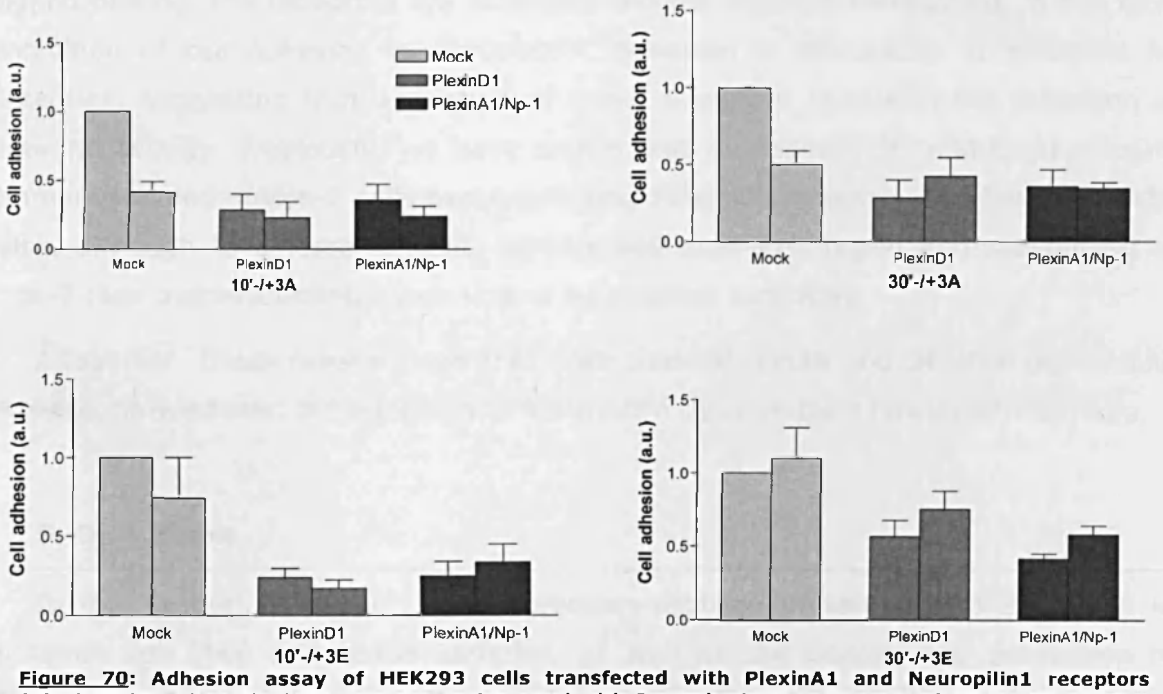

Figure 70: Adhesion assay of HEK293 cells transfected with PlexinA1 and Neuropilin1 receptors (PlexinA1/Np-1) or PlexinD1 receptor and treated with Semaphorin3A or Semaphorin3E for 10 minutes and 30 minutes. Results are mean of three independent experiments, with standard error of the mean (SEM). ANOVA statistical analysis has been applied, which showed that the effects of receptor, ligand, and time are significant (p value < 0.001).

The results in figure 70 show that cell adhesion to fibronectin of untransfected HEK293 cells is reduced by approximately 2 fold following incubation with Semaphorin3A (top panels), whereas in the presence of Semaphorin3E protein cell adhesion of HEK293 cells is not significantly changed (lower panels). HEK293 cells express low levels of PlexinA1 and NP1 (M. Williamson, personal communication) and so the decrease in adhesion observed in untransfected HEK293 cells in response to Semaphorin3A is likely to be a result of activation of the endogenous receptors. In contrast, HEK293 cells express undetectable levels of plexinD1, accounting for the minimal response of untransfected HEK293 cells to Semaphorin3E.

The results also show that cell adhesion to fibronectin of HEK293 cells overexpressing PlexinA1 and Neuropilin1 receptors or PlexinD1 receptor is reduced by approximately 2 fold relative to vector controls, whether in the presence or absence of their respective ligands, Semaphorin3A and Semaphorin3E (figure 70). It has previously been shown that overexpression of certain plexins results in receptor clustering and mimics ligand binding (Giordano et al., 2002). Plexins are indeed activated by clustering of their ligands. Our results suggest that overexpression of PlexinA1 and Neuropilin1 or PlexinD1 may act similarly, by clustering thus mimicking ligand binding, the receptors are activated and the signal is transduced, in this case inhibition of cell adhesion to fibronectin. Adhesion to fibronectin is mediated by integrins, suggesting that activation of these receptors results in the inhibition of integrin activity. Previously, we have shown that Semaphorin3E inhibits β1-integrin immunostaining of Cos-7 cells overexpressing PlexinD1 receptor, and Semaphorin3A also, although to a lesser extent, inhibits activated-β1-integrin immunostaining of Cos-7 cells overexpressing PlexinA1 and Neuropilin1 receptors.

Altogether, these results show that both Semaphorin3A and 3E strongly inhibits β1-integrin-mediated cell adhesion to fibronectin through their functional receptors.

5. Discussion

In this section, we report the expression profiling of semaphorin 3e mRNA in prostate cell lines and tissue samples, as well as the cloning and production of Semaphorin3E protein, and the study of its effects on cell morphology and behaviour.

Expression levels of semaphorin 3e mRNA were assessed by quantitative RT-PCR in the same 8 prostate cell lines as previously described, as well as in the six paired non-neoplastic and carcinoma prostate tissue samples. The results confirm the RT-PCR results from section 1, i.e. semaphorin 3e mRNA expression levels are higher in the non-neoplastic "normal" prostate stromal cell line than in the epithelial counterpart. In contrast, in benign hyperplasic prostate (BPH), there is a stronger expression of semaphorin 3e in the derived epithelial cell line than in the stromal counterpart, which may suggest roles for Semaphorin3E protein in BPH development. Further experiments could include immunostaining of normal prostate and BPH tissues with antibodies directed against Semaphorin3E protein and its receptor PlexinD1, to appreciate their distribution *in situ*. BPH is a benign enlargement of the prostate that originates within the transition zone of the gland, whereas the peripheral zone is a most frequent site of cancer. Interestingly, semaphorin 3e expression levels found in six non-neoplastic tissues surrounding cancers (graded 5 to 7) were 3 to 5 times higher than within the tumours themselves. This may reflect the (q)RT-PCR results obtained with the cell lines, i.e. prostate primary tumour and matched non-neoplastic epithelial cell lines express similar levels of semaphorin 3e mRNA, whereas the matched non-neoplastic stromal cell line and normal prostate tissue, which has more stroma express higher levels than the epithelial counterpart. It would be of interest to appreciate the distribution of Semaphorin3E and its receptor by immunostaining *in situ*.

In the prostate cancer cell line derived from a bone metastasis, mRNA expression levels of semaphorin 3e are higher than in the non-neoplastic "normal" prostate cell line. In contrast, they are much lower in the other two prostate cancer cell lines derived from a lymph node and brain metastases, which may suggest that Semaphorin3E may be involved differently in prostate metastasis depending on the secondary sites invaded. Further experiments to understand the roles of Semaphorin3E in cancer metastasis could include orthotopic xenografts of PC3 cells (derived from a bone metastasis) in mice, with or without siRNA to Semaphorin3E to determine the effects of Semaphorin3E knockdown on metastasis formation to the bone. In addition, the effects of overexpressing Semaphorin3E in non-neoplastic "normal" prostate cells xenografts on tumour formation could be investigated.

To elucidate the roles of Semaphorin3E protein on cell morphology and behaviour in general, its complete cDNA sequence was cloned into a mammalian expression vector (pEF6/Myc/His), the protein produced, and used to assess integrin and focal

adhesion formation by immunostaining of active β1-integrin and vinculin, and adhesion to fibronectin by adhesion assays.

The results show that PlexinA1 and Neuropilin1 are functional receptors for Semaphorin3A and that PlexinD1 is a functional receptor for Semaphorin3E protein, which support findings in endothelial cells (Gu et al., 2005). In addition, the results show that overexpression of PlexinA1 and Neuropilin1 receptors by Cos-7 cells leads to stress fiber formation, whereas no stress fibers were observed with overexpression of PlexinD1. Addition of Semaphorin3A or Semaphorin3E ligands inhibited stress fiber formation in cells overexpressing PlexinA1 and Neuropilin1 receptors. It has previously been shown that RhoAGTPAse is implicated in stress fiber formation and cell-matrix adhesion (Ridley and Hall, 1992; Rottner et al., 1999). Thus we may hypothesise that overexpression of PlexinA1 and/or Neuropilin1 may activate RhoAGTPases, while the addition of ligand reduces their activity. We could go further and suggest that RhoAGTPase activation may be activated only by Neuropilin1, as results showed that Semaphorin3E also reduces stress fiber formation in cells overexpressing PlexinA1 and/or Neuropilin1. It has already been shown that Semaphorin3E binds to Neuropilin1 (Feiner et al., 1997), however, it has never been shown that Semaphorin3E binds to PlexinA1, in presence or absence of Neuropilins. Thus, these results may confirm that Semaphorin3E and Neuropilin1 interact, and that the result of such interaction is a reduction in RhoAGTPase activity. This may suggest that Neuropilin1 is able to affect RhoA activity via a co-receptor with sufficient cytoplasmic domain. Further experiments to understand the downstream effects of neuropilin activation by semaphorins in prostate cancer cells are required.

Moreover, the results confirm that Semaphorin3A protein reduces active β1-integrins immunostaining of cells overexpressing its functional receptors, as already suggested by Serini and colleagues (Serini et al., 2003). Additionally, we show that Semaphorin3E also reduces active β1-integrins immunostaining of cells overexpressing its functional receptor, and thus with a stronger effect than Semaphorin3A. Interestingly, Semaphorin3E through Neuropilin1 has no effect on active β1-integrins immunostaining of cells overexpressing PlexinA1 and/or Neuropilin1, whereas an effect on stress fiber formation was observed. These results may suggest that stress fiber formation and cell adhesion are regulated by different pathways. The reduction in stress fiber formation may come from a reduction in Rho activity, whereas the reduction in integrin activity would be through some other

pathway. Integrin activity and avidity is controlled by many pathways (called inside-out signalling) including PI3K and via RAP1, RhoA, DOCK2 and R-Ras (Kinashi, 2005). Further experiments to decipher which pathways may be involved in these processes are required.

Also, the results show that both Semaphorin3A and Semaphorin3E ligands activate vinculin specific punctate staining, which suggest that both semaphorins modulate focal adhesion formation. Vinculin plays a key role in cell migration by strengthening focal adhesions and promoting cell spreading and lamellipodia extension (Xu et al., 1998). Thus, our results would suggest that both semaphorins play roles in cell migration. Vinculin regulates cytoskeletal dynamics, promoting actin polymerization and recruitment of cytoskeletal proteins. Rac1 stimulates the formation of lamellipodia (Nobes and Hall, 1995). Further experiments, such as migration assays, or lamellipodia formation are necessary to study the roles of Semaphorin3A and 3E on the various steps of cell migration.

The adhesion assays results show that activation of PlexinA1 and/or Neuropilin1 receptors, and activation of PlexinD1, either by clustering or by addition of their respective ligands, inhibits cell adhesion to fibronectin. Cell adhesion is mediated by integrins, which are cell surface proteins that bind and mediate adhesion to the extracellular matrix (ECM), organise the cytoskeleton and activate intracellular signalling pathways small GTPases of the Rho family (Schwartz and Shattil, 2000). Each integrin is formed of one α and one β subunit (18α and 8β subunits). Different combinations bind distinct ECM ligands. Integrins exist in an inactive and active form. Activation is required for ECM binding.

At first sight, the above results may appear contradictory, as adhesion to the ECM is mediated by focal adhesions and activation of integrins (part of the focal adhesions). However, cell movement is a dynamic and complicated process which involves up to 50 different proteins in the formation and maintenance of focal adhesion complexes. Different types of integrins may be implicated at various stages of focal adhesion formation. For instance, other β-integrins (β2- to β8-integrins for example), which do not form the receptor for fibronectin (β1-integrin), may be activated in focal adhesion formation, cell-cell attachment, and lamellipodia formation. Further experiments to elucidate which integrins are involved in focal adhesion formation of cells activated by semaphorin signalling pathways could include adhesion experiments to diverse substrates, such as collagen and vitronectin.

Altogether, our results suggest that Semaphorin3A and Semaphorin3E inhibit integrin-mediated cell adhesion to a fibronectin matrix and initiate cell motility, most probably through regulation of small GTPases. Oinuma and colleagues have shown that PlexinB1 acts as a RasGAP and inactivates R-Ras (Oinuma et al., 2004b), which is an activator of integrins. Activation of PlexinB1 therefore inhibits integrins via R-Ras. PlexinD1 could possibly operate via a similar mechanism, although PlexinA1 does not bind R-Ras. PlexinA1 and/or Neuropilin1 overexpression causes stress fiber formation, whereas PlexinD1 overexpression does not. Further experiments to elucidate the mechanism of action of Semaphorin3E could include interaction experiments. For example, looking at the effects of Semaphorin3E on cells transfected with Neuropilin1 only, and study Neuropilin1 interaction with integrins. To understand the roles of Semaphorin3E in tumourigenesis and/or metastasis, the effect of semaphorin3E on cell motility and lamellipodia formation could be investigated using transwell migration and cell spread assays. Finally, to investigate the roles of Semaphorin3E in prostate cells, it would be of interest to overexpress Semaphorin3E in the matched non-neoplastic "normal" and primary tumour cell lines, and measure the effects on integrin-mediated cell adhesion to fibronectin, and cell migration (migration assays) for example.

CHAPTER 4: CONCLUSIONS AND FUTURE WORK

This thesis summarises the research work performed between Oct-2001 and Mar-2005, aiming at understanding the expression, regulation and roles of semaphorins and their receptors in normal prostate, prostate cancer and metastasis. Because of their roles as attractive and repulsive cues, semaphorins may contribute to tumour progression and metastasis, which depend on the ability of cancer cells to initiate angiogenesis, migrate, and invade. Angiogenesis is under the control of vascular endothelial growth factors (VEGFs), which are up-regulated by hypoxia. Invasion is under the control of scatter factor HGF, whose receptor MET is a member of the sema domain containing superfamily. Semaphorins control cellular movement in various tissues, including the nervous, immune, and vascular systems. We may therefore hypothesise that semaphorins also play key roles in prostate tumour progression and metastasis by controlling the movement of cancer cells.

Although semaphorins have been extensively studied in many tissues, there are no studies showing their expression in prostate. Expression profiling experiments were therefore performed in prostate cell lines and tissues, by (q)RT-PCR, showing that messenger RNAs for secreted semaphorins 3a, 3b, 3c, 3e, 3f, and the receptors plexins a1, a2, a3, b1, b3, and neuropilins 1 and 2 are synthesised by most prostate cell lines and tissues. Differences were found in the expression profiles of secreted semaphorins and receptors between stromal and epithelial cell types and between cells derived from normal prostate, BPH, primary tumour and metastases. Expression profiling experiments were also performed under hypoxic conditions in matched non-neoplastic and primary tumour prostate cell lines, which showed for the first time that the expression of secreted semaphorins is controlled by hypoxia.

In cells derived from normal prostate under normoxic conditions, semaphorins 3a, 3c, and 3e, as well as neuropilins 1 and 2 are preferentially synthesised by stromal cells, whereas plexin receptors are significantly reduced compared to epithelial cells. These results may suggest a paracrine regulation of semaphorin signalling in prostate. Further experiments to demonstrate this hypothesis would include co-culture experiments with prostate stromal cells expressing semaphorin and prostate epithelial cells expressing the receptor. If the semaphorin secreted repels the epithelial cells, islands of epithelial cells should form. Also, immunohistochemistry of plexin and semaphorin could be performed on prostate tissue sections.

In cells derived from bone metastasis under normoxic conditions, expression levels of both semaphorin 3a and its functional receptors plexin a1 and neuropilin 1

are maintained at high levels, whereas they are significantly reduced in prostate primary tumour cells. Altogether, these results may suggest an autocrine regulation of Semaphorin3A signalling in prostate metastasis to the bone. Serini and colleagues have shown that Semaphorin3A is a potent inhibitor of angiogenesis, as its autocrine signalling negatively regulate endothelial cells migration and facilitate cell reorientation by inhibiting integrin function (Serini et al., 2003). In contrast, Muller and colleagues have recently shown that Semaphorin3A promotes migration and invasion of pancreatic cancer cells (Muller et al., 2007). Our results, obtained in Cos and HEK cellular systems, confirm that Semaphorin3A inhibits integrin activity and integrin-mediated cell adhesion, while it possibly activates cell spreading (focal adhesion formation). Furthermore, expression profiling experiments under hypoxic conditions showed that semaphorin 3a expression is strongly downregulated by hypoxia in cancer cells (prostate and colon), but not in normal cells (at 48h). These results may suggest that Semaphorin3A could also function as an inhibitor of angiogenesis in prostate, and as an activator of prostate metastasis to the bone. Further experiments to study the roles of Semaphorin3A and its autocrine signalling in prostate tumour formation, metastasis to the bone, and angiogenesis would include *in vivo* experiments in mice, using normal prostate cell lines overexpressing Semaphorin3A or siRNA to Semaphorin3A.

Interestingly, expression levels under normoxic conditions of semaphorins 3b and 3f, two tumour suppressor genes, are not significantly different between stromal and epithelial cells derived from normal prostate. In contrast, they are reduced in stromal and epithelial cells derived from BPH, a benign enlargement of the prostate, and in cells derived from prostate primary tumour. The loss of expression and/or mutation of semaphorins 3b and 3f genes have also been reported in lung cancer (Tomizawa et al., 2001; Kuroki et al., 2003), nasopharyngeal carcinoma (Liu et al., 2003), melanoma (Bielenberg et al., 2004; Chabbert-de Ponat et al., 2006) and neuroblastoma (Nair et al., 2007). Noticeably, semaphorins 3b and 3f genes are located on chromosome 3p21.3, which is frequently lost (LOH) in prostate cancer (Dahiya et al., 1997). Additionally, our results show that expression levels of semaphorin 3b are significantly reduced in the three prostate metastases, and those of semaphorin 3f are significantly reduced in two out of three, the lymph node and brain metastases. Interestingly, others have shown that Semaphorin3F is a potent metastasis inhibitor that is markedly down-regulated in highly metastatic melanoma tumour cells (Kessler et al., 2004; Bielenberg et al., 2004), where Semaphorin3F

inhibits the formation of metastases in the lymph node and lung. By analogy, we could hypothesise that Semaphorin3F has a similar role in prostate cancer metastasis to the lymph node. However, the cells derived from prostate metastases to the lymph node are not highly metastatic *in vivo*. On the other hand, semaphorin 3f expression levels are unchanged in prostate cells derived from bone metastases, which are highly metastatic *in vivo*. This is contradictory with the findings in melanoma. Similarly, we could hypothesise that Semaphorin3B play similar inhibitory roles in prostate as its expression is significantly reduced in prostate cells derived from metastases. However, a group has recently demonstrated that Semaphorin3B, although inhibiting primary tumour growth, was increasing metastatic dissemination to the lung, by inducing the production of Interleukin 8 (IL8) by tumour cells, which results in the recruitment of macrophages and metastasis (Rolny et al., 2008). Additionally, Semaphorin3F and 3B proteins have been shown to inhibit VEGF-induced endothelial cell proliferation and angiogenesis (Kessler et al., 2004; Castro-Rivera et al., 2004). And Semaphorin3A and 3F have been shown to work together to repel endothelial cells and induce their apoptosis (Guttmann-Raviv et al., 2007,). Our hypoxia results show that semaphorin 3f expression is not changed by hypoxia, neither in normal prostate cells nor in primary tumour cells. However, semaphorin 3f expression is decreased by hypoxia in another cancer cell line (colon), which suggests that its behaviour in prostate is specific. Also, the hypoxia results show that semaphorin 3b expression varies depending on the origin of the cells and on the time spent under hypoxic conditions (biphasic expression in prostate).

Although contradictory, the above results may suggest that Semaphorins play different, even contradictory roles at different stages of tumour progression, and this would most probably depends on the stromal environment, i.e. on which molecules involved in their signalling are present (seed and soil theory, refer to page 28, Langley and Fidler, 2007). Some Semaphorins, like Semaphorin3B (Rolny et al., 2008), may be able to foster a pro-metastatic environment, while still inhibiting tumour growth and angiogenesis. Others might have the opposite roles, like Semaphorin3C (see next paragraph). Such processes (tumourigenesis, metastasis, and angiogenesis) involve different signalling pathways. It would therefore be of great interest to study the pathways activated by secreted semaphorins signalling and investigate further the roles of the stromal environment on these signalling pathways. Further experiments would also include *in vivo* experiments to look at the effect on tumour formation and metastasis in mice, using normal prostate cell lines

expressing siRNA to Semaphorin3B or 3F to knock down the expression of these proteins.

Expression profiling results under normoxic conditions showed that semaphorin 3c levels are not significantly changed in prostate cancer and metastases cells, compared to normal levels, except in the cells derived from lymph node metastases, where they are reduced. Others have shown that Semaphorin3C is overexpressed in ovarian tumour cell lines with invasive and metastatic behaviour (Yamada et al., 1997; Neufeld et al., 2005). And its expression was also found to be upregulated in metastatic lung adenocarcinoma cells, and in malignant melanoma cells, indicating that upregulation of semaphorin 3c expression may be linked to tumour progression (Martin-Satue and Blanco, 1999; Rieger et al., 2003). Further experiments would therefore include qRt-PCR of semaphorin 3c mRNA and western blotting of the protein in prostate cell lines and tissues in order to see whether its expression is further enhanced in prostate cancer. Additionally, Semaphorin3C has also been shown to stimulate endothelial cell (EC) proliferation and survival, and enhance EC adhesion, directional migration (increasing integrin activity, contrary to Semaphorin3A), and tube formation *in vitro* (Banu et al., 2006). Expression profiling results under hypoxic conditions showed that hypoxia strongly upregulates semaphorin 3c expression in prostate primary tumour cells. We may therefore hypothesise that, in prostate, Semaphorin3C is likely to act as an angiogenic factor, and maybe have a similar role to VEGF. Its role in cell migration could be investigated using migration assays. Further experiments would also include *in vivo* experiments to look at the effect on tumour formation, and metastasis in mice, using normal prostate cell lines stably transfected and overexpressing Semaphorin3C.

Expression profiling results under normoxic conditions revealed that expression levels of semaphorin 3e remain similar to or are higher than normal prostate levels in cells derived from BPH, prostate primary tumour, and bone metastases, while in cells derived from metastases at other sites (lymph node and brain), semaphorin 3e expression is significantly reduced. Semaphorin 3e expression has been positively correlated with the metastatic ability of breast cancer cells, and it has been shown to promote metastasis growth to the lung (Christensen et al., 1998 and 2005). Altogether these results suggest that Semaphorin3E may promote prostate cancer metastasis to the bone. Further experiments to look at the effects of Semaphorin3E on tumour formation would include *in vivo* experiments. Christensen and colleagues suggest that Semaphorin3E paracrine stimulation promotes a local angiogenic

response by stimulating endothelial cells migration, thus contributing to metastasis growth in the lung (Christensen et al., 2005). On the contrary, Gu and colleagues have shown that Semaphorin3E inhibits endothelial cell migration *in vivo* (Gu et al., 2005). Our results show that semaphorin 3e expression is strongly and progressively decreased in prostate cancer cells undergoing hypoxia, which would suggest that Semaphorin3E may act as an inhibitor of tumour angiogenesis, similarly to Semaphorin3A, which is also downregulated by hypoxia in prostate cancer cells, and contrary to Semaphorin3C, known as a potent activator of angiogenesis, whose expression is strongly upregulated by hypoxia in prostate cancer cells. These results suggest that hypoxic regions within prostate tumours, either directly downregulate semaphorin 3a and 3e transcription (possibly through HIF1) or upregulate the expression of an inhibitor, yet to be determined, of semaphorin 3a or 3e expression. Further work would include promoter reporter assay experiments to understand what downregulates semaphorin 3a and 3e, and upregulates semaphorin 3c transcription in hypoxic regions of cancer. In prostate, it has been shown that the metastatic potential of cancer cells correlates with the expression of angiogenic factors (Aalinkeel et al., 2004). It would therefore be interesting to study how angiogenesis in prostate cancer is affected by secreted semaphorins.

Altogether, these expression profiling results under normoxic conditions suggest the presence of autocrine and paracrine semaphorin signalling in normal prostate, BPH, prostate cancer and metastases, as most cell lines express the ligands and their receptors. Unfortunately at the time these profiling experiments were performed, not all ligand and receptor complexes were elucidated (e.g. Semaphorin3E and PlexinD1, Semaphorin5A and PlexinB3), and thus not all ligands and receptors were screened. Further expression profiling experiments, including the previously unknown receptors or ligands (e.g. plexin d1 and semaphorin 5a) would complete this semi-quantitative analysis, and allow the selection of some ligands and receptors whose expression levels are significantly changed in prostate, and to perform quantitative experiments (qRT-PCRs for example) on these selected molecules. Interestingly, PlexinD1 receptor is also a functional receptor for Semaphorin3C *in vivo.* Sempahorin3C binds to PlexinA1, A2, and D1, and also to both neuropilins (Banu et al., 2006). Semaphorin3A binds to all three class A plexins and to Neuropilin1 only. Semaphorin3F binds to PlexinA1 and A3 and to both neuropilins. Semaphorin3B binds to both neuropilins and VEGF receptor 2. Semaphorin3E binds to PlexinD1 and Neuropilin1, etc. The various ligand-receptor combinations probably activate different

signalling pathways, and therefore have different effects on cell movement, tumour progression and angiogenesis. Studying semaphorin signalling would shed some light on their roles.

However, the main limitations of such expression profiling experiments are that it is only semi-quantitative and it remains at a transcriptomics level. Further experiments to confirm these mRNA results at the protein level would include looking at protein expression in the cell lines by western blotting and in prostate tissue sections by tissue microarray or immunohistochemistry using antibodies to semaphorins and plexins. One of the problems remains the availability of antibodies.

In order to understand the effects of Semaphorin3E, whose protein is unfortunately not commercially available, we decided to clone its gene into a mammalian expression vector in order to obtain a recombinant protein that we could use in experiments aiming at understanding its roles in general (as not much was known about it), and, if time allowed it, in prostate. The recombinant protein was produced in presence of anti-furin protease to prevent Semaphorin3E cleavage and the loss of the Myc and His tags, which allow its detection on a western blot. Furin modulates the repulsive activity of semaphorins (Adams et al., 1997). For example, when Semaphorin3E is truncated at its C-terminal moiety by furin(-like) convertase, it converts the repelling signal into an inducer of invasive growth and lung metastasis, by mediating tumour-endothelial cells interaction, stimulating lung endothelial cells migration via Erk1/2 activation and thus contributing to a local angiogenic response (Christensen et al., 2005). In our experiments, we used anti-furin protease inhibitor to avoid loosing the tags of the recombinant Semaphorin3E protein, which may account for its repulsive activity (inhibition of integrin function and cell adhesion). It would be of interest to study the effects of the truncated form of Semaphorin3E on cell adhesion and spreading to complement this study.

Because Semaphorin3E purification on a nickel column failed when going to the large scale protocol, probably because of the cleavage of the tag, and as other groups working on semaphorins (for example 3F, Kessler et al., 2004) did not use purified proteins for their biological assays, we decided to work with the conditioned medium also (using conditioned medium from untransfected cells as a control). As not much was known about Semaphorin3E protein signalling and roles, and as the prototype Semaphorin3A protein was well studied using simple cellular systems, we decided to use Semaphorin3A as a positive control for our experiments. It had just

been published that Semaphorin3A, and more generally secreted semaphorins control vascular morphogenesis by inhibiting integrin function (Serini et al., 2003). We therefore performed immunostaining experiments using commercially available anti-active-β1-integrin and anti-vinculin antibodies, as well as adhesion assays on various substrates, with the aim to study the effects of Semaphorin3E on cell adhesion and migration.

Immunostaining experiments confirmed what others had shown, namely that PlexinA1 and Neuropilin1 are functional receptors for Semaphorin3A, and that PlexinD1 is a functional receptor for Semaphorin3E (Takahashi et al., 1999, and Gu et al., 2005). The results also confirmed that Semaphorin3A inhibits active β1-integrin staining, as previously shown by Serini and Colleagues (Serini et al., 2003). Moreover, our results showed that Semaphorin3A activates vinculin staining, and that Semaphorin3E also inhibits active β1-integrin staining and activates vinculin staining. Additionally, adhesion assays showed that Semaphorin3A, or the overexpression of its receptors PlexinA1 and Neuropilin1, inhibits integrin-mediated cell adhesion. Similarly, Semaphorin3E, or the overexpression of its receptor PlexinD1, also inhibits integrin-mediated cell adhesion. Altogether, these results suggest that Semaphorin3A and 3E may have similar roles on cell movement, i.e. inhibiting cell adhesion and activating focal adhesion formation, suggesting a role in the initial steps of cell spreading. Further experiments to study the effects of Semaphorin3E protein on cellular movement would include chemotaxis assays of prostate cancer cells to a gradient of Semaphorin3E in Dunn chemotaxis chambers using time lapse video microscopy. This would allow the speed and direction of movement to be measured. The morphology would also be assessed and lamellipodia and stress fiber formation monitored. Then addition of siRNA to plexinD1 receptor would allow us to study which signalling pathway is involved in prostate cancer.

Recently, Chauvet and colleagues have shown that gating of Semaphorin3E/PlexinD1 signalling by Neuropilin1 switches axonal repulsion to attraction during brain development (Chauvet et al., 2007). They also show that PlexinD1 is the predominant binding partner for Semaphorin3E in the brain, and that Semaphorin3E binds Neuropilin1, which is in line with our results suggesting that Semaphorin3E binds Neuropilin1, thus inhibiting stress fiber formation. Also, the authors have demonstrated that Semaphorin3E acts as a bifunctional ligand *in vivo*, depending on the composition of the receptor complex; i.e. receptor is PlexinD1 only, Semaphorin3E acts as a repellent; Neuropilin1 in addition to PlexinD1 switches

Semaphorin3E signal from repulsion to attraction. Additionally, Herman and Meadows have shown that cells derived from prostate metastases to the bone overexpressing Semaphorin3A or 3E exhibit an anti-invasive activity, i.e. inhibits adhesion and invasion, while in contrast, Semaphorin3C increase invasion and adhesion (Herman and Meadows, 2007a and 2007b). Altogether, these results are in line with ours. Further experiments would include invasion and adhesion assays with cells overexpressing PlexinD1 and Neuropilin1 receptors to see whether Neuropilin1 reverts the repulsive signal into an attractive signal (enhanced adhesion). Herman and Meadows also showed that Semaphorin3E anti-invasive effect was reversible by regulating E-cadherin and β-catenin proteins, which suggest that semaphorins, cadherins, and catenins may interact with each other during invasion. Along this line, Mol and colleagues have suggested that molecules controlling cell adhesion and migration, such as E-cadherin, N-cadherin, β-catenin, integrins, focal adhesion kinase, connexins and matrix metalloproteinases, may all be promising biological markers associated with the early stage metastatic process in prostate cancer (Mol et al., 2007). Altogether, these results may raise the possibility that Semaphorin3E could play major roles in prostate metastasis and Semaphorins may be added to this list of biological markers in the near future. Further experiments could include overexpressing Semaphorin3E in normal prostate cells and studying the regulation of cadherins and catenins.

However, there are limitations to these studies on Semaphorin3E that need to be addressed. For example, for the adhesion assay, it would be better to transfect less receptors DNA to lower their expression in order to obtain a ligand-dependant response. Also, different substrates could be used, such as collagen, vitronectin, etc... Additionally, it would be interesting to knock down PlexinD1 receptor to make sure that Semaphorin3E signals through PlexinD1 to inhibit adhesion. Further experiment could also include a time course of integrin inactivation with Semaphorin3E treatment.

The invasive growth program, which governs cancer cell invasion, is also under the control of members of the sema domain superfamily, the scatter factors receptor MET and its ligand HGF, and also the transmembrane Semaphorin4D protein and its receptor PlexinB1. PlexinB1 and MET interact independently of their ligand, but activation of PlexinB1 by Semaphorin4D stimulates MET, which enhances invasive growth (Giordano et al., 2002). Interestingly, frequent missense mutations of plexin b1 gene were detected in prostate tumours and metastases (Wong et al., 2007). Our

migration assays results in cells overexpressing wild-type PlexinB1 showed that PlexinB1, activated either by clustering or low concentrations of its ligand Semaphorin4D (<50ng/mL), inhibits cell migration, whereas high Semaphorin4D concentrations (>50ng/mL) increase cell migration. Three missense mutations of the plexin b1 gene were studied using migration assays. Two of the mutations studied (A5653G and T5714C) were the most common mutations found in prostate primary cancers and metastases. The other mutation (A5359G) was found in LNCaP, cells derived lymph node metastases. The results show that these three mutations of plexin b1 increase cell migration in the absence of Semaphorin4D. Two of the three mutations (T5714C and A5359G) further increase cell migration in presence of Semaphorin4D (50ng/mL). We may therefore hypothesise that the control of cell migration by Semaphorin4D signalling pathway through PlexinB1 may be harnessed by cancer cells during invasion and metastasis. To investigate which signalling pathways are required for the increase in migration observed for the mutant forms of PlexinB1, the experiment needs to be repeated in the presence or absence of inhibitors, for example to R-Ras, Rho, PI3K.

The main limitation is that most of the thesis is based on cell lines experiments *in vitro*. *In vivo* experiments are more representative. To assess the expression of plexins and semaphorins, immunohistochemistry experiments on prostate tissue sections would add to this study. And to assess tumour development and metastasis, *in vivo* experiments in mice should be performed.

The results obtained in this thesis demonstrate that semaphorins and their receptors, plexins and neuropilins, are synthesised in prostate cells. They also suggest that their distribution in normal prostate, prostate cancer and metastases, as well as in the benign enlargement (BPH) may play a role in the development of these diseases.

BIBLIOGRAPHIC REFERENCES

Reference List

1. **Aalinkeel R, Nair MP, Sufrin G, Mahajan SD, Chadha KC, Chawda RP, Schwartz SA** 2004 Gene expression of angiogenic factors correlates with metastatic potential of prostate cancer cells. Cancer Res 64:5311-5321

2. **Adams RH, Lohrum M, Klostermann A, Betz H, Puschel AW** 1997 The chemorepulsive activity of secreted semaphorins is regulated by furin-dependent proteolytic processing. EMBO J 16:6077-6086

3. **Alcaraz A, Takahashi S, Brown JA, Herath JF, Bergstralh EJ, Larson-Keller JJ, Lieber MM, Jenkins RB** 1994 Aneuploidy and aneusomy of chromosome 7 detected by fluorescence in situ hybridization are markers of poor prognosis in prostate cancer. Cancer Res 54:3998-4002

4. **Antipenko A, Himanen JP, van LK, Nardi-Dei V, Lesniak J, Barton WA, Rajashankar KR, Lu M, Hoemme C, Puschel AW, Nikolov DB** 2003 Structure of the semaphorin-3A receptor binding module. Neuron 39:589-598

5. **Arthur WT, Petch LA, Burridge K** 2000 Integrin engagement suppresses RhoA activity via a c-Src-dependent mechanism. Curr Biol 10:719-722

6. **Artigiani S, Comoglio PM, Tamagnone L** 1999 Plexins, semaphorins, and scatter factor receptors: a common root for cell guidance signals? IUBMB Life 48:477-482

7. **Artigiani S, Barberis D, Fazzari P, Longati P, Angelini P, van de Loo JW, Comoglio PM, Tamagnone L** 2003 Functional regulation of semaphorin receptors by proprotein convertases. J Biol Chem 278:10094-10101

8. **Artigiani S, Conrotto P, Fazzari P, Gilestro GF, Barberis D, Giordano S, Comoglio PM, Tamagnone L** 2004 Plexin-B3 is a functional receptor for semaphorin 5A. EMBO Rep 5:710-714

9. **Arya M, Patel HR, McGurk C, Tatoud R, Klocker H, Masters J, Williamson M** 2004 The importance of the CXCL12-CXCR4 chemokine ligand-receptor interaction in prostate cancer metastasis. J Exp Ther Oncol 4:291-303

10. **Bachelder RE, Lipscomb EA, Lin X, Wendt MA, Chadborn NH, Eickholt BJ, Mercurio AM** 2003 Competing autocrine pathways involving alternative neuropilin-1 ligands regulate chemotaxis of carcinoma cells. Cancer Res 63:5230-5233

11. **Bagnard D, Thomasset N, Lohrum M, Puschel AW, Bolz J** 2000 Spatial distributions of guidance molecules regulate chemorepulsion and chemoattraction of growth cones. J Neurosci 20:1030-1035

12. **Bandyk MG, Zhao L, Troncoso P, Pisters LL, Palmer JL, von Eschenbach AC, Chung LW, Liang JC** 1994 Trisomy 7: a potential cytogenetic marker of human prostate cancer progression. Genes Chromosomes Cancer 9:19-27

13. **Banu N, Teichman J, Dunlap-Brown M, Villegas G, Tufro A** 2006 Semaphorin 3C regulates endothelial cell function by increasing integrin activity. FASEB J 20:2150-2152

14. **Barberis D, Artigiani S, Casazza A, Corso S, Giordano S, Love CA, Jones EY, Comoglio PM, Tamagnone L** 2004 Plexin signaling hampers integrin-based adhesion, leading to Rho-kinase independent cell rounding, and inhibiting lamellipodia extension and cell motility. FASEB J 18:592-594

15. **Barberis D, Casazza A, Sordella R, Corso S, Artigiani S, Settleman J, Comoglio PM, Tamagnone L** 2005 p190 Rho-GTPase activating protein associates with plexins and it is required for semaphorin signalling. J Cell Sci 118:4689-4700

16. **Basile JR, Afkhami T, Gutkind JS** 2005 Semaphorin 4D/plexin-B1 induces endothelial cell migration through the activation of PYK2, Src, and the phosphatidylinositol 3-kinase-Akt pathway. Mol Cell Biol 25:6889-6898

17. **Basile JR, Castilho RM, Williams VP, Gutkind JS** 2006 Semaphorin 4D provides a link between axon guidance processes and tumor-induced angiogenesis. Proc Natl Acad Sci U S A 103:9017-9022

18. **bate-Shen C, Shen MM** 2000 Molecular genetics of prostate cancer. Genes Dev 14:2410-2434

19. **Behar O, Mizuno K, Badminton M, Woolf CJ** 1999 Semaphorin 3A growth cone collapse requires a sequence homologous to tarantula hanatoxin. Proc Natl Acad Sci U S A 96:13501-13505

20. **Bergers G, Benjamin LE** 2003 Tumorigenesis and the angiogenic switch. Nat Rev Cancer 3:401-410

21. **Bielenberg DR, Hida Y, Shimizu A, Kaipainen A, Kreuter M, Kim CC, Klagsbrun M** 2004 Semaphorin 3F, a chemorepulsant for endothelial cells, induces a poorly vascularized, encapsulated, nonmetastatic tumor phenotype. J Clin Invest 114:1260-1271

22. **Bismuth G, Boumsell L** 2002 Controlling the immune system through semaphorins. Sci STKE 2002:RE4

23. **Bladt F, Riethmacher D, Isenmann S, Aguzzi A, Birchmeier C** 1995 Essential role for the c-met receptor in the migration of myogenic precursor cells into the limb bud. Nature 376:768-771

24. **Blagosklonny MV** 2005 Molecular theory of cancer. Cancer Biol Ther 4:621-627

25. **Boland CR, Ricciardiello L** 1999 How many mutations does it take to make a tumor? Proc Natl Acad Sci U S A 96:14675-14677

26. **Bolanos-Garcia VM** 2005 MET meet adaptors: functional and structural implications in downstream signalling mediated by the Met receptor. Mol Cell Biochem 276:149-157

27. **Bork P, Holm L, Sander C** 1994 The immunoglobulin fold. Structural classification, sequence patterns and common core. J Mol Biol 242:309-320

28. **Borner C, Monney L** 1999 Apoptosis without caspases: an inefficient molecular guillotine? Cell Death Differ 6:497-507

29. **Bova GS, Isaacs WB** 1996 Review of allelic loss and gain in prostate cancer. World J Urol 14:338-346

30. **Bright RK, Vocke CD, Emmert-Buck MR, Duray PH, Solomon D, Fetsch P, Rhim JS, Linehan WM, Topalian SL** 1997 Generation and genetic characterization of immortal human prostate epithelial cell lines derived from primary cancer specimens. Cancer Res 57:995-1002

31. **Brooks PC, Stromblad S, Sanders LC, von Schalscha TL, Aimes RT, Stetler-Stevenson WG, Quigley JP, Cheresh DA** 1996 Localization of matrix metalloproteinase MMP-2 to the surface of invasive cells by interaction with integrin alpha v beta 3. Cell 85:683-693

32. **Bryan TM, Englezou A, Gupta J, Bacchetti S, Reddel RR** 1995 Telomere elongation in immortal human cells without detectable telomerase activity. EMBO J 14:4240-4248

33. **Bubendorf L, Schopfer A, Wagner U, Sauter G, Moch H, Willi N, Gasser TC, Mihatsch MJ** 2000 Metastatic patterns of prostate cancer: an autopsy study of 1,589 patients. Hum Pathol 31:578-583

34. **Cai H, Reed RR** 1999 Cloning and characterization of neuropilin-1-interacting protein: a PSD-95/Dlg/ZO-1 domain-containing protein that interacts with the cytoplasmic domain of neuropilin-1. J Neurosci 19:6519-6527

35. **Castellani V, Chedotal A, Schachner M, Faivre-Sarrailh C, Rougon G** 2000 Analysis of the L1-deficient mouse phenotype reveals cross-talk between Sema3A and L1 signaling pathways in axonal guidance. Neuron 27:237-249

36. **Castellani V, Rougon G** 2002 Control of semaphorin signaling. Curr Opin Neurobiol 12:532-541

37. **Castro-Rivera E, Ran S, Thorpe P, Minna JD** 2004 Semaphorin 3B (SEMA3B) induces apoptosis in lung and breast cancer, whereas VEGF165 antagonizes this effect. Proc Natl Acad Sci U S A 101:11432-11437

38. **Chabbert-de Ponnat I, Marie-Cardine A, Pasterkamp RJ, Schiavon V, Tamagnone L, Thomasset N, Bensussan A, Boumsell L** 2005 Soluble CD100 functions on human monocytes and immature dendritic cells require plexin C1 and plexin B1, respectively. Int Immunol 17:439-447

39. **Chambers AF, Matrisian LM** 1997 Changing views of the role of matrix metalloproteinases in metastasis. J Natl Cancer Inst 89:1260-1270

40. **Chauvet S, Cohen S, Yoshida Y, Fekrane L, Livet J, Gayet O, Segu L, Buhot MC, Jessell TM, Henderson CE, Mann F** 2007 Gating of Sema3E/PlexinD1 signaling by neuropilin-1 switches axonal repulsion to attraction during brain development. Neuron 56:807-822

41. **Chedotal A, Kerjan G, Moreau-Fauvarque C** 2005 The brain within the tumor: new roles for axon guidance molecules in cancers. Cell Death Differ 12:1044-1056

42. **Chedotal A** 2007 Chemotropic axon guidance molecules in tumorigenesis. Prog Exp Tumor Res 39:78-90

43. **Chen C, Li M, Chai H, Yang H, Fisher WE, Yao Q** 2005 Roles of neuropilins in neuronal development, angiogenesis, and cancers. World J Surg 29:271-275

44. **Chen H, Chedotal A, He Z, Goodman CS, Tessier-Lavigne M** 1997 Neuropilin-2, a novel member of the neuropilin family, is a high affinity receptor for the semaphorins Sema E and Sema IV but not Sema III. Neuron 19:547-559

45. **Chen H, He Z, Bagri A, Tessier-Lavigne M** 1998 Semaphorin-neuropilin interactions underlying sympathetic axon responses to class III semaphorins. Neuron 21:1283-1290

46. **Christensen C, Ambartsumian N, Gilestro G, Thomsen B, Comoglio P, Tamagnone L, Guldberg P, Lukanidin E** 2005 Proteolytic processing converts the repelling signal Sema3E into an inducer of invasive growth and lung metastasis. Cancer Res 65:6167-6177

47. **Christensen CR, Klingelhofer J, Tarabykina S, Hulgaard EF, Kramerov D, Lukanidin E** 1998 Transcription of a novel mouse semaphorin gene, M-semaH, correlates with the metastatic ability of mouse tumor cell lines. Cancer Res 58:1238-1244

48. **Colombo P, Patriarca C, Alfano RM, Cassani B, Ceva GG, Roncalli M, Bosari S, Coggi G, Campo B, Gould VE** 2001 Molecular disorders in transitional vs. peripheral zone prostate adenocarcinoma. Int J Cancer 94:383-389

49. **Comoglio PM, Tamagnone L, Boccaccio C** 1999 Plasminogen-related growth factor and semaphorin receptors: a gene superfamily controlling invasive growth. Exp Cell Res 253:88-99

50. **Comoglio PM, Boccaccio C** 2001 Scatter factors and invasive growth. Semin Cancer Biol 11:153-165

51. **Comoglio PM, Trusolino L** 2002 Invasive growth: from development to metastasis. J Clin Invest 109:857-862

52. **Conrotto P, Corso S, Gamberini S, Comoglio PM, Giordano S** 2004 Interplay between scatter factor receptors and B plexins controls invasive growth. Oncogene 23:5131-5137

53. **Curtis HJ** 1965 Formal discussion of: somatic mutations and carcinogenesis. Cancer Res 25:1305-1308

54. **Czopik AK, Bynoe MS, Palm N, Raine CS, Medzhitov R** 2006 Semaphorin 7A is a negative regulator of T cell responses. Immunity 24:591-600

55. **Dahiya R, McCarville J, Hu W, Lee C, Chui RM, Kaur G, Deng G** 1997 Chromosome 3p24-26 and 3p22-12 loss in human prostatic adenocarcinoma. Int J Cancer 71:20-25

56. **Daly-Burns B, Alam TN, Mackay A, Clark J, Shepherd CJ, Rizzo S, Tatoud R, O'Hare MJ, Masters JR, Hudson DL** 2007 A conditionally immortalized cell line model for the study of human prostatic epithelial cell differentiation. Differentiation 75:35-48

57. **Danen EH, Sonneveld P, Brakebusch C, Fassler R, Sonnenberg A** 2002 The fibronectin-binding integrins alpha5beta1 and alphavbeta3 differentially modulate RhoA-GTP loading, organization of cell matrix adhesions, and fibronectin fibrillogenesis. J Cell Biol 159:1071-1086

58. **Davies G, Jiang WG, Mason MD** 1999 Cell-cell adhesion molecules and their associated proteins in bladder cancer cells and their role in mitogen induced cell-cell dissociation and invasion. Anticancer Res 19:547-552

59. **Davies G, Jiang WG, Mason MD** 2001 Matrilysin mediates extracellular cleavage of E-cadherin from prostate cancer cells: a key mechanism in hepatocyte growth factor/scatter factor-induced cell-cell dissociation and in vitro invasion. Clin Cancer Res 7:3289-3297

60. **Davies G, Watkins G, Mason MD, Jiang WG** 2004 Targeting the HGF/SF receptor c-met using a hammerhead ribozyme transgene reduces in vitro invasion and migration in prostate cancer cells. Prostate 60:317-324

61. **de Lange T** 2005 Shelterin: the protein complex that shapes and safeguards human telomeres. Genes Dev 19:2100-2110

62. **Delaire S, Billard C, Tordjman R, Chedotal A, Elhabazi A, Bensussan A, Boumsell L** 2001 Biological activity of soluble CD100. II. Soluble CD100, similarly to H-SemaIII, inhibits immune cell migration. J Immunol 166:4348-4354

63. **Diaz-Gonzalez JA, Russell J, Rouzaut A, Gil-Bazo I, Montuenga L** 2005 Targeting hypoxia and angiogenesis through HIF-1alpha inhibition. Cancer Biol Ther 4:1055-1062

64. **Dickson BJ** 2002 Molecular mechanisms of axon guidance. Science 298:1959-1964

65. **Djakiew D** 2000 Dysregulated expression of growth factors and their receptors in the development of prostate cancer. Prostate 42:150-160

66. **Donate LE, Gherardi E, Srinivasan N, Sowdhamini R, Aparicio S, Blundell TL** 1994 Molecular evolution and domain structure of plasminogen-related growth factors (HGF/SF and HGF1/MSP). Protein Sci 3:2378-2394

67. **Driessens MH, Hu H, Nobes CD, Self A, Jordens I, Goodman CS, Hall A** 2001 Plexin-B semaphorin receptors interact directly with active Rac and regulate the actin cytoskeleton by activating Rho. Curr Biol 11:339-344

68. **Du Z, Fujiyama C, Chen Y, Masaki Z** 2003 Expression of hypoxia-inducible factor 1alpha in human normal, benign, and malignant prostate tissue. Chin Med J (Engl) 116:1936-1939

69. **Eichmann A, Makinen T, Alitalo K** 2005 Neural guidance molecules regulate vascular remodeling and vessel navigation. Genes Dev 19:1013-1021

70. **Ellis LM, Staley CA, Liu W, Fleming RY, Parikh NU, Bucana CD, Gallick GE** 1998 Down-regulation of vascular endothelial growth factor in a human colon carcinoma cell line transfected with an antisense expression vector specific for c-src. J Biol Chem 273:1052-1057

71. **Feiner L, Koppel AM, Kobayashi H, Raper JA** 1997 Secreted chick semaphorins bind recombinant neuropilin with similar affinities but bind different subsets of neurons in situ. Neuron 19:539-545

72. **Ferrara N, Gerber HP, LeCouter J** 2003 The biology of VEGF and its receptors. Nat Med 9:669-676

73. **Furge KA, Zhang YW, Vande Woude GF** 2000 Met receptor tyrosine kinase: enhanced signaling through adapter proteins. Oncogene 19:5582-5589

74. **Gagnon ML, Bielenberg DR, Gechtman Z, Miao HQ, Takashima S, Soker S, Klagsbrun M** 2000 Identification of a natural soluble neuropilin-1 that binds vascular endothelial growth factor: In vivo expression and antitumor activity. Proc Natl Acad Sci U S A 97:2573-2578

75. **Gao CF, Vande Woude GF** 2005 HGF/SF-Met signaling in tumor progression. Cell Res 15:49-51

76. **Gentile A, Comoglio PM** 2004 Invasive growth: a genetic program. Int J Dev Biol 48:451-456

77. **Gerstein M, Altman RB** 1995 Average core structures and variability measures for protein families: application to the immunoglobulins. J Mol Biol 251:161-175

78. **Gherardi E, Youles ME, Miguel RN, Blundell TL, Iamele L, Gough J, Bandyopadhyay A, Hartmann G, Butler PJ** 2003 Functional map and domain structure of MET, the product of the c-met protooncogene and receptor for hepatocyte growth factor/scatter factor. Proc Natl Acad Sci U S A 100:12039-12044

79. **Gherardi E, Love CA, Esnouf RM, Jones EY** 2004 The sema domain. Curr Opin Struct Biol 14:669-678

80. **Giacinti C, Giordano A** 2006 RB and cell cycle progression. Oncogene 25:5220-5227

81. **Giannelli G, Falk-Marzillier J, Schiraldi O, Stetler-Stevenson WG, Quaranta V** 1997 Induction of cell migration by matrix metalloprotease-2 cleavage of laminin-5. Science 277:225-228

82. **Giordano S, Corso S, Conrotto P, Artigiani S, Gilestro G, Barberis D, Tamagnone L, Comoglio PM** 2002 The semaphorin 4D receptor controls invasive growth by coupling with Met. Nat Cell Biol 4:720-724

83. **Gitler AD, Lu MM, Epstein JA** 2004 PlexinD1 and semaphorin signaling are required in endothelial cells for cardiovascular development. Dev Cell 7:107-116

84. **Gleason DF** 1966 Classification of prostatic carcinomas. Cancer Chemother Rep 50:125-128

85. **Gleason DF** 1992 Histologic grading of prostate cancer: a perspective. Hum Pathol 23:273-279

86. **Gogvadze V, Orrenius S** 2006 Mitochondrial regulation of apoptotic cell death. Chem Biol Interact 163:4-14

87. **Gu C, Yoshida Y, Livet J, Reimert DV, Mann F, Merte J, Henderson CE, Jessell TM, Kolodkin AL, Ginty DD** 2005 Semaphorin 3E and plexin-D1 control vascular pattern independently of neuropilins. Science 307:265-268

88. **Guttmann-Raviv N, Kessler O, Shraga-Heled N, Lange T, Herzog Y, Neufeld G** 2006 The neuropilins and their role in tumorigenesis and tumor progression. Cancer Lett 231:1-11

89. **Guttmann-Raviv N, Shraga-Heled N, Varshavsky A, Guimaraes-Sternberg C, Kessler O, Neufeld G** 2007 Semaphorin-3A and semaphorin-3F work together to repel endothelial cells and to inhibit their survival by induction of apoptosis. J Biol Chem 282:26294-26305

90. **Haggman MJ, Macoska JA, Wojno KJ, Oesterling JE** 1997 The relationship between prostatic intraepithelial neoplasia and prostate cancer: critical issues. J Urol 158:12-22

91. **Halaby DM, Mornon JP** 1998 The immunoglobulin superfamily: an insight on its tissular, species, and functional diversity. J Mol Evol 46:389-400

92. **Halaby DM, Poupon A, Mornon J** 1999 The immunoglobulin fold family: sequence analysis and 3D structure comparisons. Protein Eng 12:563-571

93. **Hanahan D, Weinberg RA** 2000 The hallmarks of cancer. Cell 100:57-70

94. **Hao P, Chen X, Geng H, Gu L, Chen J, Lu G** 2004 Expression and implication of hypoxia inducible factor-1alpha in prostate neoplasm. J Huazhong Univ Sci Technolog Med Sci 24:593-595

95. **Hayflick L** 1997 Mortality and immortality at the cellular level. A review. Biochemistry (Mosc) 62:1180-1190

96. **Hayflick L** 2003 Living forever and dying in the attempt. Exp Gerontol 38:1231-1241

97. **Hayward SW, Rosen MA, Cunha GR** 1997 Stromal-epithelial interactions in the normal and neoplastic prostate. Br J Urol 79 Suppl 2:18-26

98. **He Z, Tessier-Lavigne M** 1997 Neuropilin is a receptor for the axonal chemorepellent Semaphorin III. Cell 90:739-751

99. **Henson JD, Neumann AA, Yeager TR, Reddel RR** 2002 Alternative lengthening of telomeres in mammalian cells. Oncogene 21:598-610

100. **Herman JG, Meadows GG** 2007 Transferrin reverses the anti-invasive activity of human prostate cancer cells that overexpress sema3E. Int J Oncol 31:1267-1272

101. **Herman JG, Meadows GG** 2007 Increased class 3 semaphorin expression modulates the invasive and adhesive properties of prostate cancer cells. Int J Oncol 30:1231-1238

102. **Hinck L** 2004 The versatile roles of "axon guidance" cues in tissue morphogenesis. Dev Cell 7:783-793

103. **Hofmann UB, Westphal JR, Van Kraats AA, Ruiter DJ, van Muijen GN** 2000 Expression of integrin alpha(v)beta(3) correlates with activation of membrane-type matrix metalloproteinase-1 (MT1-MMP) and matrix metalloproteinase-2 (MMP-2) in human melanoma cells in vitro and in vivo. Int J Cancer 87:12-19

104. **Horoszewicz JS, Leong SS, Chu TM, Wajsman ZL, Friedman M, Papsidero L, Kim U, Chai LS, Kakati S, Arya SK, Sandberg AA** 1980 The LNCaP cell line--a new model for studies on human prostatic carcinoma. Prog Clin Biol Res 37:115-132

105. **Horoszewicz JS, Leong SS, Kawinski E, Karr JP, Rosenthal H, Chu TM, Mirand EA, Murphy GP** 1983 LNCaP model of human prostatic carcinoma. Cancer Res 43:1809-1818

106. **Hsing AW, Devesa SS** 2001 Trends and patterns of prostate cancer: what do they suggest? Epidemiol Rev 23:3-13

107. **Huber AB, Kolodkin AL, Ginty DD, Cloutier JF** 2003 Signaling at the growth cone: ligand-receptor complexes and the control of axon growth and guidance. Annu Rev Neurosci 26:509-563

108. **Humphrey PA, Zhu X, Zarnegar R, Swanson PE, Ratliff TL, Vollmer RT, Day ML** 1995 Hepatocyte growth factor and its receptor (c-MET) in prostatic carcinoma. Am J Pathol 147:386-396

109. **Jackson MW, Bentel JM, Tilley WD** 1997 Vascular endothelial growth factor (VEGF) expression in prostate cancer and benign prostatic hyperplasia. J Urol 157:2323-2328

110. **Jacobs SC** 1983 Spread of prostatic cancer to bone. Urology 21:337-344

111. **Jenkins RB, Qian J, Lieber MM, Bostwick DG** 1997 Detection of c-myc oncogene amplification and chromosomal anomalies in metastatic prostatic carcinoma by fluorescence in situ hybridization. Cancer Res 57:524-531

112. **Kaighn ME, Lechner JF, Narayan KS, Jones LW** 1978 Prostate carcinoma: tissue culture cell lines. Natl Cancer Inst Monogr17-21

113. **Kaighn ME, Narayan KS, Ohnuki Y, Lechner JF, Jones LW** 1979 Establishment and characterization of a human prostatic carcinoma cell line (PC-3). Invest Urol 17:16-23

114. **Kang Y, Siegel PM, Shu W, Drobnjak M, Kakonen SM, Cordon-Cardo C, Guise TA, Massague J** 2003 A multigenic program mediating breast cancer metastasis to bone. Cancer Cell 3:537-549

115. **Kessler O, Shraga-Heled N, Lange T, Gutmann-Raviv N, Sabo E, Baruch L, Machluf M, Neufeld G** 2004 Semaphorin-3F is an inhibitor of tumor angiogenesis. Cancer Res 64:1008-1015

116. **Khidr L, Chen PL** 2006 RB, the conductor that orchestrates life, death and differentiation. Oncogene 25:5210-5219

117. **Kinashi T** 2005 Intracellular signalling controlling integrin activation in lymphocytes. Nat Rev Immunol 5:546-559

118. **Klostermann A, Lohrum M, Adams RH, Puschel AW** 1998 The chemorepulsive activity of the axonal guidance signal semaphorin D requires dimerization. J Biol Chem 273:7326-7331

119. **Kobayashi T, Honke K, Miyazaki T, Matsumoto K, Nakamura T, Ishizuka I, Makita A** 1994 Hepatocyte growth factor specifically binds to sulfoglycolipids. J Biol Chem 269:9817-9821

120. **Kolodkin AL, Matthes DJ, Goodman CS** 1993 The semaphorin genes encode a family of transmembrane and secreted growth cone guidance molecules. Cell 75:1389-1399

121. **Kolodkin AL, Levengood DV, Rowe EG, Tai YT, Giger RJ, Ginty DD** 1997 Neuropilin is a semaphorin III receptor. Cell 90:753-762

122. **Komada M, Hatsuzawa K, Shibamoto S, Ito F, Nakayama K, Kitamura N** 1993 Proteolytic processing of the hepatocyte growth factor/scatter factor receptor by furin. FEBS Lett 328:25-29

123. **Komada M, Kitamura N** 1993 The cell dissociation and motility triggered by scatter factor/hepatocyte growth factor are mediated through the cytoplasmic domain of the c-Met receptor. Oncogene 8:2381-2390

124. **Kong-Beltran M, Stamos J, Wickramasinghe D** 2004 The Sema domain of Met is necessary for receptor dimerization and activation. Cancer Cell 6:75-84

125. **Koppel AM, Feiner L, Kobayashi H, Raper JA** 1997 A 70 amino acid region within the semaphorin domain activates specific cellular response of semaphorin family members. Neuron 19:531-537

126. **Koppel AM, Raper JA** 1998 Collapsin-1 covalently dimerizes, and dimerization is necessary for collapsing activity. J Biol Chem 273:15708-15713

127. **Kornau HC, Seeburg PH, Kennedy MB** 1997 Interaction of ion channels and receptors with PDZ domain proteins. Curr Opin Neurobiol 7:368-373

128. **Kozlov G, Perreault A, Schrag JD, Park M, Cygler M, Gehring K, Ekiel I** 2004 Insights into function of PSI domains from structure of the Met receptor PSI domain. Biochem Biophys Res Commun 321:234-240

129. **Kruger RP, Aurandt J, Guan KL** 2005 Semaphorins command cells to move. Nat Rev Mol Cell Biol 6:789-800

130. **Kumanogoh A, Watanabe C, Lee I, Wang X, Shi W, Araki H, Hirata H, Iwahori K, Uchida J, Yasui T, Matsumoto M, Yoshida K, Yakura H, Pan C, Parnes JR, Kikutani H** 2000 Identification of CD72 as a lymphocyte receptor for the class IV semaphorin CD100: a novel mechanism for regulating B cell signaling. Immunity 13:621-631

131. **Kumanogoh A, Kikutani H** 2003 Roles of the semaphorin family in immune regulation. Adv Immunol 81:173-198

132. **Kumanogoh A, Kikutani H** 2004 Biological functions and signaling of a transmembrane semaphorin, CD100/Sema4D. Cell Mol Life Sci 61:292-300

133. **Kumar S** 2007 Caspase function in programmed cell death. Cell Death Differ 14:32-43

134. **Kuroki T, Trapasso F, Yendamuri S, Matsuyama A, Alder H, Williams NN, Kaiser LR, Croce CM** 2003 Allelic loss on chromosome 3p21.3 and promoter hypermethylation of semaphorin 3B in non-small cell lung cancer. Cancer Res 63:3352-3355

135. **Lalani SR, Safiullah AM, Molinari LM, Fernbach SD, Martin DM, Belmont JW** 2004 SEMA3E mutation in a patient with CHARGE syndrome. J Med Genet 41:e94

136. **Lange PH, Vessella RL** 1998 Mechanisms, hypotheses and questions regarding prostate cancer micrometastases to bone. Cancer Metastasis Rev 17:331-336

137. **Langley RR, Fidler IJ** 2007 Tumor cell-organ microenvironment interactions in the pathogenesis of cancer metastasis. Endocr Rev 28:297-321

138. **Latil A, Bieche I, Pesche S, Valeri A, Fournier G, Cussenot O, Lidereau R** 2000 VEGF overexpression in clinically localized prostate tumors and neuropilin-1 overexpression in metastatic forms. Int J Cancer 89:167-171

139. **Lepelletier Y, Moura IC, Hadj-Slimane R, Renand A, Fiorentino S, Baude C, Shirvan A, Barzilai A, Hermine O** 2006 Immunosuppressive role of semaphorin-3A on T cell proliferation is mediated by inhibition of actin cytoskeleton reorganization. Eur J Immunol 36:1782-1793

140. **Liu XQ, Sun M, Chen HK, Li JX, Pan ZG, Long QX, Wang XZ, Zeng YX** 2003 [Mutation and expression of SEMA3B and SEMA3F gene in nasopharyngeal carcinoma]. Ai Zheng 22:16-20

141. **Liu Y** 1998 The human hepatocyte growth factor receptor gene: complete structural organization and promoter characterization. Gene 215:159-169

142. **Lokker NA, Mark MR, Luis EA, Bennett GL, Robbins KA, Baker JB, Godowski PJ** 1992 Structure-function analysis of hepatocyte growth factor: identification of variants that lack mitogenic activity yet retain high affinity receptor binding. EMBO J 11:2503-2510

143. **Love CA, Harlos K, Mavaddat N, Davis SJ, Stuart DI, Jones EY, Esnouf RM** 2003 The ligand-binding face of the semaphorins revealed by the high-resolution crystal structure of SEMA4D. Nat Struct Biol 10:843-848

144. **Macaluso M, Montanari M, Giordano A** 2006 Rb family proteins as modulators of gene expression and new aspects regarding the interaction with chromatin remodeling enzymes. Oncogene 25:5263-5267

145. **Maestrini E, Tamagnone L, Longati P, Cremona O, Gulisano M, Bione S, Tamanini F, Neel BG, Toniolo D, Comoglio PM** 1996 A family of transmembrane proteins with homology to the MET-hepatocyte growth factor receptor. Proc Natl Acad Sci U S A 93:674-678

146. **Martin-Satue M, Blanco J** 1999 Identification of semaphorin E gene expression in metastatic human lung adenocarcinoma cells by mRNA differential display. J Surg Oncol 72:18-23

147. **Masters JR, Thomson JA, Ly-Burns B, Reid YA, Dirks WG, Packer P, Toji LH, Ohno T, Tanabe H, Arlett CF, Kelland LR, Harrison M, Virmani A, Ward TH, Ayres KL, Debenham PG** 2001 Short tandem repeat profiling provides an international reference standard for human cell lines. Proc Natl Acad Sci U S A 98:8012-8017

148. **Maulik G, Shrikhande A, Kijima T, Ma PC, Morrison PT, Salgia R** 2002 Role of the hepatocyte growth factor receptor, c-Met, in oncogenesis and potential for therapeutic inhibition. Cytokine Growth Factor Rev 13:41-59

149. **McNeal JE, a** 1981 The zonal anatomy of the prostate. Prostate 2:35-49

150. **McNeal JE, b** 1981 Normal and pathologic anatomy of prostate. Urology 17:11-16

151. **Miao H, Nickel CH, Cantley LG, Bruggeman LA, Bennardo LN, Wang B** 2003 EphA kinase activation regulates HGF-induced epithelial branching morphogenesis. J Cell Biol 162:1281-1292

152. **Miao HQ, Soker S, Feiner L, Alonso JL, Raper JA, Klagsbrun M** 1999 Neuropilin-1 mediates collapsin-1/semaphorin III inhibition of endothelial cell motility: functional competition of collapsin-1 and vascular endothelial growth factor-165. J Cell Biol 146:233-242

153. **Miao HQ, Lee P, Lin H, Soker S, Klagsbrun M** 2000 Neuropilin-1 expression by tumor cells promotes tumor angiogenesis and progression. FASEB J 14:2532-2539

154. **Mickey DD, Stone KR, Wunderli H, Mickey GH, Paulson DF** 1980 Characterization of a human prostate adenocarcinoma cell line (DU 145) as a monolayer culture and as a solid tumor in athymic mice. Prog Clin Biol Res 37:67-84

155. **Miller JR, Moon RT** 1996 Signal transduction through beta-catenin and specification of cell fate during embryogenesis. Genes Dev 10:2527-2539

156. **Miura H, Nishimura K, Tsujimura A, Matsumiya K, Matsumoto K, Nakamura T, Okuyama A** 2001 Effects of hepatocyte growth factor on E-cadherin-mediated cell-cell adhesion in DU145 prostate cancer cells. Urology 58:1064-1069

157. **Mol AJ, Geldof AA, Meijer GA, van der Poel HG, van Moorselaar RJ** 2007 New experimental markers for early detection of high-risk prostate cancer: role of cell-cell adhesion and cell migration. J Cancer Res Clin Oncol

158. **Monvoisin A, Bisson C, Si-Tayeb K, Balabaud C, Desmouliere A, Rosenbaum J** 2002 Involvement of matrix metalloproteinase type-3 in hepatocyte growth factor-induced invasion of human hepatocellular carcinoma cells. Int J Cancer 97:157-162

159. **Moretti S, Procopio A, Boemi M, Catalano A** 2006 Neuronal semaphorins regulate a primary immune response. Curr Neurovasc Res 3:295-305

160. **Morgia G, Falsaperla M, Malaponte G, Madonia M, Indelicato M, Travali S, Mazzarino MC** 2005 Matrix metalloproteinases as diagnostic (MMP-13) and prognostic (MMP-2, MMP-9) markers of prostate cancer. Urol Res 33:44-50

161. **Muller MW, Giese NA, Swiercz JM, Ceyhan GO, Esposito I, Hinz U, Buchler P, Giese T, Buchler MW, Offermanns S, Friess H** 2007 Association of axon guidance factor semaphorin 3A with poor outcome in pancreatic cancer. Int J Cancer 121:2421-2433

162. **Nair PN, McArdle L, Cornell J, Cohn SL, Stallings RL** 2007 High-resolution analysis of 3p deletion in neuroblastoma and differential methylation of the SEMA3B tumor suppressor gene. Cancer Genet Cytogenet 174:100-110

163. **Narla G, Heath KE, Reeves HL, Li D, Giono LE, Kimmelman AC, Glucksman MJ, Narla J, Eng FJ, Chan AM, Ferrari AC, Martignetti JA, Friedman SL** 2001 KLF6, a candidate tumor suppressor gene mutated in prostate cancer. Science 294:2563-2566

164. **Nasarre P, Constantin B, Rouhaud L, Harnois T, Raymond G, Drabkin HA, Bourmeyster N, Roche J** 2003 Semaphorin SEMA3F and VEGF have opposing effects on cell attachment and spreading. Neoplasia 5:83-92

165. **Nathke I** 2005 Relationship between the role of the adenomatous polyposis coli protein in colon cancer and its contribution to cytoskeletal regulation. Biochem Soc Trans 33:694-697

166. **Nathke IS** 2004 The adenomatous polyposis coli protein: the Achilles heel of the gut epithelium. Annu Rev Cell Dev Biol 20:337-366

167. **Neufeld G, Cohen T, Shraga N, Lange T, Kessler O, Herzog Y** 2002 The neuropilins: multifunctional semaphorin and VEGF receptors that modulate axon guidance and angiogenesis. Trends Cardiovasc Med 12:13-19

168. **Neufeld G, Shraga-Heled N, Lange T, Guttmann-Raviv N, Herzog Y, Kessler O** 2005 Semaphorins in cancer. Front Biosci 10:751-760

169. **Niemann C, Brinkmann V, Spitzer E, Hartmann G, Sachs M, Naundorf H, Birchmeier W** 1998 Reconstitution of mammary gland development in vitro: requirement of c-met and c-erbB2 signaling for branching and alveolar morphogenesis. J Cell Biol 143:533-545

170. **Nobes CD, Hall A** 1995 Rho, rac, and cdc42 GTPases regulate the assembly of multimolecular focal complexes associated with actin stress fibers, lamellipodia, and filopodia. Cell 81:53-62

171. **Oinuma I, Katoh H, Harada A, Negishi M** 2003 Direct interaction of Rnd1 with Plexin-B1 regulates PDZ-RhoGEF-mediated Rho activation by Plexin-B1 and induces cell contraction in COS-7 cells. J Biol Chem 278:25671-25677

172. **Oinuma I, Katoh H, Negishi M, a** 2004 Molecular dissection of the semaphorin 4D receptor plexin-B1-stimulated R-Ras GTPase-activating protein activity and neurite remodeling in hippocampal neurons. J Neurosci 24:11473-11480

173. **Oinuma I, Ishikawa Y, Katoh H, Negishi M, b** 2004 The Semaphorin 4D receptor Plexin-B1 is a GTPase activating protein for R-Ras. Science 305:862-865

174. **Oinuma I, Katoh H, Negishi M** 2006 Semaphorin 4D/Plexin-B1-mediated R-Ras GAP activity inhibits cell migration by regulating beta(1) integrin activity. J Cell Biol 173:601-613

175. **Olumi AF, Grossfeld GD, Hayward SW, Carroll PR, Tlsty TD, Cunha GR** 1999 Carcinoma-associated fibroblasts direct tumor progression of initiated human prostatic epithelium. Cancer Res 59:5002-5011

176. **Pan Q, Chanthery Y, Liang WC, Stawicki S, Mak J, Rathore N, Tong RK, Kowalski J, Yee SF, Pacheco G, Ross S, Cheng Z, Le CJ, Plowman G, Peale F, Koch AW, Wu Y, Bagri A, Tessier-Lavigne M, Watts RJ** 2007 Blocking neuropilin-1 function has an additive effect with anti-VEGF to inhibit tumor growth. Cancer Cell 11:53-67

177. **Park YH, Ryu HS, Choi DS, Chang KH, Park DW, Min CK** 2003 Effects of hepatocyte growth factor on the expression of matrix metalloproteinases and their tissue inhibitors during the endometrial cancer invasion in a three-dimensional coculture. Int J Gynecol Cancer 13:53-60

178. **Pascual M, Pozas E, Soriano E** 2005 Role of class 3 semaphorins in the development and maturation of the septohippocampal pathway. Hippocampus 15:184-202

179. **Pennacchietti S, Michieli P, Galluzzo M, Mazzone M, Giordano S, Comoglio PM** 2003 Hypoxia promotes invasive growth by transcriptional activation of the met protooncogene. Cancer Cell 3:347-361

180. **Pisters LL, Troncoso P, Zhau HE, Li W, von Eschenbach AC, Chung LW** 1995 c-met proto-oncogene expression in benign and malignant human prostate tissues. J Urol 154:293-298

181. **Ponzetto C, Bardelli A, Zhen Z, Maina F, dalla ZP, Giordano S, Graziani A, Panayotou G, Comoglio PM** 1994 A multifunctional docking site mediates signaling and transformation by the hepatocyte growth factor/scatter factor receptor family. Cell 77:261-271

182. **Price LS, Leng J, Schwartz MA, Bokoch GM** 1998 Activation of Rac and Cdc42 by integrins mediates cell spreading. Mol Biol Cell 9:1863-1871

183. **Quinn DI, Henshall SM, Sutherland RL** 2005 Molecular markers of prostate cancer outcome. Eur J Cancer 41:858-887

184. **Ren XD, Kiosses WB, Schwartz MA** 1999 Regulation of the small GTP-binding protein Rho by cell adhesion and the cytoskeleton. EMBO J 18:578-585

185. **Renan MJ** 1993 How many mutations are required for tumorigenesis? Implications from human cancer data. Mol Carcinog 7:139-146

186. **Ridley AJ, Hall A** 1992 The small GTP-binding protein rho regulates the assembly of focal adhesions and actin stress fibers in response to growth factors. Cell 70:389-399

187. **Rieger J, Wick W, Weller M** 2003 Human malignant glioma cells express semaphorins and their receptors, neuropilins and plexins. Glia 42:379-389

188. **Rohm B, Rahim B, Kleiber B, Hovatta I, Puschel AW, a** 2000 The semaphorin 3A receptor may directly regulate the activity of small GTPases. FEBS Lett 486:68-72

189. **Rohm B, Ottemeyer A, Lohrum M, Puschel AW, b** 2000 Plexin/neuropilin complexes mediate repulsion by the axonal guidance signal semaphorin 3A. Mech Dev 93:95-104

190. **Rolny C, Capparuccia L, Casazza A, Mazzone M, Vallario A, Cignetti A, Medico E, Carmeliet P, Comoglio PM, Tamagnone L** 2008 The tumor suppressor semaphorin 3B triggers a prometastatic program mediated by interleukin 8 and the tumor microenvironment. J Exp Med 205:1155-1171

191. **Rosenthal EL, Johnson TM, Allen ED, Apel IJ, Punturieri A, Weiss SJ** 1998 Role of the plasminogen activator and matrix metalloproteinase systems in epidermal growth factor- and scatter factor-stimulated invasion of carcinoma cells. Cancer Res 58:5221-5230

192. **Roskies AL** 1998 Dissecting semaphorin signaling. Neuron 21:935-936

193. **Rossignol M, Beggs AH, Pierce EA, Klagsbrun M** 1999 Human neuropilin-1 and neuropilin-2 map to 10p12 and 2q34, respectively. Genomics 57:459-460

194. **Rossignol M, Gagnon ML, Klagsbrun M** 2000 Genomic organization of human neuropilin-1 and neuropilin-2 genes: identification and distribution of splice variants and soluble isoforms. Genomics 70:211-222

195. **Rottner K, Hall A, Small JV** 1999 Interplay between Rac and Rho in the control of substrate contact dynamics. Curr Biol 9:640-648

196. **Royal I, Lamarche-Vane N, Lamorte L, Kaibuchi K, Park M** 2000 Activation of cdc42, rac, PAK, and rho-kinase in response to hepatocyte growth factor differentially regulates epithelial cell colony spreading and dissociation. Mol Biol Cell 11:1709-1725

197. **Rubin MA, Putzi M, Mucci N, Smith DC, Wojno K, Korenchuk S, Pienta KJ** 2000 Rapid ("warm") autopsy study for procurement of metastatic prostate cancer. Clin Cancer Res 6:1038-1045

198. **Saccone S, Narsimhan RP, Gaudino G, Dalpra L, Comoglio PM, Della VG** 1992 Regional mapping of the human hepatocyte growth factor (HGF)-scatter factor gene to chromosome 7q21.1. Genomics 13:912-914

199. **Sakai T, Furuyama T, Ohoka Y, Miyazaki N, Fujioka S, Sugimoto H, Amasaki M, Hattori S, Matsuya T, Inagaki S** 1999 Mouse semaphorin H induces PC12 cell neurite outgrowth activating Ras-mitogen-activated protein kinase signaling pathway via Ca(2+) influx. J Biol Chem 274:29666-29671

200. **Sanchez P, Hernandez AM, Stecca B, Kahler AJ, DeGueme AM, Barrett A, Beyna M, Datta MW, Datta S, Altaba A** 2004 Inhibition of prostate cancer proliferation by interference with SONIC HEDGEHOG-GLI1 signaling. Proc Natl Acad Sci U S A 101:12561-12566

201. **Sattler HP, Rohde V, Bonkhoff H, Zwergel T, Wullich B** 1999 Comparative genomic hybridization reveals DNA copy number gains to frequently occur in human prostate cancer. Prostate 39:79-86

202. **Schiering N, Knapp S, Marconi M, Flocco MM, Cui J, Perego R, Rusconi L, Cristiani C** 2003 Crystal structure of the tyrosine kinase domain of the hepatocyte growth factor receptor c-Met and its complex with the microbial alkaloid K-252a. Proc Natl Acad Sci U S A 100:12654-12659

203. **Schmidt C, Bladt F, Goedecke S, Brinkmann V, Zschiesche W, Sharpe M, Gherardi E, Birchmeier C** 1995 Scatter factor/hepatocyte growth factor is essential for liver development. Nature 373:699-702

204. **Schroder FH, Hermanek P, Denis L, Fair WR, Gospodarowicz MK, Pavone-Macaluso M** 1992 The TNM classification of prostate cancer. Prostate Suppl 4:129-138

205. **Schwartz MA, Shattil SJ** 2000 Signaling networks linking integrins and rho family GTPases. Trends Biochem Sci 25:388-391

206. **Seki T, Hagiya M, Shimonishi M, Nakamura T, Shimizu S** 1991 Organization of the human hepatocyte growth factor-encoding gene. Gene 102:213-219

207. **Semenza GL** 2000 HIF-1: using two hands to flip the angiogenic switch. Cancer Metastasis Rev 19:59-65

208. **Semenza GL** 2001 HIF-1, O(2), and the 3 PHDs: how animal cells signal hypoxia to the nucleus. Cell 107:1-3

209. **Serini G, Valdembri D, Zanivan S, Morterra G, Burkhardt C, Caccavari F, Zammataro L, Primo L, Tamagnone L, Logan M, Tessier-Lavigne M, Taniguchi M, Puschel AW, Bussolino F** 2003 Class 3 semaphorins control vascular morphogenesis by inhibiting integrin function. Nature 424:391-397

210. **Shakib K, Norman JT, Fine LG, Brown LR, Godovac-Zimmermann J** 2005 Proteomics profiling of nuclear proteins for kidney fibroblasts suggests hypoxia, meiosis, and cancer may meet in the nucleus. Proteomics 5:2819-2838

211. **Shen J, Samul R, Zimmer J, Liu H, Liang X, Hackett S, Campochiaro PA** 2004 Deficiency of neuropilin 2 suppresses VEGF-induced retinal neovascularization. Mol Med 10:12-18

212. **Sheppard D** 2002 Endothelial integrins and angiogenesis: not so simple anymore. J Clin Invest 110:913-914

213. **Shi W, Kumanogoh A, Watanabe C, Uchida J, Wang X, Yasui T, Yukawa K, Ikawa M, Okabe M, Parnes JR, Yoshida K, Kikutani H** 2000 The class IV semaphorin CD100 plays nonredundant roles in the immune system: defective B and T cell activation in CD100-deficient mice. Immunity 13:633-642

214. **Soker S, Takashima S, Miao HQ, Neufeld G, Klagsbrun M** 1998 Neuropilin-1 is expressed by endothelial and tumor cells as an isoform-specific receptor for vascular endothelial growth factor. Cell 92:735-745

215. **Sonnenberg E, Meyer D, Weidner KM, Birchmeier C** 1993 Scatter factor/hepatocyte growth factor and its receptor, the c-met tyrosine kinase, can mediate a signal exchange between mesenchyme and epithelia during mouse development. J Cell Biol 123:223-235

216. **Soto AM, Sonnenschein C** 2005 Emergentism as a default: cancer as a problem of tissue organization. J Biosci 30:103-118

217. **Sperandio S, de B, I, Bredesen DE** 2000 An alternative, nonapoptotic form of programmed cell death. Proc Natl Acad Sci U S A 97:14376-14381

218. **Staller P, Sulitkova J, Lisztwan J, Moch H, Oakeley EJ, Krek W** 2003 Chemokine receptor CXCR4 downregulated by von Hippel-Lindau tumour suppressor pVHL. Nature 425:307-311

219. **Stamos J, Lazarus RA, Yao X, Kirchhofer D, Wiesmann C** 2004 Crystal structure of the HGF beta-chain in complex with the Sema domain of the Met receptor. EMBO J 23:2325-2335

220. **Steinbach K, Volkmer H, Schlosshauer B** 2002 Semaphorin 3E/collapsin-5 inhibits growing retinal axons. Exp Cell Res 279:52-61

221. **Stewart SA, Weinberg RA** 2006 Telomeres: cancer to human aging. Annu Rev Cell Dev Biol 22:531-557

222. **Stone KR, Mickey DD, Wunderli H, Mickey GH, Paulson DF** 1978 Isolation of a human prostate carcinoma cell line (DU 145). Int J Cancer 21:274-281

223. **Suchting S, Bicknell R, Eichmann A** 2006 Neuronal clues to vascular guidance. Exp Cell Res 312:668-675

224. **Suzuki K, Okuno T, Yamamoto M, Pasterkamp RJ, Takegahara N, Takamatsu H, Kitao T, Takagi J, Rennert PD, Kolodkin AL, Kumanogoh A, Kikutani H** 2007 Semaphorin 7A initiates T-cell-mediated inflammatory responses through alpha1beta1 integrin. Nature 446:680-684

225. **Swiercz JM, Kuner R, Behrens J, Offermanns S** 2002 Plexin-B1 directly interacts with PDZ-RhoGEF/LARG to regulate RhoA and growth cone morphology. Neuron 35:51-63

226. **Swiercz JM, Kuner R, Offermanns S** 2004 Plexin-B1/RhoGEF-mediated RhoA activation involves the receptor tyrosine kinase ErbB-2. J Cell Biol 165:869-880

227. **Takahashi T, Nakamura F, Jin Z, Kalb RG, Strittmatter SM** 1998 Semaphorins A and E act as antagonists of neuropilin-1 and agonists of neuropilin-2 receptors. Nat Neurosci 1:487-493

228. **Takahashi T, Fournier A, Nakamura F, Wang LH, Murakami Y, Kalb RG, Fujisawa H, Strittmatter SM** 1999 Plexin-neuropilin-1 complexes form functional semaphorin-3A receptors. Cell 99:59-69

229. **Takahashi T, Strittmatter SM** 2001 Plexina1 autoinhibition by the plexin sema domain. Neuron 29:429-439

230. **Takegahara N, Kumanogoh A, Kikutani H** 2005 Semaphorins: a new class of immunoregulatory molecules. Philos Trans R Soc Lond B Biol Sci 360:1673-1680

231. **Tamagnone L, Comoglio PM** 1997 Control of invasive growth by hepatocyte growth factor (HGF) and related scatter factors. Cytokine Growth Factor Rev 8:129-142

232. **Tamagnone L, Artigiani S, Chen H, He Z, Ming GI, Song H, Chedotal A, Winberg ML, Goodman CS, Poo M, Tessier-Lavigne M, Comoglio PM** 1999 Plexins are a large family of receptors for transmembrane, secreted, and GPI-anchored semaphorins in vertebrates. Cell 99:71-80

233. **Tantivejkul K, Kalikin LM, Pienta KJ** 2004 Dynamic process of prostate cancer metastasis to bone. J Cell Biochem 91:706-717

234. **Tomizawa Y, Sekido Y, Kondo M, Gao B, Yokota J, Roche J, Drabkin H, Lerman MI, Gazdar AF, Minna JD** 2001 Inhibition of lung cancer cell growth and induction of apoptosis after reexpression of 3p21.3 candidate tumor suppressor gene SEMA3B. Proc Natl Acad Sci U S A 98:13954-13959

235. **Tomlins SA, Rhodes DR, Perner S, Dhanasekaran SM, Mehra R, Sun XW, Varambally S, Cao X, Tchinda J, Kuefer R, Lee C, Montie JE, Shah RB, Pienta KJ, Rubin MA, Chinnaiyan AM** 2005 Recurrent fusion of TMPRSS2 and ETS transcription factor genes in prostate cancer. Science 310:644-648

236. **Tomlinson IP, Novelli MR, Bodmer WF** 1996 The mutation rate and cancer. Proc Natl Acad Sci U S A 93:14800-14803

237. **Torres-Vazquez J, Gitler AD, Fraser SD, Berk JD, Van NP, Fishman MC, Childs S, Epstein JA, Weinstein BM** 2004 Semaphorin-plexin signaling guides patterning of the developing vasculature. Dev Cell 7:117-123

238. **Toyofuku T, Zhang H, Kumanogoh A, Takegahara N, Suto F, Kamei J, Aoki K, Yabuki M, Hori M, Fujisawa H, Kikutani H** 2004 Dual roles of Sema6D in cardiac morphogenesis through region-specific association of its receptor, Plexin-A1, with off-track and vascular endothelial growth factor receptor type 2. Genes Dev 18:435-447

239. **Trusolino L, Serini G, Cecchini G, Besati C, mbesi-Impiombato FS, Marchisio PC, De FR** 1998 Growth factor-dependent activation of alphavbeta3 integrin in normal epithelial cells: implications for tumor invasion. J Cell Biol 142:1145-1156

240. **Trusolino L, Cavassa S, Angelini P, Ando M, Bertotti A, Comoglio PM, Boccaccio C** 2000 HGF/scatter factor selectively promotes cell invasion by increasing integrin avidity. FASEB J 14:1629-1640

241. **Trusolino L, Comoglio PM** 2002 Scatter-factor and semaphorin receptors: cell signalling for invasive growth. Nat Rev Cancer 2:289-300

242. **Van Den BC, Guan XY, Von HD, Jenkins R, Bittner, Griffin C, Kallioniemi O, Visakorpi, McGill, Herath J, .** 1995 DNA sequence amplification in human prostate cancer identified by chromosome microdissection: potential prognostic implications. Clin Cancer Res 1:11-18

243. **Vande Woude GF, Jeffers M, Cortner J, Alvord G, Tsarfaty I, Resau J** 1997 Met-HGF/SF: tumorigenesis, invasion and metastasis. Ciba Found Symp 212:119-130

244. **Vikis HG, Li W, He Z, Guan KL** 2000 The semaphorin receptor plexin-B1 specifically interacts with active Rac in a ligand-dependent manner. Proc Natl Acad Sci U S A 97:12457-12462

245. **Vikis HG, Li W, Guan KL** 2002 The plexin-B1/Rac interaction inhibits PAK activation and enhances Sema4D ligand binding. Genes Dev 16:836-845

246. **Vogelstein B, Kinzler KW** 2004 Cancer genes and the pathways they control. Nat Med 10:789-799

247. **Weidner N, Carroll PR, Flax J, Blumenfeld W, Folkman J** 1993 Tumor angiogenesis correlates with metastasis in invasive prostate carcinoma. Am J Pathol 143:401-409

248. **Wells CM, Ahmed T, Masters JR, Jones GE** 2005 Rho family GTPases are activated during HGF-stimulated prostate cancer-cell scattering. Cell Motil Cytoskeleton 62:180-194

249. **Wenger RH, Stiehl DP, Camenisch G** 2005 Integration of oxygen signaling at the consensus HRE. Sci STKE 2005:re12

250. **Wu C, Bauer JS, Juliano RL, McDonald JA** 1993 The alpha 5 beta 1 integrin fibronectin receptor, but not the alpha 5 cytoplasmic domain, functions in an early and essential step in fibronectin matrix assembly. J Biol Chem 268:21883-21888

251. **Xu W, Coll JL, Adamson ED** 1998 Rescue of the mutant phenotype by reexpression of full-length vinculin in null F9 cells; effects on cell locomotion by domain deleted vinculin. J Cell Sci 111 (Pt 11):1535-1544

252. **Yamada T, Endo R, Gotoh M, Hirohashi S** 1997 Identification of semaphorin E as a non-MDR drug resistance gene of human cancers. Proc Natl Acad Sci U S A 94:14713-14718

253. **Yin JJ, Pollock CB, Kelly K** 2005 Mechanisms of cancer metastasis to the bone. Cell Res 15:57-62

254. **Zamir E, Geiger B** 2001 Molecular complexity and dynamics of cell-matrix adhesions. J Cell Sci 114:3583-3590

255. **Zhang YW, Vande Woude GF** 2003 HGF/SF-met signaling in the control of branching morphogenesis and invasion. J Cell Biochem 88:408-417

256. **Zhang Z, Morla AO, Vuori K, Bauer JS, Juliano RL, Ruoslahti E** 1993 The alpha v beta 1 integrin functions as a fibronectin receptor but does not support fibronectin matrix assembly and cell migration on fibronectin. J Cell Biol 122:235-242

257. **Zhong H, De Marzo AM, Laughner E, Lim M, Hilton DA, Zagzag D, Buechler P, Isaacs WB, Semenza GL, Simons JW** 1999 Overexpression of hypoxia-inducible factor 1alpha in common human cancers and their metastases. Cancer Res 59:5830-5835

258. **Zhu H, Naujokas MA, Park M** 1994 Receptor chimeras indicate that the met tyrosine kinase mediates the motility and morphogenic responses of hepatocyte growth/scatter factor. Cell Growth Differ 5:359-366

APPENDIX 1

Semaphorin 3a:

- DU145 cell line:

TGKGGGGCTYTWRRWGMTGCTCGAGCGGCCGCCAGTGTGATGGATATCTGCAGAATTCGC
CCTTACTGCTATTTCMGCAATGGAGCTTTCCACTAAGCAGCAACAACTATATATTGGTTCAAC
GGCTGGGGTTGCCCAGCTCCCTTTACACCGGTGTGATATTTACGGGAAAGCGTGTGCTGAG
TGTTGCCTCGCCCGAGACCCTTACTGTGCTTGGGATGGTTCTGCATGTTCTCGCTATTTTCCC
ACTGCAAAGAGACGCACAAGACGACAAGATATAAGAAATGGAGACCCACTGACTCACTGTTC
AGACTTACACCATGATAATCACCATGGCCACAGCCCTGAAGAGAGAATCATCTATGGTGTAG
AGAATAGTAGCACATTTTTGGAATGCAGTCCGAAGTCGCAGAGAGCGCTGGTCTATTGGCAA
TTCCAGAGGCGAAATGAAGAGCGAAAAGAAGAGATCAGAGTGGATGATCATATCATCAGGA
CAGATCAAGGCCTTCTGCTACGTAGTCTACAACAGAAGGATTCAGGCAATTACCTCTGCCAT
GCGGTGGAACATGGGTTCATACAAACTCTTCTTAAGGTAACCCTGGAAGTCATTGACACAGA
GCATTTGGAAGAACTTCTTCATAAAGATGATGATGGAGATGGCTCTAAGACCAAAGAAATGT
CCAATAGCATGACACCTAGCCAGAAGGTCTGGTACAGAGACTTCATGCAGCTCATCAACCAC
CCCAATCTCAACACAATGGATGAGTTCTGTGAACAAGTTAAGGGCGAATTCCAGCACACTGG
CGGCCGTTACTAGTGGATCCGAGCTCGGTACCAAGCTTGATGCATAGCTTGAGTATTCTATA
GTGTCACCTAAATAGCTTGGCGTAATCATGGTCATAGCTGTTTCCTGTGTGAAATTGTTATCC
GCTCACAATTCCACACACATACGAGCCGGAAGCATAAAGTGTAAAGCCTGGGGKGCCTAAT
GRGKGAGCTAACYCAMATTAAATTGSGTTGSGC

- 1542NPTX cell line:

TKSCCYYYWKWWKMAWGCTCGAGCGGCCGCCAGTGTGATGGATATCTGCAGAATTCGCCC
TTACTGCTATTTCAGCAATGGAGCTTTCCACTAAGCAGCAACAACTATATATTGGTTCAACGG
CTGGGGTTGCCCAGCTCCCTTTACACCGGTGTGATATTTACGGGGAAGCACGTGCTGAGTG
TTGCCTCGCCCGAGACCCTTACTGTGCTTGGGATGGTTCTGCATGTTCTCGCTATTTTCCCAC
TGCAAAGAGACGCACAAGACGACAAGATATAAGAAATGGAGACCCACTGACTCACTGTTCA
GACTTACACCATGATAATCACCATGGCCACAGCCCTGAAAAGAGAATCATCTATGGTGTAGA
GAATAGTAGCACATTTTTGGAATGCAGTCCGAAGTCGCAGAGAGCGCTGGTCTATTGGCAAT
TCCAGAGGCGAAATGAAGAGCGAAAAGAAGAGATCAGAGTGGATGATCATATCATCAGGAC
AGATCAAGGCCTTCTGCTACGTAGTCTACAACAGAAGGATTCAGGCAATTACCTCTGCCATG
CGGTGGAACATGGGTTCATACAAACTCTTCTTAAGGTAACCCTGGAAGTCATTGACACAGAG
CATTTGTAAGAACTTCTTCATAAAGACGATGATGGAGATGGCTCTAAGACCAAAGAAATGTC
CAATAGCATGACACCTAGCCAGAAGGTCTGGTACAGAGACTTCATGCAGCTCATCAACCACC
CCAATCTCAACACAATGGATGAGTTCTGTGAACAAGTTAAGGGCGAATTCCAGCACACTGGC
GGCCGTTACTAGTGGATCCGAGCTCGGTACCAAGCTTGATGCATAGCTTGAGTATTCTATAG
TGTCACCTAAATAGCTTGGCGTAATCATGGTCATAGCTGTTTCCTGTGTGAAATTGTTATCCG
CTCACAATTCCACACAACATACGAGCCGGAAGCATAAGTGTAAAGCCTGGGTGCCTAATGAG
TGAGCTAACTCACATTAATTGCGTTGCGCTCACTGCCCGCTTTCCAGTCGGGAAA

Semaphorin 3b:

- DU145 cell line:

CSCMKCCSTGRMCGSSTGTTTGTGGGTGCCRAGAACCATGTGGCCTCCCTCAACCTGGACA
ACATCAGCAAGCGGGCCAAGAAGCTGGCCTGGCCGGCCCCTGTGGAATGGCGAGAGGAGT

GCAACTGGGCAGGGAAGGACATTGGTACTGAGTGCATGAACTTCGTGAAGTTGCTGCATGC
CTACAACCGCACCCATTTGCTGGCCTGTGGCACGGGAGCCTTCCACCCAACCTGTGCCTTTG
TGGAAGTGGGCCACCGGGCAGAGGAGCCCGTCCTCCGGCTGGACCCAGGAAGGATAGAGG
ATGGCAAGGGGAAGAGTCCTTATGACCCCAGGCATCGGGCTGCCTCCGTGCTGGKGGGGG
AGGAGCTATACTCAGGGGTGGCAGCAGACCTCATGGGACGAGACTTTACCATCTTTCGCAG
CCTAGGGCAACGTCCAAGTCTCCGAACAGAGA

- 1542NPTX cell line:

GTGGATTSTCGTGCKWAGTGGWGAGGAGCGTGGACGCCTGTTTGTGGGTGCCGAGAACCA
TGTGGCCTCCCTCAACCTGGACAACATCAGCAAGCGGGCCAAGAAGCTGGCCTGGCCGGCC
CCTGTGGAATGGCGAGAGGAGTGCAACTGGGCAGGGAAGGACATTGGTACTGAGTGCATG
AACTTCGTGAAGTTGCTGCATGCCTACAACCGCACCCATTTGCTGGCCTGTGGCACGGGAG
CCTTCCACCCAACCTGTGCCTTTGTGGAAGTGGGCCACCGGGCAGAGGAGCCCGTCCTCCG
GCTGGACCCAGGAAGGATAGAGGATGGCAAGGGGAAGAGTCCTTATGACCCCAGGCATCG
GGCTGCCTCCGTGCTGGTGGGGGAGGAGCTATACTCAGGGGTGGCAGCAGACCTCATGGG
ACGAGACTTTACCATCTTTCGCAGCCTAGGGCAACGTCCAAGTCTCSGGAACAGAGA

Semaphorin 3c:

- DU145 cell line:

CGSAGYAAGCACTKACKGWKWYAYYWTMYWSAWYGATRCAGATCARGACCGGATATATGT
GGGAAGCAAAGATCACATTCTTTCCCTGAATATTAACAATATAAGTCAAGAAGCTTTGAGTGT
TTTCTGGCCAGCATCTACAATCAAAGTTGAAGAATGCAAAATGGCTGGCAAAGATCCCACAC
ACGGCTGTGGGAACTTTGTCCGTGTAATTCAGACTTTCAATCGCACACATTTGTATGTCTGTG
GGAGTGGCGCTTTCAGTCCTGTCTGTACTTACTTGAACAGAGGGAGGAGATCAGAGGACCA
AGTTTTCATGATTGACTCCAAGTGTGAATCTGGAAAAGGACGCTGCTCTTTCAACCCCAACG
TGAACACGGTGTCTGTTATGATCAATGAGGAGCTTTTCTCTGGAATGTATATAGATTTCATGG
GGACAGATGCTGCTATTTTTCGAAGTTTAACCAAGAGGAATGCGGTCAGAACTGATCAACAT
AATTCCAAATGGCTAAGTGAACCTATGTTTGTAGATGCACATGTCATCCRAAWKGGTAC

- 1542NPTX cell line:

CCTWCCYTTRWSKACARGATTTTATTAATGGATGAAGATCAGGACCGGATATATGTGGGAA
GCAAAGATCACATTCTTTCCCTGAATATTAACAATATAAGTCAAGAAGCTTTGAGTGTTTTCT
GGCCAGCATCTACAATCAAAGTTGAAGAATGCAAAATGGCTGGCAAAGATCCCACACACGG
CTGTGGGAACTTTGTCCGTGTAATTCAGACTTTCAATCGCACACATTTGTATGTCTGTGGGAG
TGGCGCTTTCAGTCCTGTCTGTACTTACTTGAACAGAGGGAGGAGATCAGAGGACCAAGTTT
TCATGATTGACTCCAAGTGTGAATCTGGAAAAGGACGCTGCTCTTTCAACCCCAACGTGAAC
ACGGTGTCTGTTATGATCAATGAGGAGCTTTTCTCTGGAATGTATATAGATTTCATGGGGAC
AGATGCTGCTATTTTTCGAAGTTTAACCAAGAGGAATGCGGTCAGAACTGATCAACATAATTC
CAAATGGCTAAGTGAACCTATGTTTGTAGATGCACATGTCATC

Semaphorin 3e:

- DU145 cell line:

CCMAGTYTGACGACTCATATTTCATAGCCCTTTTGGATTTCTTGATCTCCATACAATGCTGCT
GGATGAATATCAAGAGAGGCTCTTCGTGGGAGGCAGGGACCTTGTATATTCCCTCAGCTTG
GAGAGAATCAGTGACGGCTATAAAGAGATACACTGGCCGAGTACAGCTCTAAAAATGGAAG
AATGCATAATGAAGGGAAAAGATGCGGGTGAATGTGCAAATTATGTTCGGGTTTTGCATCAC
TATAACAGGACACACCTTCTGACCTGTGGTACTGGAGCTTTTGATCCAGTTTGTGCCTTCATC
AGAGTTGGATATCATTTGGAGRATCCTCTGTTTCACCTGGAATCACCCAGATCTGAGAGAGG
AAGGGGCAGATGTCCTTTTGACCCCASCTCCTCCTTCATCTCCACTTTAATTGGTAGTGAATT
GTTTGCTGGACTCTACAGTGACTACKGRAA

- 1542NPTX cell line:

CSAGAYTGACKCAMTSATATTTCATAGCCCTTTTGGATTTCTTGATCTCCATACAATGCTGCT
GGATGAATATCAAGAGAGGCTCTTCGTGGGAGGCAGGGACCTTGTATATTCCCTCAGCTTG
GAGAGAATCAGTGACGGCTATAAAGAGATACACTGGCCGAGTACAGCTCTAAAAATGGAAG
AATGCATAATGAAGGGAAAAGATGCGGGTGAATGTGCAAATTATGTTCGGGTTTTGCATCAC
TATAACAGGACACACCTTCTGACCTGTGGTACTGGAGCTTTTGATCCAGTTTGTGCCTTCATC
AGAGTTGGATATCATTTGGAGGATCCTCTGTTTCWCCTGGAATCACCCAKATCTGAKRGARG
AAGGGGCAGATGTCCTTTTGACCCCAGCTCCTCCTTCATCTCCACTTTAATTGGTAGTGAATT
GTTTGCTGGACTCTACAGTRMCYTACTGGAA

Semaphorin 3f:

- DU145 cell line:

GGTMTCTGRSTGAKTTMGCATGGTCTTCAACGGGCCCTTWGCCCACRAMGAGGGGCCCAA
CTACCAGTGGATGCCCWTCTCRKGSAASAYGCCCTACCCACSGSCGGGMMCRTGYCCTGGT
GGAACSTTCWMGCCATSTRKGAAGTCCACCAAGGATTATCCTGATGAGGTGATCAACYTCAT
GCGCAKCCACCCACTCRTGTACCRSGCCKKGTACSCTCTRYRSMGGCGGCSCCTGGTARTC
CGCACAGGTGCTCCCTACCGCCTTACCACTATTGCCGTGGACCAGGTGGATGCAGGCGAC

- 1542NPTX cell line:

AGCAGAGGTYTMTGGCTGWATTCGCATGGTCTTCACGGGCCCTTTGCCCACAAAGAGGGGC
CCAACTACCAGTGGATGCCCTTCTCAGGGAAGATGCCCTACCCACGGCCGGGCACGTGCCC
TGGTGGAACCTTCACGCCATCTATGAAGTCCACCAAGGATTATCCTGATGAGGTGATCAACT
TCATGCGCAGCCACCCACTCATGTACCAGGCCGTGTACCCTCTGCAGCGGCGGCCCCTGGT
AGTCCGCACAGGTGCTCCCTACCGCCTTACCACTATTGCCGTGGACCAGGTGGATGCAGGC
RMGTG

Plexin a1:

- 1542NPTX cell line:

TKKGGCTYYTWRAWKMWGCTCGAGCGGCCGCCAGTGTGATGGATATCTGCAGAATTCGCC
CTTTGCTGGACGCTGCCTACAAGGGCGTGCCCTACTCCCAGCGGCCCAAGGCCGCGGACAT
GGACCTGGAGTGGCGCCAGGGCCGCATGGCGCGCATCATCCTGCAGGACGAGGACGTCAC
CACCAAGATTGACAACGATTGGAAGAGGCTGAACACACTGGCTCACTACCAGGTGACAGAT
GGGTCCTCGGTGGCACTGGTGCCCAAGCAGACGTCCGCCTACAACATCTCCAACTCCTCCA
CCTTCACCAAGTCCCTCAGCAGATACGAGAGCATGCTGCGCACGGCCAGCAGCCCCGACAG

CCTGCGCTCGCGCACGCCCATGATCACGCCCGACCTGGAGAGCGGCACCAAGCTGTGGCA
CCTGGTGAAGAACCACGACCACCTGGACCAGCGTGAGGGTGACCGCGGCAGCAAGATGGT
CTCGGAGATCTACTTGACACGGCTACTGGCCACCAAGGGCACACTGCAGAAGTTTGTGGAC
GACCTGTTTGAGACCATCTTCAGCACGGCACACCGGGGCTCAGCCCTGCCGCTGGCCATCA
AGTACATGTTCGACTTCCTGGATGAGCAGGCCGACAAGCACCAGATCCACGATGCTGACGT
GCGCCACACCTGGAAGAGCAACTGCCTGCAAGGGCGAATTCCAGCACACTGGCGGCCGTTA
CTAGTGGATCCGAGCTCGGTACCAAGCTTGATGCATAGCTTGAGTATTCTATAGTGTCACCT
AAATAGCTTGGCGTAATCATGGTCATAGCTGTTTCCTGTGTGAAATTGTTATCCGCTCACAAT
TCCACACAACATACGAGCCGGAAGCATAAAGTGTAAAGCCTGGGGTGCCTAATGAGTGAGC
TAACTCACATTAATTGCGTTGCGCTCACTGCCCGCTTTCCAGTCGGAAACCTGTCGTGCCAG
CTGCATTAATGAATCGGCCAACGCGCGGGGGAGAGGCGGTTTGCGTATTGGGCGCTCTTCC
GCTT

Plexin a2:

- DU145 cell line:

TMWTTTWCTGGTGCTGTCACTCAACCCAATCCGAGGTCCCGAGTCARRARRSACTATGGTG
ACCATTACCGGCCATTACCWTGSGGCTRGGAGCAGCGTGGCAKTCTACCTGGGCAACCAGA
CCTGCGAGTTCTACGGGAGGTCAATGAGTGAGATCGTGYGTGTCTCACCCCCATCATCCAAT
GGCCTTGGCCCGGTCCCTGTTTCTGTGAGTGTCGACCGAGCCCATGTGGATAGCAACCTGC
AGTTTGAGTACATAGATGACCCTCGGGTCCAGCGCATCGAGCCAKAGTGGAKCATTGCCAG
TGGCCACACACCCCTGACCATCACAGGCTTCAACCTGGATGTCATTCAGGAGCCAAGGATCC
SAGTCAAATTCAATGGCAAAKAATCTGTCAATGTGTGKAAAGTTGTGAACACAACCACCCTC
ACCTGSCTGGSACCCTCTCTGACCACGGACTACCGCCCTGGCCTGGACACTGTGGAAMGCC
CAGATGAGTTTGGATTTGTCTTTAACAATGTCCAATCCTTGCTAATTTACAACGACACCAAGT
TTATCTACTACCCCAACCCGACCTTTGAACTGCTTAGCCCTACTGGAGTCTTGGATCAAAAGC
CAGGATCGCCCATCATTCTGAAGGGCAAAAACCTCTGCCCTCCTGCCTCTGGAGGGGCCAA
ACTCAAYTACACTGTGYTCAWCGGAGAGACCCCTTGTGCTGTCMCCGTATCTGAGACCCAG
CTA

- 1542NPTX cell line:

AMTACKATGAACCCTTCTGTGCTGTCACTCAACCCAATCCGAGGTCCCGAGTCAKGAGGCAC
TATGGTGACCATTACCGGCCATTACCTTGGGGCTGGGAGCAGCGTGGCAGTCTACCTGGGC
AACCAGACCTGCGAGTTCTACGGGAGGTCAATGAGTGAGATCGTGTGTGTCTCACCCCCAT
CATCCAATGGCCTTGGCCCGGTCCCTGTTTCTGTGAGTGTCGACCGAGCCCATGTGGATAG
CAACCTGCAGTTTGAGTACATAGATGACCCTCGGGTCCAGCGCATCGAGCCAGAGTGGAGC
ATTGCCAGTGGCCACACACCCCTGACCATCACAGGCTTCAACCTGGATGTCATTCAGGAGCC
AAGGATCCGAGTCAAATTCAATGGCAAAGAATCTGTCAATGTGTGTAAAGTTGTGAACACAA
CCACCCTCACCTGCCTGGCACCCTCTCTGACCACGGACTACCGCCCTGGCCTGGACACTGT
GGAACGCCCAGATGAGTTTGGATTTGTCTTTAACAATGTCCAATCCTTGCTAATTTACAACGA
CACCAAGTTTATCTACTACCCCAACCCGACCTTTGAACTGCTTAGCCCTACTGGAGTCTTGGA
TCAAAAGCCAGGATCGCCCATCATTCTGAAGGGCAAAAACCTCTGCCCTCCTGCCTCTGGAG
GGGCCAAACTCAACTACACTGTGCTCATCGGAGAGACCCCTTGTGCTGTCACCGTATCTGAG
AACCCAKMTATAAA

Plexin a3:

- DU145 cell line:

AMGTCTATGCCACGGGGCTGCTCAAGCAACTGCTGGCCGACCTCATCGAGAAKAACCTCKW
GAGCAAGAACCACCCCAAGCTGCTGCTACGCAKGACWGAGTCAGTGGCTRAGAAGATGCTT
ACCAACTGGTTCACGTTCCTGCTGCATAAGTTTCTGAAGGAGTGTGCTGGGGAGCCTCTCTT
CCTGCTTTACTGTGCCATCAAGCAGCAGATGGAGAAGGGCCCCATTGATGCCATCACGGGC
GAGGCACGATACTCCCTGAGCGAGGACAAGCTCATCCGTCAGCAGATCGACTACAAGACAC
TGACCCTTCACTGCGTGTGTCCGGAGAACGAGGGCAGCGCCCAGGTCCCAGTGAAGGTTCT
CAACTGTGACAGCATCACCCAGGCCAAAGATAAGCTGCTGGACACTGTGTACAAGGGCATT
CCGTACTCCCAGCGTCCCAAAGCTGAGGACATGGACCTGGAGTGGCGCCAGGGCCGCATG
ACTCGCTYCATCCTCC

- 1542NPTX cell line:

TGACTATGCCACGGGGCTGCTCAAGCAACTGCTGGCCGACCTCATCGAGAAGAACCTCGAG
AGCAAGAACCACCCCAAGCTGCTGCTACGCAKGACAGAGTCAGTGGCTRAGAAGATGCTTA
CCAACTGGTTCACGTTCCTGCTGCATAAGTTTCTGAAGGAGTGTGCTGGGGAGCCTCTCTTC
CTGCTTTACTGTGCCATCAAGCAGCAGATGGAGAAGGGCCCCATTGATGCCATCACGGGCG
AGGCACGATACTCCCTGAGCGAGGACAAGCTCATCCGTCAGCAGATCGACTACAAGACACT
GACCCTTCACTGCGTGTGTCCGGAGAACGAGGGCAGCGCCCAGGTCCCAGTGAAGGTTCTC
AACTGTGACAGCATCACCCAGGCCAAAGATAAGCTGCTGGACACTGTGTACAAGGGCATTC
CGTACTCCCAGCGTCCCAAAGCTGAGGACATGGACCTGGAGTGGCGCCAGGGCCGCATGA
CTCGATYCMWTCCTCCC

Plexin b1:

- DU145 cell line:

AGMMGCTCWRGATGCATGCTCGAGCGGCCGCCAGTGTGATGGATATCTGCAGAATTCGCC
CTTGCTCACCGTGSCACTGCATGGGAAGCTTGAGTATTTCACTGACATCCTCCGCACTCTGC
TCAGTGACCTGGTTGCCCAGTATGTGGCCAAGAACCCCAAGCTGATGCTGCGCAGGACAGA
GACTGTGGTGGRGAAGCYGCTCACCAACTGGATGTCCATCTGTCTGTATACCTTCGTGAGGG
ACTCCGTAGGGGAGCCTCTGTACATGCTCTTTCGAGGGATTAAGCACCAAGTGGATAAGGG
GCCAGTGGACAGTGTGACAGGCAAGGCCAAATACACCTTGAACGACAACCGCCTGCTCAGA
GAGGATGTGGAGTACCGTCCCCTGACCTTGAATGCACTATTGGCTGTGGGGCCTGGGGCAG
GAGAGGCCCAGGGCGTGCCCGTGAAGGTCCTAGACTGTGACACCATCTCCCAGGCAAAGG
AGAAGATGCTGGACCAGCTTTATAAAGGAGTGCCTCTCACCCAGCGGCCAGACCCTCGCAC
CCTTGATGTTGAGTGGCGGTCTGGAAGGGCGAATTCCAGCACACTGGCGGCCGTTACTAGT
GGATCCGAGCTCGGTACCAAGCTTGATGCATAGCTTGAGTATTCTATAGTGTCACCTAAATA
GCTTGGCGTAATCATGGTCATAGCTGTTTCCTGTGTGAAATTGTTATCCGCTCACAATTCCAC
ACAACATACGAGCCGGAAGCATAAAGTGTAAAGCCTGGGGTGCCTAATGAGTGAGCTAACT
CACATTAATTGCGTTGCGCTCACTGCCCGCTTTCCAGTCGGGAAACCTGTCGTGCCAGCTGC
ATTAATGAATCGGCCAACGCGCGGGGAGAGGCGGTTTGCGTATTGGGCGCTCTTCCGCTTC
CTCGCTCACTGACTCGCTGCGCTCGGTCGTTCGGCTGCGGCGAGSGTATCAGCTCACTCAA
AGGCGGTATACGGTTATCCACAGAATCAGGGGAWAACGCAGAAAGAACATGTGARCAAAG
G

Plexin b3:

- PC3 cell line:

GKSAGGCWRACCTAGTGGCAGCCTGCCCCCAGTTCCCTGACTGTGCCAGCTGCCTCCAGGC
CCAGGACCCGCTGTGTGGCTGGTGTGTCCTCCAGGGCAGGTGTACCCGGAAGGGCCAGTG
CGGGCGGGCAGGCCAGCTGAACCAGTGGCTGTGGAGTTATGAGGAGGACAGCCACTGCCT
GCACATCCAGAGCCTGCTGCCGGGCCACCACCCCCGCCAGGAGCAGGGCCAGGTCACTTT
GTCTGTCCCCCGGCTGCCCATCCTGGATGCAGATGAATACTTCCWTTGTGCGTTCGGGGAC
TATGACAGCTTGGCTCATGTGGAAGGGCCCCACGTGGCCTGTGTCACCCCTCCCCAAGACC
AGGTGCCACTTAACCCTCCAGGCACARACCACATCACTGTGCCCCTGGCCCTGATGTTCGAG
GACGTGACTGTGGCTGCCACCAACTTCTCCTTTTATGACTGCAGTGCCGTCCAGGCCTTGGA
GGCGGCTGCCCCGTGTCGCGCTTGCGTGGGCAGCATCTGGCGGTGTCACTGGTGCCCGCA
GAGTAGCCACTGCGTGTACGGAGAGCACTGCCCAGAGGGCGAGAGGACCATCTACAGCGC
CCAGGAGGTGGACATCCAGGTGCGTGGCCCAGGGGCTTGCCCACAGGTCGAARGYKKGSC
MRGGWY

Neuropilin 1:

- DU145 cell line:

GWSGWCAYCGACTACGAAACACATGGTGCAGGATTTTCCATACGTTATGAAATTTTCAAGA
GAGGTCCTGAATGTTCCCAGAACTACACAACACCTAGTGGAGTGATAAAGTCCCCCGGATTC
CCTGAAAAATATCCCAACAGCCTTGAATGCACTTATATTGTCTTTGCGCCAAAGATGTCAGAG
ATTATCCTGGAATTTGAAAGCTTTGACCTGGAGCCTGACTCAAATCCTCCAGGGGGGATGTT
CTGTCGCTACGACCGGCTAGAAATCTGGGATGGATTCCCTGATGTTGGCCCTCACATTGGGC
GTTACTGTGGACAGAAAACACCAGGTCGAATCCGATCCTCATCGGGCATTCTCTCCATGGTT
TTTTACACCGACAGCGCGATAGCAAAAGAAGGTTTCTCAGCAAACTACAGTGTCTTGCAGAG
CAGTGTCTCAGAAGATTTCAAATGTATGGAAGCTCTGGGCATGGAATCAGGAGAAATTCATT
CTGACCAGATCACAGCTTCTTCCCAGTATAGCACCAACTGGTCTGARAARCGCTMA

- 1542NPTX cell line:

CKKKGTSRGWGRTMTMTRACTACGARCACATGGKGCAGGATTTTCCATACGTTATGAAATTT
TCAAGAGAGGTCCTGAATGTTCCCAGAACTACACAACACCTAGTGGAGTGATAAAGTCCCCC
GGATTCCCTGAAAAATATCCCAACAGCCTTGAATGCACTTATATTGTCTTTGCRCCAAAGATG
TCAGAGATTATCCTGGAATTTGAAAGCTTTGACCTGGAGCCTGACTCAAATCCTCCAGGGGG
GATGTTCTGTCGCTACGACCGGCTAGAAATCTGGGATGGATTCCCTGATGTTGGCCCTCACA
TTGGGCGTTACTGTGGACAGAAAACACCAGGTCGAATCCGATCCTCATCGGGCATTCTCTCC
ATGGTTTTTTACACCGACAGCGCGATAGCAAAAGAAGGTTTCTCASCAAACTACAGTGTCTT
GCAGAGCAGTGTCTCAGAAGATTTCAAATGTATGGAAGCTCTGGGCATGGAATCAGGAGAA
ATTCATTCTGACCAGATCACAGCTTCTTCCCAGTATAGCACCAACTGGTCTGAGAA

Neuropilin 2:

- DU145 cell line:

CGKKGGCTYCWGATGCWGCTCGAGCGGCCGCCAGTGTGATGGATATCTGCAGAATTCGCC
CTTCTACATCAAGTYCACCTCCGACTACGCCCGGCAGGGGGCAGGCTTCTCTCTGCGCTACG
AGATCTTCAAGACAGGCTCTGAAGATTGCTCAAAAAACTTCACAAGCCCCAACGGGACCATC
GAATCTCCTGGGTTTCCTGAGAAGTATCCACACAACTTGGACTGCACCTTTACCATCCTGGC
CAAACCCAAGATGGAGATCATCCTGCAGTTCCTGATCTTTGACCTGGAGCATGACCCTTTGC
AGGTGGGAGAGGGGGACTGCAAGTACGATTGGCTGGACATCTGGGATGGCATTCCACATGT
TGGCCCCCTGATTGGCAAGTACTGTGGGACCAAAACACCCTCTGAACTTCGTTCATCGACGG

GGATCCTCTCCCTGACCTTTCACACGGACATGGCGGTGGCCAAGGATGGCTTCTCTGCGCG
TTACTACCTGGTCCACCAAGAGCCACTAGAGAACTTTCAGTGCAATGTTCCTCTGGGCATGG
AGTCTGGCCGGATTGCTAATGAACAGATCAGTGCCTCATCTACCTACTCTGATGGGAGGTGG
ACCCCTCAACAAAGCCGGCTCCATGGTGATGACAATGGAAGGGCGAATTCCAGCACACTGG
CGGCCGTTACTAGTGGATCCGAGCTCGGTACCAAGCTTGATGCATAGCTTGAGTATTCTATA
GTGTCACCTAAATAGCTTGGCGTAATCATGGTCATAGCTGTTTCCTGTGTGAAATTGTTATCC
GCTCACAATTCCACACAACATACGAGCCGGAAGCATAAAGTGTAAAGCCTGGGGTGCCTAAT
GAGTGAGCTAACTCACATTAATTGCGTTGCGCTCACTGCCCGCTTTCCAGTCGGGAAACCTG
TCGTGCCAGCTGCATTAATGAATCGGCCAACGCGCGGGGAGAGGCGGTTTGCGTATTGGGC
GCTCTTCCGCTTCCTCGCTCACTG

- 1542NPTX cell line:

ABSTRACT

Prostate cancer (PCa) has become a major public health issue; it is the second most common cause of cancer-related death in the UK. PCa preferentially metastasises to the bone. Semaphorins are an important family of membrane bound or secreted signalling proteins, which control cell movement (or chemotaxis). They have a role in the nervous, immune and vascular systems, but have not previously been studied in prostate. To determine if semaphorins and their receptors are expressed in normal and pathological prostate, profiling experiments were performed by (q)RT-PCR in prostate cell lines and tissues. Results show that semaphorins and receptors are ubiquitously expressed, suggesting autocrine and paracrine regulation of semaphorin signalling in prostate; particularly an autocrine signalling of Semaphorin3A in bone metastasis derived cells. Results also show that expression of secreted semaphorins is strongly regulated by hypoxia; which strongly down-regulates semaphorin 3e in primary tumour derived cells, whereas semaphorin 3c is strongly up-regulated. Particular focus was brought on semaphorin 3e, whose expression is strongly increased in epithelial cells derived from benign prostate hyperplasia, non-neoplastic tissue, and bone metastasis derived cells. A Semaphorin3E expression construct was made and the protein produced in mammalian cells to study its effects on cell morphology and adhesion by immunocytochemistry and adhesion assays. Results show that Semaphorin3E inhibits integrin-mediated cell adhesion while it initiates vinculin-mediated focal adhesion formation, which suggest that Semaphorin3E may play important regulatory roles in prostate cancer metastasis. The effects on cell movement of frequent missense mutations of PlexinB1 receptor, associated with prostate primary tumours and metastases, was studied by migration assays. Results show that the three mutations of PlexinB1 increase cell migration in absence of ligand Semaphorin4D, and further increase migration in its presence. Together these results suggest that semaphorin signalling has a key role in prostate cancer progression.